



Cardiff
Catalysis Institute

Sefydliad Catalysis
Caerdydd

Investigating rate enhancements in alpha-keto esters using cinchona and non- cinchona alkaloids

MATTHEW EDWARDS

Miles Matthew Henderson Edwards

School of Chemistry

Cardiff Catalysis Institute

Cardiff University

December 2022

Submitted for a PhD in chemistry

Abstract

The products of the hydrogenation of alpha-ketoesters like ethyl pyruvate (EtPy), methyl benzoylformate (MBF) and ethyl benzoylformate (EBF) are used in many industries including pharmaceuticals, fragrances, solvent synthesis, and organic chemical intermediates. The rate of hydrogenation of EtPy increases substantially using cinchona alkaloid modifiers such as cinchonidine (CD) but the mechanism of rate enhancement is poorly understood, despite having been investigated extensively over the last few decades.

The objective of this thesis is to investigate the mechanism of modifier-induced rate enhancement for the hydrogenation reactions of the alpha-keto esters EtPy, MBF and EBF. Rate enhancements were observed for the reactions of all three substrates (MBF, EBF and EtPy) using the different modifiers (CD, quinuclidine (QD) 3-quinuclidinol (QL), 1,4-diazabicyclo[2.2.2]octane (DABCO), and 4-aminoquinoline (AQ)). QD, QL, DABCO and AQ are modifiers that represent parts of the CD molecule, the aim of studying them being to deduce which parts of the CD molecule were involved in the rate enhancements. The concentrations of the modifiers were optimised, and the reaction data was kinetically fitted. Theoretical calculations were also completed to see if the rate enhancement mechanism could be understood computationally.

The reaction mechanism when using CD may involve the 1:1 modifier: reactant model which stabilizes the half-hydrogenated state. This is suggested especially because of the rate enhancements observed for EBF and MBF which made the alternative theory for the mechanism of action via a 'cleaning' the catalyst model unlikely. The EtPy reaction mechanism may be a combination of the CD stabilizing the half-hydrogenated state and the cleaning effect. Concerning the achiral tertiary amines, the mechanism of action is unclear but the previous literature suggestion, supported by results from this project point to the modifier-surface

complex being stabilized by the half-hydrogenated substrate. The cleaning effect and competitive adsorption may also be involved.

Different substrates that were similar in structure to either EtPy, EBF and MBF were tested also to see if other rate enhancements could be found but none of these reactions gave significant rate enhancement. Theoretical computational results provided evidence for the existence of a solution-dimer intermediate.

Table of Contents

1. Chapter 1 Introduction ; aims and objectives	7
1.1 Reaction kinetics	8
1.1.1 Orders of reaction	9
1.1.2 Factors that affect the reaction rate	10
1.1.3 Mass Transfer effects	11
1.1.4 Pore Diffusion Resistance	11
1.1.5 Solvent	11
1.2 Stereoselective and regio-selective reactions	12
1.2.1 Stereoselective reactions	13
1.2.2 Regioselective reaction	13
1.3 History of catalysis	14
1.4 Catalyst inhibitors, poisons and promoters	16
1.4.1 Catalyst inhibitors	16
1.4.2 Catalyst poisons	17
1.4.3 Catalyst promoters	18
1.5 The EtPy hydrogenation reaction	18
1.6 1:1 Modifier to reactant model	21
1.7 Origin of the rate enhancement	23
1.8 Alternative models	26
1.9 Previous EtPy hydrogenation studies	28
1.10 Conformers of CD	34
1.11 Ethyl pyruvate hydrogenation using Pt Colloids	36
1.12 Other modifiers used in the EtPy reaction	37
1.13 Summary of published results using different modifiers	43
1.14 Different reactants that experience rate enhancement	47
1.15 Reactors	51
1.15.1 The continuous reactor	
1.15.1.1 Fixed bed reactors	52
1.15.1.2 Fluidised bed reactor	52
1.15.2 Continuous stirred tank reactor	52
1.15.3 Trickle bed reactors	53
1.15.4 Semi-batch reactors	53
1.15.5 Batch reactors	54
1.15.6 Slurry Reactors	54
1.16 The components of the catalytic system	54
1.16.1 Catalysis	54
1.16.2 Solvent	55
1.17 Side reactions of EtPy	55
1.18 Computational Analysis	56
1.19 Previous studies on the ETPY hydrogenation using computational analysis	57
1.20 Summary	59
1.21 References	60
2. Chapter 2 Experimental	64

2.1	Introduction	64
2.2	Materials	65
2.3	General synthesis and preparation of catalyst	67
2.4	Equipment	69
2.4.1	Batch reactors	69
2.4.2	Autoclave reactors	70
2.4.3	Hydrogen uptake monitor	71
2.5	How the rate is calculated	74
2.5.1	Noise rejection	74
2.5.2	Kinetic model	77
2.6	Characterisation techniques	80
2.6.1	Carbon monoxide chemisorption	80
2.6.2	Gas chromatography	83
2.6.2.1	Chiral columns	85
2.6.3	Transmission electron microscopy (TEM)	86
2.6.4	Brunauer-Emmett-Teller (BET) surface area analysis	89
2.6.5	X-ray diffraction (XRD)	92
2.7	References	95
3.	Chapter 3 Hydrogenation reactions using cinchonidine and cinchonine modifiers	96
3.1	The background of the rate enhancement caused by CD	96
3.1.1	The 1:1 Modifier to reactant model	96
3.2	Results and Discussion	97
3.2.1	Catalyst Characterization	97
3.2.1.1	Transmission electron microscopy (TEM)	98
3.2.1.2	X-ray diffraction (XRD) characterisation of the two catalysts compared to gamma alumina	102
3.2.1.3	Nitrogen adsorption measurements and BET analysis	103
3.3	Comparison of the Hydrogenation Reactivity over the Sigma-Aldrich (SA) and Johnson Matthey (JM) catalysts	105
3.3.1	EtPy hydrogenations	105
3.3.2	EBF hydrogenation	108
3.3.3	MBF hydrogenation reactions	111
3.3.4	Summary of comparison of catalysts	113
3.4	Investigation of experimental parameters using SA catalyst to determine their effect on reaction kinetics	115
3.4.1	Influence of reaction stirring speed	115
3.4.2	Order of reaction with respect to substrate	117
3.5	Discussion	121
3.5.1	The state-of-the art hydrogenation using EtPy with CD	121
3.5.2	Unmodified EtPy hydrogenation reactions	123
3.5.3	EtPy Hydrogenation Using CD	123
3.5.4	EBF hydrogenation	128
3.5.5	MBF hydrogenation using CD	133
3.6	Conclusion	138
3.7	References	140

4. Chapter 4 Understanding the mechanism of the rate enhancement of cinchonidine in α -keto ester reduction using analogues of its deconstructed parts	141
4.1 Reactions in neat toluene	143
4.2 Comparison of the two catalysts	144
4.3 EBF hydrogenation	148
4.4 MBF hydrogenation	150
4.5 Summary of catalyst comparison	152
4.6 4-aminoquinoline (AQ)	154
4.6.1 EtPy hydrogenation	156
4.7 Reactions with QD	159
4.8 Comparison of EtPy, EBF and MBF with QD modifier	163
4.9 DABCO	169
4.9.1 Comparison of EtPy, EBF and MBF with DABCO modifier	170
4.10 3-Quinuclidinol	176
4.10.1 Comparison of EtPy, EBF and MBF with QL modifier	178
4.11 Overview of the modifiers in each substrate	182
4.11.1 EtPy	182
4.11.2 MBF	184
4.11.3 EBF	186
4.12 The influence of solvent; acetic acid compared to toluene + acetic acid (0.001 M)	188
4.12.1 EtPy	188
4.12.2 MBF	191
4.12.3 EBF	193
4.13 Conclusion	196
4.14 References	197
5. Chapter 5- Extending the Pt-cinchona system to other reactants	198
5.1 Hydrogenation of β -diketo esters	200
5.1.1 EAA hydrogenation	200
5.1.2 Methyl acetoacetate hydrogenation	202
5.1.3 Ethyl benzoyl acetate hydrogenation	205
5.2 Γ - diketo ester	207
5.2.1 Methyl levulinate hydrogenation	207
5.3 Simple ketones	209
5.3.1 Acetophenone hydrogenation	209
5.3.2 Benzalacetone hydrogenation	211
5.4 Diketone	213
5.4.1 2,3-Butane-dione hydrogenation	213
5.5 Fluorine-containing compounds	215
5.5.1 1,1,1-trifluoro-2,4-pentandione hydrogenation	215
5.5.2 Ethyl trifluoropyruvate hydrogenation	216
5.6 Conclusion	219
5.7 References	221
6. Chapter 6- Computational analysis	222
6.1 Background to theoretical calculations	222
6.1.1 Periodic calculations	223

6.1.2	Molecular calculations	225
6.2	Dimer formation	227
6.2.1	ETPY	228
6.2.2	MBF	231
6.2.3	EBF	234
6.2.4	Ethyl acetoacetate	237
6.2.5	Conclusions for dimer calculation	238
6.3	Substrate-modifier- surface	239
6.3.1	ETPY	240
6.3.2	MBF	243
6.3.3	EBF	246
6.3.4	Ethylacetoacetate	249
6.3.5	Conclusion for complex calculations	252
6.4	Workfunction	253
6.5	References	256
7.	Summary and conclusions	257
7.1	Summary	256
7.2	Future work	261
8.	Acknowledgements	263
9.	Appendix	264

Chapter 1 Introduction

Aims and objectives

Catalysis is an extremely important field of chemistry as it is used in most industrial chemistry applications, with examples ranging from refinement of petroleum, production of pharmaceuticals and chemicals, to the manufacture of synthetic fibres and plastics. Catalysis is a staple for green chemistry and is essential for making a sustainable world, because reactions are achievable using lower energy, with less of the associated pollution and depletion of finite resources that this benefit brings. Hydrogenation reactions are a key type of reaction for which catalysts are needed. In these reactions a hydrogen molecule reacts with another compound, for example, the saturation of organic compounds in many industrial processes. It is an important step in the fats and oils industry as it converts liquid oils into semi-liquids for different applications, including shortenings and margarine manufacture.¹

Hydrogenation reactions are also used to recover crude oil and gases so that they can be used for industrial purposes.² Initially, hydrogenation reactions were used to retrieve oil from coal. In the 1980s, hydrogenation was used to cleanse industrial residue like oil that had chlorine in it.³

When using catalysts, a modifier can be used to enhance the rate, achieving even faster reactions than those possible using the catalyst alone. There has been considerable work on the rate enhancement of hydrogenation reactions and further study of these types of reactions is the focus for this thesis. Hydrogenation of ethyl pyruvate (EtPy) is an important reaction to investigate as the product, ethyl lactate, is commercially useful as a food flavouring and is also found in many cosmetic products. Ethyl lactate has a high solvency power, high boiling point, low vapour pressure and low surface tension. For these reasons it is sought after in the coating

industry, and it also acts as a good paint stripper and graffiti remover. Ethyl lactate has also replaced more toxic solvents like toluene and xylene making work environments safer.⁴

The overall objective of this thesis is to investigate in mechanistic detail the hydrogenation of EtPy to see how cinchona alkaloid modifiers such as cinchonidine (CD) and cinchonine (CN) provide a rate enhancement for the reaction. Once this is understood more fully, this rate enhancement may be applied successfully to other hydrogenation reactions. To achieve this objective, the aims of this thesis are to investigate the rate enhancement of EtPy using cinchona alkaloids and other nitrogen-containing hydrocarbon analogues; to investigate the rate enhancement caused by the individual structural moieties of the molecule CD, to use computer modelling techniques to explore computationally the different possible mechanisms and to investigate whether the rate enhancements seen in EtPy are present in other hydrogenation reactions. Catalysis is the process of increasing the rate of reaction by lowering its activation energy (E_a). The catalyst does this by providing an alternative pathway for the reaction to take place, i.e. the catalyst forms an intermediate with the reactant and is then recycled such that the catalyst is not consumed in the reaction. There are two types of catalysts: homogeneous and heterogeneous.

1.1 Reaction Kinetics

As catalysts are not used up in reactions, they are not involved stoichiometrically in the overall chemical equations. However, because they increase the rate of reaction, they must be involved in at least one of the intermediate steps. Catalysts lower the E_a of the reaction thus lowering the energy barrier for the reaction, hence increasing the proportion of reactants that can react causing the forward and reverse reaction to accelerate. Figure 1.1 illustrates the activation energies of a reaction with catalyst and a reaction without catalyst. The reaction with

catalyst shows a decrease in E_a compared to the reaction without catalyst, thereby, allowing the reaction to occur at a faster rate.

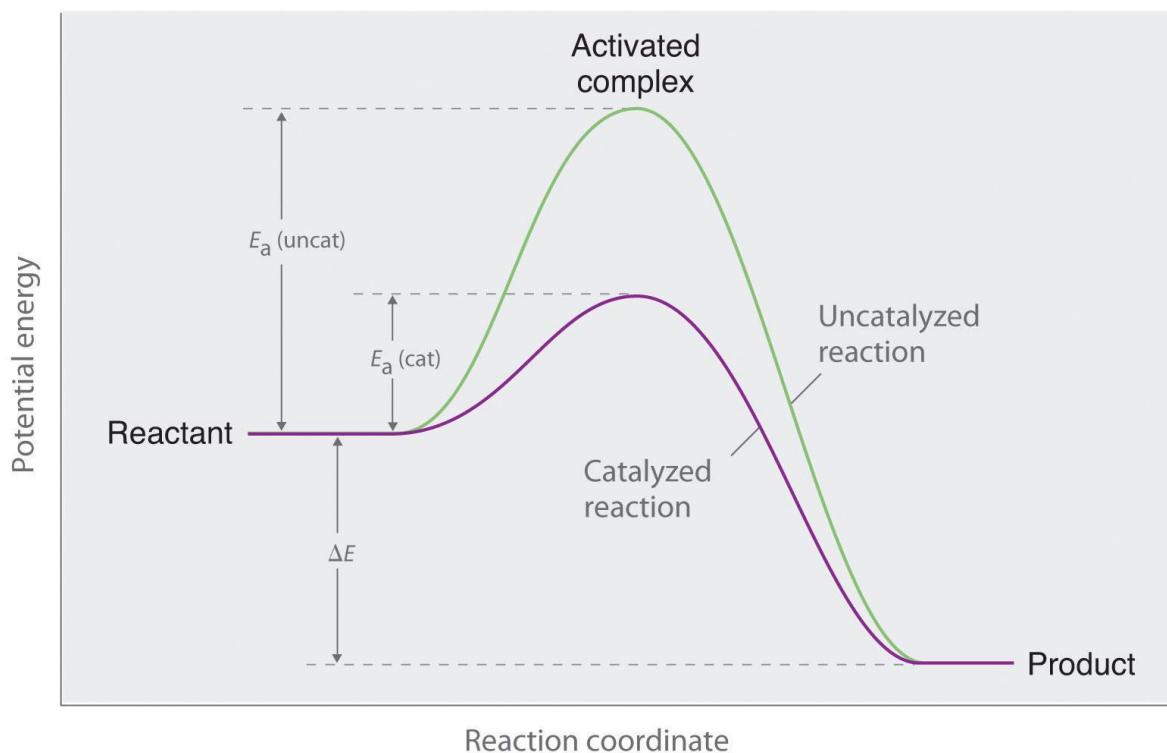
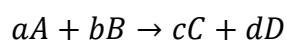


Figure 1.1: A graphical representation of what happens when a catalyst is added to a reaction.⁵

1.1.1 Orders of reaction

The order of a reaction relates the rate of reaction to the rate constant (k) and the concentration of reactants.

If a reaction has the equation:



with no intermediate steps the rate law is

$$\text{rate} = k[A]^a[B]^b$$

where k is the rate constant.

A **zero-order** reaction is a reaction where the rate does not depend on the reactant concentration; the units of k are $\text{mol dm}^{-3} \text{s}^{-1}$ and the rate equation for such reactions can be given as:

$$\text{rate} = k$$

A **first-order** reaction is a reaction that depends on the concentration of one reactant linearly, which becomes a unimolecular reaction if there are other reactants whose concentration will not make a difference to the rate. k has units of s^{-1} . Most reactions have first-order rate kinetics.

$$\text{rate} = -\frac{\Delta[A]}{\Delta t} = k[A]$$

A **second-order** reaction is a reaction where the rate depends on the concentration of a reactant to the power of 2. The units of k are $\text{mol}^{-1} \text{dm}^3 \text{s}^{-1}$. Formation of double stranded DNA from two complementary strands is an example of this.

$$\text{rate} = -\frac{\Delta[A]}{\Delta t} = k[A]^2$$

There are other order reactions where the concentration is raised to a fraction power but these three are the most common types of reaction.

1.1.2 Factors that affect the reaction rate

There are several different factors that can have an impact on the reaction rate. In addition to the catalyst, temperature, concentration, pressure and surface area are other important considerations include mass and heat transfer effects.

1.1.3 Mass Transfer effects

Mass transfer effects can influence catalytic rates. There are two types of mass transfer effects internal and external. Internal mass transfer effects occur in porous materials when the reactants and products diffuse in and out of the interior of a particle. External mass transfer effects refer to movement of reactants from the bulk solution to the catalyst surface when there is a solid-liquid interface between the reactants and the catalyst.⁶

1.1.4 Pore Diffusion Resistance

Another factor that can have an effect on rate is the pore diffusion resistance. Diffusion is assumed to take place in the pores of the catalyst. For the Pt on alumina catalyst used in this project large mesopores (pore diameter > ~12 nm) were essential to obtain maximum catalytic activity without mass transfer limitation and pore diffusion resistance and to suppress catalyst deactivation by fouling.⁷

1.1.5 Solvent

The reaction solvent can affect the reaction rate and solvent effects have been reported extensively in organic synthesis and in heterogeneous catalysis. The mechanistic understanding is more detailed in organic synthesis. It is harder to understand and characterize in heterogeneous catalysis because of the interactions between the supported metal catalysts and the reactants, which could be due to the interactions between the solvent and the support.⁸

When investigating solvent effects in reaction kinetics the reaction rates and product distribution are correlated with the solvent polarity to determine if the solvent effects make

significant changes to the rate. The dielectric constant is an important factor and can change the rate of reaction.⁸

1.2 Stereoselective and regio-selective reactions

1.2.1 Stereoselective reactions

A stereoselective reaction occurs when one stereoisomer is formed preferentially over another. The dehydrohalogenation of 2-iodobutane is an example (Figure 1.2). The *E*-isomer is the preferred product compared to the *Z*-isomers for this reaction.⁹

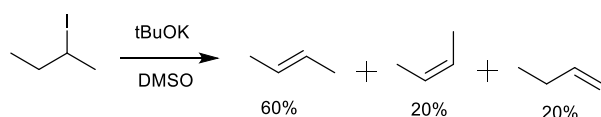


Figure 1.2: The dehydrohalogenation of 2-iodobutane. The *Z* isomer is the product on the left and the *E*-isomer is in the middle.

If the products of a reaction are enantiomers, the reaction is referred to as enantioselective when the two enantiomers are produced in unequal amounts. An example of this type of reaction is the EtPy hydrogenation which is one of the reactions focussed on during this project. Further description of the EtPy hydrogenation is contained within Section 1.5 in this chapter.

Another example of this is the asymmetric hydrogenation of olefins using Pd catalysts. Hydrogenation of olefins is a very useful reaction for the synthesis of optically active compounds. These reactions can be done over a Pd catalyst like the hydrogenation of 3-methyl-2-cyclohexenone by Drago and Pregosin (Figure 1.3). They achieved a 30% enantiomeric excess (ee) and a 40% yield.¹⁰ Yield is a quantity of moles of a product formed in a reaction

in relation to the reaction consumed. The enantiomeric excess is a measurement of purity for chiral substances.

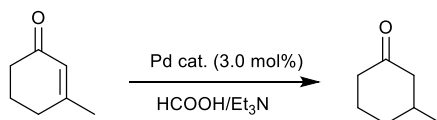


Figure 1.3: The hydrogenation of 3-methyl-2-cyclohexenone

Another example is Nickel catalysed asymmetric hydrogenation of N-sulfonyl imines (Figure 1.4). Li *et al.* used completed a few reactions to synthesise chiral amines. Chiral amines are useful building blocks for a large selection of chiral intermediates. There was a 95 % yield and a 97 % ee.¹¹

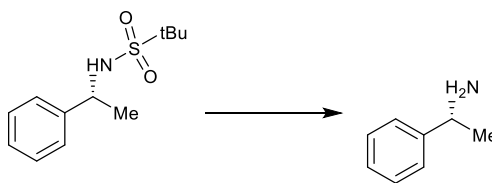


Figure 1.4: The hydrogenation of (R)-2-methyl-N-(1-phenylethyl)propane-2-sulfonamide. AlCl₃ (3.0 mmol), CH₂Cl₂ (10 mL), RT.

1.2.2 Regioselective reactions

Regio-selective reactions occur when there is a preferred area where the bonds in a reaction are made or broken. An example of this is the bromination reaction of N-bromosuccinimide (NBS) with an asymmetrical alkene such as 2-propenylbenzene; two different products are possible, but one is preferred over the other (Figure 1.5).¹²

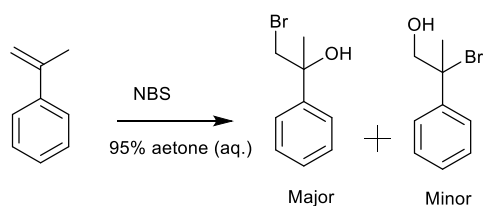


Figure 1.5: The bromination of 2-propenylbenzene showing the major and minor product

1.3 History of Catalysis

Elizabeth Fulhame invented the principle of catalysis in 1794 but the term catalysis as a word was not coined until 1835 by Jöns Jakob Berzelius (1779-1848).¹³ The word catalysis comes from the Greek words *kata* (down) and *luo* (loose). The oldest form of catalysis is homogeneous catalysis, using enzymes, which has been around for thousands of years.¹³ The earliest example of a homogeneous process is fermentation used to produce wine and beer by the Egyptians. An interesting example of catalysis is the production of sulphuric acid; in the Middle Ages they made this by burning sulphur and nitric acid together. They improved on this reaction by using lead as the construction material for the reactors which allowed larger quantities of it to be made. In 1793 two chemists, Clement and Desormés, discovered that nitre in this process was a catalyst as when they added more air, less of the nitre was needed and it was not used up in the reaction. They became aware that the nitrous vapours were intermediates and that the oxidising agent was air.¹³

The first time it became clear that a chemical reaction could be accelerated by a substance where the substance was not used up itself was in the decomposition of hydrogen peroxide, investigated by L.J. Thénard, a French chemist, in 1818.¹⁴ In 1817, a British chemist named Humphrey Davy¹⁴ discovered the first instance where two gaseous reactants can react on a surface without the metal changing. His research led to the design of the miners' safety lamp. Davy found that if you put a platinum wire above a coal-lamp and added coal gas the

fire would go out, but the platinum wire would stay hot for many minutes. He concluded that the coal gas and the oxygen combined to produce enough heat to keep the platinum wire warm. Davy had discovered heterogeneous catalytic oxidation. He also recorded the first pattern of catalytic activity as only platinum and palladium wires would stay hot so were effective, but copper, gold, silver and iron were ineffective. It was thought that the platinum and palladium were more effective than the other metals due to their low heat capacities and low thermal conductivities.¹⁵ Peregrine Phillips understood the value of catalytic oxidation in 1831 and created a way to formulate sulphuric acid. However, it was not until a few decades later that sulphuric acid became a needed chemical in industry and Messel in 1875 made fuming sulphuric acid from Phillips' research.¹⁶

The Haber process was an effort to create NH_3 catalytically. Hundreds of thousands of tonnes of NH_3 are needed every year.¹⁷ In agriculture it is used as a precursor to a fertilizer composition and significantly increases crop yields by as much as 60%. Increased amounts were needed during World War 1 where ammonia was used for the manufacture of explosives. Noncatalyzed synthetic routes which were not very effective had been used previously. Therefore, Haber started experimenting with catalysts to make NH_3 and his first successful experiment was in 1905 when he reported that he synthesised NH_3 at a low yield at 1293K. It was not until he started performing the reactions at higher pressures that he obtained higher yields. He experimented with many catalysts and found FeO_x to be the most active.

Haber teamed up with BASF chemical company to scale-up this reaction; they tested over 4000 different catalysts and managed to create plants that allowed the reaction to take place. Haber won the Nobel prize in 1919 because of his work.¹⁸ In 1923 BASF used a ZnO-chromia catalyst at high pressure to synthesise methanol. This was significant as it marked the development of synthesis of mass quantities of organic products. Then came along catalytic cracking which was first used in 1936.¹⁸ In 1938 Otto Roelen discovered oxo synthesis which

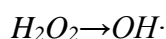
marked the emergence of homogeneously catalysed reactions. In the 1960s Chevron revived hydrocracking using metal promoted silica–aluminas, aluminas, and zeolites.¹⁹

Environmental issues drove new technologies using catalysis as well; e. g. in 1980 V, W and Ti oxides were used in the selective catalytic reduction (SCR) of NO_x by NH₃ for power plants. In 1990 the use of catalysts for diesel oxidation using only cerium were developed.²⁰

1.4 Catalyst inhibitors, poisons and promoters

1.4.1 Catalyst inhibitors

A catalyst inhibitor lowers the activity of a catalyst; typically, the inhibitor has a similar molecular structure in most cases to the reactant and so can bind to the active site of the catalyst instead of the reactant itself. The active site is the group of atoms on the surface of a heterogeneous catalyst where the reaction takes place between the reactants. An inhibitor reduces the activity of the catalyst via a reversible process and so is different from a poison, as a poison irreversibly changes the catalyst. An example of inhibition is when hydrogen peroxide decomposition is inhibited by acetanilide (Scheme 1.1). Hydrogen peroxide is thermodynamically unstable due to the unstable peroxide bonds, decomposing to water and oxygen.



Scheme 1.1: Decomposition of hydrogen peroxide

The degradation reaction can be catalysed by many types of heterogeneous, homogeneous and biological catalysts, among the most common being potassium iodide, lead dioxide and manganese (IV) oxide, and the enzyme catalase. Ferrous-catalysed degradation

can be inhibited by acetanilide, as can the un-catalysed degradation. It is thought that acetanilide binds to the surface of the iron catalyst. Hydrogen peroxide is used in many oxidation reactions, bleaching processes, as a disinfectant and in treatment of pollutants but as its decomposition is very likely to occur, it must be stored with the inhibitor acetanilide.²¹

Enzymes or biological catalysts can be inhibited either irreversibly or reversibly. Reversible inhibitors are inhibitors that nullify the enzyme by binding to it via a weak interaction that is not bound covalently. There are two types of this kind of inhibition: competitive and non-competitive inhibition. Competitive inhibition is when the inhibitor structurally resembles the substrate and therefore competes with the substrate when binding to the enzyme active site.²² Non-competitive inhibition is where the inhibitor does not bind to the active site of the enzyme, but it does bind to another part of the molecule causing a conformational change which then deforms the active site making it inactive.

Irreversible inhibition occurs when an inhibitor forms a strong covalent bond with the enzyme deactivating the enzyme irreversibly.²³ In heterogeneous catalysis irreversible inhibitors are called catalyst poisons.

1.4.2 Catalyst poisons

A catalyst poison is a substance that completely stops or inhibits the reactivity of a catalyst. A poison causes the catalyst to be chemically deactivated rather than physically altered. Lead is an example of a poison that reduces the activity of the catalysts in car catalytic converters. Catalytic converters are devices on the exhaust pipes of cars that reduce the quantity of toxic gases and pollutants emitted into the atmosphere. There are two types: the two-step converter and the three-step converter. The two-step converter works by combining unburned hydrocarbons, carbon monoxide and oxygen to produce CO₂ and H₂O. This is useful as CO is

toxic and the unburned hydrocarbons are pollutants that cause damage to human health and the environment.²⁴ Examples of the unburned hydrocarbons include small molecules such as formaldehyde and larger compounds including benzene, toluene and xylene. These molecules are toxic as they can cause cancer. Some of these molecules also can react with the nitrogen oxides to form ozone which creates a photochemical smog. The three-step converter carries out the above conversions and in addition also reduces the nitrogen oxides to nitrogen. The lead poisons the catalytic converter by forming a lead coating on the surface of the catalyst thereby blocking the harmful gases from adsorbing. For this reason, unleaded fuel is required to run cars containing catalytic converters.²⁵

1.4.3 Catalyst promoters

These are substances that enhance the reactivity of catalysts in reactions. Catalyst promoters by themselves have no catalytic effect. Catalyst promoters, sometimes called catalyst modifiers, usually work by adsorbing onto the surface of the catalyst and through intermolecular forces (hydrogen bonding, electrostatic attractions) lower the activation energy (E_a) needed for the reaction. An example of this is in the Haber process; when producing ammonia, small amounts of K_2O increase the rate of the reaction. In this example the K_2O is the catalyst promoter and osmium is the catalyst used. Other catalytic promoters include the modifiers CD and CN in the EtPy hydrogenation.²⁶

1.5 The EtPy hydrogenation reaction

Over the past three decades the hydrogenation of EtPy has been investigated and studied extensively. The main goal of these experiments and investigations was focused on improving the enantiomeric excess (ee) of the reaction. The ee is of interest in organic chemistry as it

shows the purity of one enantiomer over the other as enantiomers can have different chemical and biological properties. Rate enhancements using the modifiers CD (Figure 1.6) and its diastereoisomer CN have been observed in previous studies^{27,28,29}, as well as an enantiomeric excess^{27,28,29}. However, as the main focus for these experiments was the ee, the origin of the rate enhancement was not fully explored.

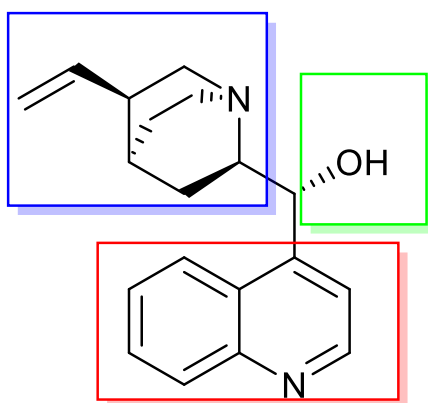


Figure 1.6: Different parts of cinchonidine. The blue part is the quinuclidine moiety; the green part is the hydroxyl group and the red part is the quinoline moiety.

The earliest publications on the EtPy hydrogenation were concerned with just cinchona alkaloids and how they gave such a significant enantiomeric excess and yield in the EtPy hydrogenation when compared to the unmodified reaction. The first publications were completed by Orito *et al.* from 1979 to 1980; in these reports α -ketoesters like methyl benzoylformate (MBF), EtPy and methyl pyruvate were hydrogenated using cinchona-modified catalysts. Optical yields of up to 90 % were found using the modified catalyst. The yield was heavily influenced by the catalyst pre-treatment and various other additives. They found that all cinchona alkaloids that had the same absolute configuration as CD produced the *R*-enantiomer (*R*-ethyl lactate) and all cinchona alkaloids with the same absolute configuration

as CN produce the *S*-enantiomer (*S*-ethyl lactate). The absolute configuration refers to the spatial arrangement of atoms within a chiral molecule and its' resultant stereochemical description. This was found through using a chiral column in gas chromatography.²⁷

Blaser *et al.* published a paper following on from Orito's work where they found that the modified cinchona catalysts were up to 100 times more active than the unmodified catalyst. In this work they stated that there was no discernible relationship between total or metal surface area and performance. They found initial rates were increased in the modified reaction by 5-100 times. They stated that thermal treatment had the biggest influence on the rate rather than catalyst pre-treatment which is in contrast to the findings found in the Orito reaction.²⁷ This paper proved using adsorption isotherms that CD adsorbs onto the metal surface and they theorized that there are interactions with the α -ketoester on the surface of the metal and not in the liquid phase. They also ruled out a basic effect where the stronger the base the faster the rate enhancement, because they could not achieve a significant rate enhancement with stronger bases compared to CD.²⁸

Baiker and Blaser were the first to look at the different aspects of the cinchona alkaloid hydrogenation to investigate what caused the rate enhancement. They reported that if there is a change to the area around the oxygen group of the cinchona alkaloid there is a large change in both sign and size of optical induction. The nature of the alkene part of the quinuclidine moiety was found to not be significant to optical induction as it is hydrogenated in the first parts of the reaction. Any substitution around the carbon that is attached to the OH group results in lower enantioselectivity. They found that if the N is alkylated the optical induction is lost completely. The partial hydrogenation of the quinoline moiety decreased the enantioselectivity. They confirmed that in the reaction using CD the *R*-enantiomer was produced and when CN was used the (*S*)-enantiomer was produced. In the EtPy hydrogenation reaction the CD modifier produces an excess of the (*R*)-enantiomer while the CN modifier produces the (*S*)-

ethyl lactate. It is unclear how they changed the modifiers chemically but they used IR, MS and NMR in order to make sure they were using the correct structures. They found the results by gas chromatography with a chiral column.²⁹

1.6 The 1:1 Modifier to reactant model

The generally accepted mechanism for the mode of action for the EtPy hydrogenation is that the CD modifier adsorbs onto the platinum surface via the quinoline moiety through its π -system.³⁰ The quinoline moiety is known to adsorb parallel to the surface of the platinum (Figure 1.7). This was supported by hydrogen-deuterium exchange between adsorbed-CD and deuterated solvents. All the hydrogens on the quinoline were exchanged with the deuterium which indicates that the modifier molecules are chemisorbed with the π -electron system parallel to the Pt.³¹

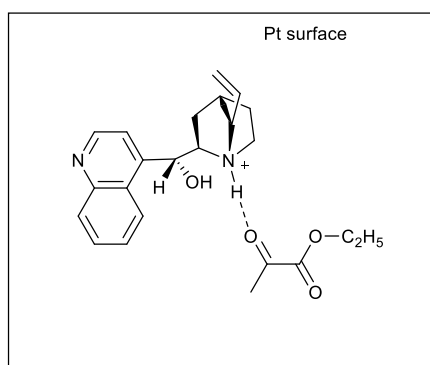


Figure 1.7: Modifier-reactant complex theorized by Baiker

It was first thought that CD worked in the reaction mechanism with two points of contact, i.e., the CD molecule adsorbs onto the Pt (111) surface via its quinoline moiety, parallel to the surface. This was shown under ultra-high vacuum conditions and investigated by near-edge X-ray absorption fine structure spectroscopy (NEXAFS).³¹ Baiker *et al.* say that in acetic acid the nitrogen on the CD is protonated which was found through NMR experiments. The

EtPy molecule adsorbs onto the platinum and, once there, it is attracted to the protonated nitrogen of the quinuclidine moiety of the modifier, where a hydrogen bond is formed between the hydrogen on the nitrogen and the oxygen (Figure 1.8). However, they propose that in non-polar solvents following theoretical observations that a protonated nitrogen on the quinuclidine moiety is not needed to form hydrogen bond with the carbonyl. The hydrogen bond could come from the half-hydrogenated state of the reactant (O-H---N). In addition, they mention that there is some hydrogen bonding between the O-H group on the CD and the carbonyl group on the substrate, but this is of minor importance. They came to this conclusion through theoretical calculations. Baiker states that the hydrogens that protonate the nitrogen and hydrogenate the substrate could either come from the solvent if it is polar or from dissociatively adsorbed hydrogen.³¹

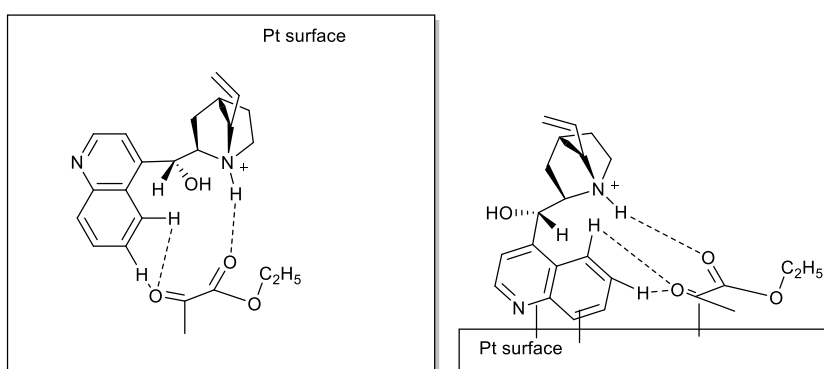


Figure 1.8: Reactant: modifier complex put forward by McBreen *et al.*³²

However, McBreen *et al.* added an additional interaction and made it into a 3-point model, where there are interactions between the C-Hs on the quinoline moiety and the carbonyl group on the substrate (Figure 1.8).³² They came to this conclusion as recent surface studies had found that aromatic C-Hs adsorbed onto Pt(111) were hydrogen bonded to carbonyl groups on substrates near them. The surface chemistry they used was reflection adsorption infrared

spectroscopy. It is mentioned that the protons on the quinoline ring are more acidic due to the redistribution of electrons in the chemisorption bond formation and the activation of the quinoline ring by bonding to the Pt surface. This allows it to form hydrogen bonds with the carbonyl on the substrate.³³ This model however is not completely likely as it would mean that the ethyl pyruvate would be in a cis conformation with carbonyls pointing the same way.

Hydrogen-deuterium exchange between adsorbed-CD and a deuterated solvent shows that all the H-atoms of the quinoline moiety are simultaneously exchanged, indicating that modifier molecules are chemisorbed with the π -electron system of the quinoline parallel with the Pt surface. They state that it is unclear how the nitrogen is protonated on the quinuclidine moiety under reaction conditions they point out. Potentially, this could be achieved through the use of a protic solvent. In aprotic solvents it has been said that it could be protonated by surface hydrogens.³⁴

Once the hydrogenation reaction occurs the hydrogen on the nitrogen stabilizes the half-hydrogenated EtPy. There is a fast transfer of the proton to the oxygen of the carbonyl on the EtPy molecule followed by the slow addition of the H atom and desorption. They mention they cannot be sure if the carbon or the oxygen is hydrogenated first. They stated that there is competitive adsorption between the hydrogen and the substrate.³⁵

1.7 Origin of the rate enhancement

Baiker *et al.* link thermodynamic and kinetic reasons for the rate enhancement. The rate acceleration was found to follow a lowering of the activation barrier of the modified reaction compared to the unmodified reaction. As a correlation between the keto-carbonyl orbital energy and the hydrogen rate was found, they show that the more stabilized diastereoisomer complex

gives a larger stabilization to the keto-carbonyl compounds and this was claimed to give rise to the rate enhancement.³¹

Garland *et al.* first used the term ligand accelerated catalysis when describing the EtPy hydrogenation and show that the reaction with CD added has a faster rate as CD is involved in the reaction mechanism.³⁶ Another reason for the rate enhancement put forward is that CD reduces the catalyst deactivation. The catalyst deactivation comes from by-products from the EtPy reaction or decomposition products from EtPy adsorbing to the surface of the catalyst and taking up the active sites. There have been different reports published on why the catalyst deactivation and ligand origin theory happens.

Jenkins *et al.* report that the reason CD gives a rate enhancement is due to its suppression of side reactions of the EtPy (pyruvate dimerization/ polymerization). These side reaction products go on to adsorb to the Pt surface and stop the substrate from adsorbing, therefore deactivating the catalyst. They came to this conclusion as scanning tunnelling microscopy has shown that the EtPy polymerise at the platinum surface. Furthermore, they found that quinuclidine (QD) increased the chiral product when added with CD. This they believe means that the QD helps inhibit the EtPy from polymerizing and freeing up more active sites on the catalyst.³⁷

In support of the work of Jenkins *et al.*, Toukoniitty *et al.* showed that the EtPy-CD interactions resulted in ligand acceleration.³⁸ In this paper they showed for the first time that a high ee can be achieved (87%) without a ligand acceleration effect. However, they also hypothesised that the EtPy could deactivate the catalyst via decomposition or side reactions of EtPy such as oligomerisation. They make mention in this paper that the exact reactions causing the catalyst deactivation is not known. The catalyst deactivated quicker at higher reactant concentrations of the unmodified reaction. They show that at low EP concentrations there was

no difference in the rate between the unmodified reaction and the modified reaction which provided evidence that the ligand acceleration is due to their catalyst deactivation theory as most of the reactions reported had used high levels of EtPy. Another reason that supports their catalyst deactivation theory is that they tried much lower catalyst amounts with a constant [CD]; at lower [EtPy] the racemic reaction was reported to be faster than the enantioselective reaction presumably due to the CD strongly adsorbing onto the sites and blocking some of the active sites. So, they report at higher [EtPy] that addition of CD reduced or prevented this deactivation as it adsorbed onto the catalyst surface sites thus preventing the EtPy molecules from deactivating it via side-reactions. Specifically, Toukoniitty *et al.* reported that CD caused the rate enhancement due to it suppressing side reactions of EtPy, although the side-reactions were not described.³⁸ Attenuated total reflectance (ATR)–infrared spectroscopy (IR) was also used to show that EtPy decomposed 60-times faster when CD was absent further suggesting that CD-suppression of degradation is a potential reason for the rate enhancement. It was mentioned that when the EtPy decomposed CO fragments were left on the Pt catalyst. The side reactions for the EtPy could be aldol-type polymerisation, similar to the findings of Bonello *et al.* for methyl pyruvate that hydrogen starvation on the surface of the Pt catalysts could lead to polymerization of methyl pyruvate. In contrast to Toukoniitty *et al.* many publications say that this is an intrinsic part of the reaction mechanism of the substrate-modifier interaction.^{39,40,41,42}

However, Meier *et al.* suggest that the rate enhancement is not due to catalyst deactivation in contrast to Toukoniitty *et al.* They found that catalyst deactivation does not occur under appropriate conditions (15 bar of H₂ pressure, 20°C and acetic acid) in the unmodified reaction.⁴³ They used acetic acid to minimise side reactions and also to avoid catalyst deactivation. Acetic acid was used because it had been previously reported that acetic acid prevents the alumina of the catalyst from catalysing EtPy degradation by adsorbing onto the alumina.⁴⁴

In addition, it was reported that amine modifiers catalyse the EtPy decomposition (by aldol- condensation) when in toluene but not in acetic acid.⁴⁵ In this paper Ferri *et al.* go one step further to say that hydrogen transport limitation in the system leads to a lower surface hydrogen concentration and then a lower enantioselectivity. Hydrogen transport limitations can be reduced by increasing the hydrogen pressure. CD, CN and quinidine (Figure 1.9) were compared and the order of superiority in terms of ee and rate enhancement was found to be CD > CN > quinidine. They attribute this to adsorption strengths as the quinoline moiety is much more effective than the methoxy quinoline moiety. They were able to calculate the adsorption strengths of the modifiers by switching the major enantiomer of the product by changing the modifier. This provided information on the adsorption strength and the geometry of the modifier.⁴³

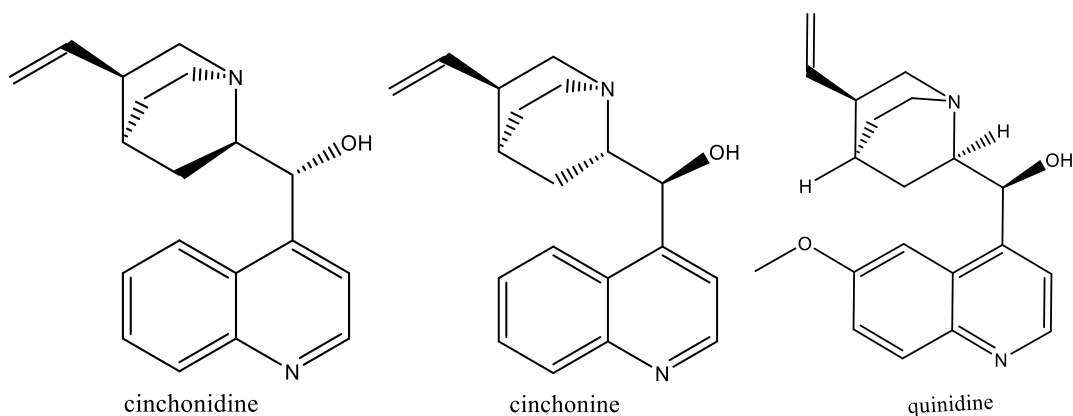


Figure 1.9: Comparison of the molecular structures of CD, CN and quinidine.

1.8 Alternative models

Another model for the rate enhancement put forward from Margitfalvi *et al.* is the shielding effect model which involves an interaction between molecules of EtPy and CD in the liquid phase.⁴⁶ They state there is π - π stacking between the ester group and the end quinoline moiety and there is an interaction with the quinuclidine nitrogen and the keto group. The

unshielded part of this complex is where the hydrogenation occurs; the shielded side is where the EtPy interacts with platinum surface (Figure 1.10). They based this model off of NMR results they previously had obtained but also molecular modelling.⁴⁶

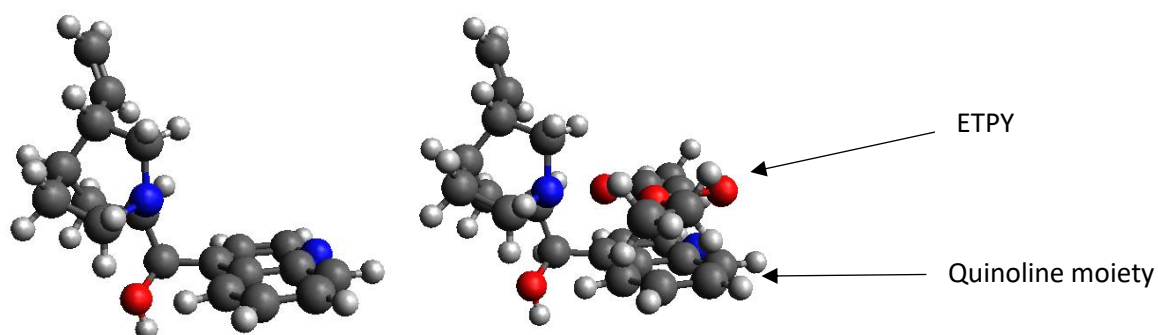


Figure 1.10: Margitfalvi *et al.* shielding model. The left image is the CD in its closed conformer. The right image is the closed conformer with EtPy. Blue (●) circle: nitrogen, grey (●) circle: carbon, white (○) circle: hydrogen and red (●) circle: oxygen.

It was reported by Baiker *et al.* that forming a closed complex CD and EtPy complex is not a prerequisite to chiral induction as using cinchonidine in its open 3 conformer gives similar enantiodifferentiation providing evidence that the conformers do not make a difference in this reaction which suggests that Margitfalvi's model is inaccurate.⁴⁷

Another model was put forward by Augustine *et al.* and studied computationally by Vayner *et al* suggests that the CD and the EtPy form a strong covalent bond (Figure 1.11) forming a zwitterionic adduct which adsorbs to the platinum and then is reduced via inversion. An ethyl pyruvate molecule is covalently bonded to the nitrogen from the quinuclidine moiety, which has a positive charge, to the carbon in the carbonyl group. They proposed this model as amines are likely to undergo nucleophilic attack with the carbonyl group. In this model G.Vayner *et al.* state that the adduct is stabilized by hydrogen bonding in acidic media. The C-

N bond is said to then go through hydrogenolysis with inversion of configuration.⁴⁸ However, this is unlikely as the highest achieved ee's and rates are in acetic acid (see state of the art section number 1.8) which would mean the quinuclidine moiety of the CD would be protonated and therefore would not be able to form a covalent bond with the EtPy.⁴⁹

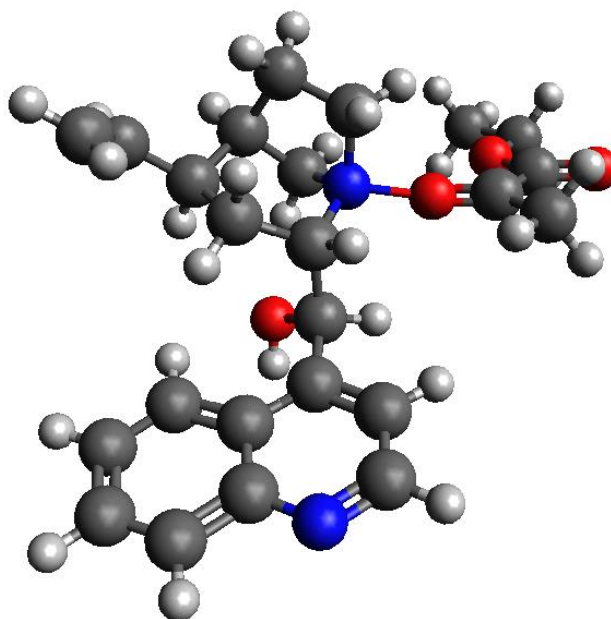


Figure 1.11: The zwitterionic adduct model proposed by Augustine *et al.* Atoms: grey: carbon; white: hydrogen; red: oxygen; blue: nitrogen.

1.9 Previous EtPy hydrogenation studies

There have been many studies completed on the EtPy hydrogenation reaction where each one has attempted to look at the reaction from a different perspective. Some of the completed studies are described in this section.

Following on from rate investigations Blackmond *et al.* showed that product distribution was altered by bulk diffusion limitations, i.e., the transport of H₂ was limited from

the gas phase to the liquid phase. They mention that bulk mass transfer limitation suppressed production of the *R*-enantiomer but do not state why.⁸

Lou *et al.* investigated a new Pt/3DC (3D carbon) catalyst (5 μmol) for EtPy (0.2 mL) hydrogenation, with CD (4 mg) as the modifier, in various solvents (1.6 mL). The Pt on this catalyst was ordered on a 3D mesoporous structure. The reaction was carried out in a stainless-steel autoclave at room temperature and with 5 MPa of H_2 . They achieved high enantioselectivities in the hydrogenation of ethyl and methyl pyruvate which could be obtained in solvents with dielectric constants between 2 and 10. The prepared catalyst Pt/3DC afforded high catalytic performance after chiral modification of CD (Table 1.1). Much better catalytic activity, with a high TOF (turnover frequency) of 11800 h^{-1} , was achieved compared with CD-modified Pt/C and Pt / Al_2O_3 catalysts. The Pt/3DC catalyst was more stable and durable than Pt / Al_2O_3 under the reaction conditions used.⁵⁰

Table 1.1 The results of EtPy hydrogenation at 5 minutes over Pt/3DC catalyst ⁵⁰				
	Catalyst	Solvent	Conv (%)	ee(%)
1	Pt/3DC	Acetic acid	100	79.5
2	Pt/3DC	Toluene	99.4	40.5
3	Pt/3DC	Ethanol	83.5	37.9
4	Pt/C	Acetic acid	41.1	48.1
5	Pt / Al_2O_3	Acetic acid	89.0	84

Guan *et al.* used carbon nanotubes (CNT) as the support. The CNTs act as a nano-reactor where they enrich the molecules inside the channels but also stabilize the chemical state of the Pt in the higher oxidation state (Pt^{+4}). This was shown by XPS. This is important as the

more electrophilic Pt species promotes the interaction between the chiral modifier/ reactant with the platinum nanoparticles. They found that highly oxidized Pt species are stabilized inside the channels of CNTs when Na⁺ is present. The Pt atoms inside the channels also had a stronger adsorption to hydrogen which also improved the enantioselectivity. The Pt nanoparticles encapsulated in the channels are denoted by (in) and the Pt nanoparticles outside of the channels are denoted by (out).⁵¹

Catalyst	Conversion (%)	ee (%)
Pt/CNT (in)	>95	95
Pt/CNT (out)	>95	75
Pt/CNT (in-H ₂)	56	60

The state-of-the-art currently for the EtPy hydrogenation reaction is 0.88 mol of modifier to mol of Pt ratio, acetic acid as solvent, 100 bar of hydrogen pressure, 3,461 Pt to substrate of EtPy to platinum 5 wt. % Pt / Al₂O₃. This method was developed by Blaser *et al.*⁴⁰ It has been reported that the best catalyst is a 5 % Pt / Al₂O₃ which has low dispersion and a large pore volume.

Following on from this work Blaser *et al.* performed three series of experiments:

1. Catalyst 5 wt. % Pt on alumina E4759 was used in ethanol, 0 - 2 mg of CD, 20 bar;
2. The second series was conducted in toluene with the same catalyst, 0 - 50 mg, 20 bar;
3. Acetic acid was used with catalyst 5R94, 0 - 50 mg MeOHCd, 100 bar.

They found increasing the modifier concentration at low concentrations increased the yield but at higher modifier concentrations the pattern changed. The yield of *R*-lactate started to decrease after 2 mmol / litre.

It was found that if more than 2 mmol / litre of modifier was added, the reaction rate and ee would decrease. This implies that too much of the modifier would take up all the active sites on the platinum therefore poisoning the reaction. They found a linear relationship between the amount of modifier and the degree of modification under 2 mmol / litre of modifier. The line deviated and no longer showed a linear relationship at greater than 2 mmol / litre. This assumed that only modified sites could induce chirality. Blaser *et al.* then went on to conclude that if the modifier became chiral when adsorbed onto the platinum the reaction could be performed enantioselectivity. However, this only worked for a certain number of reactions due to the high substrate specificity of the catalyst and it was suggested that it could only happen with α -keto-esters.⁵²

Blaser *et al.* showed that the modified reaction was approximately 20 – 30 times faster than the unmodified reaction. A significant increase of the enantiomeric excess was noticed from 1 to 40 bar. On a chiral site, the rate determining step (RDS) to the major enantiomer was proposed to be the addition of the second hydrogen, whereas the RDS for the minor enantiomer remained the first H addition. For the unmodified site they theorize that there is competitive adsorption between the hydrogen and the EtPy and the addition of the first hydrogen is the rate determining step.³⁵

When using cinchona alkaloids as modifiers, high ee and rate enhancements in hydrogenation of α -keto-esters have been seen.⁸ There is still no definitive explanation of why this occurs, and a few theories have been put forward to explain this. Early work gave different explanations to why this rate enhancement occurred: ethyl pyruvate (EtPy) is activated by

quinuclidine, there is more H coverage on the modified catalyst than on the unmodified catalysts and the quinoline moiety adsorbing on the platinum gives it an electronic interaction. This was found by using a H₂/D₂ exchange experiment to vary the surface coverage of the hydrogen. All three of these effects give an enhanced rate of the reaction. Bond *et al.* ordered the significance of these effects as the first being the most significant and the last being the least.⁵³

Jenkins *et al.* describe the rate enhancement in their work as a reaction occurring at a normal rate at an enhanced number of sites rather than due to an enhanced rate at a normal number of sites. They did this by blocking step or terrace sites with inert adatoms and observing the chiral performance of the remaining surface. They found that when adding bismuth, the step sites were blocked and therefore the ee decreased implying that the step sites are the most important for enantioselective hydrogenation. They also found that the most important sites for increasing the rate of reaction were the terrace sites. The steps (Pt(111)×(111) and Pt(100)×(111)) and terraces (Pt(100) and Pt(111)) of a 5 % Pt / graphite were used and these terraces and steps were identified using cyclic voltammetry.³⁷

Furthermore, Jenkins *et al.* described two types of adduct formed, a semi-ketal formed by the reaction of the product and the substrate, and a dimer of the substrate formed in a dimerization reaction. For this explanation, the enol and the keto forms of the substrate were formed.³⁷

Minder *et al.* investigated the EtPy hydrogenation in supercritical fluid (ethane and CO₂) and gave a different insight into the reaction. In supercritical ethane the reaction time was reduced by 3.5 compared to the reaction in toluene without any loss of enantioselectivity. An advantage of using supercritical fluids is that the enantioselectivity remains high even at high

catalyst/reactant ratio. They also observed a catalyst deactivation in supercritical carbon dioxide. The CO₂ was reduced on the platinum, as indicated by FT-IR spectroscopy.⁵⁴

Xin You *et al.* used a high-pressure reaction system and fixed-bed reactor and compared this reactor to the usual batch reactor. The batch reactor resulted in an ee of 90 % and the fixed-bed reactor resulted in an ee of 60 %. They believed this was due to the adsorbed CD being removed from the surface of the platinum over time under *continuous* conditions. They found that a side reaction of the polymerization of EtPy decreased under high pressure. They also found that the presence of a solvent could alleviate the competitive adsorption of hydrogen and substrate. Like Minder *et al.* they found that CO₂ and C₂H₆ improved the reaction greatly giving it higher activity at first but over time the CO₂ caused deactivation of the catalyst by the adsorbed CO and carbonate species and the C₂H₆ removed the CD from the surface over time.^{54,55}

Margitfalvi *et al.* describes reaction as two parallel reactions; racemic hydrogenation resulting in *R*- and *S*- product in equal amount and enantioselective hydrogenation to produce only one of the two enantiomers. Their findings suggested that CD accelerated the reaction to synthesise the *R*-enantiomer but importantly it decelerated the *S*- enantiomer; this was a new observation. However, they did not report the exact nature of the rate acceleration and the rate deceleration. Margitfalvi *et al.* suggested the acceleration was not due to the suppression of the poisoning effect of CO or oligomers of EtPy. It is interesting to note that they also tried achiral tertiary amines with CD and they found a strong acceleration effect which they attribute to the ATAs preventing cinchonidine forming a dimer and also to stop the quinoline on the cinchonidine ring being hydrogenated.⁵⁶

Toukoniitty *et al.* investigated the use of dissolved oxygen. In their investigation they added trace amounts of oxygen which increased the overall rate and the ee. In batch reactors it

is suggested that the rate deceleration is due to the presence of side reactions resulting in catalyst deactivation. The side reactions are polymerization and EtPy decomposition. They say the rate enhancement could be attributed to reduction in catalyst deactivation effects and not associated with intrinsic kinetics of the reaction. They attribute the rate acceleration because of the oxidative removal of the CO surface impurities by oxidizing the molecule to CO₂. The CO comes from the decomposition of the EtPy. The EtPy decomposition has been shown to take place at the surface using IR analysis.⁵⁷

Ma *et al.* looked at different dissolved gases and their effect on the adsorption of CD via an IR study. Ar, N₂, O₂, air or CO₂ do not enhance the adsorption of CD. The only gas they investigated that increased the adsorption of CD was hydrogen as they reported that the H₂ removed CO which freed up sites for the CD to adsorb. They found O₂ also removes CO from the surface but does not increase the adsorption of CD. They mention CO is a strong inhibitor of the EtPy hydrogenation because it stops CD adsorbing onto the platinum surface.⁵⁸

As the modifier mediated EtPy mechanism of rate enhancement has not been fully understood there is room for more investigation to see if this mechanism can be better understood. In this project the mechanism of rate enhancement using a modified Pt catalyst was explored for EtPy with different modifiers, both experimentally and computationally to gain insight into the reaction mechanism.

1.10 Conformers of CD

Eleven different conformations of CD and CN have been identified: 1 closed, 2 closed, 3 open, 4 open, 5 open, 6 open, 7 close, 8 open, 9 open, 10 open, 11 open (Figure 1.12).⁵⁹ The conformers are said to be open if the nitrogen on the quinuclidine moiety is pointing away from the quinoline ring whereas the closed conformers are pointing towards the quinoline moiety.

These conformations were found using NOESY-DFT analysis. They investigated different temperature-induced changes of the conformational populations using this type of analysis. In this work they also state that the most stable conformer is open (3).⁵⁹

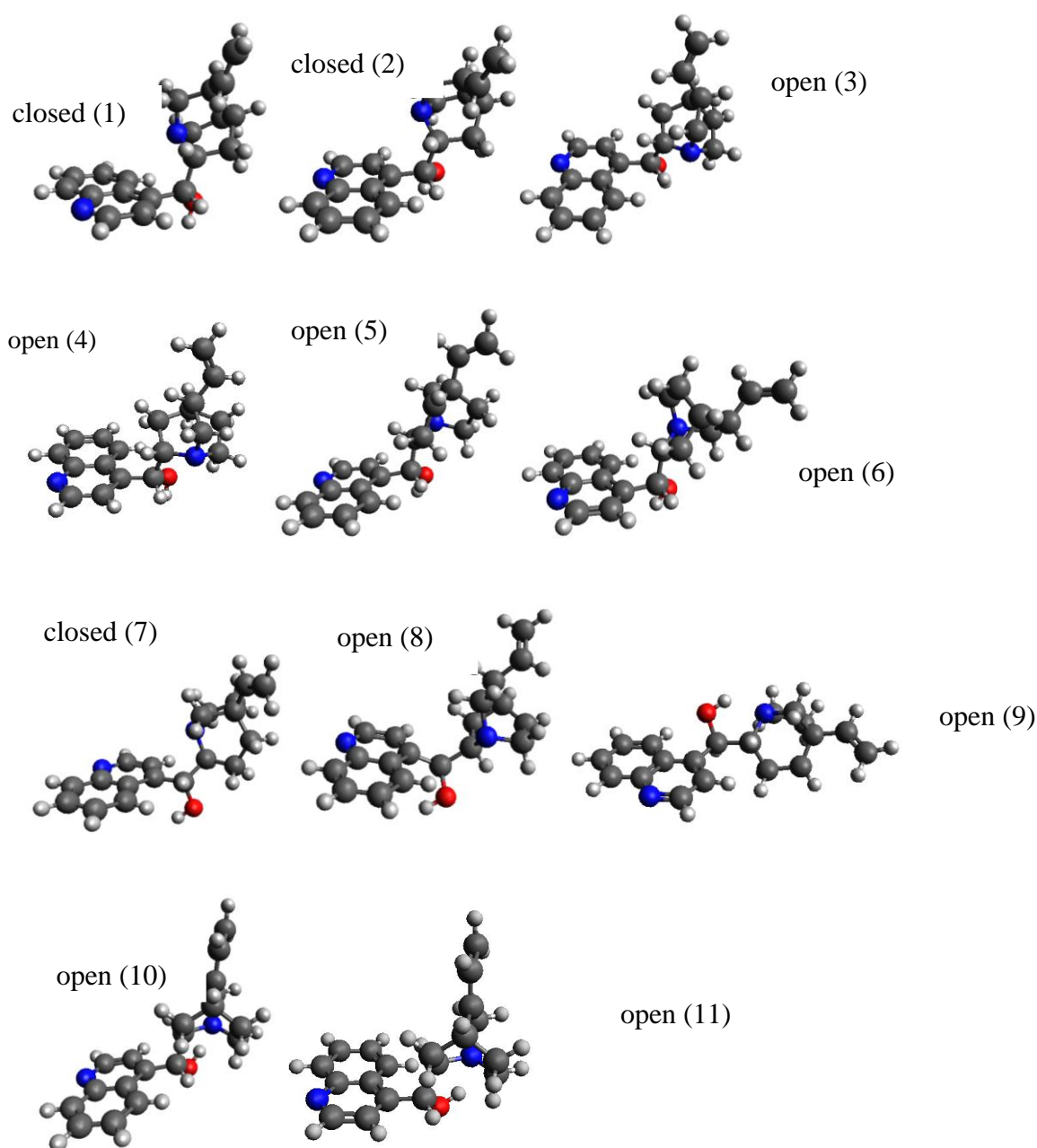


Figure 1.12: Eleven different conformers of cinchonidine. Their conformers were made in this project computationally and were adapted from A. Baiker *et al*'s work.⁶⁰ Top left to bottom right: closed (1), closed (2), open (3), open (4), open (5), open (6), closed (7), open (8), open (9), open (10), open (11)

Ab initio calculations show that the conformation that is mostly used by the CD in apolar solvents is the open 3 conformer. However, using polar solvents the closed 1 and closed 2 conformers are greatly stabilized with regards to open 3. At room temperature it was found that just over 50 % of the conformers were closed.⁶⁰

1.11 Ethyl pyruvate hydrogenation using Pt Colloids

EtPy hydrogenation using colloids rather than the conventional supported catalysts have been reported.^{61,62,63,64} There has been significant progress where reports suggest that colloids gave a very similar reaction rate and ee compared to that of the conventionally supported catalysts.

Jochem *et al.* investigated EtPy hydrogenation over colloidal catalysts on platinum sols. When they added HCl and then removed HCl via dialysis they obtained very high rates of EtPy hydrogenation, higher than the reactions without HCl. In this paper, they show that when the acidity of the colloidal system is reduced the rate and ee increases. Using colloids is advantageous as they have the benefit of not showing the effects often seen with supported catalysts.⁶¹ This can be helpful as usually for supported catalysts there is a competition for modifier molecules between the metal sites and the support surface. The colloids were made so that the nanoparticles were highly dispersed in the stabilizing agent, polyvinylpyrrolidone. This was also measured by a hydrogen uptake monitor.⁶¹

Collier *et al.* completed reactions on the EtPy hydrogenation using Pt colloids with CD and they found an increase in rate of 50-85. These rates were measured from the hydrogen uptake monitor.⁶² In this study Pt (2.3 nm-2.8 nm) and Pd (2.7 nm -3.8 nm) solvent-stabilised nanoparticles were investigated for EtPy hydrogenation. These reactions were compared to the conventional supported catalysts (5 wt.% Pt on alumina). They exhibited parallel rates and

enantioselective excess was also observed in the ethyl lactate reaction. It was found that the Pd nanoparticles resulted in a reversal of the sense of the enantioselectivity in the ethyl lactate. For the Pt nanoparticles the rate and enantiomeric excess were the same as the conventionally supported platinum catalyst.⁶²

Kohler *et al.* undertook hydrogenation of EtPy using Pt colloids stabilized in ethanol with poly(vinylpyrrolidone). It was found that the stabilizer adsorbs onto the particle surface which provides a steric barrier to interparticle collision, although the surface areas of the catalytic particles might be reduced. They compared a traditional Pt / Alumina catalyst with a colloidal catalyst and found that for the colloidal system the enantiomeric excess and the reaction rate were lower than the traditional system. They measured these rates by using a hydrogen pressure monitor.⁶³

In another study Pt (2.3 nm - 2.8 nm) and Pd (2.7 nm - 3.8 nm) solvent-stabilised nanoparticles were investigated for EtPy hydrogenation. These reactions were compared to the conventional supported catalysts (5 wt. % Pt on alumina). They exhibited parallel rates and enantioselective excess was also observed in the ethyl lactate reaction. It was found that the Pd nanoparticles resulted in a reversal of the sense of the enantioselectivity in the ethyl lactate. For the Pt nanoparticles the rate and enantiomeric excess were the same as the conventionally supported platinum catalyst.⁶⁴

1.12 Other modifiers used in the EtPy reaction

Other modifiers have been investigated to better understand why the CD-EtPy system gives a rate enhancement and to see if any modifiers can enhance this rate further. Minder *et al.* used (*R*)-2-(1-pyrrodidnyl)-1-(1-naphthyl)ethanol (Figure 1.13) in acetic acid using the reaction conditions 1-10 bar of H₂ pressure at 0-25 °C. At low hydrogen pressure it was found

that there was enantio-differentiation of the modifier. They suggest that there could be a rate enhancement in the acetic acid due to base catalysis of carbonyl reduction. They attribute the rate acceleration to base catalysis of the carbonyl reduction and suppression of side reactions e. g. polymerisation of EtPy and interactions between the modifier as a ligand (when adsorbed onto the catalyst surface) and the reactant.⁶⁴

Schurch *et al.*⁶⁵ noted that to have an efficient chiral modifier a basic, secondary and tertiary N atom and an adsorptive anchoring of the complex on Pt were advantageous. They synthesised 1-(9-anthracenyl)-2-(1-pyrrolidinylnyl)ethanol and (*R*)-2-(1-pyrrodidnyl)-1-(1-naphthyl)ethanol (Figure 1.13). They obtained an ee of 87 % which is 12 × higher than the naphthalene derivative of this modifier. The modifier was found to have a higher stability against self-hydrogenation compared to that of the naphthalene derivative. They substituted the 9-anthracenyl group of the previous modifier with a 9-triptycenylnyl moiety. This led to a complete loss of enantio-differentiation. This suggested to them that an extended flat aromatic ring system is needed to be an efficient modifier of α -ketoester hydrogenation.

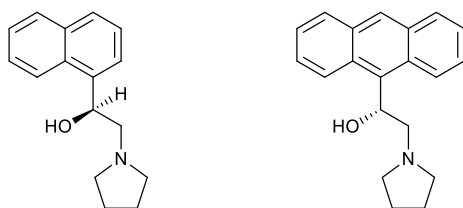


Figure 1.13: The structure of (*R*)-2-(1-pyrrodidnyl)-1-(1-naphthyl)ethanol (left), of 1-(9-anthracenyl)-2-(1-pyrrolidinylnyl)ethanol (right)

The modifier 1-(9-anthracenyl)-2-(1-pyrrolidinylnyl)ethanol gave a rate acceleration and the ee was higher than for the 1-(naphthalen-1-yl)-2-(pyrrolidin-1-yl)ethan-1-ol. When they increased the pressure from 10-100 bar the rate increased but the ee stayed the same. For the

other molecule when the pressure went higher than 10 bar the performance was poor due to partial hydrogenation. The modifier 1-(9-anthracenyl)-2-(1-pyrrolidinyl)ethanol was found to have a rate enhancement and ee similar to that of the cinchona alkaloids.⁶⁵

Blaser *et al.* found that a modifier, *O*-methyl-10,11-dihydrocinchonidine, (Figure 1.14) gave a high ee of 93 at 10 bar; this is more efficient than CD or 11-dihydrocinchonidine. However, they did not compare rates to the unmodified reaction and the CD/CN reactions.⁶⁶

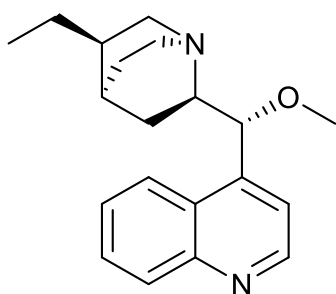


Figure 1.14: Structure of *O*-methyl-10,11-dihydrocinchonidine

O-methyl-10,11-dihydrocinchonidine was found to be the best modifier, with 93 % ee in all of the solvents, which were toluene, acetic acid (AcOH) and ethanol (EtOH).⁶⁷ They also report that a basic nitrogen moiety close to a stereogenic centre that is connected to an aromatic ring are needed to give an ee. They found that CD and quinine derivatives give higher ees than the CN and quinidine families. When a methoxy group was added to the quinoline moiety a lower enantioselectivity was observed. When acetic acid was used as a solvent the best ee values were obtained. Substituents of OH or OMe at C9 were optimal and larger substituents on the O-atom increased optical induction. Other substituents led to lower enantioselectivities.⁶⁶

New modifiers were synthesised from L-tryptophan. (*S*)-3-(1-methyl-indolyl-3-yl)-2-methylamino-propan-1-ol (Figure 1.15) was the most efficient modifier which gave an ee of 43 % using toluene at 1 bar of pressure and 273K. Raising the H₂ pressure decreased the enantioselectivity. This was explained by weaker resistance of the indolyl to hydrogenation which gave lower ees. They found that, similar to the quinoline moiety for cinchonas alkaloids, the indolyl moiety of L-tryptophan modifiers was the aromatic system that adsorbed onto the platinum surface.⁶⁷

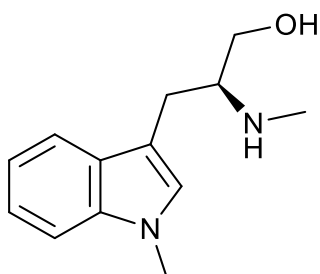


Figure 1.15: Structure (*S*)-3-(1-methyl-indolyl-3-yl)-2-methylamino-propan-1-ol

Heinz *et al.* found that amines can be used to give enantiomeric excess in this hydrogenation reaction. The amines make an imine with the EtPy and then proceed to form ethyl lactate. The rate is also enhanced but less than when they used CD and CN. They found this modifier (Figure 1.16) gave better ee's and gave a rate enhancement of 6-fold.⁶⁸

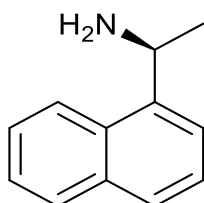


Figure 1.16: The structure of (*S*)-1-(naphthalen-1-yl)ethan-1-amine

Wang *et al.* found that CD was better at higher pressures as the naphthalene ring can be hydrogenated. The ee was always lower when the modifier was hydrogenated in their reactions. (*R*)-2-(pyrrolidin-1-yl)-1-(quinolin-4-yl)ethan-1-ol gave a better ee at higher pressures than (*R*)-1-(naphthalen-1-yl)-2-(pyrrolidin-1-yl)ethan-1-ol. At lower pressures the quinoline derivative (Figure 1.17) is inferior for ee. For the (*R*)-1-(naphthalen-1-yl)-2-(pyrrolidin-1-yl)ethan-1-ol modifier they found that the influence of the modifier concentration was significant regarding the rate of the reaction as at lower concentration there was a rate enhancement but not at higher concentration.⁶⁹

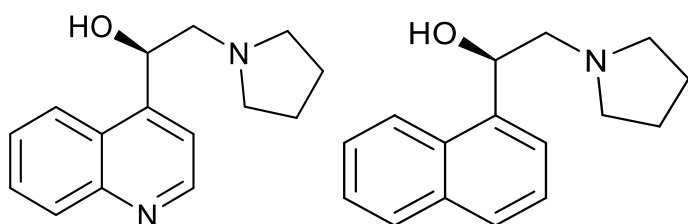


Figure 1.17: The structures of (*R*)-2-(pyrrolidin-1-yl)-1-(quinolin-4-yl)ethan-1-ol (left) and (*R*)-1-(naphthalen-1-yl)-2-(pyrrolidin-1-yl)ethan-1-ol (right).

Solladié-Cavallo *et al.* showed that the ee using both modifiers, naphthalen-1-yl(piperidin-2-yl)methanol and anthracen-9-yl(piperidin-2-yl)methanol (Figure 1.18) were lower than that of CD. They showed this by finding the ees using a chiral column. However, the reaction rates were not reported in this paper.⁷⁰

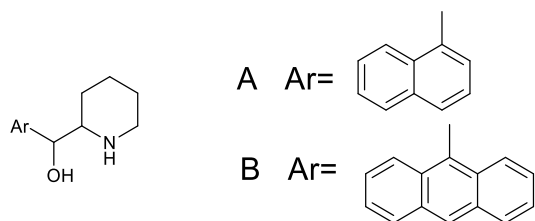


Figure 1.18: The structures of two modifiers, A- naphthalen-1-yl(piperidin-2-yl)methanol, B- anthracen-9-yl(piperidin-2-yl)methanol⁷⁰

Bartok *et al.* used the modifiers quinidine and quinine (Figure 1.19) which gave similar ee values as CD and CN. A hydrogen consumption graph plotted against time in this paper implies a rate enhancement compared to the unmodified reaction but did not give any values.⁷¹

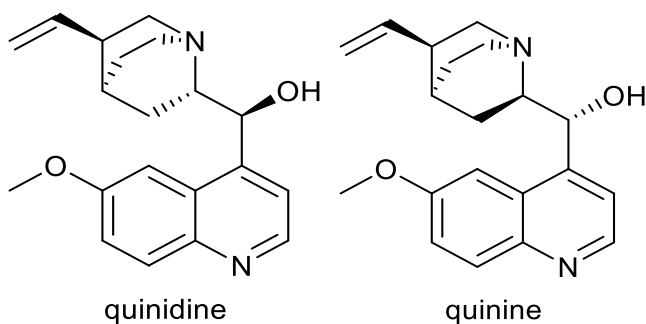


Figure 1.19: Structure of quinidine (left) and quinine (right)

Under mild conditions of millipascals (mPa) 1 H₂ pressure at 273K, 2-propanol on Pt/SiO₂, Ruggera *et al.* found that the rate of the (*S*)-(+)-1-aminoindan-modified reaction (7.35) gave a comparable rate to CD (7.97). (*S*)-(+)-1-indanol (which is *S*-(+)-aminoindan (Figure 1.20) with a hydroxy group attached adjacent to the NH₂ group) gave a racemic mixture and no ee.⁷²

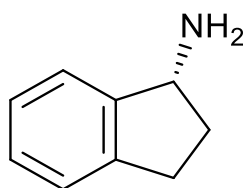


Figure 1.20: Structure of S-(+)-aminoindan

(S)-proline 2-(2-naphthyl)-ethyl ester (Figure 1.21) gave a 5 % enantiomeric excess which was much lower than the ee given by CD (98 %) It was the highest ee given by a set of proline esters tested in the hydrogenation by Sipos *et al* . They make no mention of rate values in this paper.⁷³

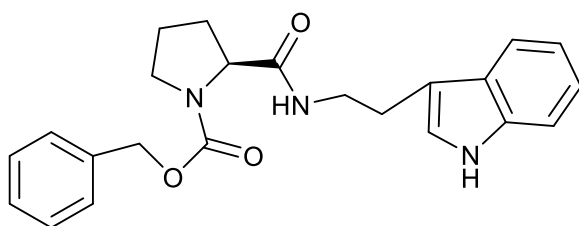
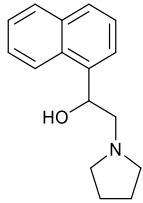
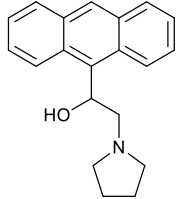
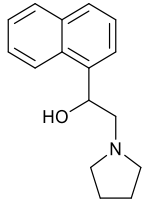
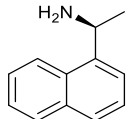
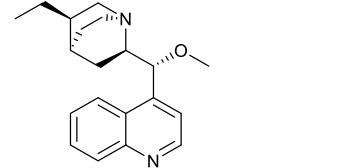
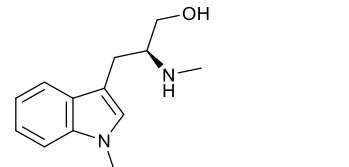
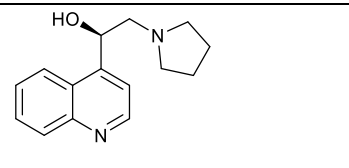
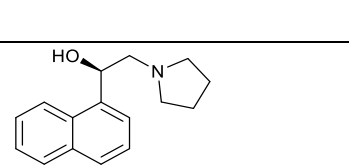
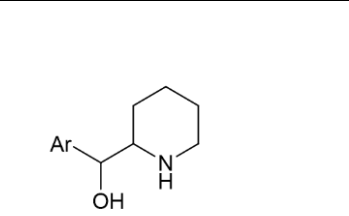
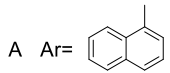
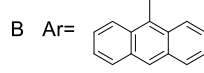


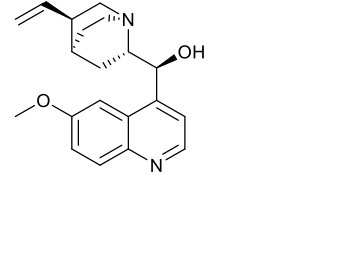
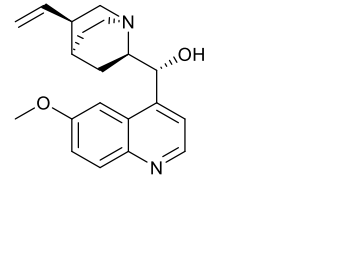
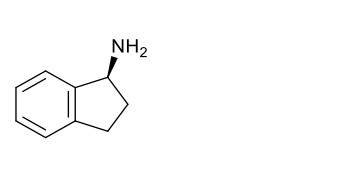
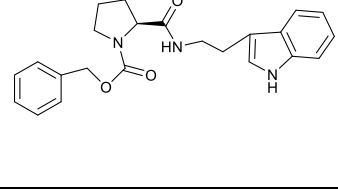
Figure 1.21: The structure of (S)-proline 2-(2-naphthyl)-ethyl ester

1.13 Summary of published results using different modifiers

A summary of the published results using different modifiers is shown in Table 1.3. In conclusion, previous studies show that in order to maximise the ee and rate enhancement the main components needed in the modifier include a moiety that can adsorb to the surface of the catalyst usually an aromatic group and a basic nitrogen which stabilizes the half-hydrogenated EtPy molecule (or another α -keto ester).

Table 1.3 A summary of published results using different modifiers						
Modifier		Solvent	Temperature / °C	H ₂ pressure / bar	Rate enhancement	ee / %
Name	Structure					
(R)-2-(1-pyrrodidnyl)-1-(1-naphthyl)ethanol		Acetic acid	0-25	1-10	7	
1-(9-anthracenyl)-2-(1-pyrrolidyinyl)ethanol		Acetic acid	10	10-100	20-21	87 %
1-(naphthalen-1-yl)-2-(pyrrolidin-1-yl)ethan-1-ol		Acetic acid	10	10-100	7-8	68 %
(S)-1-(naphthalen-1-yl)ethan-1-amine		Acetic acid	9	8	6	82 %

<i>O</i> -methyl-10,11-dihydrocinchonidine		Acetic acid	RT	100	23.75	93 %
(<i>S</i>)-3-(1-methyl-indolyl-3-yl)-2-methylamino-propan-1-ol		Toluene	0	1	4	43 %
(<i>R</i>)-2-(pyrrolidin-1-yl)-1-(quinolin-4-yl)ethan-1-ol		Acetic acid	25	1	N/A	75 %
(<i>R</i>)-1-(naphthalen-1-yl)-2-(pyrrolidin-1-yl)ethan-1-ol		Acetic acid	25	1	N/A	66 %
A= naphthalen-1-yl(piperidin-2-yl)methanol B= anthracen-9-yl(piperidin-2-yl)methanol	 A Ar=  B Ar= 	Acetic acid	RT	A= 40 B= 40	N/A	A= 72 % B= 47 %

Quinidine		Acetic acid	RT	1	N/A (rate enhancement but no values reported)	81 %
Quinine		Acetic acid	RT	1	N/A (rate enhancement but no values reported)	85 %
S-(+)-1-aminoindan		2-propanol	0	10	2.2	63 %
(S)-proline 2-(2-naphthyl)-ethyl		MeOH	25	50	N/A	23 %
Footnotes- rate enhancement is the rate of the modified reaction over the unmodified reaction						

Other molecules that do not have all three of these components have been reported to give a rate enhancement in the EtPy-CD hydrogenation; e. g. quinuclidine (QD), 1,4-diazabicyclo [2.2.2]octane (DABCO) and 3-quinuclidinol (QL) in a Pt-cinchona system.^{74,75} QD has also been reported to give a rate enhancement where there is no CD present.³⁷ These three molecules do not contain an aromatic ring to adsorb to the surface of the catalyst. However, it was found using theoretical calculations completed in this project that they are able to adsorb to the surface. Each of these compounds still contains a basic nitrogen that can stabilize the half-hydrogenated EtPy reactant. From the computational and experimental work in this project it was therefore concluded that the most important component is the basic nitrogen. However, the rate enhancement is less significant using these achiral tertiary amines. These studies show that there is the possibility of different modifiers giving rate enhancements in the ETPY hydrogenation.

1.14 Different reactants that experience rate enhancement

Ketopantolactone and MBF (Figure 1.22) hydrogenation reactions were compared^{76,77} using a Pt / Al₂O₃ catalyst and it was found that the MBF rate enhancement was more significant than the EtPy hydrogenation. The reaction rate could be enhanced for hydrogenation of ketopantolactone but this was less significant than EtPy hydrogenation. It was concluded that the rate enhancement must be an intrinsic feature of the asymmetric hydrogenation of alpha-keto esters. The hydrogenation of ketopantolactone was also investigated by Schurch *et al.* and it was found that a high ee (79 %) can be obtained using toluene and a 5 wt. % Pt on alumina catalyst if oxygen and water were removed during pre-treatment of the catalyst and the hydrogenation reaction itself.⁷⁷

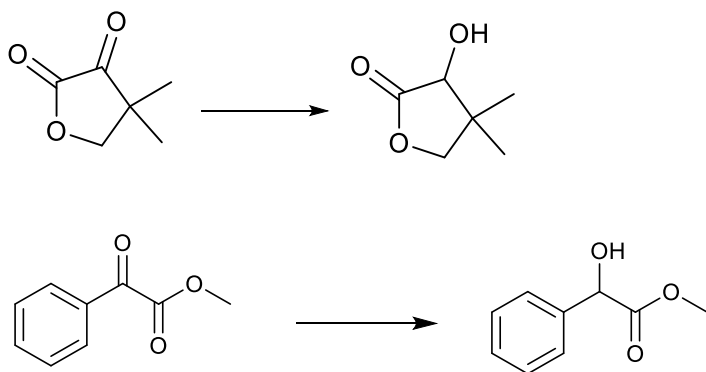


Figure 1.22: Reaction schemes showing the hydrogenation of ketopantolactone (above) and MBF (below)

Sharma *et al.* compared a multi walled nanoparticle support with graphene (G), carbon nanotube (CNT), activated carbon (AC) (Figure 1.23, Table 1.4). In this paper they were investigating the hydrogenation of methyl pyruvate.⁷⁸ The conditions used for the reaction were Pt/C (300 mg), CD (40 mg, 0.13 mmol), acetic acid (15 mL, 23.7 mmol), methyl pyruvate (0.75 mL, 8.3 mmol). The reaction was carried out in a stainless-steel vessel under varying hydrogen pressures.

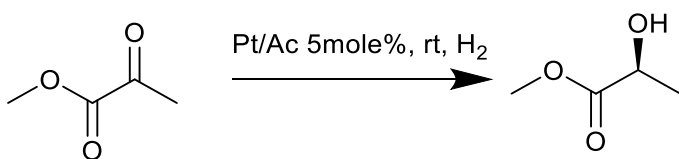


Figure 1.23: Reaction scheme showing the reduction of methyl pyruvate to methyl lactate

Table 1.4: Yield and ee ⁷⁸ obtained using nanoparticle support with graphene in the methyl pyruvate hydrogenation			
Entry	Catalyst	Yield (%)	ee (%)
1	Pt / AC	97	31
2	Pt/G	87	91
3	Pt/CNT	75	89
4	Pt/MWNT	99	99

MWNTs (multi walled nanotubes) provide high specific area, good electrical conductivity and good thermal and chemical stability. They form a highly stable system that is unreactive in many acidic and basic media, which do not promote any side reactions. The rate of reaction increased as the pressure was increased.⁷⁸

Campos *et al.* found that immobilising a chiral inducer on 1 % platinum mesoporous nanotubes produced interesting results.⁷⁹ The chiral influencers were (-)-11-trimethoxysilyl-cinchonidine moieties which were created via surface anchorage. They investigated each modifier in the hydrogenation of 1-phenylpropane-1,2-dione (Figure 1.24) finding that the more they added the more the conversion increased as well as the ee up until 15 %. Increasing beyond the optimal 15 %, the modifier worked as a poison and reduced the effectiveness of the reaction. The conversions and ee's were taken as averages as there were seven components to the reaction.⁷⁹

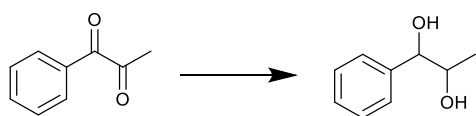


Figure 1.24: The hydrogenation of 1-phenylpropane-1,2-dione

Gzolloso *et al* used CD modified 5 % Pd / Al₂O₃ and observed a six-fold rate increase (8 – 49 %) for the hydrogenation of itaconic acid (Figure 1.25). The ee of the itaconic acid also increased from 7 % to 32 %. (E)- α -Phenyl-cinnamic acid on the other hand caused a decrease in rate with addition of the benzylamine. However, the ee increased from 0 to 46 % for the (E)- α -phenyl-cinnamic acid. This work was different from other publications discussed as the alkene bond was hydrogenated rather than a carbonyl group.⁸⁰

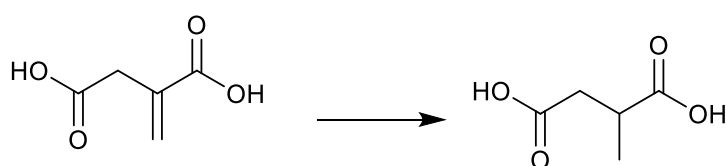


Figure 1.25: Hydrogenation of itaconic acid

EBF has also been shown to give a slight rate enhancement using CD (Martin *et al*). They used a Pt / Al₂O₃ catalyst with toluene as the solvent to afford an ee of 85 % (Figure 1.26) in a semi-batch reactor. The maximum rate enhancement was 36 % more than the unmodified reaction. When more of the modifier was added after the optimum it decreased and the rate decreased to a lower level than the unmodified reaction after more addition of modifier. They do not mention why this may be the case.⁸¹

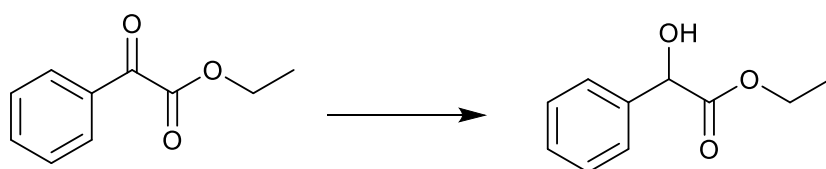


Figure 1.26: EBF hydrogenation

Ethyl trifluoropyruvate hydrogenation (Figure 1.27) was carried out using CD modifier and afforded a poor ee of 5

%; the rate is not mentioned however. In this reaction Pt / Al₂O₃ and toluene was used.⁸²

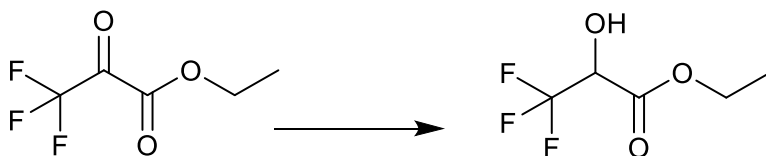


Figure 1.27: Hydrogenation of ethyl trifluoropyruvate

In conclusion, in addition to EtPy, other α -keto esters such as methyl pyruvate, MBF, ketopantolactone, itanoic acid, 1-phenylpropane-1,2-dione and EBF have all been used as substrates together with CD as a modifier; all have shown a rate enhancement in previous studies. As all of these molecules have shown rate enhancements it allows for the possibility that this Pt-cinchona system could potentially give rate enhancements on molecules that are similar in structure to EtPy but have not been reported.

1.15 Reactors

There are many types of reactors that are used for homogeneous and heterogeneous catalysis. These include continuous reactors, semi batch and batch reactors.

1.15.1 The continuous reactor

In the continuous reactor the reactants are fed through one point and the products come out at another. Example of continuous reactors are fluidised bed and fixed bed reactors, as well as slurry reactors.

1.15.1.1 Fixed bed reactors

It is the simplest type of reactor and is available in many sizes facilitating laboratory scale, pilot-plant scale, or commercial scale reactions. The catalysts in fixed bed reactors are in the form of pellets which are placed in a tube which the reactant flows through, reacting to form the product. However, there can be problems with small surface areas of the catalyst particles inside the reactor.⁸³

1.15.1.2 Fluidised bed reactor

Fluidised bed reactors are like fixed bed reactors except the catalysts are very fine and the gaseous reactant is passed over the catalyst. These fine particles are then carried with the reactant forming a fluid. This ensures effective mixing of the catalyst which minimizes the temperature gradients and offers a more enhanced mass and heat transfer. This overcomes some of the problems of the fixed bed reactor. An application of this is the oxychlorination of ethene to chloroethene (vinyl chloride).⁸⁴

Fluidised bed reactors are used in a range of applications including the pyrolysis of plastics. This application involves subjecting plastics to high temperatures of 400 to 500 °C without any oxygen. This will thermally decompose the plastic instead of burning it.⁸⁵

1.15.2 Continuous stirred tank reactor

The continuous stirred tank reactor has a stirrer and the reactants are added and the products are removed continuously. The stirring ensures that everything is mixed perfectly, and that the mixture is homogeneous. Continuous stirred tank reactors are used in different industries like chemical and environmental engineering. Examples include fermentation, biogas production and wastewater treatment.⁸⁶

1.15.3 Trickle bed reactors

Trickle bed reactors are used in the petrochemical, mineral, coal, waste and pharmaceutical industries. The trickle bed reactor allows the downward movement of the liquid reagent and the downward movement or upward (counter movement) of the gaseous reagent over a catalyst bed. They offer several advantages including that they are simplistic in operation as there are no moving parts or catalyst separation unit. They also allow high catalyst loadings and low costs. The disadvantages are that they are vulnerable to liquid maldistribution, there are intraparticle diffusion limitations and heat transfer rates are poor externally and between the particles. This is where a slurry reactor is better suited.⁸⁷

1.15.4 Semi-batch reactors

Semi-batch reactors are similar to batch reactors. However, they have a modified part which allows addition of reactants during the reaction. The product can be removed through creating a purge stream and the selectivity can be improved. Semi-batch reactors are run on an unsteady-state basis. They are usually a single-stirred tank.

Batch and semi-batch reactors are usually liquid phase at a small-scale. They cost less per unit than a stirring, continuous tank reactor. It costs more however when the production is scaled. The cost includes protective measures, non-productive times when there has to be a switch in batches and handling of the reaction like cleaning it, filling and emptying it.⁸⁸ In this project a semi-batch reactor was used.

1.15.5 Batch reactors

Batch reactors are a closed system where there is no continuous flow of reactants and products in and out of the reactor. They have many applications and are used in industry and pharmaceuticals.⁸⁹ They are simplistic as they usually only have a tank and an agitator or stirrer. The reason batch reactors are so widely used is because of their versatility. They can carry out reactions without breaking containment which is advantageous for toxic and potent compounds. They are used in the treatment of wastewater.⁹⁰

1.15.5.1 Slurry Reactors

One example of a batch reactor is the slurry reactor. In a slurry reactor the solid catalyst is suspended in a closed system for a batch version. It can also be setup to accommodate flow reactions. The slurry reactor can be considered the usual substitute for trickle-bed reactors. A slurry reactor allows good temperature control and stability as there is a high heat capacity which is very useful for exothermic reactions. Temperature conditions are uniform throughout the reactor and heat transfer and heat recovery can be achieved. The diffusion resistance between the particles is low as the particles are small. Also, as an added advantage the catalyst can be easily replaced. Slurry reactors can be used in the formation of ethylene glycol and glycolic acid.⁹¹

1.16 The components of the catalytic system

In this section the different parts of the catalytic system are discussed in terms of the optimum components for the EtPy hydrogenation.

1.16.1 Catalyst

The best catalyst available for the EtPy hydrogenation commercially is 5 % Pt / Al₂O₃ with low dispersion and a large pore volume. Webb *et al.* showed metal particles <2 nm are

less selective and also lower the turnover frequency (TOF). It was found that the enantioselectivity did not change with the acidity or the support.⁴⁰ Other supports such as SiO₂, TiO₂ and CaCO₃ can also be used but are not as optimal as alumina in terms of yield and ee. Catalysts with a lower dispersion were less selective and had a lower turnover frequency.⁹² Compared to Pt, Ir and Pd catalysts were much less selective for α -keto ester hydrogenation. There was also no rate acceleration in any of the hydrogenation reactions using these catalysts.^{93,40}

1.16.2 Solvent

There have been reports of many different solvents in the literature like toluene, EtOH and acetic acid.⁴⁰ Many solvents are suitable for the EtPy hydrogenation. Solvents with a dielectric constant between 2-10 give the highest optical selectivity.⁹⁴ Acetic acid and toluene are the most common but also tend to give the highest ee's and rates seen. The reaction rates showed no correlation with solvent polarity.

1.17 Side reactions of EtPy

Like with many reactions the EtPy hydrogenation has side reactions that can suppress the rate and the ee of the primary reaction. It has been reported that oligomers formed from EtPy can poison the catalyst. As well as EtPy dimerization (Figure 1.28), other by-products include: semi-ketal formation from the solvent and the substrate; semi-ketal formation of the CD and substrate; transesterification to create methyl pyruvate and methyl lactate from EtPy in methanol; formation of the by-products from oligomers and modifier and hydrogenated derivatives of CD.⁹⁵

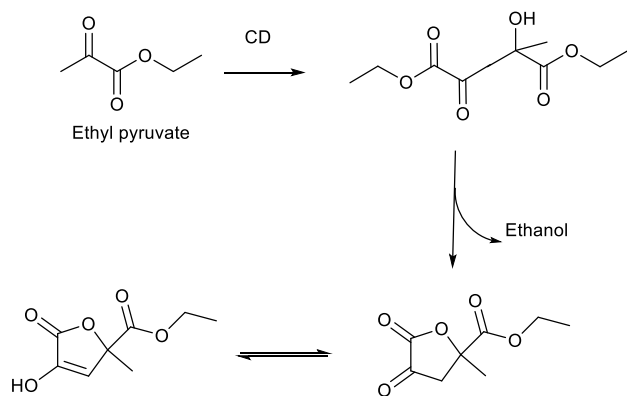


Figure 1.28: Dimerization of EtPy enhanced enantioselectivity in EtPy hydrogenation due to competing enantioselective aldol reaction catalyzed by cinchonidine

1.18 Computational Analysis

As part of this thesis, there is an investigation into conformers of different modifiers to provide insight into the mechanism of action. Recently, there has been considerable development in the field of computational design of solid catalysts. Computational methods have been used to screen for the design of new catalysts which can give increased activity and catalyse with improved selectivity. This is important because most chemicals currently are synthesised through technologies based on catalysts.⁹⁶

The essential reasons as to why finding new catalysts is a priority through screening are environmental and sustainability concerns. There is a need to find catalysts that are more selective, not expensive and that are made from materials that have an abundance on Earth. Some examples of catalysts that have been discovered are used in batteries, hydrogen storage, optical absorption, and molecules for homogeneous catalysis.

A key development of computer-based catalyst design was that the methods in calculations for surface processes have been greatly improved. Theoretical calculations on the interaction energies of molecules and atoms with metal surfaces can be achieved together with

trends in reactivity for transition metals (TMs) and alloys.⁹⁶ This can be investigated through the basis of density functional theory (DFT) calculations of reaction barriers, reaction energies and the associated entropies. Through experimentation it has been shown that real catalyst particles have well defined geometrical features. Computational studies are useful for identification of characteristics because the activation energies for elementary surface reactions are highly correlated with adsorption energies.

1.19 Previous studies on the ETPY hydrogenation using computational analysis

Theoretical calculations have been completed on the EtPy hydrogenation previously:

1. In 1997 Margitfalvi *et al.* used results found in computational studies of CD interactions with the substrates EtPy, EBF, pantolactone and trifluoroacetophenone as evidence that there are interactions in the liquid phase. In this work they discuss the ‘shielding effect model’ the accuracy of which is disputed later (see section 1.17). They used the 3-21 G basis sets for their computational calculations. In this work they also find that CD can exist in nine different conformers.⁴⁶
2. Martin *et al.* used Density functional theory calculations to study EBF adsorption on Pt(111) and were able to estimate the number of adsorption sites needed. They estimate that EBF covers 8 - 12 Pt atoms through their calculations.⁹⁷
3. Baiker *et al.* reported the use of DFT studies on CD adsorption on Pt(100) and Pt(111) surfaces. There was a much stronger adsorption of CD to the Pt(100) surface than the Pt(111) surface. Therefore, they concluded that the best catalytic surface for the hydrogenation of ketones is the Pt(111) surface. The electronic structure was modelled by means of DFT.⁹⁸

There has been work using computational studies to model other modifiers. Baiker *et al.* minimised the energies of (*R*)-2-(1-pyrrolidinyl)-1-(1-naphthyl) ethanol, (*R*)-2-(1-pyrrolidinyl)-1-(2-naphthyl)ethanol, (*R*)-2-(1-pyrrolidinyl)-1-[1-(8-methyl-naphthyl)]ethanol (Figure 1.29) and EtPy. They found the most stable conformations for those three modifiers. The theoretical calculations were made at the Hartree–Fock (HF) level with the Gaussian 98 program using the 6-31G* basis set. They identify in this work that repulsion between the EtPy molecule and the anchoring group is important to enantiodifferentiation.⁹⁹

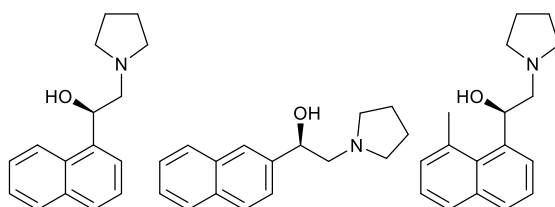


Figure 1.29: The synthetic modifiers (*R*)-2-(1-pyrrolidinyl)-1-(1-naphthyl) ethanol **1** (left), (*R*)-2-(1-pyrrolidinyl)-1-(2-naphthyl)ethanol **2** (centre), and (*R*)-2-(1-pyrrolidinyl)-1-[1-(8-methyl-naphthyl)]ethanol **3** (right)

M.Casella *et al.* were studying some new modifiers using computational calculations. These modifiers were (*S*)-(+)-1-aminoindan, (*R*)-(–)-1-aminoindan, (1*R*,2*S*)-(+)-cis-1-amino-2-indanol, (1*S*,2*R*)-(–)-cis-1-amino-2-indanol, (*S*)-(+)-1-indanol and (*R*)-(–)-1-indanol (Figure 1.30). They optimised the structures formed between these modifiers and the EtPy. They found that there is hydrogen bonding between the OH and the NH₂ parts on the (1*R*,2*S*)-(+)-cis-1-amino-2-indanol and (1*S*,2*R*)-(–)-cis-1-amino-2-indanol modifiers. They found due to their calculations that the -OH group has a smaller proton affinity than the -NH₂ group. They suggested that the ee can be predicted from computational calculations and in this

instance, they could predict the two modifiers had lower ee's due to their intramolecular interactions.⁷³

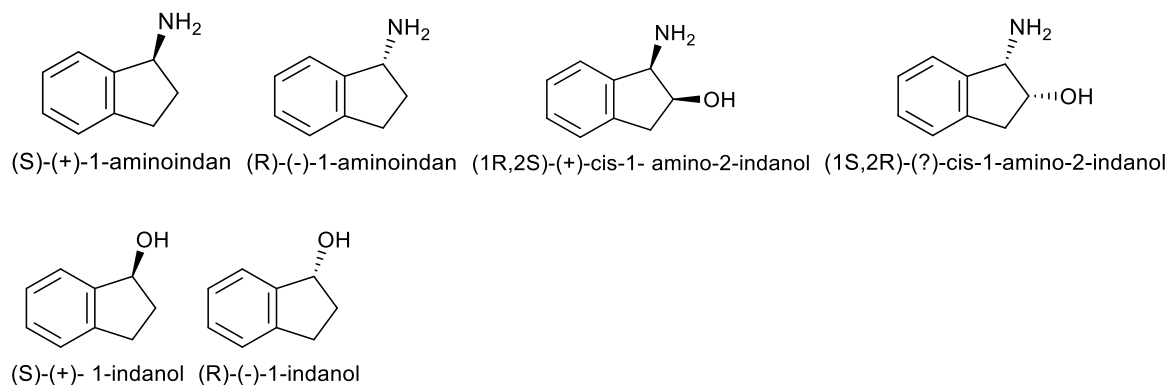


Figure 1.30: Structures of the synthetic modifiers: (S)-(+)-1-aminoindan, (R)-(-)-1-aminoindan, (1R,2S)-(+)-cis-1-amino-2-indanol, (1S,2R)-(-)-cis-1-amino-2-indanol, (S)-(+)-1-indanol and (R)-(-)-1-indanol.

1.20 Summary

The EtPy hydrogenation using cinchona alkaloids has been studied extensively. However, the reason for the rate enhancement has not been fully understood. Although several theories of how the rate enhancement occurs have been put forwards none of them are definitive. This makes room for more work to be conducted experimentally and computationally to see why the rate enhancement occurs.

There have been many different modifiers used to see which parts of the modifiers are needed and from this the main components have been found to be the basic nitrogen, aromatic moiety and hydroxy group. More reactions are needed to understand the difference in rates when modifiers have all these components and do not give a rate enhancement and why some modifiers only have one or two of these components and they give a rate enhancement. Also,

the type of catalyst has a big effect with the 5 % Pt on alumina catalyst giving the best ee and rate values.

The third chapter of this thesis will focus on the CD and CN modifiers and the rate enhancements that are obtained using these modifiers in the EtPy, MBF and EBF hydrogenations over the unmodified reaction. In the fourth chapter reactions using modifiers that are analogues of parts of cinchonidine will be investigated in detail. The rate enhancements will focus on the substrates EtPy, MBF and EBF, again over the unmodified reaction. In the fifth chapter, results for the other substrates that had similar structures to EtPy, MBF and EBF will be described with all the modifiers. In the sixth chapter the computational analysis and calculations are shown. In this chapter calculations on dimer formation, adsorption energies of EtPy and workfunctions using the different modifiers are carried out.

1.21 References

1. Lauren S. Jackson, Fadwa Al-Taher, in *Ensuring Global Food Safety*, Academic press, Momence IL, 2010
2. Ioannis S. Arvanitoyannis, in *Waste Management for the Food Industries*, 2008
3. I. Arvanitoyannis, *Waste Management for the Food Industries (Food science and technology. International series)*, Academic Press, 2008.
4. M. Doble and A. K. Kruthiventi, *Green Chemistry and Processes*, Academic Press, 2010.
5. Catalysis, https://saylordotorg.github.io/text_general-chemistry-principles-patterns-and-applications-v1.0/s18-08-catalysis.html, (accessed december 2022)
6. S. Mosleh M. Ghaedi, *Interface Science and Technology*, 2021, **32**, 761-790
7. J. T. Wehrli, A. Baiker, D. M. Monti and H. U. Blaser, *Journal of Molecular Catalysis*, 1989, **49**, 195–203.
8. U. K. Singh, M. A. Vannice, *Applied Catalysis A: General*, 2001, **213**, 1–24.
9. R. Bartsch, G. Pruss, B. Bushaw and K. Wiegers, *Journal of the American Chemical Society*, 1973, **95**, 3405-3407.
10. D. Drago and P. S. Pregosin, *Organometallics*, 2002, **21**, 1208–1215.
11. B. Li, J. Chen, Z. Zhang, I. D. Gridnev and W. Zhang, *Angewandte Chemie*, 2019, **131**, 7407–7412.
12. B. Andersh, K. N. Kilby, M. E. Turnis and D. L. Murphy, *Journal of Chemical Education*, 2008, **85**, 102.
13. H.S.Taylor, in *studies surface science and catalysis*, 1999, vol 79.
14. P. Fouilloux, *Applied Catalysis*, 1983, **8**, 145.

15. J. Wisniak, *Educación Química*, 2010, **21**, 60–69.
16. Big Chemical Encyclopedia, https://chempedia.info/info/phillips_peregrine/, (accessed December 2022)
17. S. M. McGinn, H. H. Janzen, *Canadian Journal of Soil Science*, 1998, **78**, 139–148.
18. 1902-1924 BASF, <https://www.basf.com/ca/en/who-we-are/history/1902-1924.html>, (accessed December 2022)
19. R. Sullivan, J. Scott, *Heterogenous Catalysis*, 1983, **24**, 293-313
20. P. Pędziwiatr, F. Mikołajczyk, D. Zawadzki, K. Mikołajczyk and A. Bedka, *Acta Innovations*, 2018, 45-52.
21. W. C. Bray and S. Peterson, *Journal of the American Chemical Society*, 1950, **72**, 1401–1402.
22. Difference Between Reversible and Irreversible Inhibition, <https://www.differencebetween.com/difference-between-reversible-and-irreversible-inhibition/>, accessed on June 2020
23. eMedicalPrep, <https://www.emedicalprep.com/study-material/chemistry/surface-chemistry/catalytic-promoters/>, accessed on June 2020.
24. G. C. Koltsakis, I. P. Kandylas, A. M. Stamatelos, *Chemical Engineering Communications*, 1998, **164**, 153–189.
25. [Catalytic Converters](https://www.catalyticconverters.com/faq/frequently-asked-questions-about-catalytic-converters/), <https://www.catalyticconverters.com/faq/frequently-asked-questions-about-catalytic-converters/>, (accessed 2022)
26. J. Humphreys, R. Lan and S. Tao, *Advanced Energy and Sustainability Research*, 2020, **2**, 2000043.
27. Y. Orito, S. Imai, S. Niwa, Nguyen G-H; *J. Synth. Org. Chem. Jpn.* 1979, **37**,173. b) Y. Orito, S. Imai and S. Niwa, *J. Chern. Soc. Jpn.* 1979, 18. c) Y. Orito, S. Imai and S. Niwa, *J. Chern. Soc. Jpn.* 1980, 670. d) Y. Orito, S. Imai and S. Niwa, *J. Chem. Soc. Jpn.* 1982, 137
28. H.U. Blaser, H.P. Jalett, D.M. Monti, J.F. Reber and J.T. Wehrli, *Studies and Surface Science and Catalysis*, 1988, **41**, 153-163
29. H. U. Blaser*, H. P. Jalett, D. M. Monti, A. Baiker, J. T. Wehrli+, *Studies in Surface Science and Catalysis*, 1991, **67**, 147-155
30. G. Webb, P.B. Wells, *Catal. Today*, 1992, **12**, 319.
31. T. Bürgi and A. Baiker, *Accounts of Chemical Research*, 2004, **37**, 909-917.
32. Lavoie, S.; Laliberte, M. A.; Temprano, I.; McBreen, P. H. *A generalized two-point H-bonding model for catalytic stereoselective hydrogenation of activated ketones on chirally modified platinum. J. Am. Chem. Soc.* 2006, **128**, 7588–7593.
33. S, Lavoie, P. McBreen, *Phys. Chem. B* 2005, **109**, 986-990.
34. A. Vargas, D. Ferri, A. Baiker, *J. Catal.* 2005, **236**, 1-8.
35. H. Blaser, H. Jalett, M. Garland, M. Studer, H. Thies and A. Wirth-Tijani, *Journal of Catalysis*, 1998, **173**, 282-294.
36. M. Garland, H.U. Blaser, *J. Am. Chem. Soc.*, 1990, **112**, 7048.
37. D. Jenkins, A. Alabdulrahman, G. Attard, K. Griffin, P. Johnson. P. Wells, *Journal of Catalysis*, 2005, **234**, 230-239.
38. E. Toukoniitty, D. Murzin, *Journal of Catalysis*, 2006, **241**, 96-102
39. M. Bartók, *Curr. Org. Chem.*, 2006, **10**, 1533
40. H. U. Blaser, H.P. Jalett, M. Müller, M. Studer, *Catal. Today*, 1997, **37**,441.
41. A. Baiker, H.U. Blaser, G. Ertl, H. Knözinger, J. Weitkamp *Handbook of Heterogeneous Catalysis*, Wiley–VCH, Weinheim, 1997, 2442.
42. A. Vargas, T. Bürgi, A. Baiker, *New J. Chem.*, 2002. **26**, 807
43. D. Meier, D. Ferri, T. Mallat. A. Baiker, *Journal of Catalysis*, 2007, **248**, 68-76.

44. D. Ferri, S. Diezi, I. M. Maciejewski. A. Baiker, *Applied Catalysis A: General*, 2006, **297**, 165-173.
45. D. Ferri, T. Bürgi, K. Borszeky, T. Mallat and A. Baiker, *Journal of Catalysis*, 2000, **193**, 139-144.
46. J. Margitfalvi. E. Tfirst, *Journal of Molecular Catalysis A: Chemical*, 1999, **139**, 81-95.
47. T. Bürgi. A. Baiker, *ChemInform*, 2005, **36**.
48. G. Vayner, K. Houk and Y. Sun, *Journal of the American Chemical Society*, 2003, **126**, 199-203.
49. R. Augustine, S. Tanielyan, K. Doyle, *Enantioselective heterogeneous catalysis. 1. A working model for the catalyst modifier-substrate interactions in chiral pyruvate hydrogenations. Tetrahedron: Asymmetry* 1993, **4**, 1803-1827.
50. L. Lou, T. Yang, W. Yu, H. Qu, Y. Feng, H. Li, K. Yu and S. Liu, *Catalysis Today*, 2017, **298**, 197-202.
51. Z. Guan, S. Lu and C. Li, *Chinese Journal of Catalysis*, 2015, **36**, 1535-1542.
52. H. Blaser, M. Garland, H. Jallet, *Journal of Catalysis*, 1993, **144**, 569-578.-
53. G. Bond, P. Meheux, A. Ibbotson and P. Wells, *Catalysis Today*, 1991, **10**, 371-378.
54. B. Minder, T. Mallat, K. Pickel, K. Steiner and A. Baiker, *Catalysis Letters*, 1995, **34**, 1-9.
55. Xin.You, Xiaohong Li, Song Xiang, Suizhi Zhang, Qin Xin, Xuyuan Li *Studies in Surface Science and Catalysis*, 2000, **130**, 3375-3380
56. J. Margitfalvi, E. Tálas, *Topics in Catalysis*, 2006, **39**, 77-87.
57. E. Toukoniitty and D. Murzin, *Catalysis Letters*, 2004, **93**, 171-176.
58. Z. Ma, *Journal of Catalysis*, 2003, **219**, 404-416.
59. A. Urakawa, D. Meier, H. Rügger, and A. Baiker, *The Journal of Physical Chemistry A*, 2008, **112**, 7250-7255.
60. T. Bürgi, A. Baiker, *Journal of the American Chemical Society*, 1998, **120**, 12920-12926.
61. J.U. Kohler, J.S Bradley, *Catalysis Letters*, 1997, **45**, 203-208
62. P. Collier, J. Iggo and R. Whyman, *Journal of Molecular Catalysis A: Chemical*, 1999, **146**, 149-157
63. J. Köhler and J. Bradley, *Langmuir*, 1998, **14**, 2730-2735.
64. a) H.S.Taylor, in *Studies Surface Science and Catalysis*, 1999,79; b) P. Fouilloux, *Applied Catalysis*, 1983, **8**, 145.
65. M. Schürch, T. Heinz, R. Aeschmann, T. Mallat, A. Pfaltz and A. Baiker, *Journal of Catalysis*, 1998, **173**, 187-195.
66. H. Blaser, H. Jalett, W. Lottenbach and M. Studer, *Journal of the American Chemical Society*, 2000, **122**, 12675-12682.
67. G. Szöllösi, C. Somlai, P.T. Szabó, M. Bartók, *Journal of Molecular Catalysis A: Chemical*, 2001, **170**,165-173
68. T. Heinz, G. Wang, A. Pfaltz, B. Minder, M. Schürch, T. Mallat and A. Baiker, *J. Chem. Soc., Chem. Commun.*, 1995, 1421-1422.
69. G. Wang, T. Heinz, A. Pfaltz, B. Minder, T. Mallat and A. Baiker, *ChemInform*, 2010, **26**,
70. A. Solladié-Cavallo, C. Marsol and F. Garin, *Tetrahedron Letters*, 2002, **43**, 4733-4735.
71. M. Bartók, K. Felföldi, G. Szöllösi and T. Bartók, *Reaction Kinetics and Catalysis Letters*, 1999, **68**, 371-377.
72. J. Ruggera, A. Merlo, R. Diez and M. Casella, *Journal of Molecular Catalysis A: Chemical*, 2016, **423**, 233-239.

73. É. Sípos, A. Tungler and I. Bitter, *Journal of Molecular Catalysis A: Chemical*, 2003, **198**, 167-173
74. J. Margitfalvi, E. Tálas, E. Tfirst, C. Kumar and A. Gergely, *Applied Catalysis A: General*, 2000, **191**, 177-191.
75. E. Tálas, F. Zsila, P. Szabó and J. Margitfalvi, *Journal of Molecular Catalysis A: Chemical*, 2012, **357**, 87-94.
76. E. Tálas, J. Margitfalvi and O. Egyed, *Journal of Catalysis*, 2009, **266**, 191-198.
77. M. Schürch, O. Schwalm, T. Mallat, J. Weber and A. Baiker, *Journal of Catalysis*, 1997, **169**, 275-286.
78. P. Sharma and R. Sharma, *RSC Advances*, 2015, **5**, 102481-102487.
79. A. Campos, C. Torres, P. Osorio-Vargas, C. Mella, J. Belmar, D. Ruiz, J. Fierro and P. Reyes, *Journal of Molecular Catalysis A: Chemical*, 2015, **398**, 190-202.
80. G. Szollosi, T. Hanaoka, S. Niwa, F. Mizukami and M. Bartok, *Journal of Catalysis*, 2005, **231**, 480-483.
81. G. Martin, P. Mäki-Arvela, D. Murzin and T. Salmi, *Catal. Sci. Technol.*, 2014, **4**, 170-178.
82. M. von Arx, T. Mallat and A. Baiker, *Journal of Catalysis*, 2000, **193**, 161-164.
83. S. Hafeez , E. Pallari, G. Manos and A. Constantino, *Catalytic Conversion and Chemical Recover*, 2015.
84. The essential chemistry industry online, <https://www.essentialchemicalindustry.org/processes/chemical-reactors.html>, April accessed 2020
85. J. Saad, M. Nahil and P. Williams, *Journal of Analytical and Applied Pyrolysis*, 2015, **113**, 35-40.
86. Linqip, [Continuous Stirred-Tank Reactor: Comprehensive Overview \(linquip.com\)](https://www.linqip.com/continuous-stirred-tank-reactor-comprehensive-overview), (accessed December 2022)
87. V. Ranade, R. Chaudhari and P. Gunjal, *Trickle bed reactors*, Elsevier, Oxford, 2011.
88. Visual encyclopedia of chemical engineering equipment, <https://encyclopedia.che.engin.umich.edu/semi-batch/>, (accessed december 2022)
89. Shijie Liu, in *Bioprocess Engineering (Second Edition)*, 2017
90. T. Kuba, G. Smolders, M. C. van Loosdrecht and J. J. Heijnen, *Water Science and Technology*, 1993, **27**, 241–252.
91. J. H. Santos, J. T. Gomes, M. Benachour, E. B. Medeiros, C. A. Abreu and N. M. Lima-Filho, *Reaction Kinetics, Mechanisms and Catalysis*, 2020, **131**, 139–151.
92. H.U. Blaser, M. Mtiller, *Stud. Surf. Sci. Catal.* 1991, **59**, 73
93. K.E. Simons, A. Ibbotson, P. Johnston, H. Plum, P.B. Wells, *J. Catal.*, 1994, **150**, 321.
94. H. Blaser, H. Jalett and J. Wiehl, *Journal of Molecular Catalysis*, 1991, **68**, 215-222.
95. J. Margitfalvi, M. Hegedüs, *Tetrahedron: Asymmetry*, 1996, **7**, 571-580.
96. J. K. Nørskov, T. Bligaard, J. Rossmel and C. H. Christensen, *Nature Chemistry*, 2009, **1**, 37–46.
97. G. Martin, P. Mäki-Arvela, J. Wärnä, K. Honkala, D. Y. Murzin and T. Salmi, *Industrial & Engineering Chemistry Research*, 2014, **53**, 11945–11953.
98. E. Schmidt, A. Vargas, T. Mallat and A. Baiker, *Journal of the American Chemical Society*, 2009, **131**, 12358-12367.
99. A. Vargas, T. Bürgi and A. Baiker, *Journal of Catalysis*, 2001, **197**, 378-384

Chapter 2

Experimental

2.1 Introduction

The focus of this project was to gain a better understanding of why the rate enhancement observed with the hydrogenation of ethyl pyruvate (EtPy) (Figure 2.1) over a modified-Pt system is so pronounced. To facilitate the investigation into the hydrogenation of EtPy and other related substrates, reactions were carried out using several different modifiers. Chapter 3 describes experiments using different amounts of modifiers where the mol additive per mol of Pt were compared with each other. Two other substrates were found to have significant rate enhancements using the same modifiers in toluene and 0.001 M of acetic acid; these were ethyl benzoylformate and methyl benzoylformate (EBF and MBF). Reports of the hydrogenation of MBF and EBF have been scarcely reported and these novel results are described in Chapter 4. In addition to EtPy, a library of other substrates that have a similar structure to EtPy were tested to see if rate enhancements could be observed. These included beta and gamma diketo esters. The results of experiments using these other substrates are described in Chapter 5. Theoretical studies were also completed to try and obtain a greater understanding of the rate enhancement, and these are reported in Chapter 6.

A hydrogen uptake monitor was used to monitor the amount of hydrogen pressure (bar) used up in the reaction once it was completed. Gas chromatography (GC) was used to measure the conversion of reactant to product for the reactions. The reaction mixtures for the EtPy hydrogenation using cinchonidine (CD), (*R*)-quinuclidinol ((*R*)-QL) and 3-quinuclidinol (QL) were analysed using a GC with a chiral column to check the enantiomeric excesses. The catalyst was characterized using powder X-ray diffraction (XRD), transmission electron microscopy

(TEM), carbon monoxide chemisorption (CO) and Brunauer-Emmett-Teller surface area analysis (BET). The 5 % wt. on Pt / Al₂O₃ was reduced prior to use by heating to 400 °C with H₂ for four hours. Reactions were evaluated in a glass liner within a 50 mL stainless steel autoclave.

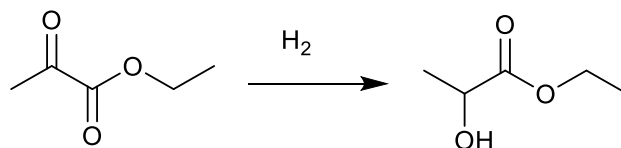


Figure 2.1: Reaction scheme of the EtPy hydrogenation

2.2 Materials

Typically, a commercially sourced 5 % wt. Pt / Al₂O₃ catalyst (Sigma Aldrich) was used in the hydrogenation of these substrates. This catalyst was used for every reaction except for a few reactions I used with a 5 % wt. Pt / Al₂O₃ catalyst. The modifiers used in these reactions were aminoquinoline (AQ (1)), quinuclidine (QD (2)), 3-quinuclidinol (QL (3)), (R)-quinuclidinol ((R)-QL (4)), cinchonidine (CD (5)), cinchonine (CN (6)) and DABCO (7) (Figure 2.2).

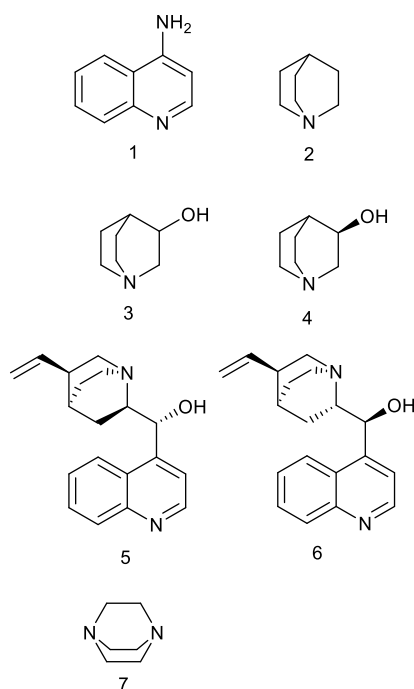


Figure 2.2: Chemical structure of the modifiers used in this study. Key: AQ (1); QD (2); QL (3); (R)-QL (4); CD (5); CN (6) and DABCO (7)

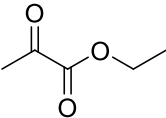
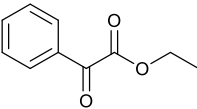
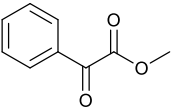
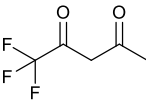
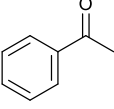
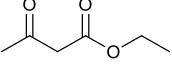
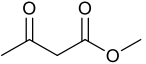
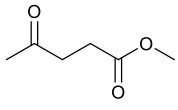
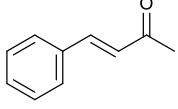
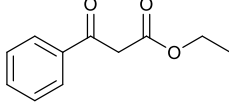
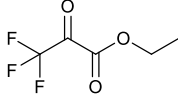
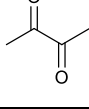
The materials used as received were:

- (98 %) EtPy (Sigma Aldrich +Alfa Aesar)
- (95 %) EBF (Sigma Aldrich)
- (98 %) MBF (Sigma Aldrich)
- (98 %) 1,1,1-trifluoro-2,4-pentadione (Sigma Aldrich)
- (99 %) Acetophenone (Sigma Aldrich)
- (99 %) ethyl acetoacetate (Sigma Aldrich)
- (99 %) methyl acetoacetate (Alfa Aesar)
- (98 %) methyl levulinate (Sigma Aldrich)
- (98 %) Benzalacetone (Sigma Aldrich)
- (95 %) ethyl benzoylacetate (Sigma Aldrich)
- (96 %) CD (Sigma Aldrich)
- (98 %) CN (Sigma Aldrich)
- 4-AQ (Sigma Aldrich)
- (97 %) QD (Sigma Aldrich)
- (98 %) QL (Alfa Aesar)

- (99 %) (R)-QL (Sigma Aldrich)
- (99 %) 1,4-diazabicyclo[2.2.2]octane (DABCO) (Sigma Aldrich)
- (99 %) R-Ethyl lactate (Sigma Aldrich)
- S-Ethyl lactate (Sigma Aldrich)
- Toluene (Sigma Aldrich)
- Acetic acid (Sigma Aldrich)
- γ -alumina (Sigma Aldrich)
- 5 % Pt on alumina (Sigma Aldrich)
- 5 % Pt on alumina (Johnson Matthey)

2.3 General synthesis and preparation of the catalyst

The substrate (see Table 2.1 for the different substrates used), Pt / Al₂O₃ catalyst (0.25 g, 1.25 mmol) and toluene +acetic acid (0.001 M) (5 mL) solvents were added to a glass liner. The modifiers of this reaction (see Table 2.1 for the different amounts added) were added also. The glass liner was put into a 50 mL stainless steel autoclave and the system was purged three times with 10 bar of hydrogen. The system was put under 20 bar of H₂ and the stirrer was started at 1000 rpm. This stirring speed was chosen as it was the same stirring speed used in the literature.¹ A hydrogen uptake monitor was used to observe how much hydrogen was taken up by the reaction. The reaction was carried out at room temperature and the reactions were left for one and a half hours or until the reaction went to completion. The reactions were completed in batches for each substrate and modifier. For each substrate and modifier the reactions would be completed within a week which limits the variability of room temperature. Although, there was variability in room temperature as the room would heat up and cool down throughout the day. Once the reaction was completed the reaction mixture was filtered using filter paper to remove the catalyst so that the reaction mixture could be analysed by GC to check the ee and to make sure there was no starting material or by-products in the reaction mixture.

Table 2.1- The substrates used and the amounts of each used in the reaction		
Chemical	structure	Amount added (mmol)
EtPy		45
EBF		43
MBF		41
1,1,1-trifluoro-2,4-pentadione		45
Acetophenone		41
Ethyl acetoacetate		45
Methyl acetoacetate		45
Methyl levulinate		45
Benzalacetone		45
Ethyl benzoylacetate		41
Ethyl trifluoropyruvate		45
2,3-butandione		45

In Table 2.1 the amount of each of the substrates used in the reaction are shown. The amounts were lowered sometimes so an accurate hydrogen uptake graph could be made. This was because if there was too much substrate more hydrogen would be taken up in the reaction than could be detected by the software that was being used. The software used was called RaspberryPii. The modifiers, and their quantities used, are shown in Table 2.2.

Table 2.2 - Modifiers that were investigated in the reactions	
Chemical	Amount added (mmol)
4-AQ	0.7, 1.4, 1.05, 0.35, 0.07
CD	4.25×10^{-8} - 8.5×10^{-5}
CN	0.0085 μ mol
Quinuclidine	0.9, 0.45, 0.23, 0.67, 1.37, 2.2, 0.09
QL	0.024, 0.039, 0.063, 0.078, 0.16, 0.24
R-QL	0.078
DABCO	101, 202, 303, 150, 50, 10

2.4 Equipment

2.4.1 Batch reactors

In this project a batch reactor was used for the hydrogenation reactions. The advantages of a batch reactor include that it is very reliable and robust, it is easy and simple to use and it is versatile so you can use it for several types of reactions. The disadvantages include that it can only create a limited quantity of the product and the purity can decline if you use it for different reactions as it can be difficult to clean completely. Typical reactions that use the batch

reactor include food processing, beverage processing, pharmaceutical formulations and biotechnology products manufacturing.²

2.4.2 Autoclave Reactor

In Figure 2.3 a schematic representation of the autoclave reactor that was used in the reaction is shown. When the glass liner containing the reaction mixture was placed into the autoclave the valve on the left was opened to allow around 10 bar of hydrogen into the autoclave to purge the system. The valve on the left was closed and the valve on the right was opened to release the pressure and vent the hydrogen out of the system. This was repeated twice more and then 20 bar of hydrogen was flushed into the system. The glass liner was placed in the autoclave where there was an overhead impeller driven by a magnetic drive system. The autoclave used in the reaction was from the Parr instrument company with the model number 4597 and had a maximum restricted operating pressure at 70 bar and 350 °C.

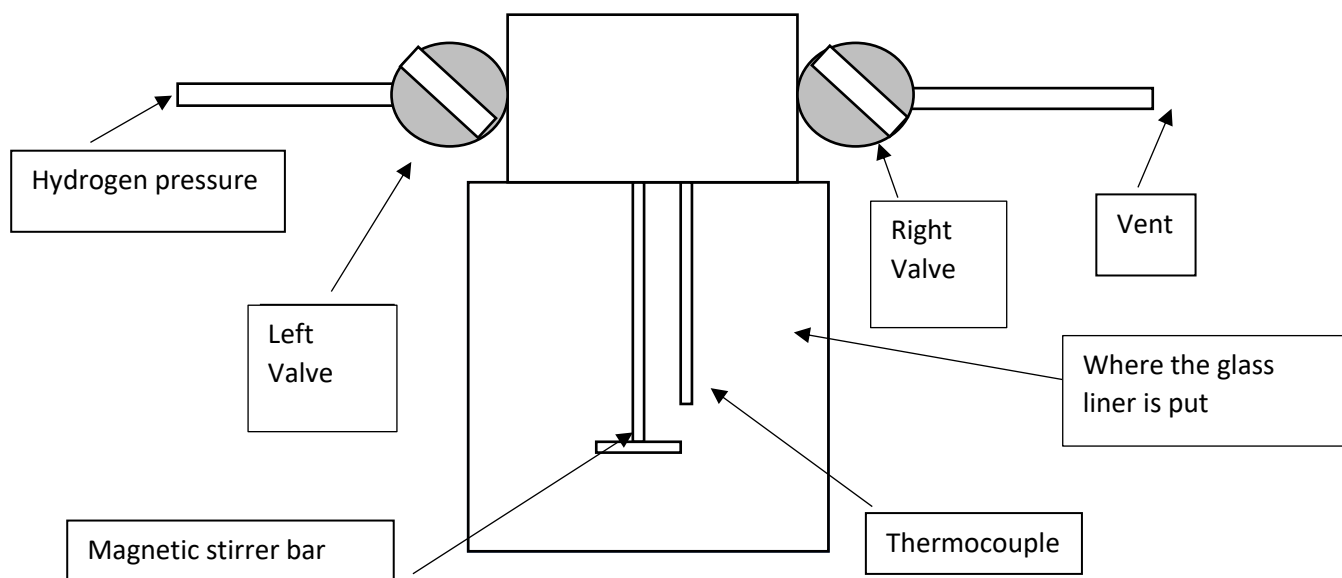


Figure 2.3: Schematic of a Parr instrument stainless autoclave. A glass liner was put in the autoclave and the volume of reaction mixture goes above the stirrer bar and thermocouple.

2.4.3 Hydrogen uptake monitor

The reactions were monitored by a hydrogen uptake monitor (Figure 2.4). Hydrogen uptake monitors measure the amount of hydrogen pressure (bar) that is used up in the hydrogenation reaction.

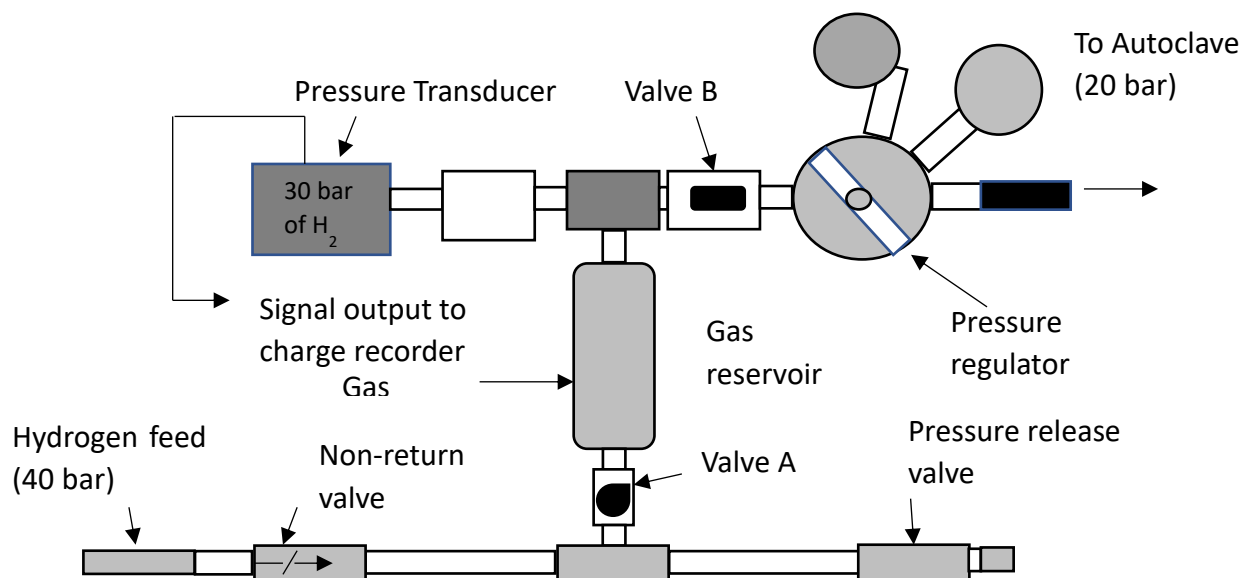


Figure 2.4: Hydrogen uptake monitor

A schematic diagram of the hydrogen uptake monitor used to assess the performance of each modifier and substrate in Chapters 3-5 is shown Figure 2.4. For each reaction the hydrogen was fed through valve A to the gas reservoir which would hold approximately 30 bar of hydrogen. The hydrogen gas from the reservoir flowed from the gas reservoir through valve B and to the pressure regulator. From here 20 bar of hydrogen was allowed to flow to the autoclave (Figure 2.4). Before the reaction started valve A was shut so no more hydrogen could flow into the gas reservoir. Once the reaction had started the gas reservoir was monitored by the pressure transducer and the drop in hydrogen pressure was detected by the Pi computer programme software (Figure 2.5).

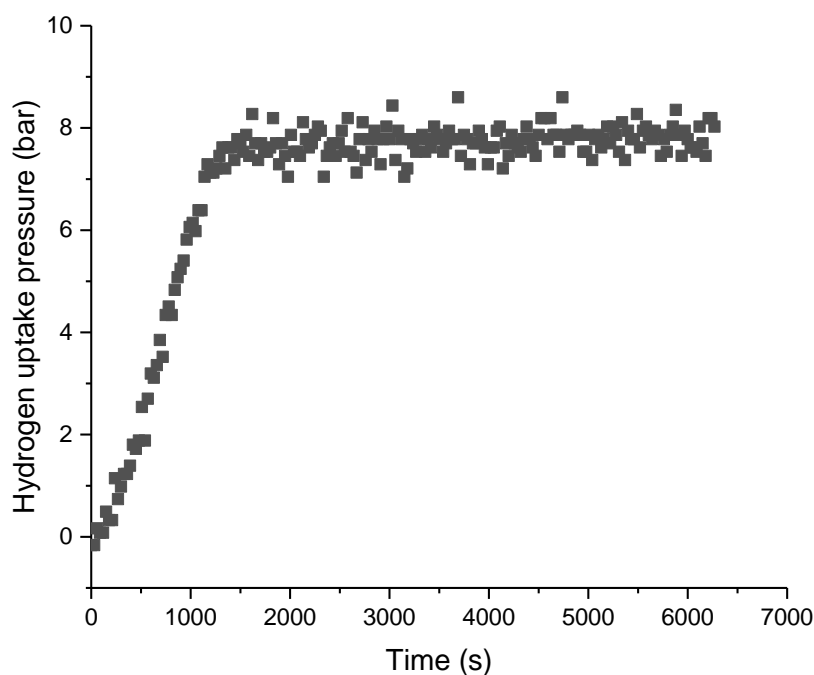


Figure 2.5: Hydrogen uptake of the EtPy hydrogenation using CD; Reaction conditions: H₂ (20 bar); RT; 5 wt.% Pt / Al₂O₃ (1.25 mmol, 250 mg); EtPy (45 mmol, 5.2 mL); Toluene + 0.001 M acetic acid); CD (8.5 μmol, 2.5 mg). This graph excludes outliers.

In Figure 2.5 the hydrogen uptake graph is shown. The software that analyses the reaction shows the change in hydrogen pressure in the reactor and as more hydrogen is used up in the reaction the higher the change in hydrogen pressure. The software takes records the pressure every 30 seconds. Hydrogen uptake pressure is on the y-axis and time (s) is on the x-axis.

2.5 How the rate is calculated

2.5.1 Noise rejection

The data was affected by electrical noise on the pressure monitoring system which was a major issue for some of the reactions. When electrical interference occurred, this caused the data points to appear as outliers which detracted from the trends in the pressure measurements to which kinetic models was fitted (Figure 2.6). These outliers needed to be excluded from further analysis and to do this a Savitzky-Golay filter^{3,4} was implemented in the SciPy Python library⁴ to obtain a trend line by fitting a moving polynomial. Outlying datapoints were detected in the smoothed data and then automatically excluded. 200 data points were collected over the course of an experiment and the window for the running polynomial was chosen as 101 points. This would allow a 4th order polynomial to be fitted. This choice of fitting parameters was found to produce a trend line which followed the main trend of the data and so provided a good reference from which to reject outlier points. A tolerance of 0.5 units was chosen on the scale shown in Figure 2.6, rejecting points that were further from the Savitzky-Golay trendline than this reference.

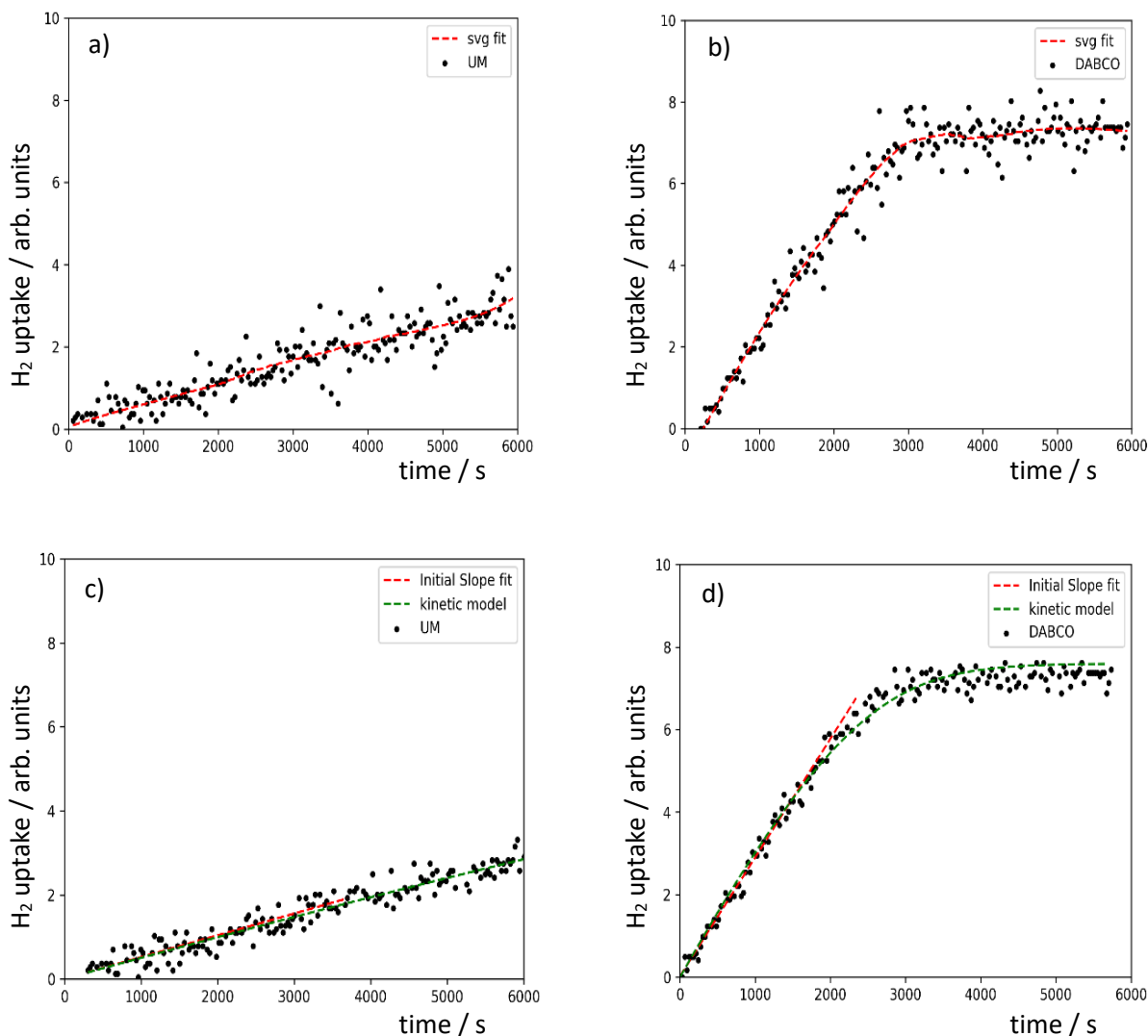


Figure 2.6- H₂ uptake measurements using Sigma Aldrich 5 wt. % Pt/Al₂O₃. a) Unmodified and b) DABCO modified catalyst. In both cases the points are the original data and the “svg fit” line is fitted using the Savitzky-Golay approach. c) Unmodified and d) DABCO modified catalyst following outlier rejection. The fitted lines here are a linear fit to the first 1000 s (red dash line) and a kinetic model fit to the data set (green dashed line).

In Figure 2.6 the aR values are calculated using the red dashed line on the bottom two graphs of Figure 2.6 and the iRs values are calculated using the green dash line.

The kinetic models used in this work assume that there is no hydrogenation at time zero for the experiment. This is difficult to achieve practically as data collection can start a few seconds before the reaction reaches the stirring speed. So before fitting, the time origin was reset so that the zero time is when the reaction begins.

For all data sets the first 1000 seconds of data was found to give a good approximation to linear hydrogen uptake, H_{up} , with respect to time. Using a Python script, a standard linear function can be fitted to this portion of the data (Equation 2.1).

$$H_{up} = mt_{orig} + c$$

Equation 2.1- Equation of the linear function fitted to the data where, t_{orig} is the original time series of the measurements and m and c are the slope and intercept of the linear fit. The zero reaction time should be set as the time at which this equation gives $H_{up} = 0$, i.e., we require a time shift, t_{shift} (Equation 2.2).

$$t_{shift} = -\frac{c}{m}$$

Equation 2.2- Equation for the time shift used in the analysis

The data set was then adapted to this time origin by offsetting all time values in the data according to:

$$t_{new} = t_{orig} - t_{shift}$$

Equation 2.3- Equation to find the new time in the analysis

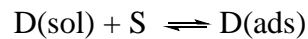
This gives a time series, t_{new} , in which $H_{up} = 0$ when $t_{new}=0$. Data that now had a negative time value was removed from the data set. A new linear fit to the data was carried out giving the equation (Equation 2.4). A check was made that this linear fit gave the same slope as the original and gave $c_{new} = 0$.

$$H_{up} = m_{new}t_{new} + c_{new}$$

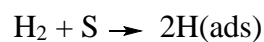
Equation 2.4- Equation for the linear fit

2.5.2 Kinetic model

In terms of the chemical reaction the reactant, D, is first adsorbed onto the surface and then hydrogenated following the reaction scheme (Equations 2.5 and 2.6):



Equation 2.5- Equation for the reactant adsorbing onto the surface



Equation 2.6- Equation for the dissociative adsorption of hydrogen to the surface



Equation 2.7- Equation for the adsorbed reactant being hydrogenated.

For the initial surface adsorption step, we assume Langmuir adsorption will give the surface coverage, $\Theta(D_{ads})$, of the adsorbed reactant:

$$\Theta(D_{ads}) = \frac{K_{ads}D_{sol}}{(1+K_{ads}D_{sol})}$$

Equation 2.8- Equation for the surface coverage of the adsorbed reactant, where K_{ads} is the equilibrium constant for the adsorption of the reactant to the catalytic surface sites and D_{sol} is the concentration of reactant in solution.

The kinetic equations are integrated numerically using the increments:

$$\delta H_{up} = \Theta(D_{ads})k_2\delta t$$

Equation 2.9- Shows the change in hydrogen uptake pressure. It also shows the slope of the graph at the linear portion.

$$\delta D_{sol} = -\Theta(D_{ads})k_2\delta t$$

Equation 2.10- Shows the change of concentration of reactant in solution where k_2 is the pseudo rate constant which includes active site concentration, for the surface hydrogenation reaction (Equation 2.8).

So, it is assumed that the equilibrium between the solution and surface adsorption is maintained throughout the reaction and that hydrogen does not compete for adsorption sites with the reactant.

The numerical integration is carried out using a Python code which calculates changes in H_{up} and D_{sol} with a time step of $\delta t = 1$ s, so that the time step is significantly shorter than the time interval between data points (30 s). At each time step the surface coverage is recalculated from Equation 2.8.

Equation 2.9 shows that the gradient obtained in the linear fit to the initial part of the data (Equation 2.4) will be the product of the surface coverage of the reactant and the rate constant for the surface hydrogenation reaction. As such, the interpretation of the initial slope as demonstrating differences in the rate constant when comparing catalyst modifiers can be mis-leading as the modifiers would also be expected to influence the surface coverage of reactants.

The kinetic model has only three variable parameters: k_2 , K_{ads} and D_0 . Where D_0 is the reactant concentration at the start of the experiment, which corresponds to the maximum hydrogen uptake observed. As D_0 is measured we restrict the fitting process to only allow +/- 5 % variation in this parameter.

Equation 2.9 shows that the slope of the graph in the linear portion at early times is related to the adsorption equilibrium constant as well as the rate constant. So, the linear fit slope is not a direct measure of the intrinsic rate of a catalytic site on the surface. By fitting the model, we can try to separate the surface coverage and the rate constant for hydrogenation. Only a pseudo rate constant has been defined as it also contains the concentration of active sites. A rate enhancement suggests that the modifiers are able to increase the intrinsic rate but the adsorption of the modifiers will also cover over some active sites, reducing their number. So, the enhancement seen is a balance between the increased activity and reduced number of sites. Once the values from the fittings were obtained, they were multiplied by $6.158 \text{ mmol bar}^{-1}$ as this is the calibration factor to convert bar to mmol at 293K. Error bars were added as three reactions of EtPy and CD were completed and the error was found to be +/- 5% for the linear fit and +/-10% for the kinetic fit.

The aR that is used in the results section relates to the rate values obtained from the linear fit. These linear fit rate values of the modified reactions are divided by the linear fit of

the unmodified reactions and this gives the aR values. The iR values are found from the rate values obtained from the kinetic fit model. The kinetic fit values for the modified reaction are then divided by the unmodified kinetic fit values and that gives the iR values.

The software was written in python and installed on the Raspberry Pi, it just uses the A/D convertor on the Pi to read the output of the pressure monitor.

The device was calibrated by comparison with the standard lab gauge (see appendix for error). The biggest error with the system was due to fluctuations due to electrical interference which were removed by the smoothing software.

2.6 Characterization Techniques

2.6.1 Carbon Monoxide Chemisorption

Carbon monoxide chemisorption is an extremely useful analytical technique in heterogenous catalysis as it can be used to measure the specific surface area of the metal and dispersion of a catalyst which is necessary when comparing the effectiveness and activity of catalysts. Carbon monoxide (CO) binds very strongly to the transition metals and blocks access to other gases and reactants. As it binds strongly the amount of carbon monoxide used to cover a surface of a heterogenous catalyst can be used to determine the surface area of the solid. A fixed amount of CO gas is flown through the metal sample and adsorbs to the metal surface. This is repeated until the surface of the metal is completely saturated. This allows the calculation of the total surface area (equation 2.11) as well as the dispersion of the metal on the support (equation 2.12).

A CO molecule binds to the transition metal to form a partially triple bond (Figure 2.7).

This happens by:

- Two π - bonds are formed through an overlap of the d-orbitals with the antibonding pi orbitals from the carbon. For the electrons from the metal to fill the electrons of the π -

antibonding orbital on the carbon monoxide molecule (back-bonding) there must be electrons in its d-orbitals, and it must be in a low oxidation state (0, +1, +2).

- The orbitals from the metal (a mix of the s, p and d orbitals) form a σ - bond with the sp hybridised molecule from the carbon monoxide molecule.

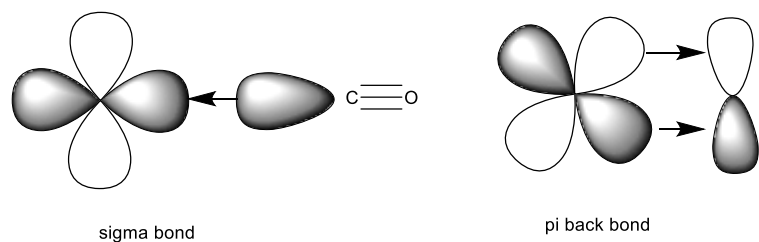


Figure 2.7: representation of the bonding between CO and the metal

$$\text{Metal dispersion \%} = n \times \frac{V_{ads}}{V_g} \times \frac{m.w}{M} \times 100$$

Equation 2.11- The equation to work out the metal dispersion using the number of surface atoms and the total number of atoms. V_{ads} = volume of CO adsorbed, V_g = molar volume gas of CO, m.w = molecular weight, M= % metal loading n= stoichiometric factor

The specific surface area is calculated using Equation 12:

$$A_m \left(\frac{m^2}{gm} \text{ sample} \right) = \left[\left(n \times \frac{V_{ads}}{V_g} \right) \times N_A \right] \times \alpha$$

Equation 2.12– Equation to calculate specific surface area using the surface area occupied metal atom. V_{ads} = volume of CO adsorbed, V_g = molar volume gas of CO, n = stoichiometric factor, N_A = Avogadro number, α = cross- sectional area of active site metal atom m^2

The instrument that was used was a Micromeritics Autochem II. The Important parameters were:

1. A pre-reduction step was required prior to CO chemisorption analysis, to ensure that all PtO was full reduced to Pt metal. CO does not bind to PtO, so it is incredibly important that this is done in order to achieve quality analysis.
2. After this step, the catalyst is cooled down to room temperature and a sample loop containing the CO is passed over the catalyst. The sample loop contains a precise known volume. This process of CO being introduced is continued until no more CO is adsorbed.
3. It is assumed that Pt - CO stoichiometry is exactly 1. It is important to know that this is an assumption. Therefore, by knowing the total moles of CO that is adsorbed in a given experiment (from the CO purging) we can work out the moles of Pt active site (per gram of catalyst).

In this project the flow rate of the CO is not important as it runs on a parallel line to the one that goes over the catalyst bed. Fixed amounts (volumes) of CO are directed into the gas line that flows over the catalyst bed which are introduced through a sample loop.

Thus, the flow rate does not matter. The catalyst bed temperature was heated to and fixed at 35 °C for the entire of the analysis.

2.6.2 Gas chromatography

Gas chromatography is an analytical technique that is used to analyse and separate compounds in a reaction mixture. It is a versatile analytical technique and is used extensively in many industries including pharmaceuticals, pesticides and cosmetics and many analytical laboratories, including environmental and forensic. The main uses for GC are to identify chemicals and determine their concentration relative to the other chemicals in the reaction mixture. GC can also be used to calculate the vapour pressure, activity coefficients and the heat of different solutions and to see if a reaction has gone to completion or if there are any by-products.

The sample/reaction mixture being analysed is introduced to the GC column via a sample port. A few microlitres of the sample, contained within a GC sample vial, are injected into a GC injection port. Here the sample is heated so that it is in the gas phase and then it enters the gas stream along with the carrier gas. The carrier gas is usually nitrogen, helium or hydrogen as it must be inert, dry and oxygen-free. In this project nitrogen was used. The carrier gas is known as the mobile phase and the column is known as the stationary phase (Figure 2.8). This carrier gas moves along a column which is heated in the column oven to a specific temperature. The compounds are separated along the column due to the difference in affinities of the compounds in the reaction mixture relative to the stationary phase. As the compounds leave the column they go towards the detector. The separation of the analytes depends on the vapour pressure and the activity coefficients of the solutes.

In this project the GC samples were detected by a flame ionization detector. The flame ionization detector is one of the most common types of detectors as well as a thermal

conductivity detector. In the flame ionisation detector once the liquid enters the detector it is heated and then it mixes with hydrogen and an oxidizer (hydrogen flame) and the compounds are pyrolyzed in between two electrodes. This releases electrons and ions. Therefore, the current between the two electrodes changes. These changes are detected, amplified and integrated using an integrator and display system.⁵

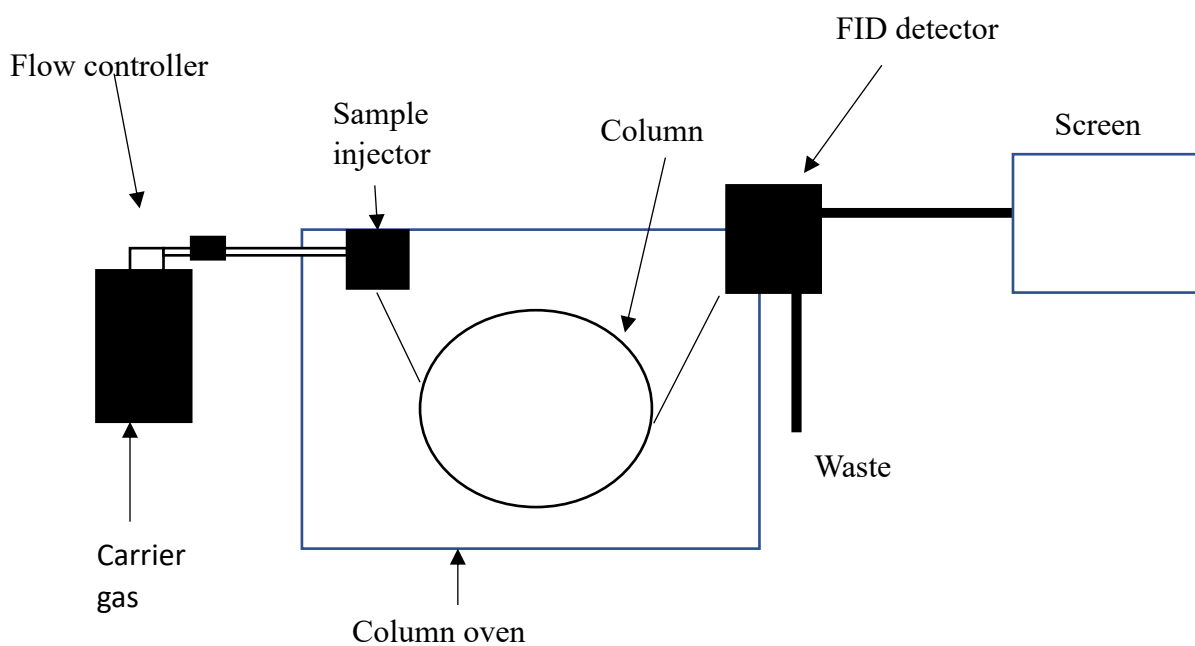


Figure 2.8: Schematic diagram of a gas chromatography system

A Perkin Elmer TGA-FTIR-GC/MS was used for the GCs. The parameters used in this project for the GC are: 0.5 μL of sample was injected, CP wax column, ramp rate of $10\text{ }^{\circ}\text{C min}^{-1}$; a carrier gas flow rate of 1.6136 mL/min; pressure of 8.11071 psi; average velocity of 29.792 cm/sec; no splitter and no external standard was added. PerkinElmer Chromatography Data System (CDS) Software was used.

2.6.2.1 Chiral column

A chiral column was used to determine the enantiomeric excess (ee) of some of the reactions performed for these investigations. The reactions that were analysed by the chiral column were the EtPy hydrogenation reactions using the modifiers CD, R-QL and QL. Capillary columns using a chiral stationary phase were able to separate enantiomers in all cases. The most common chiral stationary phases are cyclodextrin derivatives.⁶ The chiral column used was a chiraldex – beta column, 30 m column length, column OD 0.32 mm and film

thickness 0.25 microns. Column OD is a column that is filled with a packing of octadecylsilyl groups chemically bonded to a silica gel carrier. In order to find the selectivity, the R and S peak areas are subtracted from each other and divided by the total peak area and that value is times by 100 in order to get the ee. The conversion is found through adding the product peaks and dividing them by the product peaks and the starting material peaks and then times that value by 100.

2.6.3 Transmission electron microscopy (TEM)

Transmission electron microscopy (TEM; Figure 2.9) is a highly useful type of microscopy that can analyse surfaces of materials on the nanoscale and allows the user to look in-depth at the crystal structure and different features in that structure. Some features that can be provided by TEM include the size of the nanoparticles and the topography of the material. TEM works by transmitting a high intensity beam of electrons through a thin sample in order to form an image of the sample. It is a widely used analytical technique in heterogenous catalysis. The images created have a much higher resolution than those made using light microscopy. This is due to the small de Broglie wavelength of the electrons.

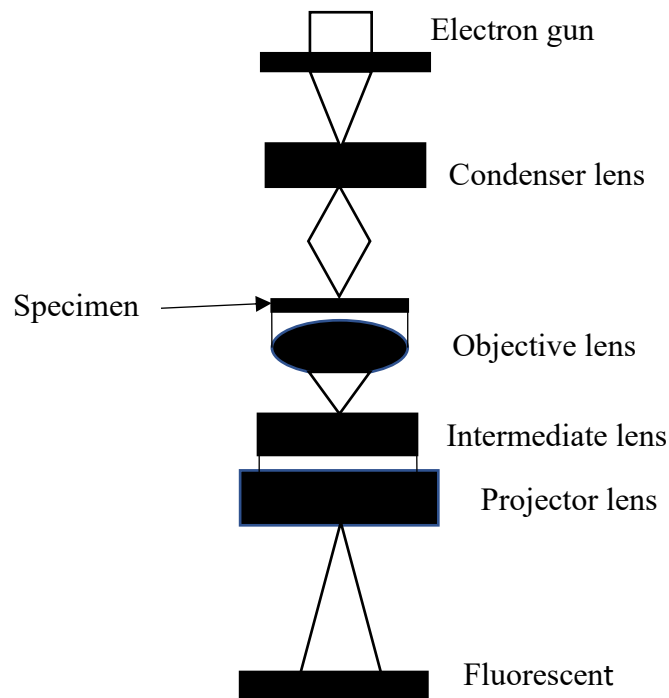


Figure 2.9: Schematic diagram of a transmission electron microscope

The mode of action of the TEM is as follows: the electron gun shoots a high intensity beam of electrons. This high intensity beam of electrons is focused onto the condenser lens where the high angle electrons are excluded by the condenser aperture. The electrons then hit the sample and the electrons are transmitted depending on the electron transparency and the thickness of the sample (Figure 2.9). The transmitted electrons are then focused by the objective lens into an image on a fluorescent screen. The electrons are converted to light so that the image is created. The densities in specimen are shown by the darkness in the image. The images that are made on the fluorescent screen can be taken at different magnifications which allows the user to look in detail at the structure of the surface.⁷

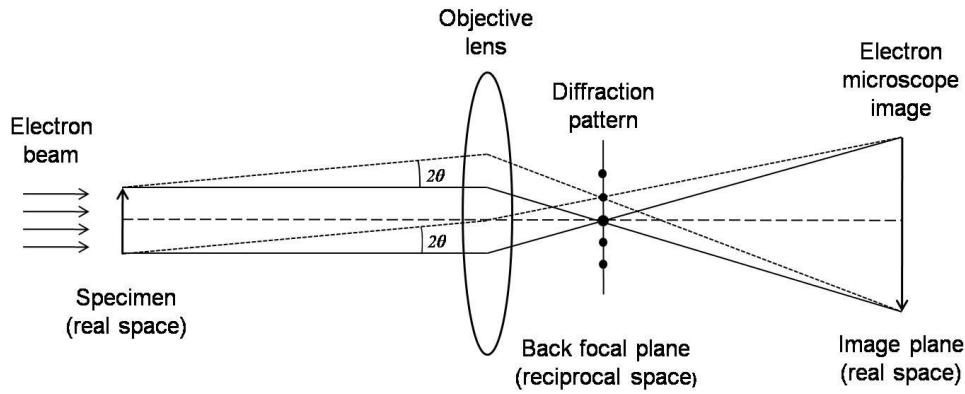


Figure 2.10: The optical electron beam diagram of TEM.⁸ Image obtained from libre texts⁹

Figure 2.10 shows what happens when the electron beam is transmitted through sample. When a crystal lattice has electrons transmitted through it with the wavelength λ , diffracted waves are formed at angles of 2Θ (incidence and scattering angle) and the Bragg equation is satisfied (Equation 2.13).

$$\lambda = 2d \sin \Theta$$

Equation 2.13- Bragg equation

In the image a diffraction pattern would be seen and when the transmitted electrons and the diffracted beams combine a magnified image can be seen. By changing the focal lengths of the lenses, the diffraction pattern and the electron microscope image can be seen. TEM can be used in the analysis of the microstructure of materials.¹⁰ In this project a Jeol JEM 2100 LaB6 TEM was used. The sample was dry dispersed onto copper grids and analysed as is. Imaging was done at 200kV.

2.6.4 Brunauer-Emmett-Teller (BET) surface area analysis

The BET theory was developed by Stephen Brunauer, Paul Emmett and Edwards Teller in 1938 and it was an addition to the Langmuir theory which was developed in 1916. BET theory extends monolayer adsorption (Langmuir adsorption) to multi-layer adsorption. The Langmuir theory connects the monolayer adsorption of gas molecules onto a solid surface to the gas pressure above the surface at a set temperature.¹¹

$$\theta = \frac{\alpha \cdot P}{1 + (\alpha \cdot P)}$$

Equation 2.14- Langmuir theory: θ – fractional coverage of the surface, P is the gas pressure and α is a constant.

Langmuir theory has the following assumptions:

- Gas molecules (adsorbates) form a monolayer on the surface
- Each active site of the surface/ catalyst can be occupied by one particle only
- All surface sites have the same adsorption energy for the adsorbate.
- The solvent can adsorb at one site but is independent of adsorption at neighbouring sites.
- The surface site is where a molecule can adsorb onto.

In BET theory it is also assumed that:

- Gas molecules will adsorb onto a solid in layers infinitely.
- The adsorption layers do not interact with each other
- This Langmuir theory can be applied to each layer.

In BET analysis nitrogen is usually used because of its strong interaction with solids and its high purity as well as its availability. The surface is cooled with liquid N₂ so it can detect adsorption between the gaseous and solid phase as these interactions are weak most of the time. Nitrogen is then released stepwise into the sample cell with the surface that needs analysing. The conditions of a partial vacuum are created. After the saturation pressure no more adsorptions occur. Pressure transducers monitor the pressure changes as the adsorption takes place. When the adsorption layers have all formed the sample is removed and the cell is heated so the adsorbed nitrogen is released from the material. This adsorbed nitrogen is then quantified. The data is then shown as a BET isotherm.¹² BET allows the surface area of surfaces to be calculated.¹³ °

For this project a Quantrochrome QuadroWin instrument version 6.0 was used. The BET was run with 20 adsorption and 20 desorption points. There was a degas time of 3 hours at a temperature of 200 °C.

The volume of gas required to fill the pores is based on the difference of pressure from adsorption to desorption measurements. The nitrogen condenses in pores and as the pressure is changed the difference can be measured and micro- meso-vol can be calculated.

Brunauer, Emmett and Teller found that monolayers that form between relative pressures of 0.05 to 0.30 the monolayer evenly covers the previous one. In order to work out the metal surface area the Langmuir adsorption theory is applied to those monolayers.

$$\frac{1}{W\left(\left(\frac{P_o}{P}\right) - 1\right)} = \frac{1}{W_m C} + \frac{C - 1}{W_m C} \left(\frac{P}{P_o}\right)$$

Equation 2.15- BET equation used to describe the specific surface area. W = weight of gas adsorbed, P/P_0 = relative pressure, W_m = weight of adsorbate as monolayer and C = BET constant.

Using equation 2.15 a linear plot of the left-hand side of that equation against P/P_0 .
From the linear plot.

$$s = \frac{C - 1}{W_m C} \quad i = \frac{1}{W_m C}$$

Equation 2.16- intercept and slope values from the linear graph created from equation 2.15. W_m = weight of monolayer, C = BET constant, s = slope and i = intercept

$$W_m = \frac{1}{s + i}$$

Equation 2.17- the weight of the monolayer can be worked out from the intercept and the slope.

$$S_t = \frac{W_m N_A A_{cs}}{M}$$

Equation 2.18- equation to work out the total surface area

$$S = S_t/w$$

Equation 2.19- equation to work out a specific total surface area is the total surface area divided by the weight

2.6.5 X-ray Diffraction (XRD) Analysis

XRD is the most common technique to study crystalline structure. It is a non-destructive fast analytical technique that can be used for phase identification and can provide information on unit cell dimensions. XRD can be carried out on single crystals or powders. It can be used to find if a sample is amorphous or crystalline. If the sample is amorphous the peaks would be broad and if they are crystalline they would be sharp.¹⁴

The three basic elements are an x-ray tube, a sample holder, and an x-ray detector. X-rays are produced when charged particles of sufficient energy are decelerated. Inside the X-ray tube there are electrodes, and the tube is maintained at high voltage to draw the electrons towards the anode. The X-rays are produced when electrons with sufficient energy eject the inner shell electrons of the metal. These X-rays radiate in all directions. X-rays are used because they have a similar wavelength to the spacing between atoms in a crystallite structure. The X-ray source is a Cu K α ($\lambda = 1.5406 \text{ \AA}$).¹⁵

When the crystal lattice is hit by the incident beam scattering takes place. Bragg's Diffraction takes place when scattering in a certain direction is in phase with scattered rays in other atomic planes. The reflections then combine and reinforce one another. This is known as constructive interference. Most scattering interferes with itself and is eliminated which is called destructive interference.

The electron density of the crystallite structure can be found by measuring the intensities and angles of the diffracted beams. The electron density will show the mean positions of the atoms in the crystals.

Bragg's Diffraction will occur only if the interactions between the substance and the x-rays meets the conditions of Bragg's law. These requirements are that the angle of incidence is

the same as the angle of scattering (constructive interference) and that the path length difference is equal to an integer number of wavelengths. (Figure 2.11).

$$2d(\sin\theta) = \lambda$$

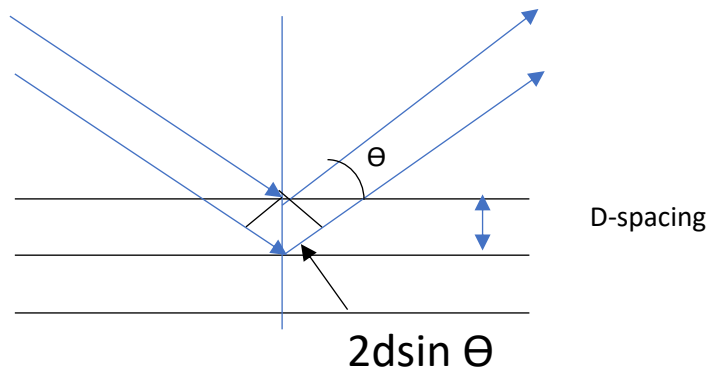


Figure 2.11: Graphical representation of the incident x-ray beam hitting the crystallite structure.

Once XRD has been completed on the sample the mean particle size can be determined using the Scherrer equation. When the crystallite size is less than 100 nm line broadening occurs (Equation 2.20).

$$\tau = \kappa\lambda/\beta\cos\theta$$

Equation 2.20: The equation relates the broadening of a peak in a diffraction pattern to the size of the particle in the crystal lattice where: τ is the mean particle size, κ is the shape factor which is dimensionless, λ is the X-ray wavelength, β is the line broadening at half the maximum intensity and θ is the bragg angle.

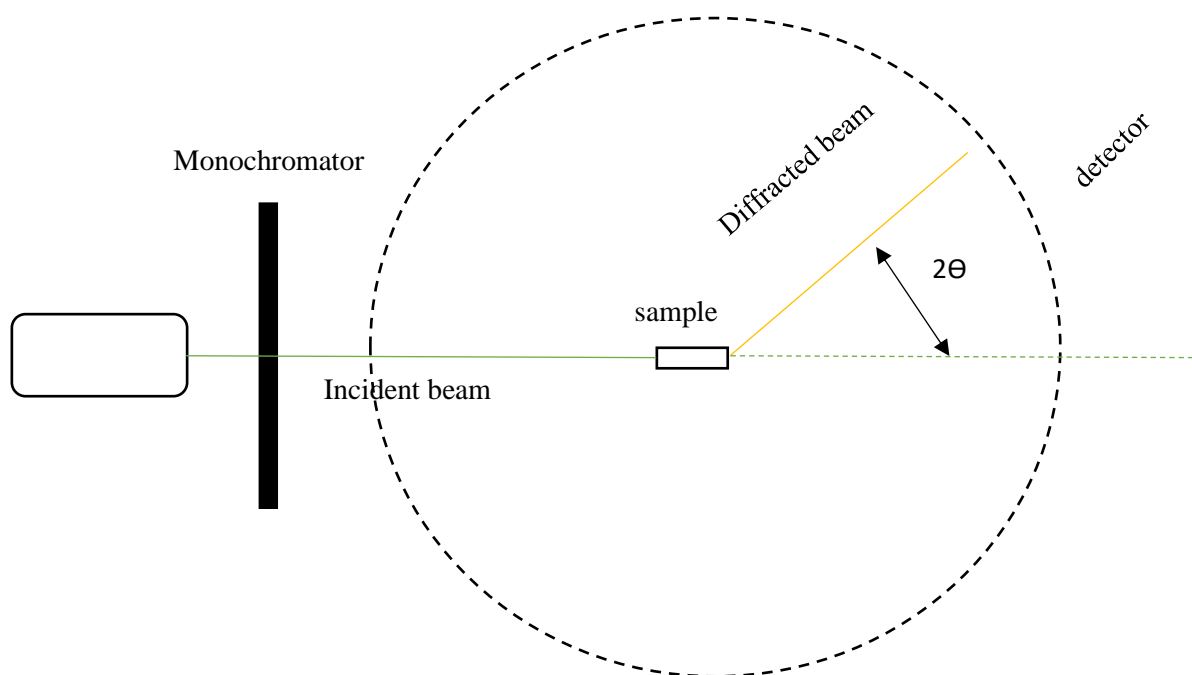


Figure 2.12: Simple schematic diagram of a XRD diffractor system.

A simple schematic diagram of a XRD diffractor system similar to the one used in this project is shown in Figure 2.12. Powder X-ray diffraction (XRD) spectra were acquired using an X'Pert Pro PAN Analytical powder diffractometer employing a Cu K_{α} radiation source operating at 40 keV and 40 mA. The spectra were analysed using X'Pert High Score Plus software. The mean crystallite size of the metallic gold nanoparticles, where possible, were determined using the Scherrer equation assuming a spherical particle shape and a K factor of 0.89 at the reflection arising from the set of (111) Au planes, at $2\theta = 38^{\circ}$. The diffractograms of the catalysts were compared to the following reference files: Pd (00-001-1201), PdO (03-065-5065), Pt (01-080-3828), PtO(01-085-0714) and Au(01-071-4614).

2.7 References

- 1- A. Kraynov and R. Richards, *Applied Catalysis A: General*, 2006, **314**, 1–8.
- 2- M. Barker, J. Rawtani, S. Mackay, *Practical batch process management*, 2005, Elsevier Science, London
- 3- A. Savitzky and M.J.E. Golay, *Anal. Chem.*, 1964 **36**, 1627-1639.
- 4- https://docs.scipy.org/doc/scipy/reference/generated/scipy.signal.savgol_filter.html, (accessed november 2022)
- 5- Gas Chromatography, [Gas Chromatography - Chemistry LibreTexts](#), (accessed August 2021)
- 6- R. A. Patil, D. W. Armstrong, *Chiral Analysis (Second Edition)*, Elsevier Science, 2018
- 7- D. B. Williams, C. B. Carter, *Transmission electron microscopy*, Springer, 2009,
- 8- Transmission electron microscopy, [Transmission Electron Microscopy \(TEM\) \(warwick.ac.uk\)](#), (accessed August 2021)
- 9- Libre texts, [https://chem.libretexts.org/Bookshelves/Analytical_Chemistry/Physical_Methods_in_Chemistry_and_Nano_Science_\(Barron\)/08%3A_Structure_at_the_Nano_Scale/8.02%3A_Transmission_Electron_Microscopy](https://chem.libretexts.org/Bookshelves/Analytical_Chemistry/Physical_Methods_in_Chemistry_and_Nano_Science_(Barron)/08%3A_Structure_at_the_Nano_Scale/8.02%3A_Transmission_Electron_Microscopy), (accessed November 2022)
- 10- Chemlibre texts, 8.2: Transmission electron microscopy, [8.2: Transmission Electron Microscopy - Chemistry LibreTexts](#), (accessed August 2021)
- 11- D. Tiab, E. C. Donaldson, *Petrophysics (Fourth Edition)*, Elsevier, 2016
- 12- Libre texts chemistry, [https://chem.libretexts.org/Bookshelves/Analytical_Chemistry/Physical_Methods_in_Chemistry_and_Nano_Science_\(Barron\)/02%3A_Physical_and_Thermal_Analysis/2.03%3A_BET_Surface_Area_Analysis_of_Nanoparticles](https://chem.libretexts.org/Bookshelves/Analytical_Chemistry/Physical_Methods_in_Chemistry_and_Nano_Science_(Barron)/02%3A_Physical_and_Thermal_Analysis/2.03%3A_BET_Surface_Area_Analysis_of_Nanoparticles), (accessed December 2022)
- 13- S. Brunauer, P. H. Emmett and E. Teller, *J. Am. Chem. Soc.*, 1938, **60**, 309.
- 14- J. P. Patel, P. H. Parsania, *Biodegradable and Biocompatible Polymer Composites*, 2018, 55-79
- 15- V. Vishwakarma, S. Uthaman, *Smart Nanoconcretes and Cement-Based Materials*, 2020, **9**, 250,

Chapter 3

Hydrogenation reactions using cinchonidine and cinchonine modifiers

The enantioselective asymmetric hydrogenation of ethyl pyruvate has been studied whereupon a rate enhancement is seen on addition of certain modifiers. A variety of theories have been put forward for the rate enhancement observed in this reaction, however, the mechanism is still not fully understood. In this chapter the rate enhancement induced by cinchonidine (CD) has been investigated for several substrates, i.e., ethyl pyruvate (EtPy), ethyl benzoyl formate (EBF) and methyl benzoyl formate (MBF). The benzoyl formate reactants have been chosen to investigate the mechanism of rate enhancement as they contain structural moieties that are similar to EtPy, but they differ in key regions that may influence the substrate-modifier-catalyst interaction. Furthermore, two 5 wt. % Pt / Al₂O₃ catalysts (Sigma Aldrich and Johnson Matthey) were compared to evaluate the differences in rate that may relate to the physical properties of the catalyst. These reactions will form the baseline of catalyst performance for comparison with achiral modifiers such as QD in Chapter 4.

3.1 The background of the rate enhancement caused by CD

3.1.1 The 1:1 Modifier to reactant model

CD is needed to induce ee in the product, which is thought to produce a rate enhancement in the EtPy hydrogenation. The most recent and generally accepted mechanism for the mode of action is that the quinoline moiety adsorbs onto the platinum surface (Figure 3.1), the protonated nitrogen then attracts the EtPy molecule and then stabilises its half-hydrogenated state. There is a fast transfer of a proton to the oxygen on the carbonyl and a slow addition of hydrogen onto the carbon and then the substrate desorbs (see introduction section 1.6).

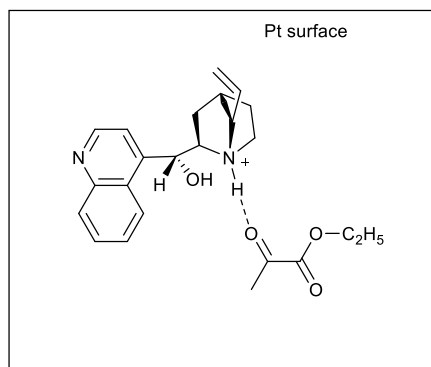


Figure 3.1: Reactant: modifier complex put forward by Blaser *et al.*¹ illustrating the half-hydrogenated ethyl pyruvate being stabilised by CD. Both of these substrates have adsorbed onto the Pt.

3.2 Results and Discussion

3.2.1 Catalyst Characterization

Two commercial catalysts are compared; a 5 wt. % Pt / Al₂O₃ sourced from Sigma-Aldrich (SA) and a 5 wt. % Pt / Al₂O₃ sourced from Johnson Matthey (JM). As the nanostructure of heterogeneous catalysts have an impact on their activity, both catalysts were analysed by transmission electron microscopy (TEM) to provide morphological information, which may then correlate with any differences in activity. Powder X-ray diffraction (XRD) was used to compare the two catalysts with gamma alumina in terms of their bulk crystalline properties and particle size. Brunauer-Emmett-Teller (BET) analysis was used to look at the surface area of the entire catalyst and CO chemisorption was used to investigate the surface area of the Pt nanoparticles on the catalyst. The surface properties found using these techniques are shown below in Table 3.1.

Catalyst	Particles size (mean) (nm)	Particle size (minimum) (nm)	Particle size (maximum) (nm)	Standard deviation (nm)	Total specific Surface area/ m^2g^{-1}	Pore radius (\AA)	Pore volume cc/g	metal specific surface area/ m^2g^{-1}	Pt loading (%)
SA	5.9	2.3	22.4	2.7	99	41	0.07	3.6	5
JM	2.6	0.8	6.2	0.7	146	113	0.09	3.6	4.6

3.2.1.1 Transmission electron microscopy (TEM)

Particle size, morphology and dispersion has been shown to change the enantioselectivity of the ethyl pyruvate hydrogenation in previous work² and in view of this the samples (SA and JM catalysts) were imaged by TEM. This was in order to understand the particles size and morphology of the Pt particles.

In Figure 3.2 the 5 % wt Pt / Al_2O_3 (SA) catalyst can be seen at different magnifications. Notably, the Pt nanoparticles appear to be encapsulated by the Al_2O_3 (alumina) (Figure 3.2 b-f). The alumina does not resemble typical gamma alumina, which usually have sharper rod-like shapes.³ The mean particle diameter was measured at 5.9 nm with a standard deviation of 2.7 nm (Figure 3,2 a). The largest particle was measured at 22.4 nm, which illustrates that the range of particle sizes is broad and can be expected to impact on the rate of reaction.

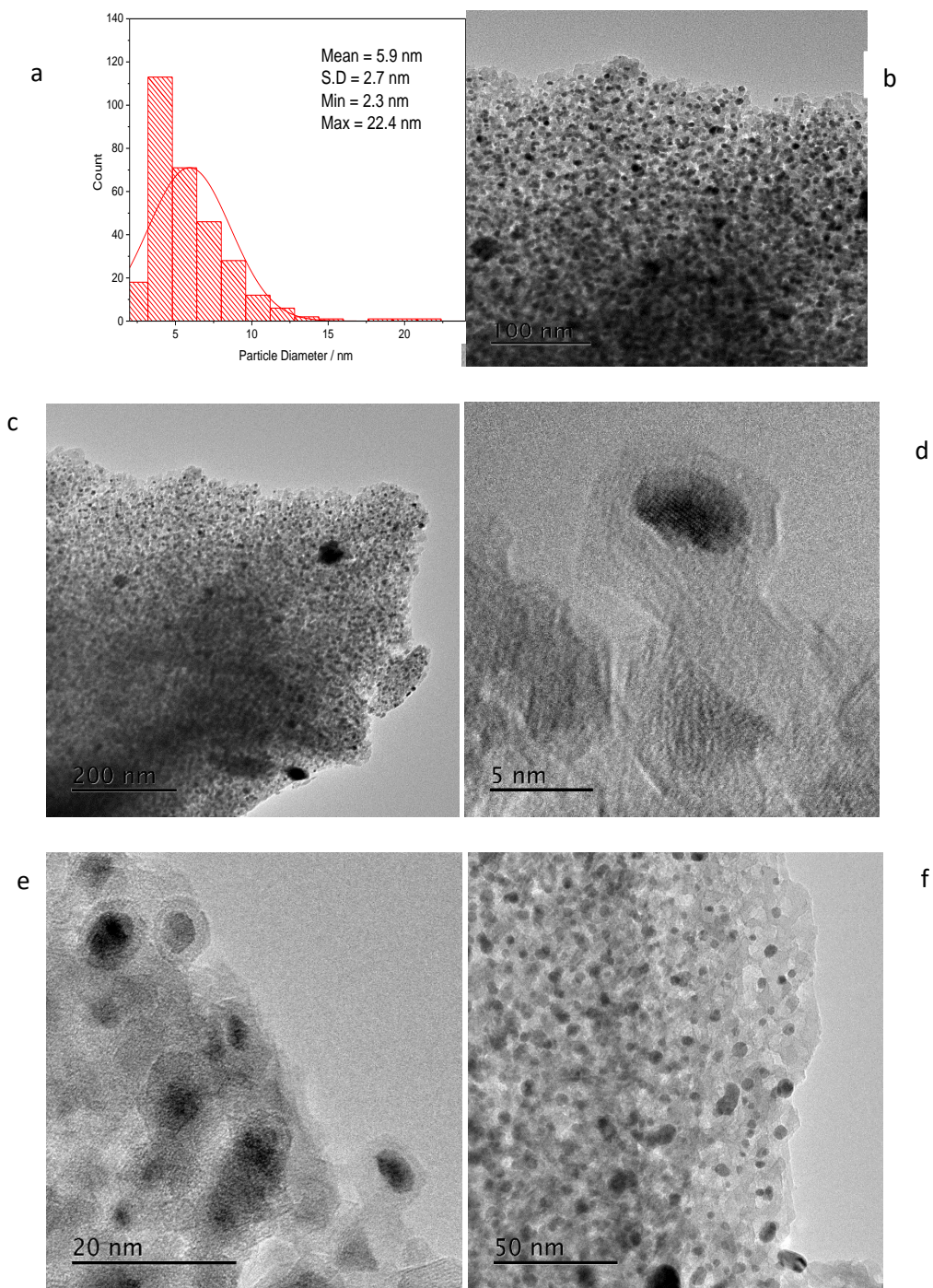


Figure 3.2: TEM images and particle size distribution of the 5 wt. % Pt / Al₂O₃ (SA) catalyst at different magnifications, showing the Pt atoms and alumina coating. Key; the Pt nanoparticles appear as dark circles and the alumina is the lighter part.

In Figure 3.3 the images of the JM catalyst and its particle size distribution can be seen. The images of the JM sample show particles consistent with gamma alumina. Alumina overlay is difficult to exclude in the JM catalyst images due to smaller particle size, but it is not observed and therefore not present to the extent of the SA catalyst. The particle diameter of the JM catalyst is narrower, where the average particle diameter is 2.6 nm (SD 0.7 nm) and the maximum particle size is 6.2 nm. It is reasonable to expect that the rate of reaction over the SA and JM catalysts will differ due to the particle size differences and the alumina overlayer observed on the SA catalyst.

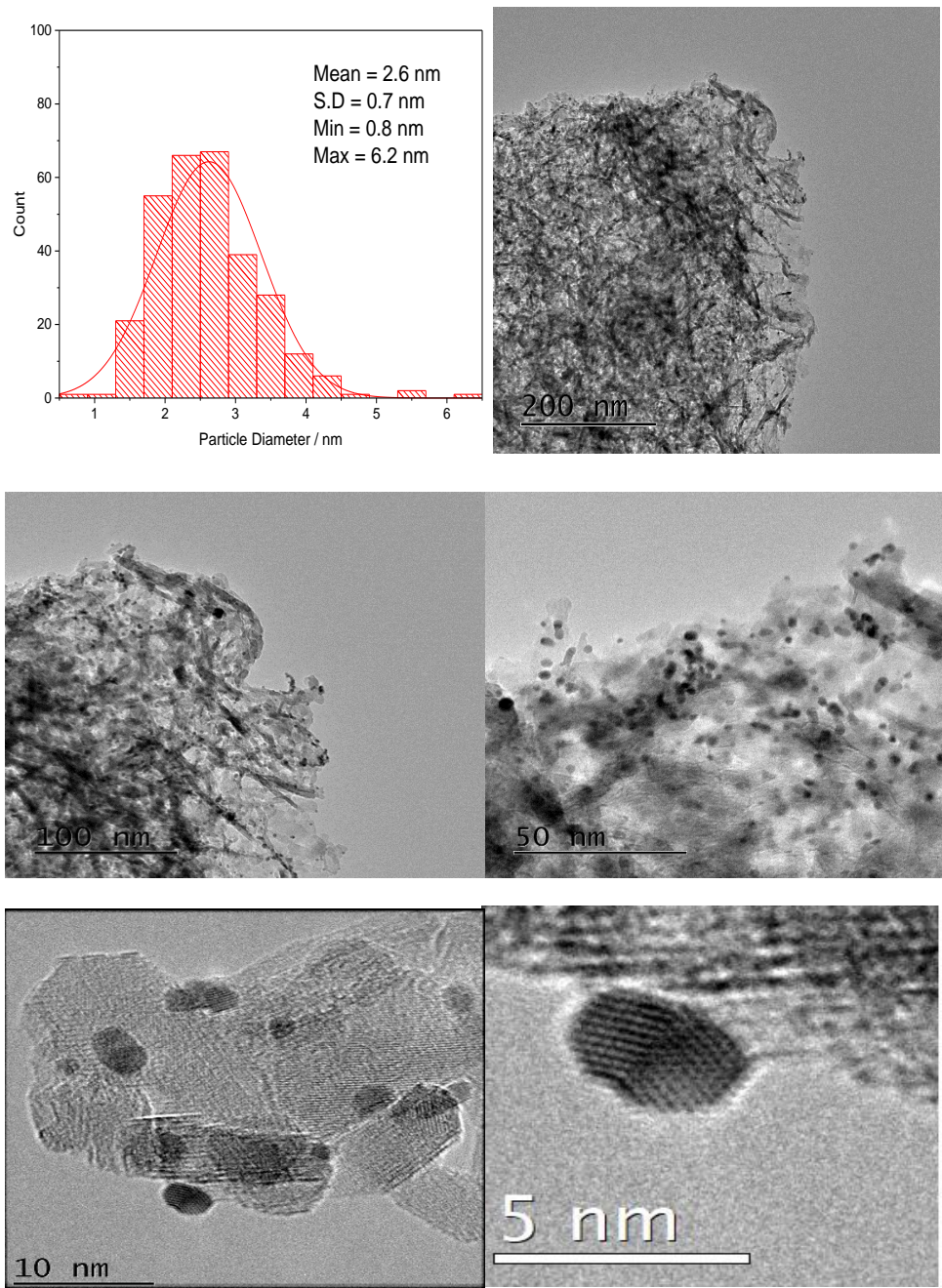


Figure 3.3: TEM Images and particle size analysis of the 5 wt. % Pt / Al₂O₃ (JM) catalyst at different magnifications.

There are many factors that can influence the catalysts activity such as specific surface area and metal surface area. The catalysts were analysed by Brunauer-Emmett-Teller (BET) analysis to estimate the surface and pore volume of each catalyst.

In Table 3.1 the information found on the two different catalysts can be seen. The JM particle sizes appear to be significantly smaller than the SA catalysts at a similar Pt loading. The metal specific surface area is the same for both catalysts, but the overall surface area and average pore radius of the SA catalyst is smaller compared to those properties of the JM catalyst.

As there are smaller particles in the JM catalyst there is a much tighter distribution. The smaller particles in the alumina overlay mean that: the particles are more hemispherical; there is a higher energy surface; i.e., there are less Pt(111) sites; there are more edge sites and the dispersion is possibly higher. These have influences on reactivity and selectivity and how chemicals adsorb.

3.2.1.2 X-ray diffraction (XRD) characterisation of the two catalysts compared to gamma alumina

In Figure 3.4 the three XRD diffraction patterns of the SA and JM catalysts and also the γ -alumina are compared. There is a peak at 39 degrees 2θ corresponding to Pt(111) (JCPDS 04-0802) there are reflections in the pattern for both the JM and SA catalysts and there is not one in the γ -alumina sample. There is an unknown reflection from the JM catalyst at $32^\circ 2\theta$ in the JM which is absent in the diffraction pattern of the SA catalyst, potentially an impurity as it cannot be indexed to aluminium from the holder.

The reflections are labelled with the hkl values of the alumina and the Pt. The platinum reflections are broad which imply the particles are quite small. The platinum reflection is largest in the SA catalyst. This could suggest that the particles are larger than the JM catalyst which is in agreement with the particle sizes found through TEM analysis. However, through XRD analysis alone it isn't clearly shown as there are alumina peaks underneath.

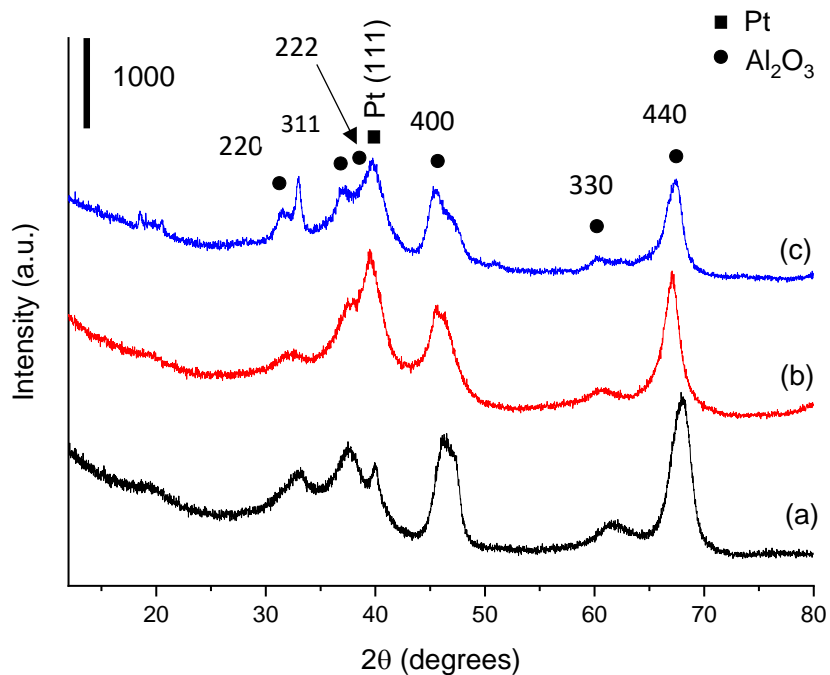


Figure 3.4: Powder XRD patterns of γ -Al₂O₃ (a), SA Pt / Al₂O₃ (b) and JM Pt / Al₂O₃ (c).^{4,5}

3.2.1.3 Nitrogen adsorption measurements and BET analysis

The two catalysts were analysed via BET analysis in order to determine the total surface area and pore radius and volume. In Table 3.1 and Figure 3.5 the nitrogen adsorption analysis is shown. The SA catalyst has a significantly smaller pore radius and a smaller total specific area than the JM catalyst. It has been reported previously that a smaller pore area and larger nanoparticles had shown to decrease the enantioselectivity and turnover frequency of the ethyl pyruvate hydrogenation.⁶

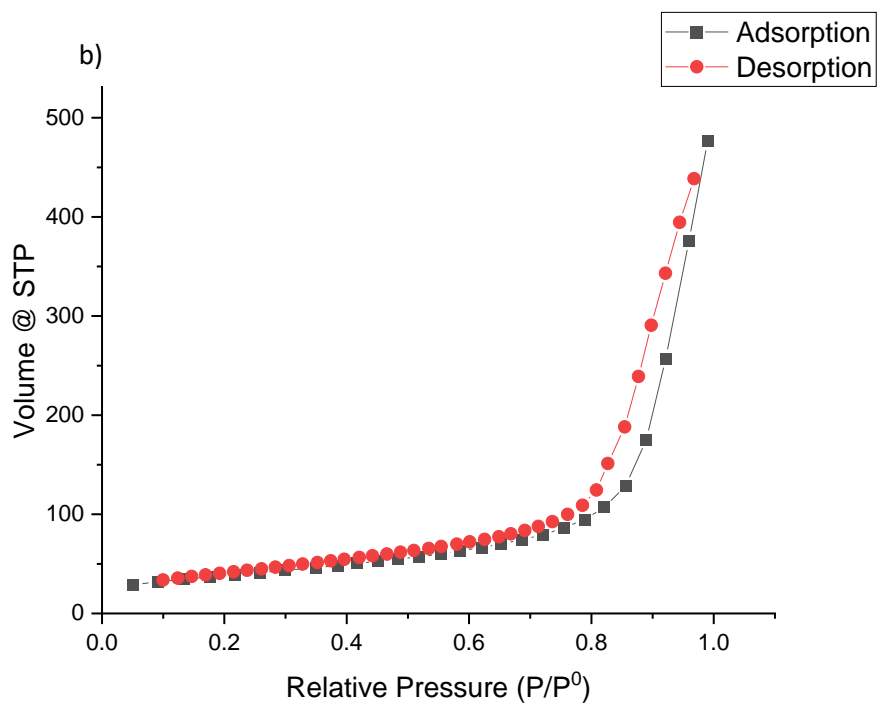
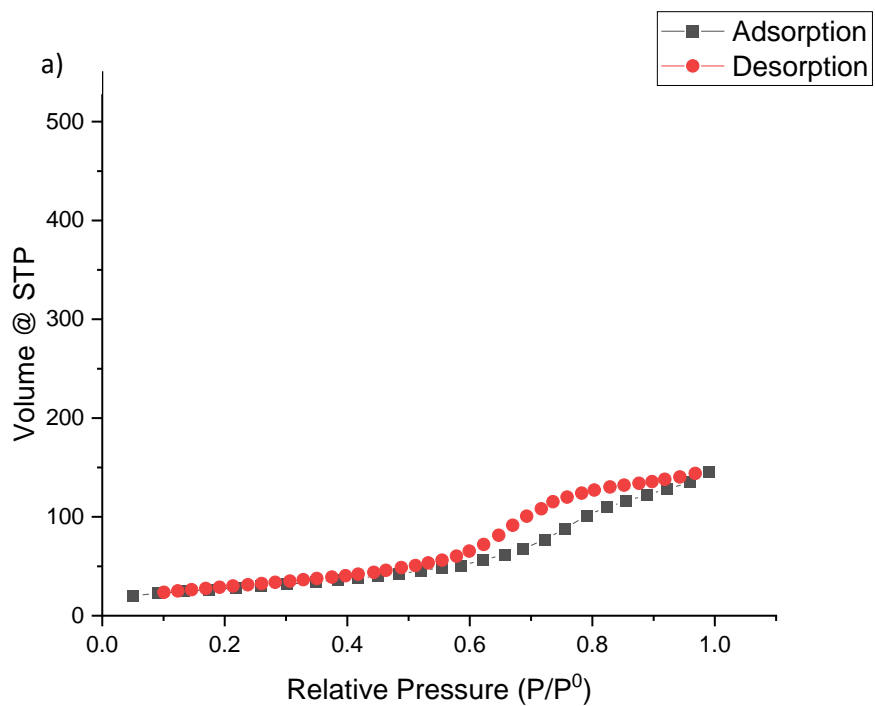


Figure 3.5: The adsorption and desorption isotherms of the SA (a) catalyst and the JM (b) catalyst.

3.3 Comparison of the Hydrogenation Reactivity over the Sigma-Aldrich (SA) and Johnson Matthey (JM) catalysts

3.3.1 EtPy hydrogenations

Figure 3.6 shows the hydrogen uptake (bar) curves of the EtPy hydrogenation using the SA (a) and JM (b) catalysts. The profiles of the modified and unmodified reactions are typical of the hydrogenation of pyruvates.⁷ This profile corresponds to a slow reaction rate over the unmodified catalyst, where addition of a modifier (CD or CN) greatly improves the reaction rate. Here the slope of the uptake profile increases in a linear fashion until the reaction is close to completion, whereupon the rate decreases and plateaus. Approximately 8 bar of hydrogen (45 mmol) is required to hydrogenate one of the carbonyls of ethyl pyruvate at a reaction pressure of 20 bar. Table 3.3 illustrates the rate information calculated from the uptake profiles according to the methods described in Chapter 2. The apparent rate enhancement is calculated using the linear slope (lin_fit slope) which is the product of the surface coverage of the reactant on the catalyst and the rate constant. The apparent rate enhancement illustrates the combination of the modifier enhancing the adsorption of the reactant to the active site and lowering the barrier to the hydrogenation step. Therefore, the intrinsic rate enhancement is the rate enhancement that is not including the surface coverage of the reactants and is showing the intrinsic rate enhancement given by the system and if the modifier lowers the barrier to the hydrogenation step. The lin_fit slope is the initial gradient of the uptake curve, and the intrinsic rate enhancement is calculated using the kinetic slope which is the initial gradient and the rest of the hydrogen uptake curve.

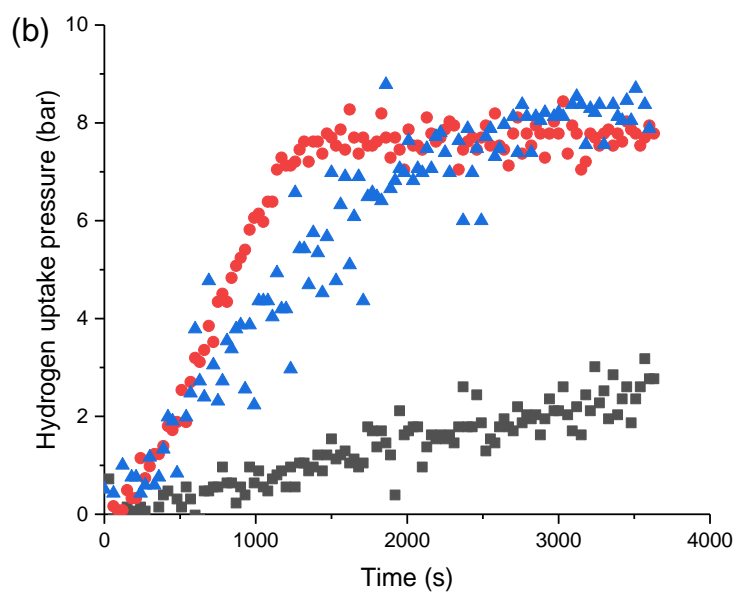
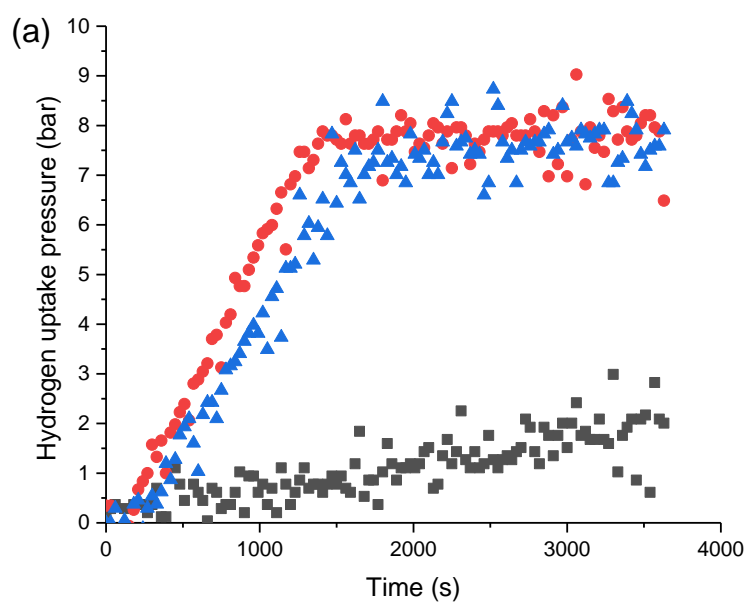


Figure 3.6: The hydrogen uptake profiles of the EtPy hydrogenation using cinchonidine (red), cinchonine (blue) and no modifier (black) and the two different catalysts SA (a) and JM (b). : H_2 (20 bar), RT, 5 wt.% Pt / Al_2O_3 (1.25 mmol, 250 mg); EtPy (45 mmol, 5.2 mL); Toluene + 0.001 M acetic acid); CD ($0.14 \text{ mmol}_{\text{CD}} \text{ mol}_{\text{Pt}}^{-1}$, 8.5 μmol , 2.5 mg), CN ($0.14 \text{ mmol}_{\text{CN}} \text{ mol}_{\text{Pt}}^{-1}$, 8.5 μmol , 2.5 mg).

Table 3.2- Comparison of the apparent and intrinsic rate values calculated over the JM catalyst and Sigma Aldrich catalyst								
Modifier	lin fit_slope/ mmol s ⁻¹ (10 ⁻³)		aR		Kinetic slope/ mmol s ⁻¹ (10 ⁻³)		iR	
	JM	SA	JM	SA	JM	SA	JM	SA
UM	4.6	3.0	1.0	1.0	6.4	3.8	1.0	1.0
CD	42.3	37.7	9.2	11.8	42.3	38.6	6.7	9.5
CN	23.1	30.8	5.0	9.6	32.9	32.3	5.2	7.9

aR = apparent rate enhancement over unmodified reaction

iR = intrinsic rate enhancement over unmodified reaction.

In Table 3.2 the different rates and hydrogen uptake curves can be seen for these reactions. The SA data shows that CD and CN gives the faster intrinsic and apparent rate enhancements when compared to the unmodified reaction. This is because the unmodified reaction gives a larger lin_fit and kinetic slope values for the JM catalyst (see Table 3.2) which in turn meant that the aRs and iRs were lower for the JM catalyst. This may be due to the smaller platinum particles sizes of the JM catalyst which then in turn means that the overall rate enhancements calculated for the CD modified reaction is less than that of the SA catalysts. However, the cinchonine modified reaction gave larger lin_fit_slope values in the reaction using the SA catalyst compared to the JM catalyst. It is unclear why this happened maybe because it allowed the substrate to adsorb more easily onto the Pt surface for the SA catalyst and not for the JM catalyst. The SA catalyst gave lower rate results for the unmodified, CD and the kinetic slope of cinchonine because it has larger platinum nanoparticles and perhaps the alumina overlay caused a lower reactivity. Another reason could be that the SA catalyst has a lower pore radius and volume than the JM catalyst which has been reported previously to influence the turnover frequency and enantioselectivity.⁶

3.3.2 EBF hydrogenation

The different catalysts SA (a) and JM (b) were tested in the EBF hydrogenation using CD and CN in order to compare the rates of the two catalysts. There is a slow reaction rate over the unmodified catalyst and addition of a modifier (CD or CN) greatly improves the reaction rate. Here the slope of the uptake profile is more rounded and is more of a curve than the EtPy uptake graphs. Approximately 6 bar of hydrogen (43 mmol) is required to hydrogenate one of the carbonyls of EBF. Table 3.3 illustrates the rate information calculated from the uptake profiles (Figure 3.7) according to the methods described in Chapter 2.

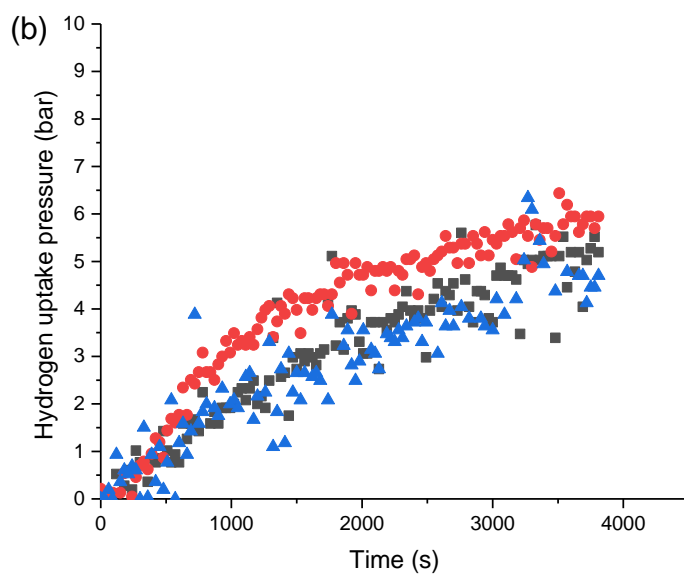
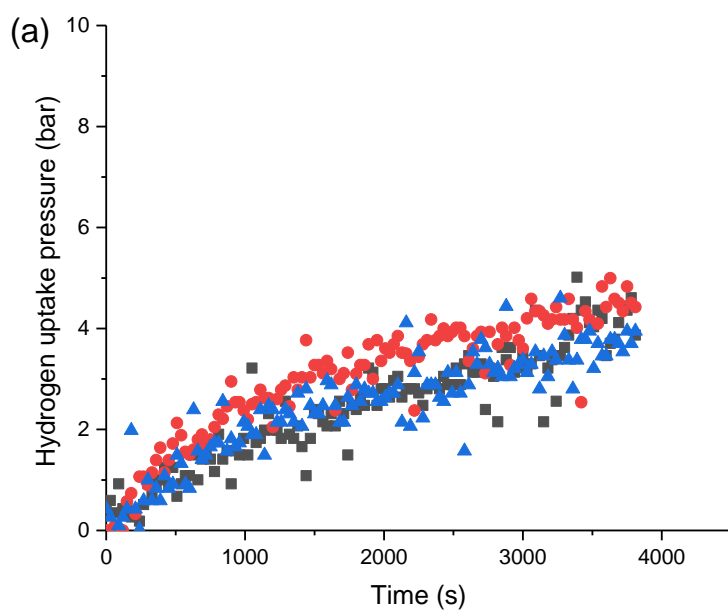


Figure 3.7: The hydrogen uptake graphs of the EBF hydrogenation using cinchonidine (red), cinchonine (blue) and no modifier (black) and the two different catalysts SA (a) and JM (b). Reaction condition: H_2 (20 bar), RT, 5 wt.% Pt / Al_2O_3 (1.25 mmol, 250 mg); EBF (43 mmol, 6.8 mL); Toluene + 0.001 M acetic acid); CD ($0.14 \text{ mmol}_{\text{CD}} \text{ mol}_{\text{Pt}}^{-1}$, 8.5 μmol , 2.5 mg), CN ($0.14 \text{ mmol}_{\text{CN}} \text{ mol}_{\text{Pt}}^{-1}$, 8.5 μmol , 2.5 mg)

Table 3.3- Comparison of the rate values calculated for the JM catalyst and Sigma Aldrich catalyst								
Modifier	lin fit_slope/ mmol s ⁻¹ (10 ⁻³)		aR		Kinetic slope/ mmol s ⁻¹ (10 ⁻³)		iR	
	JM	SA	JM	SA	JM	SA	JM	SA
UM	9.6	6.4	1.0	1.0	24.4	7.6	1.0	1.0
CD	19.6	8.4	2.0	1.3	58.7	25.3	2.4	2.8
CN	8.1	5.7	0.8	0.9	24.4	17.1	1.0	2.0

aR = apparent rate enhancement over unmodified reaction

iR = intrinsic rate enhancement over unmodified reaction.

In Table 3.3 the rates for the EBF hydrogenation using CD and CN are shown. Compared to the EtPy reaction the rates are much slower in the EBF reaction which must be due to steric hinderance as the EBF has a large benzene ring attached. In the unmodified reaction, for example using EtPy, the JM catalyst gave a faster lin_fit slope and kinetic slope. Furthermore, in the CD and CN reaction the lin_fit slope and the kinetic slope were faster for the JM catalyst due to the smaller particle sizes and larger pore volume. Under TEM analysis the Pt nanoparticles appeared to be encapsulated by alumina which could have also lowered the catalytic activity. The SA reactions gave a higher iR but this was due to the JM catalyst giving a much faster kinetic slope in the unmodified reaction than the SA catalyst in turn making the rate enhancements lower. The CN reaction only gave slight rate enhancements compared to the CD reaction. It is not clear as to why there is a difference.

3.3.3 MBF hydrogenation reactions

The different catalysts SA (a) and JM (b) were tested in the MBF hydrogenation using CD and CN as modifiers in order to compare the rates of the two catalysts. There is a slow reaction rate over the unmodified catalyst and addition of a modifier (CD or CN) greatly improves the reaction rate. In these graphs there is more of a linear slope where the rate then decreases and plateaus. Approximately 6 bar of hydrogen (41 mmol) is required to hydrogenate one of the carbonyls of MBF. Table 3.4 illustrates the rate information calculated from the uptake profiles according to the methods described in Chapter 2.

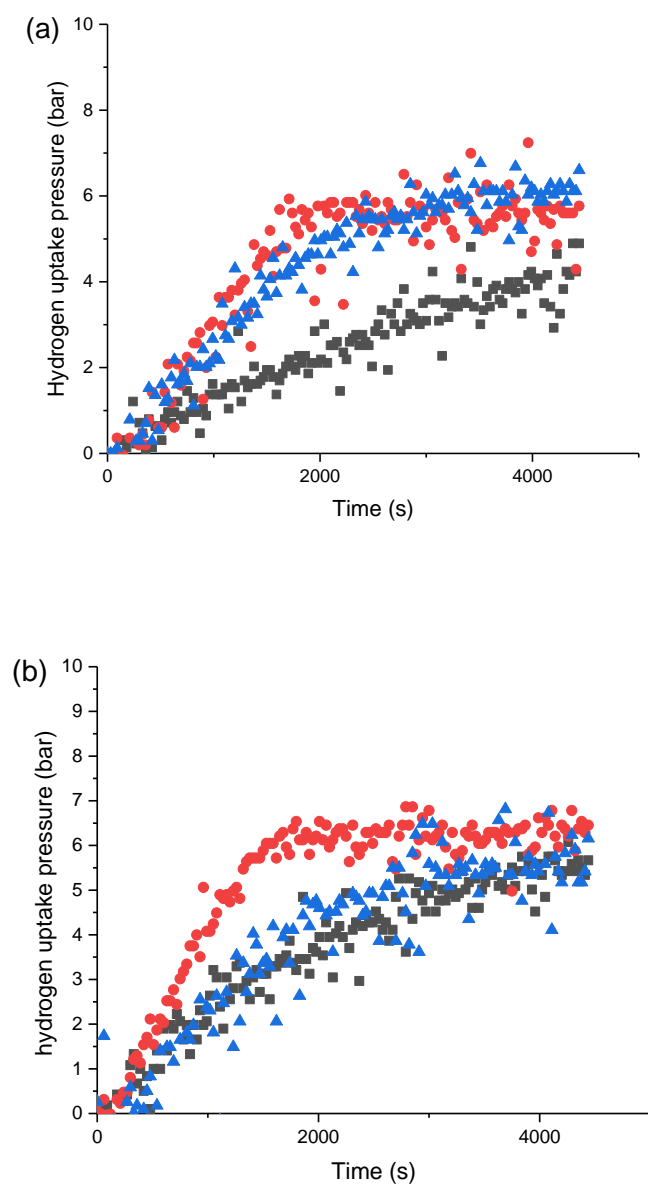


Figure 3.8: The hydrogen uptake graphs of the MBF hydrogenation using cinchonidine (red), cinchonine (blue) and no modifier (black) and the two different catalysts SA (a) and JM (b). Reaction conditions: H_2 (20 bar), RT, 5 wt. % Pt / Al_2O_3 (1.25 mmol, 250 mg); MBF (41 mmol, 5.8 mL); Toluene + 0.001 M acetic acid); CD ($0.14 \text{ mmol}_{\text{CD}} \text{ mol}_{\text{Pt}}^{-1}$, 8.5 μmol , 2.5 mg) and CN ($0.14 \text{ mmol}_{\text{CN}} \text{ mol}_{\text{Pt}}^{-1}$, 8.5 μmol , 2.5 mg)

Table 3.4- Comparison of the rate values calculated for the JM catalyst and Sigma Aldrich catalyst								
Modifier	lin fit_slope/ mmol s ⁻¹ (10 ⁻³)		aR		Kinetic slope/ mmol s ⁻¹ (10 ⁻³)		iR	
	JM	SA	JM	SA	JM	SA	JM	SA
UM	10.2	5.5	1.0	1.0	15.5	10.1	1.0	1.0
CD	22.4	21.6	2.2	3.9	24.5	27.2	1.6	3.9
CN	16.2	15.8	1.6	2.7	28.7	24.1	1.9	3.5

aR = apparent rate enhancement over unmodified reaction

iR = intrinsic rate enhancement over unmodified reaction.

In Table 3.4 and Figure 3.8 the hydrogen uptake curves and the rates for the MBF hydrogenation using CD and CN are shown. Like the results shown for the other two substrates the SA catalyst produced better intrinsic and apparent rate enhancements for the CD and CN modifiers in this reaction. This is because in the unmodified reaction the lin_fit and kinetic slope were faster for the JM catalyst than the SA catalyst which in turn made the aRs and iRs lower for the JM catalyst. The JM catalyst gave faster lin_fit slopes for all the reactions and the JM catalyst gave faster kinetic slopes for the CN and unmodified reaction but not the CD reaction. Overall, the faster rates were shown in the JM catalyst. This could be because of what was found when characterizing the catalysts: the JM nanoparticles were smaller; the pore radius and volume was larger and there was alumina overlay in Pt nanoparticles in the SA catalyst.

3.3.4 Summary of comparison of catalysts

When comparing the reaction rate over two catalysts using the CD and CN modifiers, the SA catalyst gave better aRs and iRs for all three substrates except for aR for the CD reaction in the ethyl benzoylformate reaction. This is because for the unmodified reaction for all three

substrates the JM catalyst gave faster lin_fit and kinetic slope values than in the SA catalyst which led to lower iR_s and aR_s for the modified JM catalyst reactions. The reasons for this were found when the catalysts were characterized: the JM catalyst had a larger pore radius and pore volume; the JM catalysts nanoparticles were smaller, and the SA catalysts nanoparticles were encapsulated in alumina. When comparing the three substrates the unmodified reactions were faster for the MBF and EBF reactions compared to the EtPy reactions but the modified reactions in general were faster in the EtPy reactions. This would be likely due to steric hinderance as MBF and EBF both have a benzene ring attached which could make it more difficult for the modifier to interact with the substrate (see Figure 3.9).

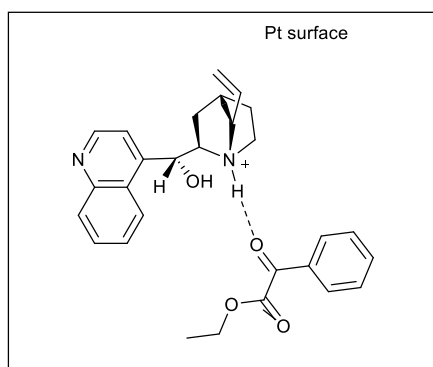


Figure 3.9: CD and EBF interaction.

For both MBF and EBF the CN reaction only gave slight rate enhancements compared to the CD reaction. It is not clear why there is such a difference between CN and CD.

3.4 Investigation of experimental parameters using SA catalyst to determine their effect on reaction kinetics

To further understand the influence of the experimental parameters on the reaction rate experiments were conducted where the stirring rate was changed (600 rpm, 800 rpm, 1000 rpm, 1200 rpm and 1400 rpm), the hydrogen pressure was changed (10 bar, 13 bar, 16 bar and 20 bar) and the amount of EtPy used in the reaction (0.025 - 0.059 mol) was changed. These experiments are intended to find the order of reaction with respect to hydrogen and with respect to the substrate EtPy, and also if there is an optimum stirring speed.

3.4.1 Influence of reaction stirring speed

A comparison of different stirring speeds was carried out on the hydrogenation reaction of EtPy substrate using CD modifier. These reactions were done using the 5 %wt. Pt on alumina catalyst from Sigma Aldrich. This showed that there was a strong dependence of rate on the stirring speed (Figure 3.10 and Table 3.5). The rate, shown as the kinetic slope, increased linearly with stirring speed.

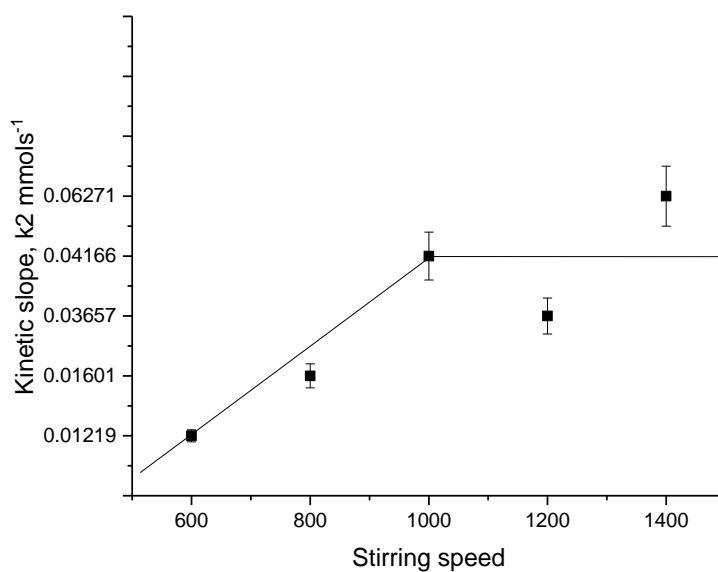


Figure 3.10: A graph showing the dependence of the kinetic slope on the stirring speed. Reaction conditions: H₂ (20 bar), RT, 5 wt.% Pt / Al₂O₃ (1.25 mmol, 250 mg); EtPy (45 mmol, 5.2 mL); CD (0.0085 mmol, 2.5 mg); Toluene + 0.001 M acetic acid)

Table 3.5- Different rate values at different stirring speeds		
Stirring speed	lin_fit slope / mmol s ⁻¹	kinetic fit, k2 / mmol s ⁻¹
600	1.1×10 ⁻²	1.2×10 ⁻²
800	1.5×10 ⁻²	1.6×10 ⁻²
1000	3.9×10 ⁻²	4.2×10 ⁻²
1200	3.6×10 ⁻²	3.7×10 ⁻²
1400	5.3×10 ⁻²	6.3×10 ⁻²

Figure 3.10 shows the values obtained from the kinetic fit for the different stirring speeds; the higher the stirring speed large the kinetic slope (k2) and hence the faster the rate. In Table 3.5 the linear fit and kinetic fit of the k2 values clearly show that increased stirring speed increases the rate. This rate increase is as expected due to the predicted effect faster stirring will have on increasing the rate of particle collisions. The error bars on these points is

very big so these reactions could be repeated. For the reaction to be mass transport limited the rate would increase as the stirring rate increases. In this reaction it appears that at 1000 rpm it plateaus which would mean that the reaction is not limited by mass transport at 1000 rpm stirring speed.

3.4.2 Order of reaction with respect to substrate

The order of reaction was investigated to better understand the reaction mechanism. The unmodified EtPy hydrogenation and the CD-modified EtPy hydrogenations were completed using different amounts of EtPy to confirm the order with respect to hydrogen pressure and EtPy concentration.

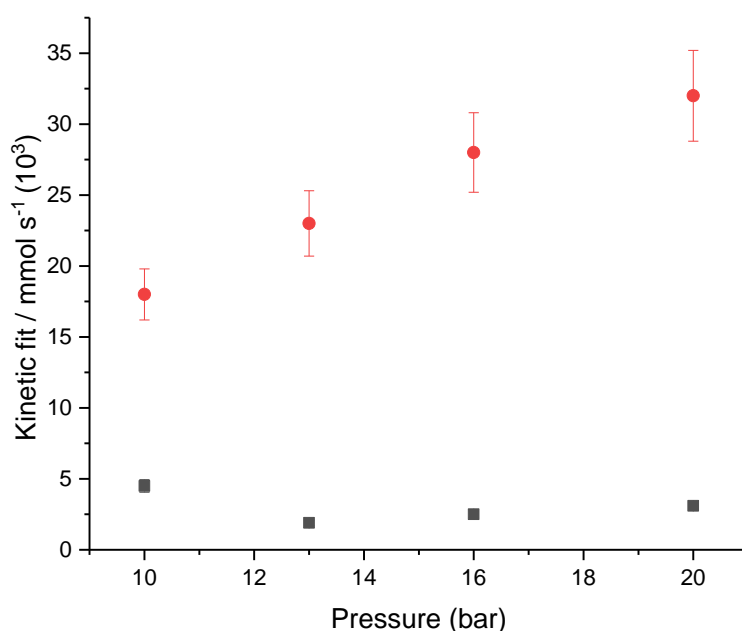


Figure 3.11: A graph showing the lin_fit slope vs the pressure of H₂ for the unmodified (black) reaction and modified (red) reaction. Reaction conditions: H₂ (varies), RT, 5 wt. % Pt /Al₂O₃ (1.25 mmol, 250 mg); EtPy (45 mmol, 5.2 mL); CD (0.0085 mmol, 2.5 mg); toluene + 0.001 M acetic acid)

Pressure of H ₂ (bar)	lin_fit slope / mmol s ⁻¹	kinetic fit, k ₂ / mmol s ⁻¹
10	2.6×10^{-3}	4.7×10^{-3}
13	1.8×10^{-3}	1.9×10^{-3}
16	2.4×10^{-3}	2.5×10^{-3}
20	3.0×10^{-3}	3.1×10^{-3}

In the unmodified reactions (Figure 3.11, Table 3.6) the reaction rates were uncorrelated to the amount of pressure confirming that the reaction was zero-order with regards to hydrogen pressure. The significance of this is that increasing or decreasing the concentration of hydrogen does not affect the reaction rate.

Pressure of H ₂ (bar)	lin_fit slope / mmol s ⁻¹	kinetic fit, k ₂ / mmol s ⁻¹
10	1.8×10^{-2}	1.8×10^{-2}
13	2.3×10^{-2}	2.3×10^{-2}
16	2.8×10^{-2}	2.8×10^{-2}
20	2.9×10^{-2}	3.2×10^{-2}

In the CD-modified reactions, however, the rates increased with increasing pressure, showing first-order kinetics (Figure 3.12, Table 3.7). First-order kinetics of the H₂ pressure in the CD-modified reaction has been reported previously.⁸ For the unmodified reaction there is no change but that is likely because there is little uptake of hydrogen in the reaction which makes it difficult to compare the gradients. In the modified reaction there is an increase in gradient as the pressure rises which would mean that it is not zero-order but first-order which is what has been reported previously.⁸

In order to better understand the reaction, the order of reaction with respect to EtPy was calculated. This was done by varying the amount of EtPy in the unmodified reaction and the CD reaction.

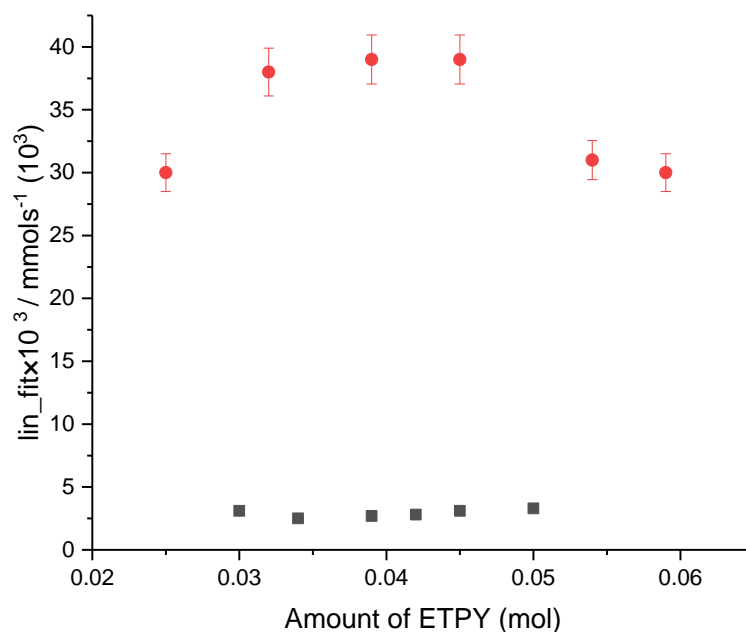


Figure 3.12: A graph showing lin_fit slope (mmol s^{-1}) for the unmodified (black) reaction and modified (red) reaction as a function of the amount of ETPY (mol). Reaction conditions: H_2 (varies), RT, 5 wt. % Pt / Al_2O_3 (1.25 mmol, 250 mg); EtPy (Varied); CD (0.0085 mmol, 2.5 mg); Toluene + 0.001 M acetic acid)

Different amounts of EtPy (mol)	Mol of substrate per mmol of Pt	lin_fit slope / mmol s ⁻¹	kinetic fit, k2 / mmol s ⁻¹
0.025	0.4	3.1×10 ⁻²	3.4×10 ⁻²
0.032	0.5	3.8×10 ⁻²	4.5×10 ⁻²
0.039	0.6	3.9×10 ⁻²	3.9×10 ⁻²
0.045	0.7	3.9×10 ⁻²	4.1×10 ⁻²
0.054	0.8	3.1×10 ⁻²	3.1×10 ⁻²
0.059	0.9	3.0×10 ⁻²	3.0×10 ⁻²

Mol of EtPy	Mol of substrate per mmol of Pt	lin_fit slope / mmol s ⁻¹	kinetic fit, k2 / mmol s ⁻¹
0.03	0.50	3.1×10 ⁻³	9.3×10 ⁻³
0.034	0.53	2.5×10 ⁻³	2.8×10 ⁻³
0.039	0.60	2.7×10 ⁻³	8.1×10 ⁻³
0.042	0.70	2.8×10 ⁻³	3.3×10 ⁻³
0.045	0.71	3.1×10 ⁻³	3.7×10 ⁻³
0.05	0.78	3.3×10 ⁻³	9.8×10 ⁻³

The rate values for the reactions confirm that rate is unrelated to the amount EtPy in both the CD-modified reaction and the unmodified reaction (Table 3.9, Table 3.8, Figure 3.12), confirming that this reaction is also zero order with respect to EtPy. Zero-order kinetics for both the unmodified and modified reactions have been reported before for the EtPy hydrogenation.⁹ This shows that the reaction rate is unchanged by the concentration of EtPy added. If the reaction is zero-order it means that there is enough EtPy on the surface of the reaction so the rate is unchanged when more is added.

3.5 Discussion

3.5.1 The state-of-the art hydrogenation using EtPy with CD

The currently accepted state-of-the-art, optimal conditions for the EtPy hydrogenation and the conditions used in this thesis are shown in Table 3.10. Previous experiments using the state-of-the-art method were aimed at raising the ee whereas the main aim of this work was to understand the influence the reaction parameters and modifiers have on reaction rate. There was no conversion reported and the only products created were ethyl lactate enantiomers.

Conditions	State-of-the-art method	This project
Catalyst	5 wt. % Pt / Al ₂ O ₃ (50 - 100 mg)	5 wt. % Pt / Al ₂ O ₃ (250 mg)
Modifier	Cinchona alkaloid modifiers (1-10 mg) or 0.08 μM concentration	Cinchona alkaloids (1-10 mg)
Solvent	Acetic acid (20 mL)	Toluene + acetic acid (0.001 M) (10 mL)
Hydrogen pressure	100 bar	20 bar
EtPy	5 mL	5.8 mL
Reactor	Autoclave	Autoclave
Apparent rate enhancement	18	14.9
ee	92 % (R)	90 % (R)

For the experiments presented in this thesis the amount of substrate for the EtPy hydrogenation was limited by the sensitivity of the hydrogen uptake monitor (discussed in Chapter 2). The amount of solvent used was limited to 5 mL due to the total volume of the glass liner used in the autoclave. The lower H₂ pressure of 20 bar was used due to the sensitivity of the hydrogen uptake monitor and a high H₂ pressure (> 50 bar) may render the reaction rates difficult to differentiate. In general, toluene with a minor amount of acetic acid was chosen as the reaction solvent as it gave slower rates than acetic acid which made analysis of the curves easier than in neat acetic acid. Acetic acid was used in the state of art because it gave the fastest rate enhancements. Minor amounts of acetic acid were used in this reaction because it allowed the CD to be dissolved. Solvents with a dielectric constant between 2 and 10 are the best suited for the EtPy hydrogenation with acetic acid giving the optimal yield.¹¹ Toluene is a suitable solvent as it has a dielectric constant of 2.4.

Reports indicate that using toluene as the reaction solvent reduce the reaction rate by 8% compared to acetic acid. Alcoholic solvents like ethanol have been reported to react and form hemi-ketals with EtPy which could provide an explanation for the lower yield.¹² Gamez *et al.* highlights that solvents with lower dielectric constants give better enantiomeric excess and rates. It was for these reasons that toluene was used as a solvent in this project. The reason they give for these differences is that the solvents will dissolve the modifiers differently which could then affect the adsorption equilibria of the modifier and the catalyst surface. They also state that the kinetics of the reaction changes depending on what solvent is used; apolar solvent such as toluene showed zero-order rate kinetics and polar solvents like ethanol and propylene carbonate showed first-order rate kinetics.¹³ Potentially this could be due to the polar solvents having interactions with the reactant although they do not state why polar solvents show first order kinetics.

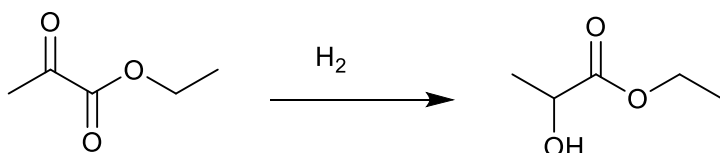
3.5.2 Unmodified EtPy hydrogenation reactions

The unmodified EtPy reactions were carried out in both solvent systems used throughout this project, i.e., toluene/ glacial acetic acid and glacial acetic acid alone, and the results compared.

Solvent	Lin_fit slope/ mmol s ⁻¹	Kinetic fit, k ₂ / mmol s ⁻¹
Toluene (0.001 M acetic acid)	2.7×10 ⁻³	8.0×10 ⁻³
Acetic acid	4.0×10 ⁻³	4.9×10 ⁻³
CD toluene (0.001 M acetic acid)	3.8×10 ⁻²	3.8×10 ⁻²
CD Acetic acid	3.8×10 ⁻²	4.2×10 ⁻²

The linear fit and kinetic fit results in the different solvent systems (Table 3.11) confirmed that there were different EtPy hydrogenation rates in each solvent. Interestingly, in the acetic acid reactions completed they gave very similar rate values for the modified reaction and slower kinetic fit rates for the unmodified reaction which goes against what is said in state of the art (see previous section).

3.5.3 EtPy Hydrogenation Using CD



Scheme 1- EtPy hydrogenation

Initially, the influence of altering the CD modifier concentration was investigated with EtPy reactant under the standard reaction conditions (Scheme 1). Reactions were completed so that the minimum amounts of CD needed for a rate enhancement to be achieved were found. Low concentrations of CD ($0.007 \text{ mmol}_{\text{cd}} \text{ mmol}_{\text{Pt}}^{-1}$) were required to induce a slight rate enhancement in the production of ethyl lactate. However, above this value significant gains in rate could be achieved. That is, the intrinsic rate of reaction at $0.04 \text{ mmol}_{\text{cd}} \text{ mmol}_{\text{Pt}}^{-1}$ gave an intrinsic rate enhancement of 3.5 and the intrinsic rate enhancement given at $0.28 \text{ mmol}_{\text{cd}} \text{ mmol}_{\text{Pt}}^{-1}$ was 4.8.

After completing reactions with different amounts of CD there was no improvement in the rate enhancement above $0.06 \text{ mmol}_{\text{cd}} \text{ mmol}_{\text{Pt}}^{-1}$; the rate enhancement decreased when lower amounts were used. Increases of between 5 times and 100 times have been reported in the literature.¹¹

Amount of CD (mg)	Amount of CD (mmol)	mmol additive per mmol of Pt	lin_fit slope/ mmol s ⁻¹	Apparent enhancement	kinetic fit, k ₂ / mmol s ⁻¹	Intrinsic enhancement
0	0	0	2.8×10^{-3}	1.0	8.4×10^{-3}	1.0
0.0125	0.000042	0.0007	3.3×10^{-3}	1.2	9.8×10^{-3}	1.2
0.125	0.00042	0.007	1.0×10^{-2}	3.7	1.4×10^{-2}	1.6
0.75	0.0025	0.04	2.2×10^{-2}	7.5	3.8×10^{-2}	3.5
1	0.0034	0.06	4.1×10^{-2}	14.5	4.5×10^{-2}	5.4
2.5	0.0085	0.14	3.8×10^{-2}	13.6	3.8×10^{-2}	4.5
3.75	0.0127	0.2	4.0×10^{-2}	14.5	4.0×10^{-2}	4.8
5	0.017	0.28	4.0×10^{-2}	14.3	4.0×10^{-2}	4.8
CN	0.0085	0.14	3.1×10^{-2}	10.9	3.1×10^{-2}	3.7

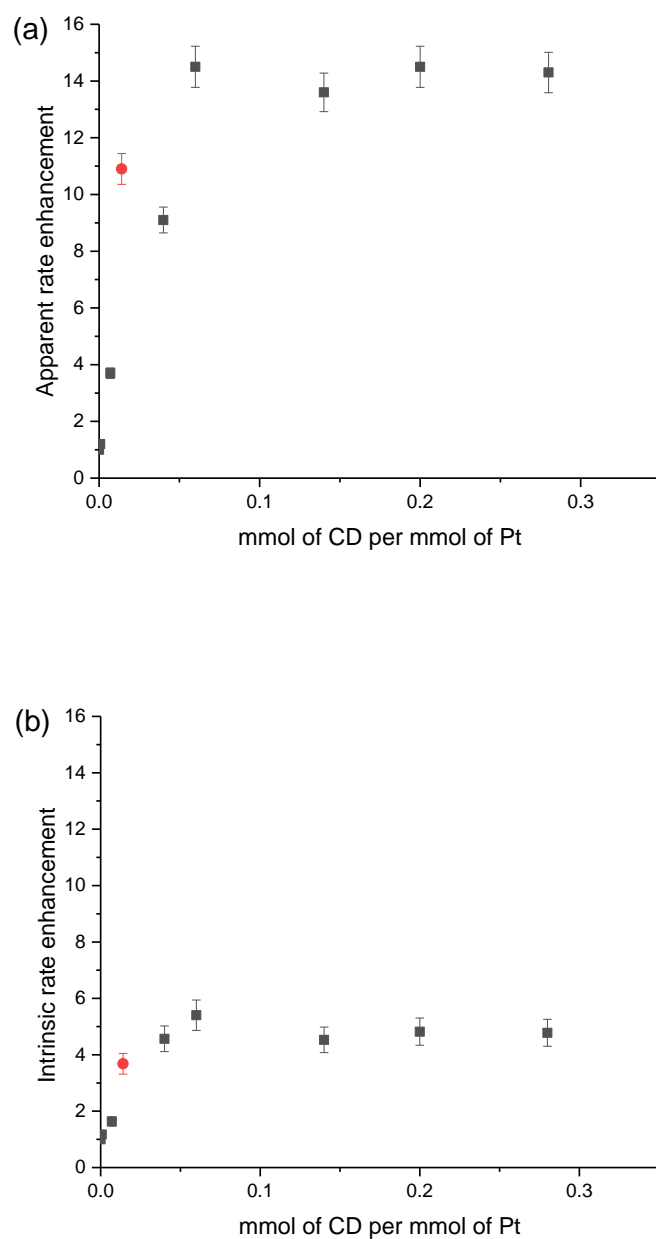


Figure 3.13: Apparent (a) and Intrinsic (b) rate enhancements for the different amounts of CD ($\text{mmol}_{\text{CD}} \text{mmol}^{-1}_{\text{Pt}}$) and CN (red circle) for comparison. Reaction conditions: H_2 (20 bar), RT, 5 wt. % Pt / Al_2O_3 (0.06 mmol, 250 mg); EtPy (45 mmol, 5.2 mL); neat Acetic acid) and Cinchonidine. CN ($0.14 \text{mmol}_{\text{CN}} \text{mmol}^{-1}_{\text{Pt}}$). The error bars were calculated by doing the same EtPy-CD reaction three times and the `lin_fit` values differed by 5 % whereas the kinetic slope values differed by 10 %.

As can be seen in Table 3.12 and Figure 3.13 the apparent rate enhancements from $0.04 \text{ mmol}_{\text{cd}} \text{ mmol}_{\text{Pt}}^{-1}$ to $0.28 \text{ mmol}_{\text{CD}} \text{ mmol}_{\text{Pt}}^{-1}$ are much higher than the intrinsic rate enhancements which implies that the surface coverage of the reactants of the adsorption equilibria influences the rate significantly. The high apparent rate enhancement shows that CD not only helps it adsorb to the surface but also increases the rate intrinsically in this system. CN ($0.014 \text{ mmol}_{\text{CN}} \text{ mmol}_{\text{Pt}}^{-1}$) was also tested and gave a lower rate enhancement than the same amount of CD. This has been previously-reported in the literature by M. Bartok *et al.* They found that not only is the rate slower but the ee is also lower; one reason they give for this is that the adsorption strength is weaker for CN than CD. Bartok *et al.* also give the TOF of CD at 0.1 modifier to Pt surface as 1.6 s^{-1} and that of CN as 1.1 s^{-1} . Another reason they gave was that the rotation around the C8-C9 is hindered as the ethyl group attached to the QD moiety is close to the surface and because of this the CN quinoline moiety would be adsorbed off -parallel or in a tilted geometry (Figure 3.14).¹⁴

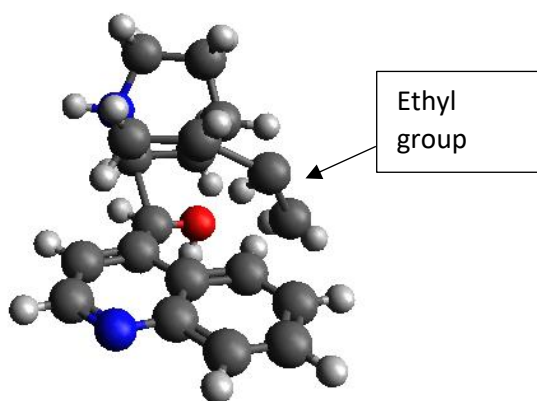


Figure 3.14: CN showing the ethyl group close to the quinoline which would be near the surface and illustrates why Bartok *et al.* suggests that it slightly restricts the favourable intermediate being formed. Key: Carbon atoms in grey, hydrogen atoms in white, nitrogen atoms in blue and the oxygen atom in red.

CD adsorbs onto the surface of the catalyst and creates an enhanced site, which increases the rate and produces more of the *R*-enantiomer. It has been reported that up to a certain concentration of CD that the yield as well as the initial rate decrease although this has not been found during the study presented here. Simmons *et al.* suggest the reason for the decrease in rate is due to a second adsorption of a CD molecule to the enhanced site. This interferes with the space where the EtPy molecule can adsorb.¹⁵

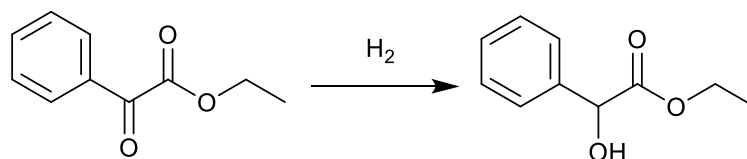
The standard amount of CD was chosen (see Table 3.10) as it was similar to what has been reported in the past by Blaser *et al.*; the optimum amount of CD is between 1-10 mg with a 50-100 mg 5 wt. % Pt on alumina catalyst. Blaser *et al.* obtained a slightly higher rate enhancement using 0.08 μM of CD in acetic acid; they achieved an apparent rate enhancement of 18 with an ee of 92 % of the *R*-ethyl lactate.¹⁶

The apparent rate enhancement of nearly 15 (see Table 3.12) using 0.2 $\text{mol}_{\text{CD}} \text{mol}_{\text{Pt}}^{-1}$ CD modifier is similar to reported values in the literature. For example, Tálas *et al.* achieved a rate enhancement of 15.8 which is the equivalent to the actual rate enhancement in this project.¹⁷ They worked out the rate enhancements by using the ratio of enantioselective and racemic hydrogenation rate constants.

It is likely that the rate enhancement is due to the 1:1 mechanism outlined earlier as well as a cleaning effect where the CD helps ‘clean’ the surface of EtPy oligomers and CO molecules. Unfortunately, throughout this chapter definitive evidence of how CD enhances the rate of the EtPy hydrogenation has not been found.

GC chiral analysis was completed (see appendix) using EtPy with CD and it was found that the an ee of 81% was given for the *R*-ethyl lactate. No other products were found in the reaction mixture. The racemic unmodified reaction was also analysed by chiral GC and the two enantiomer peaks can be seen.

3.5.4 EBF hydrogenation



Scheme 2- the EBF hydrogenation

Reports on the enantioselective hydrogenation of EBF (Scheme 2) are rare. There have been papers that report rate enhancements when CD is used, although there is a smaller rate enhancement found than in the EtPy hydrogenation. Below is a summary of the papers that have reported this reaction.

Martin *et al.* found an ee of 72 % of ethyl acetate using CD. Furthermore, the reaction was noted to be heavily solvent-dependent, due to the different dielectric constants which changed the conformation of the molecule. The highest initial rates reported were given by toluene ($21 \text{ mmol dm}^{-3} \text{ min}^{-1} \text{ g}_{\text{cat}}^{-1}$) hence why toluene was used in the following reactions. Protic solvents in general gave higher initial rates. This is because the protic solvents can act as a H donor and provide more hydrogen to the reaction. The initial rates were said to be low, however, with the cited reason being because of competitive adsorption. Competitive adsorption is seen when the adsorption strength of the reactant and solvent is similar; because of the higher solvent concentration most of the sites are taken up by the solvent, thus inhibiting the reaction. This paper shows that selecting the right solvent is important so that the mechanism of this reaction can be investigated. They also state in this paper that the order of reaction concerning hydrogen is close to zero.¹⁸

M.Bartok *et al.* reported an ee of 98% *R*-ethyl mandelate using CD in acetic acid. They found that the initial rate using CD only increased modestly, which they state infers that ligand

acceleration is not linked to high enantioselectivity. They also postulate that there is heavy competition between the CD molecule and the EBF molecule so higher amounts of CD are needed to obtain a high ee when compared to the hydrogenation of EtPy. The conditions they used were 25 mg of Pt / Al₂O₃, 1 bar of H₂, 0.16 mL of EBF, 2 mL of AcOH. The rate of reaction of EBF modified with CD (1 mmol / L) was calculated as (0.1 mmol g_{cat}⁻¹ s⁻¹) and the EBF unmodified rate was calculated as (0.087 mmol g_{cat}⁻¹ s⁻¹). The CD increased the rate by 15 % or gave an apparent rate enhancement by 1.15.¹⁹

Bartok *et al.* used derivatives of CD as modifiers; CD, CN, quinine, quinidine, isocinchonine, isoquinidine²⁰ They found that iso-cinchonine gave the same ee of 76 % compared to the reaction involving CD when reacted under 1 bar of H₂. This work suggests that some of these derivatives (isocinchonine, isoquinidine and quinine) can be nearly as effective as CD in the EBF hydrogenation. The rate calculated for CD and EBF is 0.00194 mmol g_{cat}⁻¹ s⁻¹. From their results they conclude that the modifier exists in an anti-open conformation, and the data supports the presence of a 1:1 reactant: modifier complex.²⁰

Martin *et al.* found a significant rate enhancement when they used CD in the EBF hydrogenation. In this paper they optimised conditions and found that a Pt/CD ratio of 0.16 gave a rate enhancement of 54%, or an apparent rate enhancement of 1.54, when compared to the unmodified reaction with an ee of 85 %. The reactions were performed at room temperature. They used 150 mL of toluene as a solvent in this reaction, 0.85 mmol of EBF, 220 mg of Pt / Al₂O₃, 1 atm of H₂ pressure and 500 rpm stirring speed. Martin *et al.* found up to a certain point adding CD increased the rate of reaction but after that point adding CD decreased the rate.²¹

Sutyinszki *et al.* reported an ee of 98 % of *R*-ethyl mandelate but they did not report their rate measurements. They achieved this ee using a Pt / Al₂O₃ catalyst and a 1:1 acetic acid to toluene solvent. In this paper they presume the rate limiting step is the product desorption

from the catalyst surface as EBF adsorbs to the platinum strongly. They also found that there was less of a difference in rate enhancement when compared to the EtPy hydrogenation which they say means that the high reaction rate is not a prerequisite to enantiodifferentiation. In this reaction they used 25 mg of catalyst, 2 mL of AcOH, 1 bar of H₂ and 0.16 mL of EBF at room temperature. The unmodified EBF rate was calculated at 0.0088 mmol g_{cat}⁻¹ s⁻¹ and the CD-modified EBF rate was calculated at 0.01125 mmol g_{cat}⁻¹ s⁻¹. The apparent rate enhancement they obtained was 1.28.²²

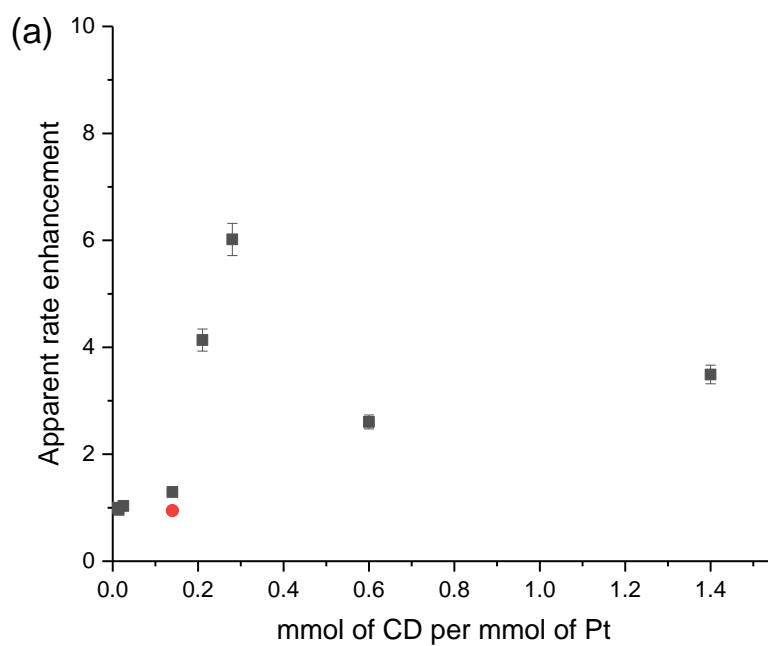
Toukoniitty *et al.* compared acetic acid and toluene in the EBF hydrogenation. Toluene gave the highest ee of 93 % but there was no rate acceleration (1.7 mmol min⁻¹ g_{cat}⁻¹). They also report a maximum conversion which implies there was some catalyst deactivation. Catalyst deactivation they suggest is due to the EBF decomposition which produces CO. They make mention of how much the solvent changes the composition of the system. They show that in acetic acid steady-state enantioselectivity is reached instantaneously as CD can adsorb quickly onto the catalyst particles, whereas in toluene it takes 10 times as long.²³

In this project EBF hydrogenation was carried out using CD at different concentrations to see what the optimised amount of CD is for rate enhancement. The reactions were carried out in toluene + acetic acid (0.001 M) following on from the EtPy hydrogenation. Previous studies by Martin *et al.* suggest that toluene gives a much greater rate enhancement than acetic acid.²¹

In Figure 3.15 the influence of CD concentration on the rate of EBF hydrogenation is illustrated. As more CD is added the hydrogenation rate increases up until it plateaus (Table 3.13) like the results found by Martin *et al.*²¹ Figure 3.15 shows the CD modifier can give a significant rate enhancement when compared to the unmodified reaction in toluene, consistent with the results of Martin *et al.*

As EBF cannot form condensation products that deactivate the catalyst the source of the rate enhancement is likely because of the 1:1 reaction model where CD creates a modified site that stabilizes the EBF half-hydrogenated state. Also, After the optimum amount of CD ($0.21 \text{ mmol}_{\text{CD}} \text{ mmol}_{\text{Pt}}^{-1}$) is added anymore then poisons the reaction it is likely that two CD molecules adsorb onto the same site which effectively deactivates that site.

GC analysis was completed to see if there were any by-products (see appendix). The GC analysis showed that there were not any.



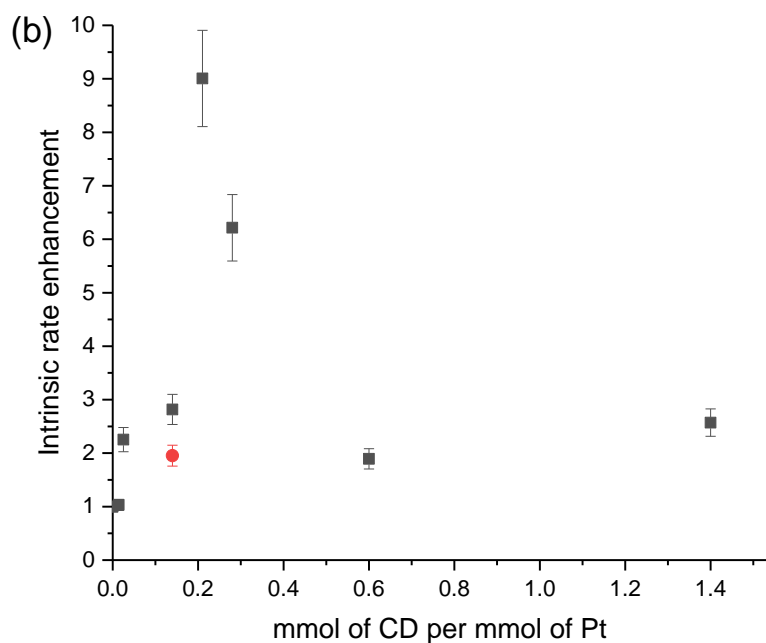


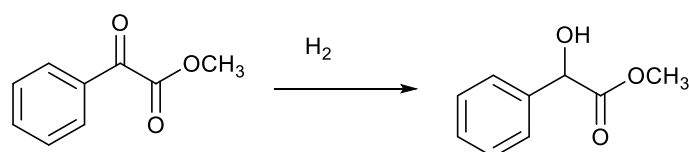
Figure 3.15: The different (a) apparent and (b) intrinsic rate enhancements can be seen in the EBF hydrogenation. CN is in (●) red. Reaction conditions: H_2 (20 bar), RT, 5 wt. % Pt / Al_2O_3 (0.06 mmol, 250 mg); EBF (43 mmol, 6.2 mL); neat acetic acid) and cinchonidine.

The rate enhancements can be seen in Figure 3.16. In Figure 3.16 the apparent rate enhancement finds a maximum at $0.6 \text{ mmol}_{CD} \text{ mmol}_{Pt}^{-1}$. However, once the intrinsic rate enhancements were calculated and the adsorption constant was separated, the highest intrinsic rate was found on addition of $0.21 \text{ mmol}_{CD} \text{ mmol}_{Pt}^{-1}$ of EBF. In both reactions the CN gave a lower rate enhancement than the CD.

Amount of CD (mg)	Amount of CD (mmol)	mmol of additive per mmol of Pt.	lin_fit slope / mmol s ⁻¹	Apparent enhancement	kinetic fit, k ₂ / mmol s ⁻¹	Intrinsic enhancement
25	0.085	1.4	2.3×10 ⁻²	2.6	2.3×10 ⁻²	1.9
10	0.034	0.6	1.7×10 ⁻²	6.0	1.7×10 ⁻²	6.2
5	0.017	0.28	3.9×10 ⁻²	3.5	5.6×10 ⁻²	2.6
3.75	0.013	0.21	2.7×10 ⁻²	4.1	8.1×10 ⁻²	9.0
2.5	0.0085	0.14	8.4×10 ⁻³	1.3	2.5×10 ⁻²	2.8
1.25	0.0015	0.025	6.7×10 ⁻³	1.0	2.0×10 ⁻²	2.3
0.25	0.00085	0.014	6.6×10 ⁻³	1.0	9.3×10 ⁻³	1.0
0	0	0	6.5×10 ⁻³	1.0	9.0×10 ⁻³	1.0
CN	0.0085	0.14	6.1×10 ⁻³	0.9	1.8×10 ⁻²	2.0

In Figure 3.16 and Table 3.13 the influence of CD concentration on the rate of EBF hydrogenation is illustrated. As more CD is added the hydrogenation rate constant increases up until 0.6 mmol_{CD} mmol_{Pt}⁻¹ and then it falls at 1.4 mmol_{CD} mmol_{Pt}⁻¹ of CD. This could be because the CD takes up too many sites and not as many EBF molecules could adsorb to the surface. The apparent rate enhancements found are higher than that have previously been published in the literature (Martin *et al.* 1.54)²¹ and (Sutyinszki *et al.* 1.28).²²

3.5.5 MBF hydrogenation using CD



Scheme 3- MBF hydrogenation

Reaction rate enhancement was achieved for MBF using CD and derivatives of CD (CN, quinidine, quinine).¹⁷ There have not been as many papers published on the MBF hydrogenation compared to the EtPy hydrogenation, but the work found has been mentioned below. Tálas *et al.* reported the rate of the MBF hydrogenation (Scheme 3) being greater than five times using CD when compared to the un-modified reaction. They used EtPy, ketopantolactone and MBF as substrates. They report that the origin of rate enhancement is not due to the decomposition of the catalyst surface. The decomposition is said to happen by CO fragments and $C_xH_yO_z$ degrading from the substrates and adsorbing to the Pt (111) surface blocking sites that could be used for hydrogenation. They argue that the rate enhancement is an intrinsic property in the Orito reaction because the rate enhancement increases as the concentration of MBF increases. They make mention of the difference in character of the substrates, mainly that EtPy can form condensation products where MBF cannot (like oligomers or polymers). However, as the rate enhancement was instantaneous, they mention that this shows that the rate enhancement occurs as part of an intrinsic feature to the reaction. The highest apparent rate enhancement they achieved was 5.5. This was with $[MBF]_0$ of 0.5, $[CD]_0(10^{-4} M)$ of 1 and 0.063 g of Pt / Al_2O_3

Szollosi *et al.* used a flow reactor to obtain high ee (80 %). In this reaction they used EtPy, ketopantolactone and MBF. They demonstrated that the hydrogenation rate of MBF was faster than for EtPy. They also mention that reducing the amount of CD in the system does not accordingly decrease the ee which could point to the chiral surface centres being very stable. They obtained a production rate of methyl mandelate of 28.5 mmol/ $g_{cat} \times h$ and 81 % ee. In this paper they only looked at the rate after varying the CD concentration they gave no unmodified rate to compare the modified reaction to.²⁴

Szollosi *et al.* reported an ee of 90 % using CD to obtain R methyl mandelate and 60 % S-methyl mandelate using CN. In this work they use CD, CN and QD which all gave rate

enhancements. The difference in effectiveness of rate enhancements is due to the adsorption strength of the cinchonas so the order of significance of rate enhancement is CD > CN > QD. They also agree with Tálás *et al.* and report that the rate enhancement is due to the ligand acceleration theory. The reasons they gave for this are; cinchona alkaloids inhibit the poisoning of the catalyst surface; they form chiral surface active-sites and the substrate and modifier forms surface intermediate complexes. However, rate values were not given in this paper.²⁵

Bartok *et al.* used methyl esters of cinchona alkaloids to hydrogenate MBF and pyruvaldehyde dimethyl acetal. Higher ees were found in toluene (88 % *R*) rather than acetic acid (76 % *R*) for the MBF hydrogenation. Methoxycinchonine (24 % *S*) and methoxyquinidine (58 % *R*) gave low ees for the MBF. They found that lower ees could be attributed to the methoxy groups repulsing the substrate. They found that CD (0.02 mmol g⁻¹ s⁻¹) and CN gave a faster rate than the methylester cinchonas. They do not state a value for the rate of CN. They also do not compare the rates to the unmodified reaction. Rates were faster in toluene for the parent cinchonas (CD, quinidine, CN, quinine). However, the rates were faster in acetic acid for the methyl ester cinchona derivative. They found the higher the ee the better adsorption strength of the modifier: CD > MeOCD > quinine > CN > MeOQN > quinidine~MeOQD.²⁶

Bartok *et al.* also published a paper using β-isochonine and CD and used them in nine methyl benzoyl acid substrates including MBF. They found again that toluene gave the faster rate for MBF and an ee of 84 %, although they do not give any rate values or raw data. They say that their work verifies previous findings; if there are aromatic groups on the substrates the solvent plays a significant role in the adsorption-desorption equilibria from the catalyst solvent.²⁷

Different amounts of CD were used to try and find the optimum amount in the MBF hydrogenation reaction and also to see how much of a rate enhancement could be seen (Figure 3.16).

GC analysis was completed to see if there were any by-products (see appendix). The GC analysis showed that there were not any.

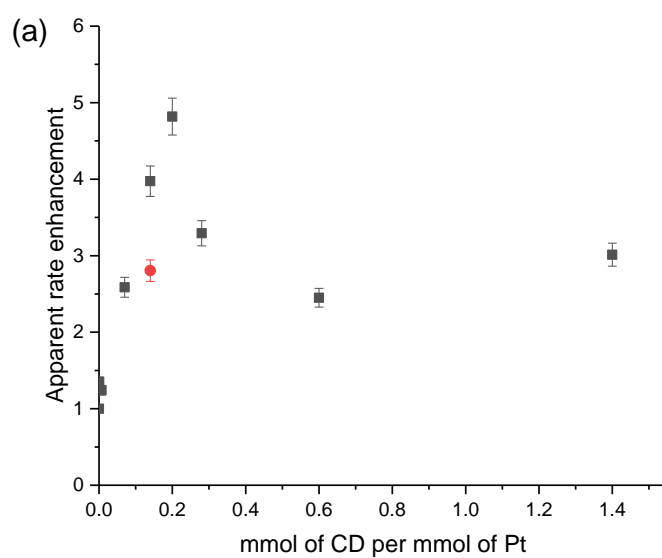
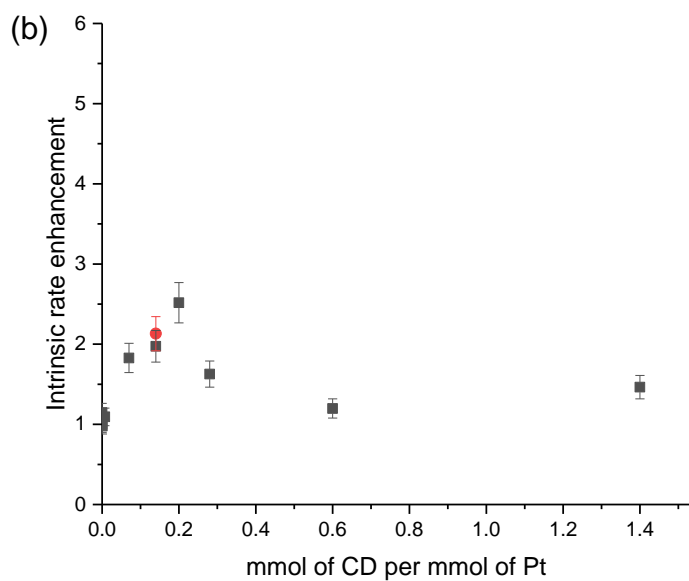


Figure 3.16: Apparent and Intrinsic rate enhancements for the different amount of CD (mmol). CN is in red (●). Reaction conditions: H₂ (20 bar), RT, 5 wt. % Pt / Al₂O₃ (0.06 mmol, 250 mg); MBF (41 mmol, 5.8 mL); neat acetic acid) and cinchonidine.

In both the graphs a volcano-type plot can be seen where the rate enhancement peaks at 0.2 mmol_{CD} mmol_{Pt}⁻¹, and then decreases after that. The decrease could be due to competitive adsorption between the CD and substrate or because of a second CD adsorbing onto a modified site.

Amount of CD (mg)	Amount of CD (mmol)	mmol of additive per mmol of Pt	lin_fit slope / mmol s ⁻¹	apparent enhancement	kinetic fit, k ₂ / mmol s ⁻¹	intrinsic enhancement
0	0	0	6.7×10 ⁻³	1.0	1.4×10 ⁻²	1.0
0.00125	0.0000042	0.00007	8.7×10 ⁻³	1.3	1.6×10 ⁻²	1.1
0.0125	0.000042	0.0007	9.0×10 ⁻³	1.3	1.4×10 ⁻²	1.0
0.125	0.00042	0.007	8.3×10 ⁻³	1.2	1.5×10 ⁻²	1.1
1.25	0.0042	0.07	1.7×10 ⁻²	2.6	2.5×10 ⁻²	1.8
2.5	0.0085	0.14	2.7×10 ⁻²	4.0	2.7×10 ⁻²	2.0
3.75	0.0127	0.2	3.2×10 ⁻²	4.8	3.5×10 ⁻²	2.5
5	0.017	0.28	2.2×10 ⁻²	3.3	2.2×10 ⁻²	1.6
10	0.034	0.6	1.6×10 ⁻²	2.5	1.7×10 ⁻²	1.2
25	0.085	1.4	2.0×10 ⁻²	3.0	2.0×10 ⁻²	1.5
CN	0.0085	0.14	1.9×10 ⁻²	2.8	2.9×10 ⁻²	2.1

In Table 3.14 and Figure 3.16 the different rate values calculated are shown for the MBF hydrogenation using different amounts of CD. The maximum rate enhancements found when $0.2 \text{ mmol}_{\text{CD}} \text{ mmol}_{\text{Pt}}^{-1}$ was used were 4.8 apparent and 2.5 intrinsic rate enhancements. This shows that the CD helps the MBF adsorb to the Pt (111) surface and also lowers the barrier for hydrogenation which helps the reaction speed up intrinsically too. After $0.2 \text{ mmol}_{\text{CD}} \text{ mmol}_{\text{Pt}}^{-1}$ the rate enhancement decreased slightly. This could be because at higher loadings of CD there is competitive adsorption between the modifier and the substrate which lowers the reaction rate and as a second cinchonidine molecule could adsorb onto the modified site. The highest apparent rate found (4.8) in these studies was similar to the rate reported by Talas *et al.* (5.5). When CN was tested there was not such a big difference between the intrinsic rate enhancement and the apparent rate enhancement compared to the same amount of CD that has been added.¹⁷

3.6 Conclusion

In conclusion, reactions using a JM and SA catalyst were used in ETPY, EBF and MBF hydrogenation reactions. CD and CN gave significant rate enhancements in the ETPY hydrogenation and slight rate enhancements in the MBF and EBF hydrogenation. There were differences between the rates the two catalysts gave, and it became clear that overall the JM catalyst gave faster rates, with two exceptions, which through characterization of the catalyst were found to be due to the JM catalyst having smaller nanoparticles, larger pore volume and the SA catalyst having alumina overlay. The CN gave slower rates in all the reactions compared to CD probably because it adsorbs in a tilted way rather than flat like CD.¹⁴ It is unclear why there were two exceptions perhaps the cinchonine modifier only helped adsorption for the SA catalyst and not the JM catalyst.

Reactions were completed using CD and CN in the EtPy, MBF and EBF hydrogenation and were found to give rate enhancements using both modifiers. For CD in all three substrate the rate enhancements hit a peak and then increased quantities of CD decreased the rate and then plateaus. In the EtPy reactions the rates plateau and it has been previously noted that the rates decrease slightly after a certain concentration of CD but not that the rates plateau. This could be that there was competitive adsorption between CD and the substrate molecules. The reason Blaser *et al.* gives for this is that there is a second adsorption of CD onto the enhanced site which stops the substrate to adsorbing onto it.⁸

For EtPy and MBF the rate enhancements found were similar to the rate enhancements found in the literature. However, the rate enhancements found in the EBF reaction using CD were much greater (6.0) than reported by Martin *et al.* (1.54) and Sutyinszki *et al.* (1.28).

Concerning the mechanism of the reaction it seems, from the literature, that the 1:1 CD:EtPy reaction model is the main reason the rate enhancement takes place and perhaps the CD does 'clean' the surface of the EtPy condensation products and decomposition products as well (See introduction). This does not happen for MBF and EBF as it has been stated that MBF cannot form condensation products although they can decompose and form CO which also adsorbs to the catalyst and can deactivate it. So, for the MBF and EBF hydrogenation the reaction rate is enhanced by this 1:1 modifier reactant model which stabilizes the half-hydrogenated state.

3.7 References

1. H. Blaser, H. Jalett, M. Garland, M. Studer, H. Thies and A. Wirth-Tijani, *Journal of Catalysis*, 1998, **173**, 282-294
2. J. Wehrli, A. Baiker, D. Monti and H. Blaser, *Journal of Molecular Catalysis*, 1989, **49**, 195-203.
3. W. Sinkler, S. Bradley, U. Ziese and K. Jong, *Microscopy and Microanalysis*, 2006, **12**, 52-53.
4. E. Rauwel, O. Nilsen, *Journal of The Electrochemical Society*, 2011, **4**, 123-130
5. Y Rozita *et al* 2010 *J. Phys.: Conf. Ser.* 2010, 241
6. H. U. Blaser, H. P. Jalett, D. M. Monti, A. Baiker and J. T. Wehrli, *Structure-Activity and Selectivity Relationships in Heterogeneous Catalysis, Proceedings of the ACS Symposium on Structure-Activity Relationships in Heterogeneous Catalysis*, 1991, 147–155.
7. E. Toukonitty, D. Murzin, *Journal of Catalysis*, 2006, **241**, 96–102.
8. H. Blaser, H. Jalett, M. Müller and M. Studer, *Catalysis Today*, 1997, **37**, 441-463.
9. A. Gamez, K. Kohler, J. Bradley, *catalysis letters*, 1998, **55**, 73-77,
10. H. Blaser, H. Jalett, W. Lottenbach and M. Studer, *Journal of the American Chemical Society*, 2000, **122**, 12675-12682.
11. H. Blaser, H. Jalett and J. Wiehl, *Journal of Molecular Catalysis*, 1991, **68**, 215-222.
12. H. Blaser, H. Jalett, M. Müller and M. Studer, *Catalysis Today*, 1997, **37**, 441-463.
13. A. Gamez, J. Kohler and J. Bradley, Solvent effects in the kinetics of the enantioselective hydrogenation of ethyl pyruvate, *Catalysis Letters*, 1998, **55**, 73–77
14. M. Bartók, M. Sutyinszki, K. Balázsik and G. Szöllösi, *Catalysis Letters*, 2005, **100**, 161-167
15. K.E. Simons, P.A. Meheux, S.P. Griffiths, I.M. Sutherland, P. Johnston, P.B. Wells, A.E Carley, M.K. Rajumon, M.W. Roberts and A. Ibbotson, *Reel. Trav. Chim. Pays-Bas*, 1994, **113**, 465.
16. H. Blaser, H. Jalett, W. Lottenbach and M. Studer, *Journal of the American Chemical Society*, 2000, **122**, 12675-12682.
17. E. Tálas, J. Margitfalvi and O. Egyed, *Journal of Catalysis*, 2009, **266**, 191-198.
18. G. Martin, P. Mäki-Arvela, D. Murzin and T. Salmi, *Catalysis Letters*, 2013, **143**, 1051-1060.
19. M. Sutyinszki, K. Szöri, K. Felföldi and M. Bartók, *Catalysis Communications*, 2002, **3**, 125-127.
20. M. Bartók, K. Felföldi, G. Szöllösi, *et al.* Rigid cinchona conformers in enantioselective catalytic reactions: new cinchona-modified platinum catalysts in the Orito reaction. *Catalysis Letters*, 1999, **61**, 1–5
21. G. Martin, P. Mäki-Arvela, D. Murzin and T. Salmi, *Catal. Sci. Technol.*, 2014, **4**, 170-178.
22. Sutyinszki, M., Szöri, K., Felföldi, K. *et al.* Heterogeneous Asymmetric Reactions. 29. Enantioselective Hydrogenation of Ethyl Benzoylformate over DihydroCD-Modified Platinum–Alumina Catalyst in Acetic Acid. *Catalysis Letters*, 2002, **81**, 281–284
23. E. Toukonitty, P. Mäki-Arvela, N. Kumar, T. Salmi and D. Y. Murzin, *Catalysis Letters*, 2004, **95**, 179–183.
24. G. Szöllösi, B. Hermán, F. Fülöp and a. Bartók, *Reaction Kinetics and Catalysis Letters*, 2006, **88**, 391-398.
25. G. Szöllösi, S. Cserényi, F. Fülöp and M. Bartók, *Journal of Catalysis*, 2008, **260**, 245-253.
26. K. Balázsik, I. Bucsi, S. Cserényi, G. Szöllösi and M. Bartók, *Journal of Molecular Catalysis A: Chemical*, 2008, **285**, 84-91.
27. K. Szori, K. Balazsik, K. Felfoldi and M. Bartok, *Journal of Catalysis*, 2006, **241**, 149-154

Chapter 4

Understanding the mechanism of the rate enhancement of cinchonidine in α -keto ester reduction using analogues of its deconstructed parts

To understand the mechanism of the rate enhancement of α -keto ester reduction produced by cinchonidine (CD) (Figure 4.1), the molecule was deconstructed into specific moieties that potentially play a role in the rate enhancement mechanism. Commercially available analogues that are structurally related to these moieties were subsequently investigated in EtPy hydrogenation reactions to determine if they caused a rate enhancement.

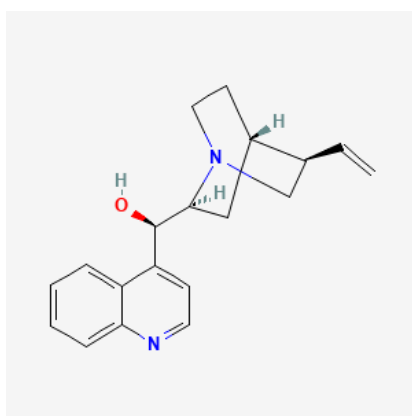
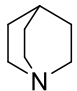
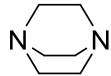
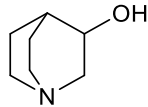
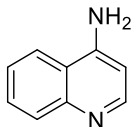


Figure 4.1: The structure of cinchonidine

Four molecules were explored that each contained some but not all the moieties present in CD as illustrated in Table 4.1 and Figure 4.2; quinuclidine (QD), DABCO, 3-quinuclidinol (QL) and aminoquinoline (AQ). QD, according to the literature, contains one of the most important parts of the CD molecule as it has the basic nitrogen that allows stabilization of the half-hydrogenated substrate. DABCO was of interest as it has two nitrogen atoms, the second one being in the 4-position on the QD ring, which could potentially produce double the rate enhancement. QL was investigated as it has the QD structure but also has an OH group at the

3-position. AQ was selected as it has a quinoline ring and a basic nitrogen but no QD moiety or OH group. The basis of discussion is centred around the apparent rate (aR) and the intrinsic rate (iR) enhancement afforded by addition of a modifier, e. g. CD, QD, QL, AQ, or DABCO, over the unmodified reaction. An apparent rate enhancement of 2 would imply that the reaction proceeds at twice the rate (mmol s^{-1}) of the unmodified reaction rate. In this case the unmodified reaction would have an apparent rate of 1. The iR enhancement as explained in the experimental section is the rate enhancement that does not include the adsorption equilibria. The modifier in some instances potentially can help the substrate adsorb onto the surface and the iR enhancement calculation does not take this into account. Therefore, the iR is the rate enhancement found intrinsically in the system.

Table 4.1 Molecules used to understand the influence of CD on rate enhancement.					
Entry	Molecule	Name	Section	pKa	Boiling point ($^{\circ}\text{C}$)
1		Quinuclidine (QD)	4.1	11 ¹	198 ¹
2		1,4-diazabicyclo[2.2.2]octane (DABCO)	4.2	9 ²	158 ²
3		3-quinuclidinol (QL)	4.3	10	207
4		4-aminoquinoline (AQ)	4.4	N/A	N/A

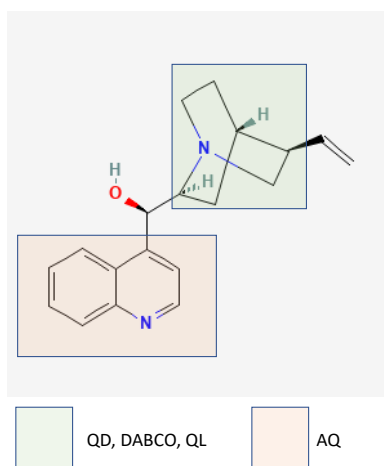


Figure 4.2: The structure of CD showing the different parts that QD, DABCO, QL and AQ mimic

4.1 Reaction in neat toluene

A reaction using QD in the enantioselective hydrogenation of ethyl pyruvate was completed using neat toluene (Figure 4.3) as the solvent to see if there is a difference in rate when acetic acid is absent from the reaction. This is important as it has been stated previously that acetic acid protonates the nitrogen on the achiral tertiary amine.³ This is said to be a reason why the rate enhancement is greater in acetic acid than in toluene + 0.001 M acetic acid.

In Figure 4.3 the hydrogen uptake pressure of the two reactions can be seen. The iRs given by both neat toluene (3.4) and toluene + 0.001 M acetic acid (3.4) were the same. So, these reactions show that acetic acid does not have a significant influence on the EtPy reaction when using QD. This shows that acetic acid protonating the modifier has no effect on the rate. This shows that adding a base (QD) to an acidified reaction mixture does not change this reaction and that the rate enhancement is the same as the QD modifier still modifies the reaction.

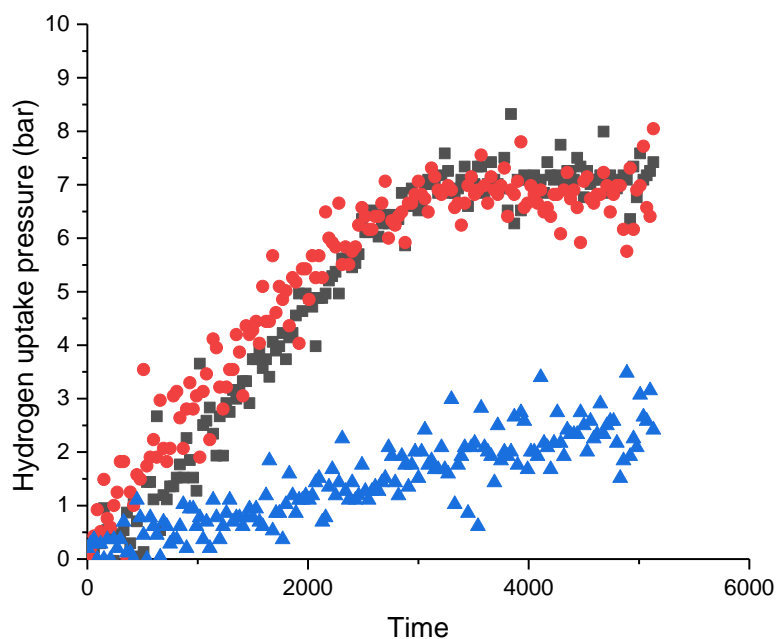


Figure 4.3: Reactions using QD in the ethyl pyruvate hydrogenation using neat toluene (■) and Toluene + 0.001 M acetic acid (●) and the unmodified reaction (▲) in toluene + 0.001 M acetic acid: Reaction conditions: H₂ (20 bar), RT, 5 wt.% Pt / Al₂O₃ (0.06 mmol, 250 mg); EtPy (45 mmol, 5.2 mL) toluene + 0.001 M acetic acid , toluene QD (0.9 mmol, 0.1 g)

4.2 Comparison of the two catalysts

In Chapter 3 the two 5% Pt on alumina catalysts coming from both Sigma Aldrich and Johnson Matthey were used in the hydrogenation reactions of MBF, EBF and EtPy with CD and CN as a modifier. It was found that overall the SA catalyst gave higher aRs and iRs as the unmodified rate values were much lower than JM so the aRs and iRs were higher for SA. This is because the aRs and iRs are found by dividing the modified rate values by the unmodified rate values. So, overall the rate values calculated were higher for JM. The reasons for this were

found when the catalysts were characterized: the JM catalyst had a larger pore radius and pore volume; the JM catalyst's nanoparticles were smaller, and the SA catalysts nanoparticles were encapsulated in alumina. In this chapter these two catalysts were used in the hydrogenation of these two substrates using the modifiers QD, DABCO and QL.

Figure 4.4 shows the hydrogen uptake (bar) curves of the EtPy hydrogenation using the SA (a) and JM (b) catalysts. There is a slow reaction rate over the unmodified catalyst as seen in Chapter 3, and on addition of the modifiers (QD, DABCO and QL) there is a significant increase in rate. Here the slope of the uptake profile increases in a linear fashion until the reaction is close to completion, whereupon the rate decreases and plateaus. Approximately 8 bar of hydrogen (45 mmol) is required to hydrogenate one of the carbonyls of ethyl pyruvate. Table 4.2 illustrates the rate information calculated from the uptake profiles according to the methods described in Chapter 2. The apparent rate enhancement is calculated using the linear slope (lin_fit slope) which is the product of the surface coverage of the reactant on the catalyst and the rate constant. The apparent rate enhancement is showing the combination of the modifier enhancing the adsorption of the reactant to the active site and lowering the barrier to the hydrogenation step. Therefore, the intrinsic rate enhancement is the rate enhancement that is not including the surface coverage of the reactants and is showing the intrinsic rate enhancement given by the system and shows if the modifier lowers the barrier to hydrogenation. The lin_fit slope is the initial gradient of the uptake curve and the intrinsic rate enhancement is calculated using the kinetic slope which is the initial gradient and the rest of the hydrogen uptake curve.

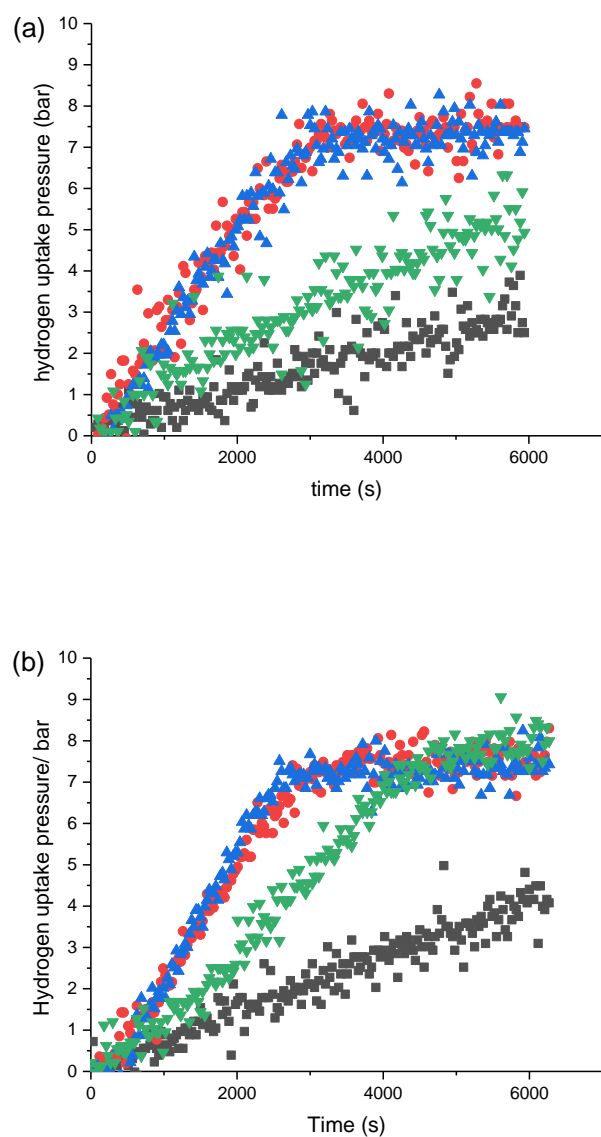


Figure 4.4: The hydrogen uptake graphs of the EtPy hydrogenation using QD (red ●), DABCO (blue ▲), QL (green ▼) and no modifier (black ■) and the two different catalysts SA (a) and JM (b): H₂ (20 bar), RT, 5 wt.% Pt / Al₂O₃ (0.06 mmol, 250 mg); EtPy (45 mmol, 5.2 mL); toluene + 0.001 M acetic acid); QD (0.9 mmol, 100 mg), QL (0.08 mmol, 10 mg), DABCO (0.9 mmol, 101 mg).

Table 4.2 - Comparison of the rate values calculated for the JM catalyst and Sigma Aldrich catalyst with different modifiers with EtPy hydrogenation.

Modifier	lin fit_slope/ mmol s ⁻¹ (10 ⁻³)		aR		Kinetic slope/ mmol s ⁻¹ (10 ⁻³)		iR	
	JM	SA	JM	SA	JM	SA	JM	SA
UM	4.6	3.0	1.0	1.0	6.4	3.8	1.0	1.0
QD	16.4	14.5	3.6	4.5	17.2	16.2	2.8	4.0
DABCO	20.7	17.2	4.5	5.4	20.2	18.9	3.3	4.6
QL	9.9	5.5	2.2	1.9	10.4	7.4	1.6	2.1

aR = apparent rate enhancement over unmodified reaction

iR = intrinsic rate enhancement over unmodified reaction.

In Figure 4.4 and Table 4.2 the different rates are shown. As discussed in Chapter three the JM catalyst gave faster rates for the unmodified reaction compared to SA and therefore the subsequent rate enhancements were lower. For the three modifiers QD, DABCO and QL the kinetic slope and the lin_fit slope were faster over the JM catalyst than over the SA catalyst. In this reaction DABCO gave better rate enhancements for both catalysts than the other two modifiers. This may be due to the other basic nitrogen on the DABCO, which increases the basicity, helping to attract and stabilise two ethyl pyruvate molecules at the same time allowing it to enhance the rate more than QD.

QL gave a significant rate enhancement in both catalysts, but it gave a smaller rate enhancement than in the other two modifiers. A smaller amount of QL was used in this reaction compared with the other modifiers.

4.3 EBF hydrogenation

The different catalysts SA (a) and JM (b) were tested in the EBF hydrogenation using QD and DABCO in order to compare the rates of the two catalysts (Figure 4.5). There is a slow reaction rate over the unmodified catalyst and addition of a modifier (QD or DABCO) greatly improves the reaction rate. Here, over the SA catalyst the slope of the uptake profile is more rounded and is more of a curve than the slopes on the JM catalyst uptake graph. Approximately 6 bar of hydrogen (43 mmol) is required to hydrogenate one of the carbonyls of EBF. Table 4.3 illustrates the rate information calculated from the uptake profiles according to the methods described in Chapter 2.

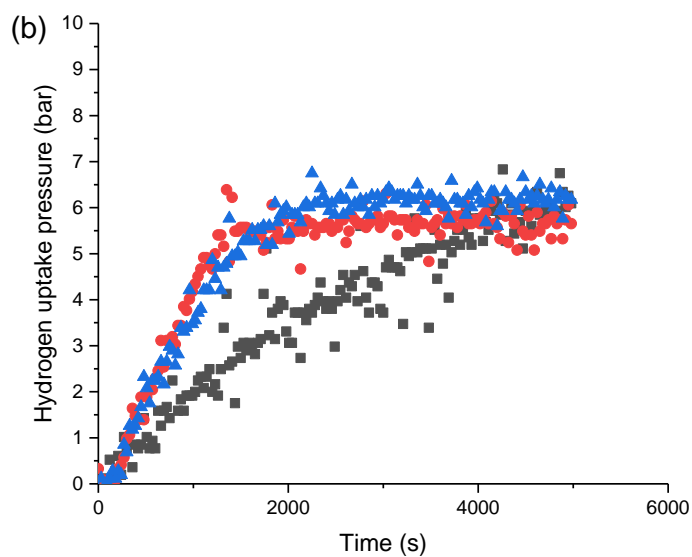
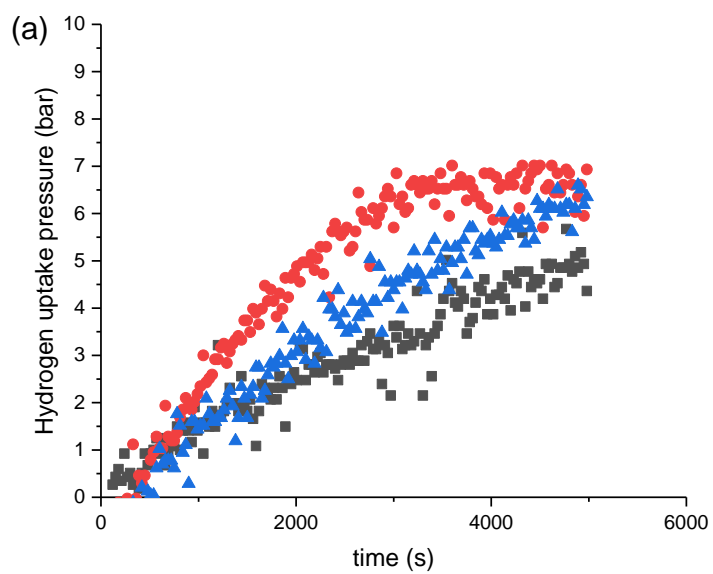


Figure 4.5: The hydrogen uptake graphs of the hydrogenation using QD (red ●) and DABCO (blue ▲) no modifier (black ■) and the two different catalysts SA (a) and JM (b). : H₂ (20 bar), RT, 5 wt.% Pt / Al₂O₃ (0.06 mmol, 250 mg); EBF (43 mmol, 6.2 mL); toluene + 0.001 M acetic acid); QD (0.9 mmol, 100 mg), DABCO (0.9 mmol, 101 mg).

Table 4.3 - Comparison of the rate values calculated for the JM catalyst and Sigma Aldrich catalyst with different modifiers with EBF hydrogenation								
Modifier	lin fit_slope/ mmol s ⁻¹ (10 ⁻³)		aR		Kinetic slope/ mmol s ⁻¹ (10 ⁻³)		iR	
	JM	SA	JM	SA	JM	SA	JM	SA
UM	9.6	6.4	1.0	1.0	24.4	7.6	1.0	1.0
QD	29.7	14.4	3.1	2.6	35.2	15.0	1.4	2.2
DABCO	25.4	10.4	2.6	1.9	34.4	13.3	1.4	1.9

aR = apparent rate enhancement over unmodified reaction

iR = intrinsic rate enhancement over unmodified reaction.

In Figure 4.5 and Table 4.3 the different rates values are shown. Like with the EtPy reaction the unmodified rates were faster using the JM catalyst than the SA catalyst and because of this the rate enhancements were found to be larger with the SA catalyst. QD gave a faster rate than DABCO so the second basic nitrogen on the DABCO did not have an effect in this reaction. Both modifiers gave a significant rate enhancement using both catalysts.

4.4 MBF hydrogenation

The different catalysts SA (a) and JM (b) were tested in the MBF hydrogenation using QD, DABCO and QL as modifiers in order to compare the rates of the two catalysts. There is a slow reaction rate over the unmodified catalyst and addition of a modifier (QD, DABCO or QL) greatly improves the reaction rate. Over the JM catalyst there is a linear slope where the rate then decreases and then plateaus (Figure 4.6a). Over the SA catalyst the uptake profile is similar to this except for the lines are more curved. Approximately 6 bar of hydrogen (41 mmol)

is required to hydrogenate one of the carbonyls of MBF. Table 4.4 illustrates the rate information calculated from the uptake profiles according to the methods described in Chapter 2.

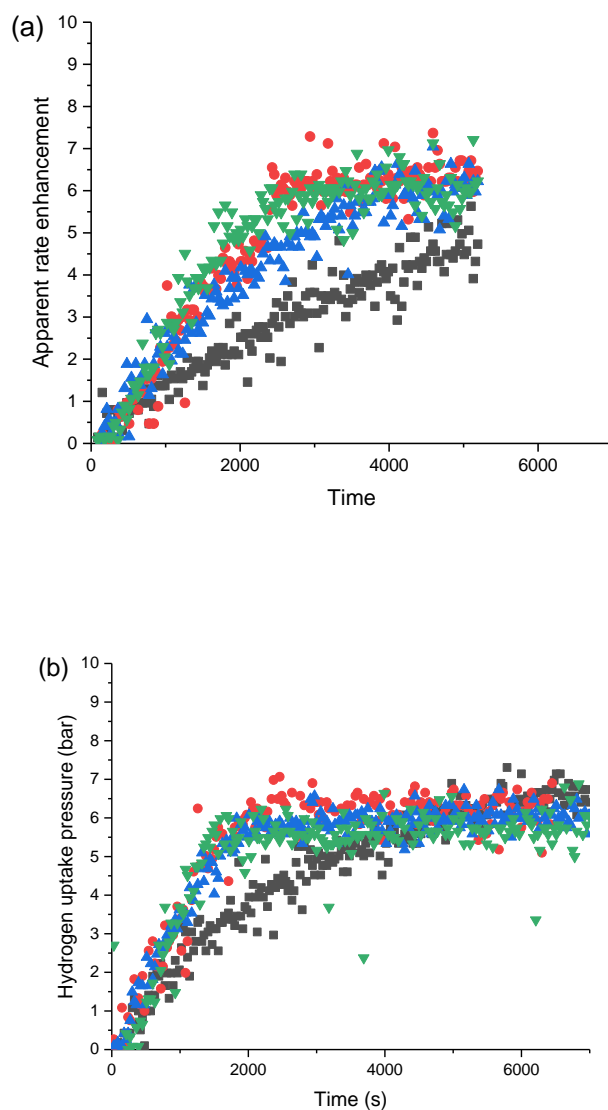


Figure 4.6: The hydrogen uptake graphs of the MBF hydrogenation using QD (●), DABCO (▲), QL (▼) and no modifier (■) and the two different catalysts SA (a) and JM (b). H₂ (20 bar), RT, 5 wt.% Pt / Al₂O₃ (0.06 mmol, 250 mg); MBF (41 mmol, 5.8 mL); toluene + 0.001 M acetic acid); QD (0.9 mmol, 100 mg), QL (0.08 mmol, 10 mg), DABCO (0.9 mmol, 101 mg).

Table 4.4- Comparison of the rate values calculated for the JM catalyst and Sigma Aldrich catalyst								
Modifier	lin fit_slope/ mmol s ⁻¹ (10 ⁻³)		aR		Kinetic slope/ mmol s ⁻¹ (10 ⁻³)		iR	
	JM	SA	JM	SA	JM	SA	JM	SA
UM	10.2	5.5	1.0	1.0	15.5	6.8	1.0	1.0
QD	20.2	14.4	2.0	2.6	22.4	15.0	1.4	2.2
DABCO	24.4	10.4	2.4	1.9	32.8	13.3	2.1	1.9
QL	28.4	14.2	2.8	2.6	28.4	16.6	1.8	2.4

aR = apparent rate enhancement over unmodified reaction

iR = intrinsic rate enhancement over unmodified reaction.

The three substrates' rates for the unmodified reaction were faster with the JM catalyst than the SA catalyst (Figure 4.6 and Table 4.4). QL gave a significant rate enhancement when used in the SA catalyst and a better rate enhancement than QD in the JM catalyst considering that a lot less QL was used compared to QD. This means that QL was very effective in this reaction enhancing the rate. It could be speculated that the OH group attached to the QL could form hydrogen bonds with one of the carbonyl groups further attracting the reactant in a similar way to CD in Baiker *et al.*'s published work.⁴ The DABCO modifier gave a faster rate in the JM catalyst whereas QD gave faster rates in the SA catalyst.

4.5 Summary of catalyst comparison

A comparison of the catalysts in the three different substrate hydrogenations using QD, DABCO and QL are shown in Figure 4.7. The apparent rate enhancements for QL for the MBF and EtPy reaction show that the JM catalyst gives the highest apparent rate enhancement. For

DABCO JM catalysts give the highest apparent rate enhancement in EBF and MBF reactions whereas the SA catalyst is highest for the EtPy reaction. For QD the JM catalyst gave higher apparent rate enhancements for the EtPy and the MBF reactions whereas the SA catalyst gave the highest apparent rate enhancement for the EtPy.

In general, the rates values given were faster using the JM catalyst than the SA catalyst in all instances. This could be for the reasons outlined in Chapter 3 in the characterization section where: the JM catalyst had a larger pore radius and pore volume; the JM catalysts nanoparticles were smaller, and the SA catalysts nanoparticles were encapsulated in alumina. As this is the case it shows that the modifiers are dependent on Pt particles on the catalyst for the rates. This implies that these modifiers are increasing the rate of reaction at the surface of the platinum. In the next sections only the SA catalyst was used not the JM catalyst.

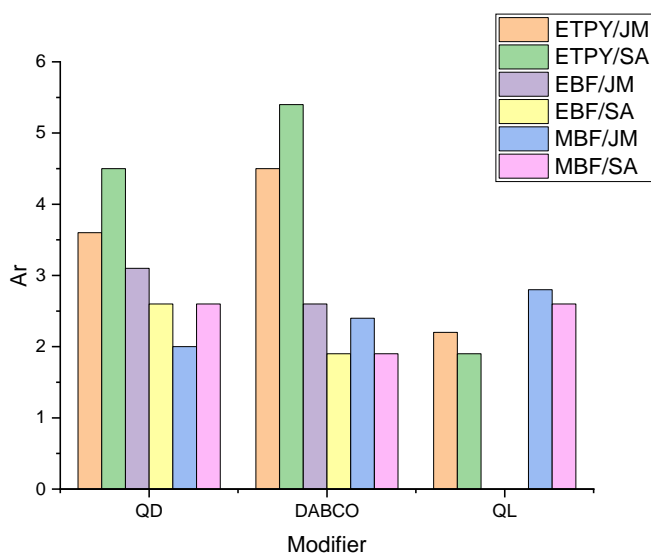


Figure 4.7: Apparent rate enhancement showing the catalyst comparison in the EtPy, MBF and EBF hydrogenation using the modifiers QD, DABCO and QL.

4.6 4-Aminoquinoline (AQ)

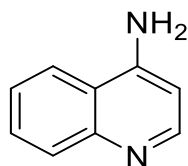


Figure 4.8: Structure of AQ

AQ (Figure 4.8) was thought of as a suitable molecule to study as a modifier as it has the quinoline moiety which is part of the reason CD is widely accepted as causing the CD-induced rate enhancement in Pt-catalysed hydrogenation reactions. The quinoline moiety is an integral part of the CD molecule which allows it to form the open 3 conformer which has been reported to yield the highest rate and ee. This is a significant difference with CD compared to AQ as AQ cannot form the open 3 conformer as the QD moiety is not present. It also has a basic nitrogen group which is thought to be essential for the rate enhancement (see Chapter 1 Introduction) as when it is protonated it attracts the substrate and stabilises its half-hydrogenated state by facilitating H-bonding. In the literature no published work has been found using AQ in the EtPy, MBF or EBF hydrogenation reactions. The only published work that has used a modifier similar to AQ is (S)-1-(1-naphthyl) ethylamine and (R)-1-(1-naphthyl) ethylamine (Figure 4.9) where it has a naphthalene ring rather than a quinoline ring and is a secondary amine that has a methyl group attached next to the amine part.⁵ In this paper they state that through NMR experiments they report that the modifier actually reacts with EtPy rapidly and forms another secondary amine which is the modifier that provides the rate enhancement in their reaction. (Figure 4.10) This could mean that AQ goes through a similar reaction with EtPy. However, NMR experiments would have to be completed using this reaction too to confirm this.

This modifier gave an apparent rate enhancement of 6 compared to the unmodified reaction and increased the ee in the EtPy hydrogenation. With this modifier it was necessary to use a different solvent as it was insoluble in toluene; the solvent used was neat concentrated acetic acid. Minder *et al.* (1996) used a 5% Pt/ Al₂O₃ catalyst (50 mg) and 5.8 mg of modifier.⁵

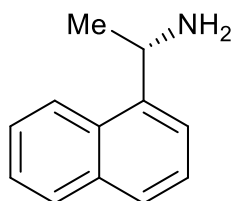


Figure 4.9: The structure of (R)-1-(1-naphthyl) ethylamine

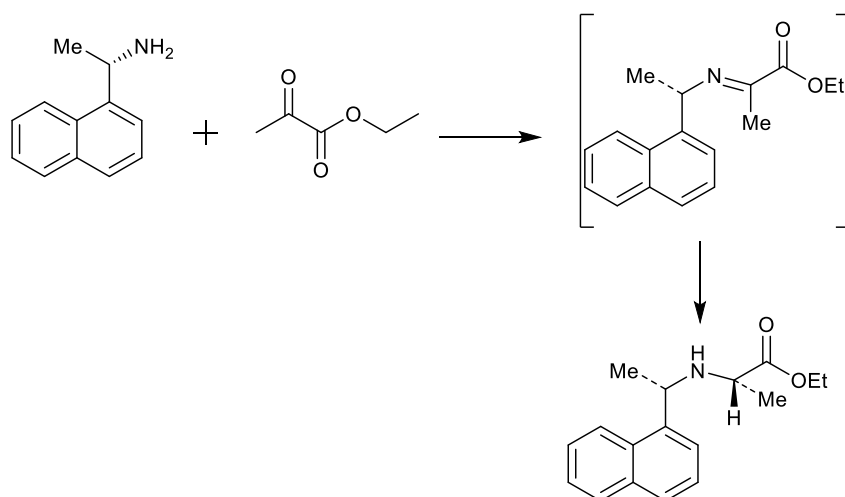


Figure 4.10: Reaction mechanism of (R)-1-(1-naphthyl) ethylamine modifier with EtPy

4.6.1 EtPy hydrogenation

AQ contains the two most important parts of the CD moiety that are needed for the rate enhancement, i. e, the basic nitrogen and aromatic group that adsorb onto the platinum. When added to the EtPy hydrogenation reaction AQ is therefore expected to give a rate enhancement. The results presented in this section are novel as there are no previous reports using AQ modifier in these types of reactions (Figure 4.11).

Table 4.5- Rate values measured and calculated for the different amounts of AQ in the EtPy reaction						
Amount of AQ (g)	Amount of AQ (mmol)	mmol additive per mmol of Pt.	lin_fit slope / mmol s ⁻¹	apparent enhancement	kinetic fit, k ₂ / mmol s ⁻¹	intrinsic enhancement
0	0	0	3.9×10 ⁻³	1.0	6.9×10 ⁻³	1.0
0.01	0.07	1.1	1.1×10 ⁻²	2.9	1.3×10 ⁻²	1.8
0.05	0.35	5.5	1.5×10 ⁻²	4.0	1.9×10 ⁻²	2.7
0.1	0.7	11	1.4×10 ⁻²	3.7	1.7×10 ⁻²	2.4
0.15	1.05	16.5	1.2×10 ⁻²	3.1	1.4×10 ⁻²	2.0
0.2	1.4	22	1.2×10 ⁻²	3.2	1.5×10 ⁻²	2.2
CD (0.0025)	0.0085	0.14	3.8×10 ⁻²	9.7	4.2×10 ⁻²	8.6

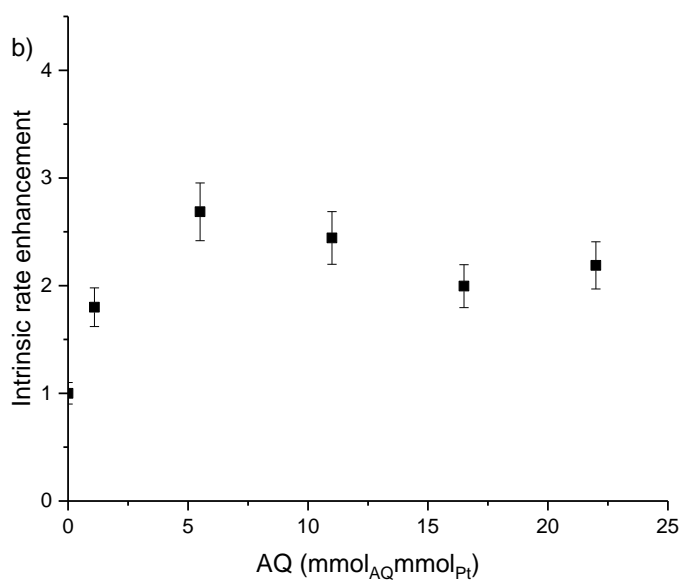
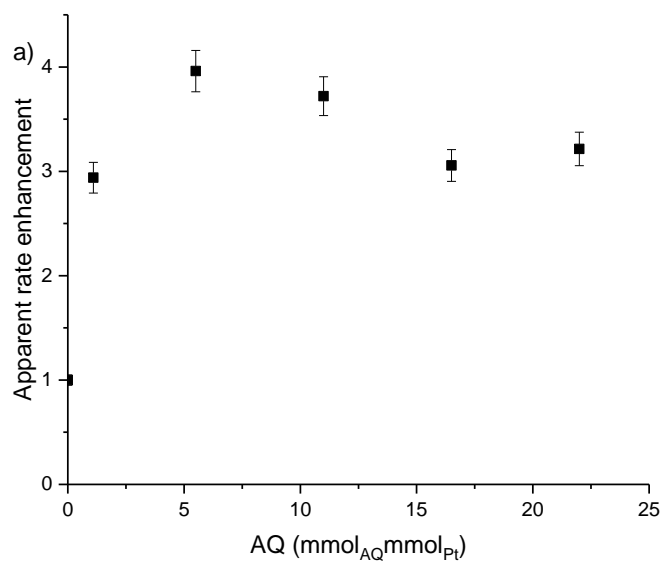


Figure 4.11: The influence of the apparent rate enhancement (a) and the intrinsic rate enhancement (b) as a function of the moles of AQ on the EtPy (■) hydrogenation reactions. Reaction conditions: H₂ (20 bar), RT, 5 wt. % Pt / Al₂O₃ (0.06 mmol, 250 mg); EtPy (45 mmol, 5.2 mL) toluene + 0.001 M acetic acid

In Table 4.5 and Figure 4.11 the optimal rate enhancement was observed using $5.5 \text{ mmol}_{\text{AQ}} \text{ mmol}_{\text{Pt}}^{-1}$. Adding further amounts of AQ caused the rate enhancement to decrease and then plateau. Additional reactions would be needed to determine if adding more aminoquinoline would increase the rate enhancement further or if this is just normal variation expected in the experiment. The apparent rate enhancement (4.0) of $5.5 \text{ mmol}_{\text{AQ}} \text{ mmol}_{\text{Pt}}^{-1}$ was much greater than its intrinsic rate enhancement (2.7). This means that AQ helps EtPy adsorb onto the surface as the aR takes the surface coverage of the reactants and the adsorption equilibria into account.

In Table 4.5 the comparison of CD and AQ is shown. CD gave a much greater aR enhancement (9.7) and iR (8.6) than any of the quantities of AQ tested. The amount of CD ($0.14 \text{ mmol}_{\text{CD}} \text{ mmol}_{\text{Pt}}^{-1}$) tested was also much smaller than AQ (Table 4.5). This shows that the QD moiety on the cinchonidine, absent on AQ, is also integral to causing the rate enhancement. The mode of action for the AQ modifier in the EtPy reaction is thought to be very similar to the CD_EtPy mode of action (Figure 4.12). This mode of action can occur as it has two of the important parts of the cinchonidine (quinoline ring and basic nitrogen), although no papers have been published using AQ as a modifier to provide evidence for this.

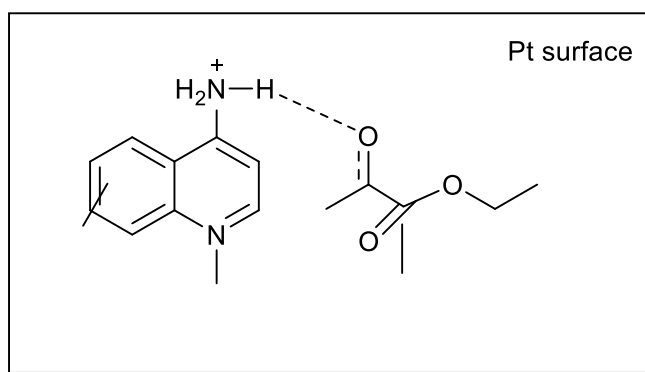


Figure 4.12: Potential mode of action of AQ and EtPy

4.7 Reactions with QD

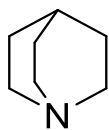


Figure 4.13; The structure of QD

The structure of QD is shown in Table 4.1 and Figure 4.13. The effect of QD modifier on the rate enhancement was investigated using three different substrates, EtPy, EBF and MBF. This section initially compares the results from all three substrates and then individually.

Toukoniity *et al.* reported that when using low concentrations of EtPy, the addition of QD alone reduced the reaction rate by 50% and the ee remained zero, the same as was obtained without QD. It was only at higher concentrations of EtPy that a rate enhancement was found. In the same paper they used CD with QD and found that there was an apparent rate enhancement factor of 1.9 above the un-modified reaction (i. e. normalised to 1). They reasoned that the rate enhancement is caused by reduction of catalyst deactivation as at lower concentrations of EtPy catalyst deactivation is negligible. Adsorbing EtPy molecules is said to deactivate the catalyst as side reactions occur (EtPy ester polymerisation) following adsorption.⁶

Wells *et al.* used bismuth and sulfur to attempt to gain a better understanding of where the reaction takes place on the catalyst; the step or terrace sites. At suitable concentrations bismuth adsorbed onto step (100) and terrace sites, and sulfur adsorbed onto the step and terrace sites but with the (111) step sites being strongly disfavoured. QD gave an apparent rate enhancement of 18 in this reaction (0.25 g of Pt / graphite, with DCM as the solvent, 65 mmol of EtPy, 30 bar of H₂, RT, 0.17 mmol of QD and 1000 rpm stirring speed). Polymerisation of

EtPy was reported to occur at step sites. In the presence of bismuth, CD and QD were reported to be as effective as each other at giving a rate enhancement. The rate enhancement using QD was thought to be due to removal of the surface oligomers of EtPy, as similarly proposed by Toukoniitty *et al.*^{6,7}

Margitfalvi *et al.* reported that achiral tertiary amines, including QD and DABCO, could be used in the Pt / Al₂O₃ /cinchona system. They found that the effect of these achiral tertiary amines was very much solvent and concentration dependent. They also discovered that the achiral tertiary amines only enhanced the rate when added to a low-concentration cinchona /Pt / Al₂O₃ system. When using QD they observed that the rate given in the first 6-10 mins was 3.6 times that of the unmodified reaction and the rate enhancement they found at 10-40 mins was 3.8 (50 bar of H₂, a temperature of 20 °C, 1 M EtPy, 1.2×10⁻⁵ M of CD, 1.2×10⁻⁵ M of QD and 0.125 g of Pt / Al₂O₃).⁸

Bond *et al.* were the first to propose that the protonated QD molecule stabilizes the half-hydrogenated alpha-keto ester (Figure 4.14). They used methyl pyruvate which is thought to have the same mechanism as the EtPy hydrogenation. It was postulated that this half-hydrogenated state would be less likely to go through H-atom loss and then the surface coverage would increase. They also used quinoline which is the aromatic part of CD that adsorbs onto the surface of the Pt(111). When added to the reaction it gave an apparent rate enhancement of 2, suggesting that the aromatic moiety contributes to significant rate enhancement with CD. Bond *et al.* also found that QD gave an initial rate enhancement of 6.5. In this paper they also investigated QL and found that it gave an initial rate enhancement of 6.5. These reactions for methyl pyruvate were performed at 10 bar H₂ pressure, 293 K, 10 mL of methyl pyruvate, 0.1 g of 6.3% Pt / silica catalyst, with 20 mL of ethanol used as a solvent.⁹

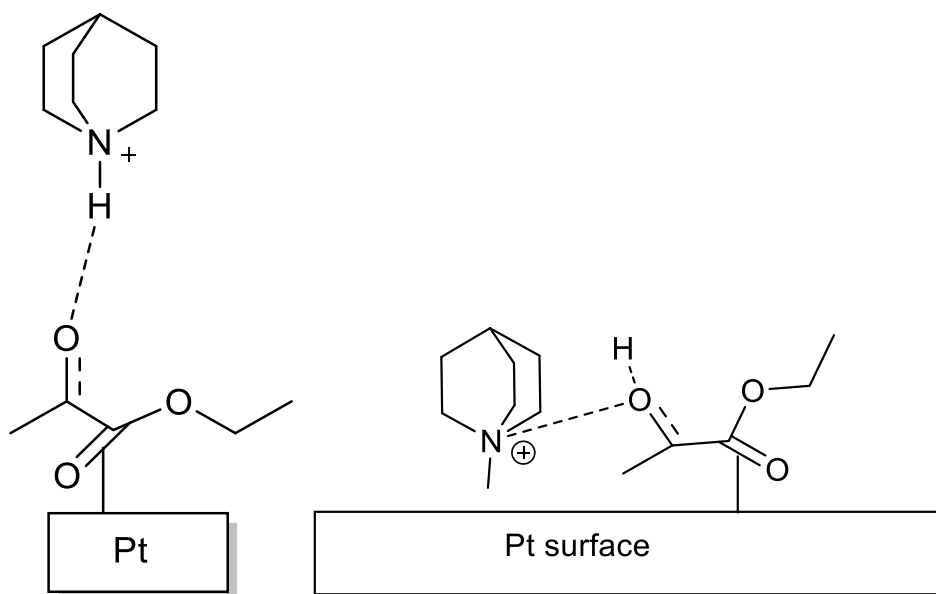


Figure 4.14: Protonated QD stabilising the half-hydrogenated state of EtPy, adapted from Figure 4 in Bond *et al.*'s work, where the QD has not adsorbed to the Pt (left).⁹ QD adsorbed to the surface through the lone pair of the nitrogen stabilising the half-hydrogenated EtPy. The right hand side is a speculated interaction from a dipole that could happen between the QD and EtPy.

It was not mentioned by Bond *et al.* if the QD adsorbs to the surface but Fierri *et al.* show through IR experiments and theoretical calculations that QD adsorbs onto the surface through the lone pair on the nitrogen (Figure 4.14).¹⁰ If it adsorbs via the nitrogen atom it would mean that it could not be protonated. However, it has been stated previously by Baiker that the QD moiety of CD did not need to be protonated to stabilize the EtPy molecule.¹¹ Although, if QD adsorbs to the Pt surface as stated in Fierri *et al.*'s paper the nitrogen would not be able to stabilize the half-hydrogenated state through the hydrogen. Therefore, it could potentially stabilize the half-hydrogenated state through dipole-dipole interaction with the oxygen on the carbonyl instead (Figure 4.14).

Furthermore, Margitfalvi *et al.* suggested that QD works together with CD to uncouple the EtPy polymers. Using circular dichroism measurements, they suggested that when achiral amines were added to the reaction mixture the virtual concentration of CD increased which therefore increased the optical yield as it decreased the dimer / monomer ratio of EtPy. The reason for this effect was unclear but one theory, suggested by adsorption measurements, was that the achiral tertiary amine prevented CD from adsorbing on the support. However, this was not seen in reactions with 9-methoxy-cinchonidine and therefore this theory was discarded. Another theory put forward is that the CD itself undergoes reduced hydrogenation when achiral tertiary amines are present. Margitfalvi *et al.* contradict the hypothesis for the rate enhancement supported by Wells *et al.*, namely that QD cleans the surface of the platinum from oligomers of EtPy, as Margitfalvi used methyl benzoyl formate (MBF) and rate enhancement was reported, although, MBF cannot form oligomers.¹²

In subsequent work Margitfalvi *et al.* show that the effects of QD are strongly concentration-dependent and that earlier NMR studies indicate there are interactions in the liquid phase between EtPy and CD and QD. The presence of QD with CD increased the enantioselectivity and the rate of hydrogenation as well as the initial rate.¹³

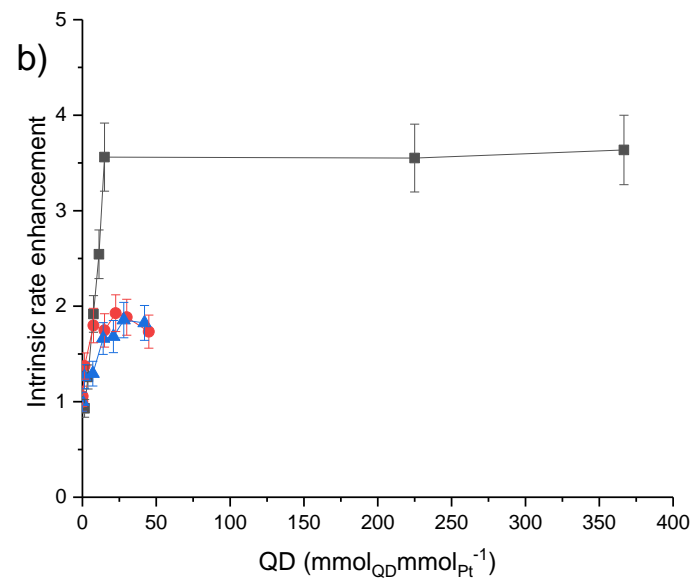
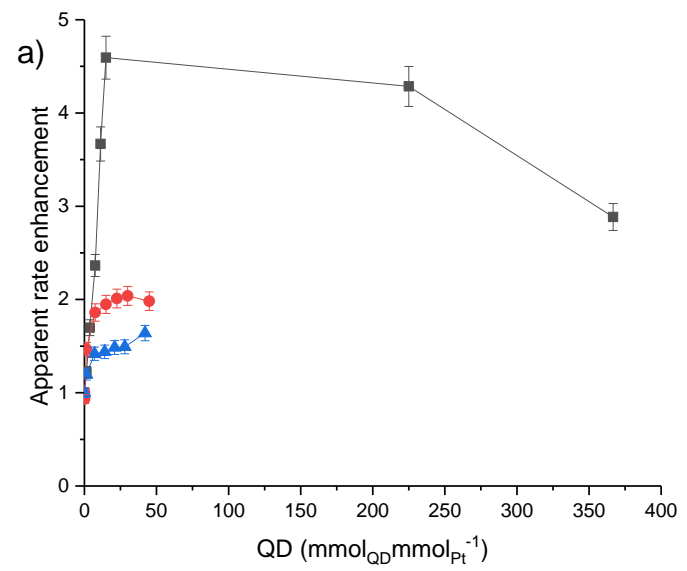
The mechanism of the mode of action of how quinuclidine increases the rate is not clear it could either be that the protonated nitrogen stabilises the half-hydrogenated substrate like CD or helps stabilize the oxygen on the carbonyl when it has adsorbed to the Pt surface (Figure 4.14) or it helps clean the catalyst of the product of side reactions and decomposition of the substrate which is a possible reason given by Toukoniitty *et al.*⁶ Although it has been said by Margitfalvi *et al.* that MBF cannot form oligomers, perhaps the MBF can still decompose and deactivate parts of the catalyst which could then be cleaned by the additives. The exact mode of action remains unclear. All that is known for sure is that the nitrogen on the quinuclidine is

important as Blaser *et al.* have shown that when the nitrogen is alkylated with a $-\text{CH}_2\text{OH}$ group on the CD molecule there is a decrease of rate from 120 to 37 $\text{mmol min}^{-1} \text{g}^{-1}$.¹⁴

GC analysis was completed using EtPy and MBF to see if there were any by products and no by products were found.

4.8 Comparison of EtPy, EBF and MBF with QD modifier

In Figure 4.15 the influence on the rate of reaction of different substrates as a function of modifier concentration of QD ($\text{mmol}_{\text{QD}} \text{mmol}_{\text{Pt}}^{-1}$) can be seen. Comparing the aRs (Figure 4.15) and iRs (Figure 4.15) for each of the substrates showed that there was a much larger rate enhancement in the EtPy reaction than for either MBF or EBF. Steric effects could be the source of this difference as both MBF and EBF have an aromatic ring attached which could make it more difficult for QD to react with EBF and MBF when they are adsorbed onto the Pt surface. In Figure 4.15 the aR for EtPy increases sharply up until 15 $\text{mmol}_{\text{QD}} \text{mmol}_{\text{Pt}}^{-1}$ is added and then as more is added (366 $\text{mmol}_{\text{QD}} \text{mmol}_{\text{Pt}}^{-1}$ and 225 $\text{mmol}_{\text{QD}} \text{mmol}_{\text{Pt}}^{-1}$) the aR decreases. The aR takes into account the adsorption constant and the surface coverage of the reactants (See Chapter 2); this suggests that $> 15 \text{mmol}_{\text{QD}} \text{mmol}_{\text{Pt}}^{-1}$ does not carry on increasing the ability of the modifier to facilitate absorption of EtPy and H_2 to the surface and it inhibits the reactants from adsorbing. This could be as it saturates the surface of the Pt and takes up active sites or as explained in Chapter 3 more than one modifier molecule could adsorb onto the same site blocking it. In Figure 4.15 there is a large difference between MBF and EBF with the apparent rate enhancements using QD results in greater apparent rate enhancements with EBF. This suggests that QD increases the surface coverage of reactants in the EBF hydrogenation.



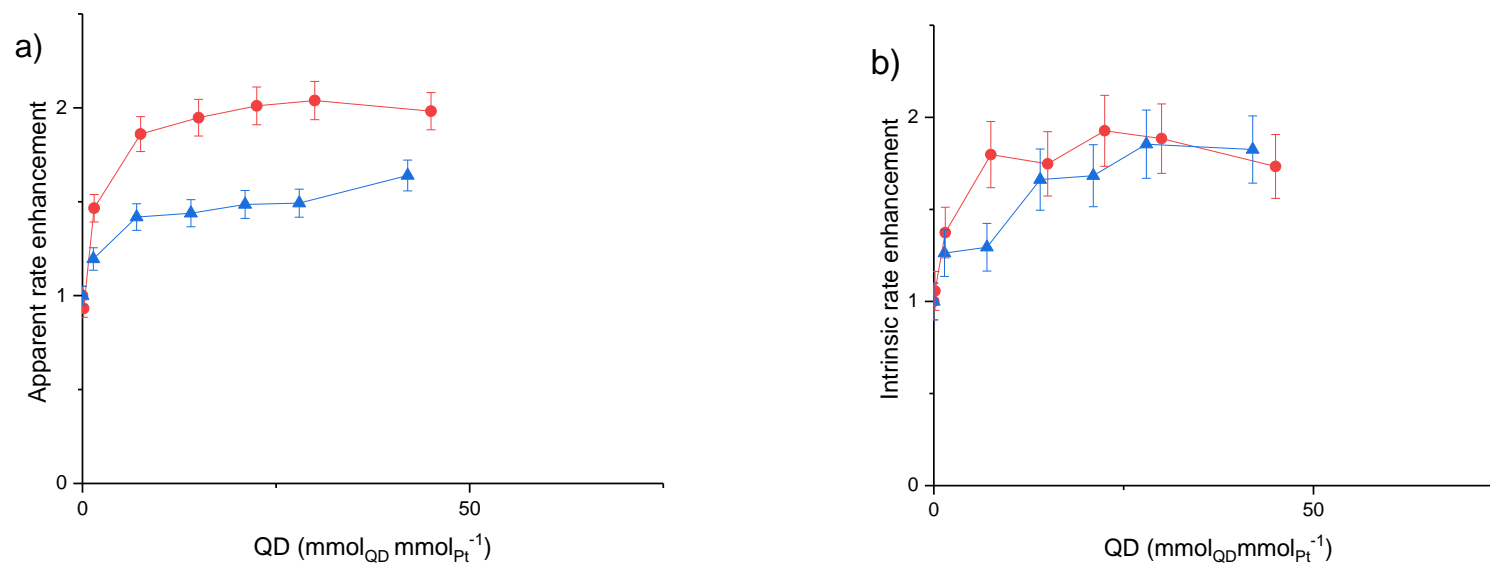


Figure 4.15: The influence on the apparent rate enhancement as a function of the moles of QD (a) and the intrinsic rate enhancement (b) on the EtPy (■), EBF (●) and MBF (▲) hydrogenation reactions. Reaction conditions: H₂ (20 bar), RT, 5 wt. % Pt / Al₂O₃ (0.06 mmol, 250 mg); EtPy (45 mmol, 5.2 mL); MBF (41 mmol, 5.8 mL); EBF (43 mmol, 6.2 mL), toluene + 0.001 M acetic acid

Figure 4.15 illustrates the iRs obtained when using QD as a modifier with these substrates (EtPy, MBF and EBF). For EtPy the rate increases sharply to $15 \text{ mmol}_{\text{QD}} \text{ mmol}_{\text{Pt}}^{-1}$ and plateaus when adding more QD. However, at greater concentrations of QD with EBF and MBF the rate decreases. The iR is the rate enhancement that comes from the system when the adsorption constant has been removed. The intrinsic rate enhancement increased up to 15 or 14 $\text{mmol}_{\text{QD}} \text{ mmol}_{\text{Pt}}^{-1}$ and was stable at higher concentrations of above $20 \text{ mmol}_{\text{QD}} \text{ mmol}_{\text{Pt}}^{-1}$ (Figure 4.15b)).

MBF and EBF have very similar iRs with no obvious difference unlike the aRs shown in Figure 4.15a. Both EBF and MBF appear to have optimum concentration of QD for the fastest rate enhancement: EBF at $22.5 \text{ mmol}_{\text{QD}} \text{ mmol}_{\text{Pt}}^{-1}$ and $30 \text{ mmol}_{\text{QD}} \text{ mmol}_{\text{Pt}}^{-1}$ and MBF at $28 \text{ mmol}_{\text{QD}} \text{ mmol}_{\text{Pt}}^{-1}$.

In Table 4.6 the different iRs and aRs for the EtPy hydrogenation using QD are shown. The iRs for QD peak at $15 \text{ mmol}_{\text{QD}} \text{ mmol}_{\text{Pt}}^{-1}$ at 3.6 and then plateau after this. This could be because as more and more modifier adsorbs onto the Pt surface it can become saturated and another QD molecule could adsorb onto the modified site making it difficult for the substrate to adsorb and manoeuvre. This has been seen when cinchonidine was used as a modifier.¹⁵

In Table 4.7 the hydrogenation for EBF using different amounts of QD are shown. The data in Table 4.7 show clear rate enhancements using QD, the aR increasing up to $15 \text{ mmol}_{\text{QD}} \text{ mmol}_{\text{Pt}}^{-1}$ and then plateauing. After more QD was added the rates plateaued. It is unclear why it plateaued and did not decrease.

In Table 4.8 the hydrogenation of MBF using different amounts of QD are shown. QD used on its own gives a rate enhancement (Table 4.8) from $7 \text{ mmol}_{\text{QD}} \text{ mmol}_{\text{Pt}}^{-1}$. The iR enhancement peaks at $28 \text{ mmol}_{\text{QD}} \text{ mmol}_{\text{Pt}}^{-1}$ and then levels off. From $14 \text{ mmol}_{\text{QD}} \text{ mmol}_{\text{Pt}}^{-1}$ to

42 mmol_{QD} mmol_{Pt}⁻¹ gave very similar aRs and iRs and the rates did not increase after the optimum had been found. The use of QD in the MBF hydrogenation has been sparsely reported; Margitfalvi *et al.* reports that QD was used in the MBF hydrogenation but only as a part of a Pt / Al₂O₃ CD system, not as QD alone. However, rate enhancement was observed when QD was added to a low concentration CD reaction.¹²

For the mode of action of the MBF and EBF hydrogenations, as neither of these two substrates from oligomers, it is likely that the QD stabilises the half-hydrogenated substrate either in the liquid phase or adsorbed to the surface. It is unlikely that a cleaning effect is responsible for the rate enhancements in these reactions as these substrates cannot form condensation products. However, EtPy gives a much greater rate enhancement compared to MBF and EBF so perhaps for EtPy there is both this cleaning effect and stabilization of the half-hydrogenated state working together. As the rate increases and then plateaus this would imply that there is adsorption of the modifier.

Table 4.6- Rate measurements and calculations in the EtPy hydrogenation reaction using different amounts of QD (mmol).

Amount of QD (g)	Amount of QD (mmol)	mmol additive per mmol of Pt	lin_fit slope / mmol s ⁻¹	Apparent enhancement	Kinetic fit, k ₂ / mmol s ⁻¹	Intrinsic enhancement
0	0	0	3.0×10 ⁻³	1.0	4.4×10 ⁻³	1.0
0.01	0.09	1.5	3.7×10 ⁻³	1.2	4.1×10 ⁻³	0.9
0.025	0.22	3.7	5.2×10 ⁻³	1.7	5.6×10 ⁻³	1.3
0.05	0.45	7.5	7.2×10 ⁻³	2.4	8.5×10 ⁻³	1.9
0.075	0.67	11.2	1.1×10 ⁻²	3.7	1.1×10 ⁻²	2.5
0.1	0.9	15	1.4×10 ⁻²	4.6	1.6×10 ⁻²	3.6
1.5	13.5	225	1.3×10 ⁻²	4.3	1.6×10 ⁻²	3.6
2.5	22	366.7	8.8×10 ⁻³	2.9	1.6×10 ⁻²	3.6

Table 4.7 - Rate measurements and calculations in the EBF hydrogenation reaction using different amounts of QD (mol).

Amount of QD (g)	Amount of QD (mmol)	mmol of additive per mmol of Pt	lin_fit slope / mmol s ⁻¹	apparent enhancement	kinetic fit, k ₂ / mmol s ⁻¹	intrinsic enhancement
0	0	0	6.6×10 ⁻³	1.0	8.2×10 ⁻³	1.0
0.001	0.009	0.15	6.1×10 ⁻³	0.9	8.6×10 ⁻³	1.1
0.01	0.09	1.50	9.6×10 ⁻³	1.5	1.1×10 ⁻²	1.4
0.05	0.45	7.50	1.2×10 ⁻²	1.9	1.5×10 ⁻²	1.8
0.1	0.9	15.00	1.3×10 ⁻²	1.9	1.4×10 ⁻²	1.7
0.15	1.35	22.50	1.3×10 ⁻²	2.0	1.6×10 ⁻²	1.9
0.2	1.8	30.00	1.3×10 ⁻²	2.0	1.5×10 ⁻²	1.9
0.3	2.7	45.00	1.3×10 ⁻²	2.0	1.4×10 ⁻²	1.7

Table 4.8 Rate measurements and calculations in the MBF hydrogenation reaction using different amounts of QD (mol).

Amount of QD (g)	Amount of QD (mol)	mmol of additive per mmol of Pt	lin_fit slope / mmol s ⁻¹	apparent enhancement	kinetic fit, k ₂ / mmol s ⁻¹	intrinsic enhancement
0	0	0	6.5×10 ⁻³	1.0	8.2×10 ⁻³	1.0
0.01	0.09	1.4	7.7×10 ⁻³	1.2	1.0×10 ⁻²	1.3
0.05	0.45	7	9.2×10 ⁻³	1.4	1.1×10 ⁻²	1.3
0.1	0.9	14	9.3×10 ⁻³	1.4	1.4×10 ⁻²	1.7
0.15	1.35	21	9.6×10 ⁻³	1.5	1.4×10 ⁻²	1.7
0.2	1.8	28	9.6×10 ⁻³	1.5	1.5×10 ⁻²	1.9
0.3	2.7	42	1.1×10 ⁻²	1.6	1.5×10 ⁻²	1.8

4.9. DABCO

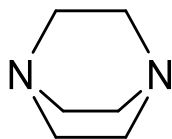


Figure 4.16: The structure of DABCO

DABCO (Figure 4.16) is an achiral tertiary amine that has a very similar structure to QD. The difference between the two compounds is that DABCO has two nitrogen-containing moieties rather than one. Due to the success of QD as a modifier in previous studies and in this project (Section 4.2) DABCO was the natural next choice of modifier. This is because DABCO could potentially increase the rate even more than QD if the rate enhancement relies on a basic nitrogen as it has two rather than one. The literature related to the use of DABCO as a modifier is very sparse. There have been no published studies to date using DABCO in either the EBF or MBF hydrogenation reactions. There has been research completed on DABCO being used in a CD-EtPy hydrogenation reaction where Margitfalvi *et al.* make mention of an achiral tertiary amine (ATA) effect where they use DABCO, QD and QL. The reason they give for these ATAs increasing the rate enhancement is that they prevent dimerization of cinchonidine.¹⁶

The mode of action of DABCO as a modifier in this reaction on its own has not been described in the literature so in this project it is postulated to be similar to the mechanism of action of QD (see QD section) proposed by Bond *et al.* (Figure 4.17)⁹ or it could clean the surface of oligomers of EtPy⁶ or clean the decomposition of the substrates or a mixture of all of these.

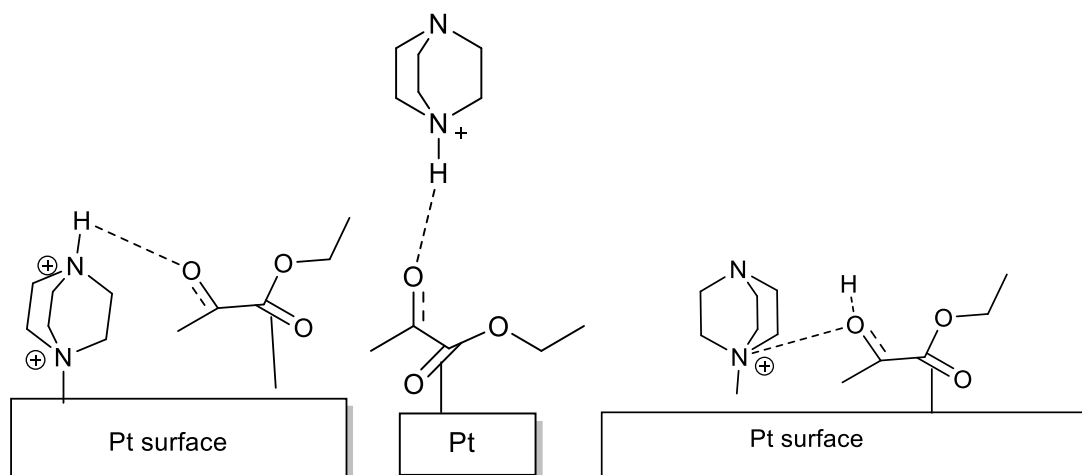


Figure 4.17: Possible mode of actions of DABCO with EtPy

GC analysis was completed using EBF with DABCO and it was found that there were no by-products. (see appendix)

4.9.1 Comparison of EtPy, EBF and MBF with DABCO modifier

In Figure 4.18 there were significant differences in rates between EtPy and the other two substrates, where MBF and EBF gave similar rates whereas EtPy gave much more significant aRs. The optimum amount of DABCO used in the EtPy reaction was $22 \text{ mmol}_{\text{DABCO}} \text{ mmol}_{\text{Pt}}^{-1}$; when more DABCO was added to the EtPy reaction the aR dipped and then levelled off. This suggests that $> 22 \text{ mmol}_{\text{DABCO}} \text{ mmol}_{\text{Pt}}^{-1}$ of DABCO modifier does not influence the surface coverage of the reactants (EtPy, MBF or EBF) on the Pt surface. For both MBF and EBF DABCO only gave slight rate enhancements when compared to the unmodified reaction. For both substrates when $> 7.5 \text{ mmol}_{\text{DABCO}} \text{ mmol}_{\text{Pt}}^{-1}$ was added there was not a large change in aRs.

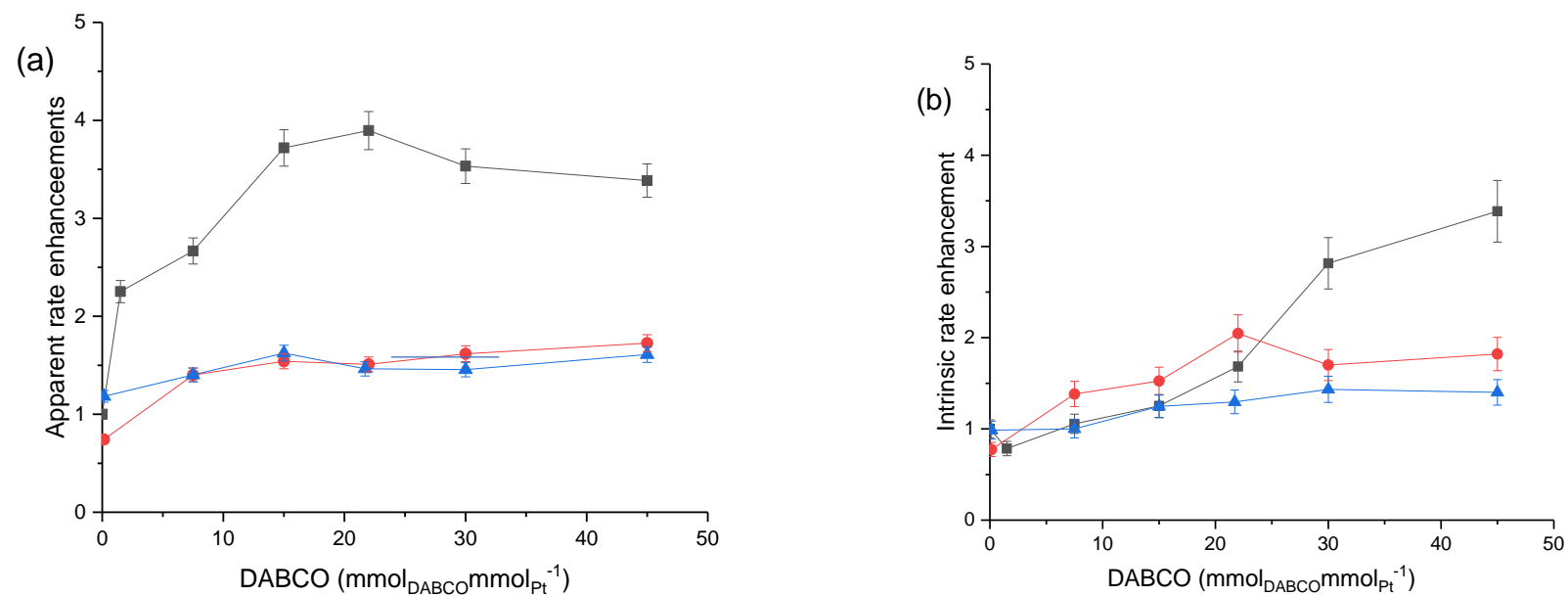


Figure 4.18; The influence of the apparent rate enhancement as a function of the moles of QD (a) and the intrinsic rate enhancement (b) on the EtPy (■), EBF (●) and MBF (▲) hydrogenation reactions. Reaction conditions: H_2 (20 bar), RT, 5 wt. % Pt / Al_2O_3 (0.06 mmol, 250 mg); EtPy (45 mmol, 5.2 mL); MBF (41 mmol, 5.8 mL); EBF (43 mmol, 6.2 mL), toluene + 0.001 M acetic acid

The values for the iRs (Figure 4.18) are very different to the aRs. For EtPy up until 22 mmol_{DABCO} mmol_{Pt}⁻¹ gave very similar intrinsic rates to MBF and EBF until 30 mmol_{DABCO} mmol_{Pt}⁻¹ where the iR for EtPy rose sharply; the optimum amount of DABCO in the EtPy reaction found was 45 mmol_{DABCO} mmol_{Pt}⁻¹. However, as the iR kept rising more reactions at even higher amounts of DABCO would be needed to see what the real optimum value is. EBF seemed to give slightly higher iRs at certain points (22 mmol_{DABCO} mmol_{Pt}⁻¹ and 45 mmol_{DABCO} mmol_{Pt}⁻¹) than MBF. The difference between EtPy and the other two substrates could be due to electronic reasons in the MBF and EBF hydrogenations as there could be resonance effects with MBF and EBF (Figure 4.19).

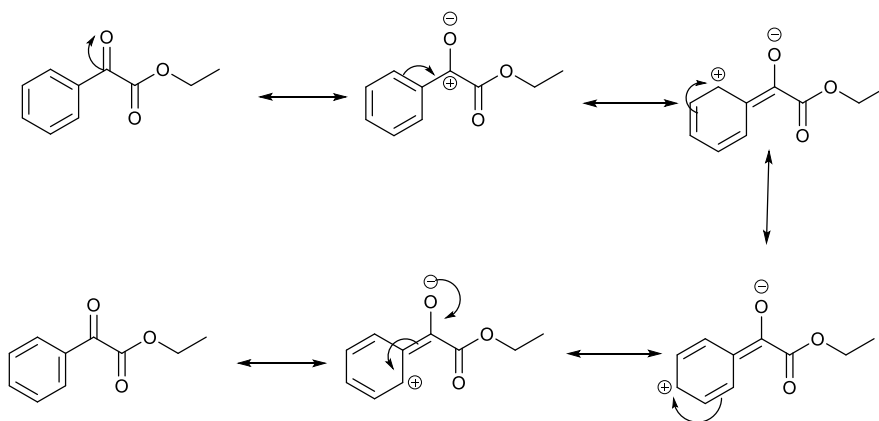


Figure 4.19: Resonance effects that could occur in ethyl benzoylformate

DABCO as an achiral tertiary amine additive into a Pt / Al₂O₃/ CD/ EtPy system has been reported by Margitfalvi *et al.* In this paper they found that DABCO in a cinchona- EtPy system increased the k₁ rate (rate from 0-10 mins) by 2 and the k₂ rate (rate from 25 mins to 60 mins) by 1.7 (Reaction conditions: [EtPy]₀ = 1.0 M, [CD] = 1.2 × 10⁻⁵ M, DABCO = 6 × 10⁻⁵ M, T = 20°C, hydrogen pressure = 50 bar, toluene, 0.125 g of 5 % wt Pt / Al₂O₃). They also reported that DABCO gave a greater rate enhancement than QD when used with cinchonidine.^{16,13,8}

The rate values calculated for the EtPy hydrogenation using different amounts of DABCO are shown. In Table 4.9 the aR enhancement increases up to $22 \text{ mmol}_{\text{DABCO}} \text{ mmol}_{\text{Pt}}^{-1}$ of DABCO and then decreases slightly in the subsequent increased concentrations. However, the iR enhancement (Table 4.9) increases with increasing amounts of DABCO above $22 \text{ mmol}_{\text{DABCO}} \text{ mmol}_{\text{Pt}}^{-1}$. This highlights that more points are needed to explore how much better the rate enhancement can potentially be. The highest rate enhancement found was 3.9 in this project which is nearly double that which has been reported in the literature (2).¹⁶ It also shows that at lower amounts DABCO enhances the adsorption of the EtPy substrate.

In Table 4.10 the rate values calculated for the EBF hydrogenation using DABCO are shown. There has not been any published literature found on DABCO being used in the EBF hydrogenation. The following findings are thought to be novel. A clear rate enhancement was observed using DABCO modifier at different concentration (Table 4.10). The optimal iR was obtained using $22 \text{ mmol}_{\text{DABCO}} \text{ mmol}_{\text{Pt}}^{-1}$ of DABCO. The iR obtained using $22 \text{ mmol}_{\text{DABCO}} \text{ mmol}_{\text{Pt}}^{-1}$ of DABCO was considerably more at 2 compared to the aR of 1.5 (Table 4.10). The rate enhancement then levels off with no further increase using higher amounts of DABCO, confirming $22 \text{ mmol}_{\text{DABCO}} \text{ mmol}_{\text{Pt}}^{-1}$ of DABCO as the optimal amount.

In Table 4.11 the rate values for the MBF hydrogenation can be seen. In Table 4.11 a clear rate enhancement can be seen after only $7.5 \text{ mmol}_{\text{DABCO}} \text{ mmol}_{\text{Pt}}^{-1}$ was added. The highest rate given was when $21.7 \text{ mmol}_{\text{DABCO}} \text{ mmol}_{\text{Pt}}^{-1}$ was added and then it reduced after that. The aR kept increasing although the iR stayed the same after greater amounts than $30 \text{ mmol}_{\text{DABCO}} \text{ mmol}_{\text{Pt}}^{-1}$ were added. This means that slightly more DABCO ($45 \text{ mmol}_{\text{DABCO}} \text{ mmol}_{\text{Pt}}^{-1}$) helps the MBF and H_2 adsorb to the Pt(111) surface. These findings of DABCO giving a rate enhancement on its own are novel for the MBF hydrogenation.

The mechanism of the reactions with DABCO with the modifier is unclear. As it has been stated previously that the nitrogen can adsorb onto the Pt surface with QD (see previous section) it is likely that that happens with DABCO. So the DABCO could stabilize the half-hydrogenated substrate either when it is adsorbed onto the surface or in the liquid phase. It could also help clean the catalyst of EtPy oligomers for the EtPy hydrogenation which could account for why the rate enhancement is much larger in EtPy than the other two substrates. However, as the graph shows that DABCO enhances the EtPy adsorption significantly at lower amounts added the rate enhancement is more likely to be because of 1:1 modifier: reactant stabilization model.

Table 4.9- Rate measurements and calculations in the EtPy hydrogenation reaction using different amounts of DABCO (mmol).

Amount of DABCO (g)	Amount of DABCO (mmol)	mmol of additive per mmol of Pt	lin_fit slope / mmol s ⁻¹	apparent enhancement	kinetic fit, k ₂ / mmol s ⁻¹	intrinsic enhancement
0	0	0	2.7×10 ⁻³	1.0	8.0×10 ⁻³	1.0
0.01	0.09	1.5	6.0×10 ⁻³	2.3	6.3×10 ⁻³	0.8
0.05	0.45	7.5	7.1×10 ⁻³	2.7	8.4×10 ⁻³	1.1
0.1	0.9	15	9.9×10 ⁻³	3.7	10×10 ⁻³	1.3
0.15	1.3	22	1.×10 ⁻²	3.9	1.3×10 ⁻²	1.7
0.2	1.8	30	9.4×10 ⁻³	3.5	2.2×10 ⁻²	2.8
0.3	2.7	45	9.0×10 ⁻³	3.4	2.7×10 ⁻²	3.4

Table 4.10- Different rate values measured and calculated for different amounts of DABCO (g) in the EBF reaction

Amount of DABCO (g)	Amount of DABCO (mmol)	mmol additive per mmol of Pt.	lin_fit slope / mmol s ⁻¹	apparent enhancement	kinetic fit, k ₂ / mmol s ⁻¹	intrinsic enhancement
0	0	0	6.6×10 ⁻³	1	8.4×10 ⁻³	1
0.001	0.009	0.15	4.9×10 ⁻³	0.7	6.0×10 ⁻³	0.8
0.05	0.45	7.5	9.2×10 ⁻³	1.4	1.2×10 ⁻²	1.4
0.1	0.9	15	1.0×10 ⁻²	1.5	1.3×10 ⁻²	1.5
0.15	1.3	22	9.9×10 ⁻³	1.5	1.7×10 ⁻²	2.0
0.2	1.8	30	1.1×10 ⁻²	1.6	1.4×10 ⁻²	1.7
0.3	2.7	45	1.1×10 ⁻²	1.7	1.5×10 ⁻²	1.8

Table 4.11- Different rate values measured and calculated for different amounts of DABCO (g) in the MBF reaction.

Amount of DABCO (g)	Amount of DABCO (mmol)	mmol additive per mmol of Pt	lin_fit slope / mmol s ⁻¹	apparent enhancement	kinetic fit, k ₂ / mmol s ⁻¹	intrinsic enhancement
0	0	0	6.6×10 ⁻³	1.0	1.1×10 ⁻²	1.0
0.001	0.009	0.15	7.8×10 ⁻³	1.2	1.1×10 ⁻²	1.0
0.05	0.45	7.5	9.2×10 ⁻³	1.4	1.1×10 ⁻²	1.0
0.1	0.9	15	1.1×10 ⁻²	1.6	1.3×10 ⁻²	1.2
0.15	1.3	21.7	9.6×10 ⁻³	1.5	1.4×10 ⁻²	1.3
0.2	1.8	30	9.6×10 ⁻³	1.5	1.5×10 ⁻²	1.4
0.3	2.7	45	1.1×10 ⁻²	1.6	1.5×10 ⁻²	1.4

4.10 3-Quinuclidinol

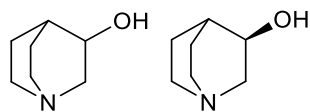


Figure 4.20: 3- Quinuclidinol (left) and R-3-quinuclidinol

As the nitrogen-containing moiety of cinchonidine, QD, shows a significant rate enhancement using each of the three substrates EtPy, EBF and MBF it was thought that adding a hydroxy group to the QD moiety would produce a further enhancement of the rate. Margitfalvi *et al.* used QL (Figure 4.20) in the EtPy hydrogenation in a Pt / Al₂O₃ - CD system. They found that the apparent rate enhancement was 2 when adding QL in this reaction. It also increased the ee slightly from 83 % to 88 %.¹⁶ However, this is the only report of using QL as a modifier.

The mode of action of QL has been suggested to by Bond *et al.* to stabilise the half-hydrogenated substrate like CD (Figure 4.22).⁹ It could be speculated that the OH group attached to the QL could form hydrogen bonds with one of the carbonyl groups further attracting the reactant in a similar way to CD in Baiker *et al.*'s published work (Figure 4.21).⁴ Although, Bond *et al.* found that there was no difference in rate enhancement between QD and QL which they state shows that the OH group does not affect the rate.⁹

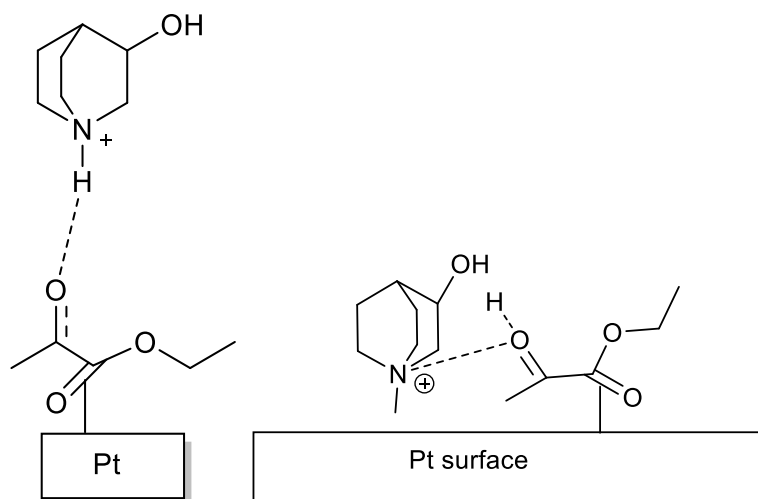


Figure 4.21: Modes of action QL and EtPy

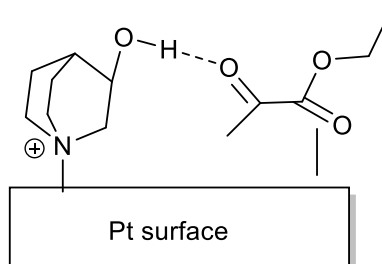


Figure 4.22: Speculated mode of action QL and EtPy if the OH group on the QL stabilised the half-hydrogenated state.

4.10.1 Comparison of EtPy, EBF and MBF with QL modifier

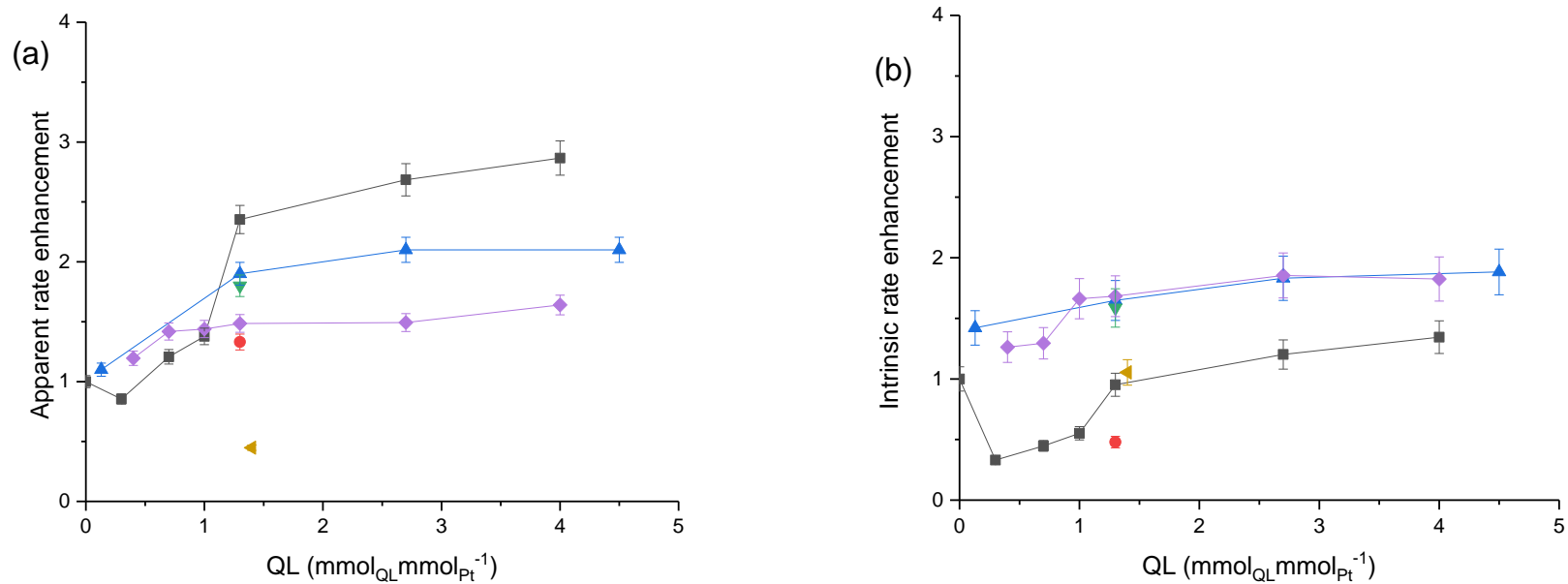


Figure 4.22: The influence of the apparent rate enhancement as a function of the moles of QL (a) and the intrinsic rate enhancement (b) on the EtPy (■), EBF (▲) and MBF (◆) hydrogenation reactions as well as the *R*-QL for EtPy (●), EBF (▼) and MBF (►). Reaction conditions: H₂ (20 bar), RT, 5 wt. % Pt / Al₂O₃ (0.06 mmol, 250 mg); EtPy (45 mmol, 5.2 mL); MBF (41 mmol, 5.8 mL); EBF (43 mmol, 6.2 mL), toluene + 0.001 M acetic acid.

In Figure 4.22 the aR for EtPy, EBF and MBF using QL and R-QL are shown. For EtPy at lower amounts of 3-QL (up to 1 mmol_{QL} mmol_{Pt}⁻¹) there is no significant aR but at higher amounts the aR is significant and increases. Unfortunately, more QL could not be tested in these reactions because it is not soluble in the toluene + .001 M of acetic acid solvent. EBF gave a more significant rate enhancement than MBF but less significant than EtPy at (1.3 mmol_{QL} mmol_{Pt}⁻¹, 2.7 mmol_{QL} mmol_{Pt}⁻¹ and 4 mmol_{QL} mmol_{Pt}⁻¹). Interestingly, R-QL for the EBF reaction gave the highest aR and R-QL for MBF actually poisoned the reaction. It is unclear why this occurred.

In Figure 4.22 for EtPy the rates appeared to be poisoned by the QL up until 1 mmol_{QL} mmol_{Pt}⁻¹ and then after that the rates give a similar rate to the unmodified reaction, whereas both EBF and MBF give similar rate enhancements when compared to the unmodified reaction. This suggests that QL influences the surface coverage of the reactants but does not give a rate enhancement intrinsically when the adsorption equilibrium has been removed. Interestingly, the only substrate that gave both aR and iR using R-QL was EBF, whereas for EtPy it decreased the iR and for MBF gave a similar rate to the unmodified reaction. The rates given by 3-QL change considerably when comparing the iR and aRs but also when compared to the other modifiers like DABCO and QD. So, the OH- group attached to the QL appears to have an effect.¹⁶

For the EtPy hydrogenation (Table 4.12), there was a clear rate enhancement observed when adding QL but not R-QL. A sample of the product mixture obtained from the reaction with R-QL was analysed by GC using a chiral column (see Chapter 2 for details) to determine the ee. The ee measured was found to be 0 indicating that the product was a racemic mixture (see Appendix 1 for GC chromatograms). A problem encountered using QL was that the maximum amount that could be dissolved was 4 mmol_{QL} mmol_{Pt}⁻¹. These findings are novel as

there have been no papers found that have used QL on its own as a modifier in the EtPy hydrogenation.

No publications have been found using QL in the MBF hydrogenation. As this modifier gave a significant rate enhancement in the EtPy hydrogenation it was of interest to test it in the MBF reaction to see if the same effect was witnessed. A clear rate enhancement (Table 4.13) was observed in this reaction from as low as $0.7 \text{ mmol}_{\text{QL}} \text{ mmol}_{\text{Pt}}^{-1}$, and the rate nearly doubled when $2.7 \text{ mmol}_{\text{QL}} \text{ mmol}_{\text{Pt}}^{-1}$ was added. The results obtained in the MBF reaction using QL are thought to be novel as no prior publication on this system has been found. As a significant rate enhancement was seen in the MBF hydrogenation it was likely, as they have very similar structures, that QL would give a rate enhancement in the EBF hydrogenation. Rate measurements were recorded at different concentrations of QL modifier (Table 4.14).

A clear, previously unreported, rate enhancement was observed using QL in the EBF reaction (Figure 4.22, Table 4.14). Interestingly using *R*-QL gave a significant rate enhancement for EBF even though, in the MBF hydrogenation, it poisoned the reaction. This is an unexpected effect as the substrates only differ by one CH_3 group. Concerning, the racemic QL it gave a significant rate enhancement and levelled off after $2.7 \text{ mmol}_{\text{QL}} \text{ mmol}_{\text{Pt}}^{-1}$ was used.

In the EtPy reaction the aRs were much greater than the iRs which show that the QL modifier was enhancing the adsorption of the EtPy molecules. As the modifier enhances the adsorption it shows that the modifier was likely in the 1:1 modifier: reactant model for the EtPy reaction.

Table 4.12- Rate values measured and calculated for the different amounts of QL in the EtPy

Amount of QL (g)	mmols of QL (mmol)	mmol additive per mmol of Pt.	lin_fit slope / mmol s ⁻¹	apparent enhancement	kinetic fit, k ₂ / mmol s ⁻¹	intrinsic enhancement
0	0	0	2.7×10 ⁻³	1.0	8.2×10 ⁻³	1.0
0.003	0.02	0.3	2.3×10 ⁻³	0.9	2.7×10 ⁻³	0.3
0.005	0.04	0.7	3.3×10 ⁻³	1.2	3.7×10 ⁻³	0.4
0.008	0.06	1	3.8×10 ⁻³	1.4	4.5×10 ⁻³	0.6
0.01	0.08	1.3	6.4×10 ⁻³	2.4	7.8×10 ⁻³	1.0
0.02	0.16	2.7	7.3×10 ⁻³	2.7	9.8×10 ⁻³	1.2
0.03	0.24	4	7.8×10 ⁻³	2.9	1.1×10 ⁻³	1.3
R (QL)	0.08	1.3	3.6×10 ⁻³	1.3	3.9×10 ⁻³	0.5

Table 4.13- Rate values measured and calculated for the different amounts of 3-QL in the MBF reaction

Amount of QL (g)	Amount of QL (mmol)	mmol of additive per mmol of Pt.	lin_fit slope / mmol s ⁻¹	apparent enhancement	kinetic fit, k ₂ / mmol s ⁻¹	intrinsic enhancement
0	0	0	6.5×10 ⁻³	1.0	8.2×10 ⁻³	1.0
0.003	0.024	0.4	7.7×10 ⁻³	1.2	1.0×10 ⁻²	1.3
0.005	0.04	0.7	9.2×10 ⁻³	1.4	1.1×10 ⁻²	1.3
0.008	0.06	1	9.3×10 ⁻³	1.4	1.4×10 ⁻²	1.7
0.01	0.08	1.3	9.6×10 ⁻³	1.5	1.4×10 ⁻²	1.7
0.02	0.16	2.7	9.6×10 ⁻³	1.5	1.5×10 ⁻²	1.9
0.03	0.24	4	1.1×10 ⁻²	1.6	1.5×10 ⁻²	1.8
R(QL)	0.08	1.4	2.9×10 ⁻³	0.4	8.7×10 ⁻³	1.1

Table 4.14- Rate values measured and calculated for the different amounts of 3-QL in the EBF reaction						
Amount of QL (g)	Amount of QL (mmol)	mmol additive per mmol of Pt	lin_fit slope / mmol s ⁻¹	apparent enhancement	kinetic fit, k ₂ / mmol s ⁻¹	intrinsic enhancement
0	0	0	6.6×10 ⁻³	1.0	8.5×10 ⁻³	1.0
0.001	0.008	0.13	7.0×10 ⁻³	1.1	1.2×10 ⁻²	1.4
0.01	0.08	1.3	1.3×10 ⁻²	1.9	1.4×10 ⁻²	1.6
0.02	0.16	2.7	1.4×10 ⁻²	2.1	1.6×10 ⁻²	1.8
0.03	0.27	4.5	1.4×10 ⁻²	2.1	1.6×10 ⁻²	1.9
R(QL)	0.08	1.3	1.2×10 ⁻²	1.8	1.4×10 ⁻²	1.6

4.11 Overview of the modifiers in each substrate

The rate enhancements produced by each modifier for each reaction were compared graphically in order to deduce their relative activities as modifiers.

4.11.1 EtPy

As can be seen in Figure 4.23. QL gave, at lower concentrations due to the solubility in the solvent, faster apparent rate than both DABCO and QD. This shows that it can help the substrate adsorb to the surface. This could be due to the hydrogen bonding from the OH attracting the substrate on the surface. The QD at similar amounts of DABCO gave better intrinsic rate enhancements. Their apparent rate enhancements were similar which means that DABCO helps the substrate adsorb to the surface more easily.

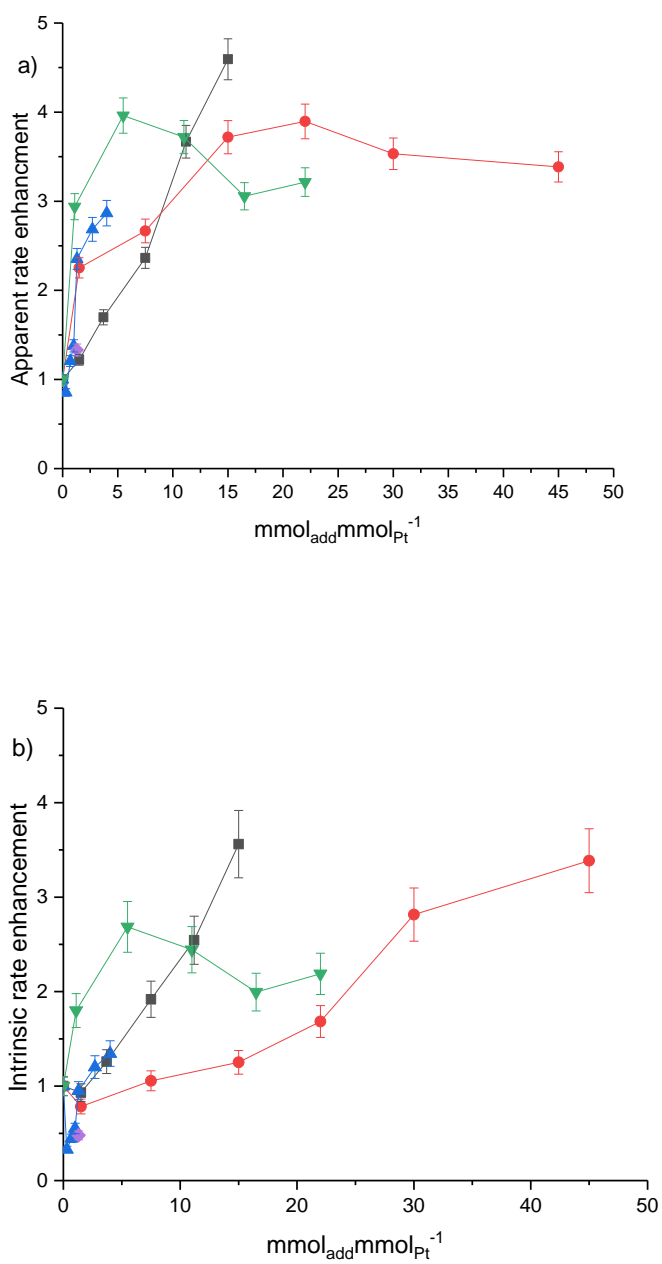


Figure 4.23: A comparison of each modifier at different quantities (mol additive per mol of Pt) and the apparent (a) and intrinsic (b) rate enhancements they give. (See Table for abbreviations; (R)3-quinuclidinol = RQL). QD (black ■), DABCO (red ●), QL (blue ▲), RQL (purple ●), AQ (▲)

4.11.2 MBF

In Figure 4.24 QL at lower quantities gives a slightly higher rate enhancement than DABCO and QD, increasing the rate by slightly more than twice that of the unmodified reaction at its peak. This suggests that the extra OH group attached to the molecule influences the reaction. It is likely that the OH group forms hydrogen bonds with the carbonyl of the substrates and helps attract the substrate to the surface or to the modifier. This is additional evidence to support the theory that the addition of the hydroxy group helps the rate enhancement.¹¹

DABCO and QD both gave similar aRs. DABCO's iRs in general were less than QD. It is not known why this is but DABCO only gave a slight rate enhancement in this reaction.

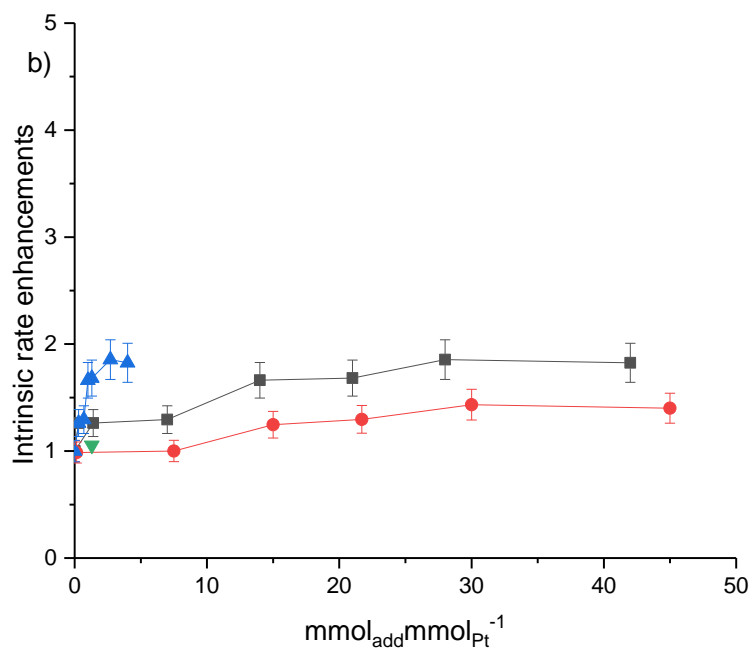
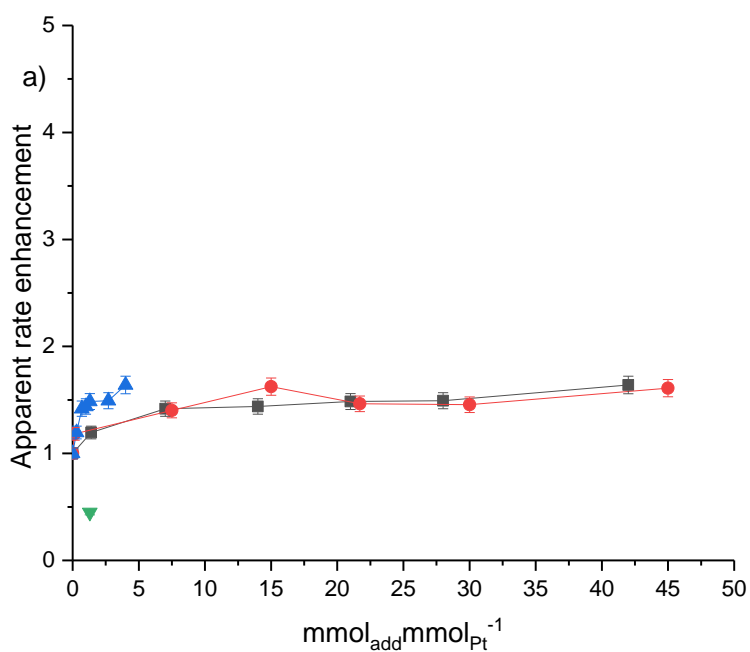


Figure 4.24: A comparison of the apparent (a) and intrinsic (b) rate enhancements using different amounts of each modifier: QD (black ■), DABCO (red ●), QL (blue ▲), RQL (green ▼).

. 4.11.3 EBF

Figure 4.25 shows that, at lower amounts, QL gives a higher iR and aR than both DABCO and QD which suggests that the extra OH group attached to the molecule influences the reaction. This could be due to the OH group forming hydrogen bonds with the carbonyl of the substrate, thus helping attract the substrate to the surface or to the modifier. Adding more QD and DABCO did not increase the iR very much, indicating that the addition of another nitrogen to the modifier does not increase the rate. This is interesting as the basic nitrogen is thought to be key in the rate enhancement and by adding another one it would be expected to have increased the rate enhancement. The aRs and iRs of these modifiers are shown in Figure 4.25 and it can be seen that the QL gives a better aR than QD and DABCO at the lowest mmol_{add} tested.

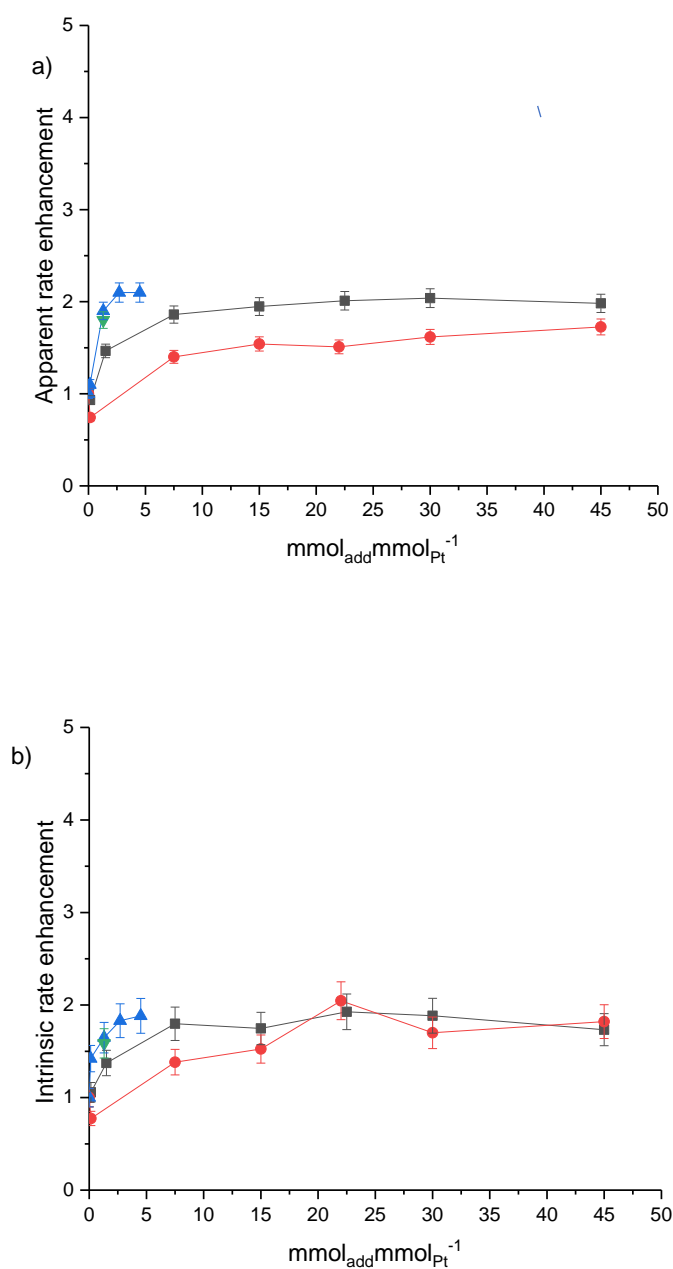


Figure 4.25: Different apparent (a) and intrinsic (b) rate enhancements of the EBF reaction using different modifiers at different quantities (Mol of additive per mol of Pt), QL- quinculidinol, R-QL- R-quinuclidinol, QD- QD and DABCO- 1,4-diazabicyclo [2.2.2]octane. QD (black ■), DABCO (red ●), QL (blue ▲).

4.12 The influence of solvent; acetic acid compared to toluene + acetic acid (0.001 M)

AQ required acetic acid as a solvent and many papers have published data in toluene + 0.001 M acetic acid for hydrogenation of alpha-ketoesters making it difficult to compare the data without knowing the general effects of different solvents on the rate. Therefore, a comparison of the two solvent systems was carried out for the three substrates, EtPy, MBF and EBF, using the same amount of modifier across both systems.

4.12.1 EtPy

In Figure 4.26, Tables 4.15 and Table 4.16 the differences between rate enhancements of the modifiers in acetic acid versus toluene + 0.001 M acetic acid can be seen. DABCO and QD produce much greater aRs and iRs in toluene + 0.001 M acetic acid than neat acetic acid and the rate values found were much greater for these two modifiers in toluene + acetic acid (0.001 M) than glacial acetic acid. CD gave a faster aR and slightly faster iR in toluene + acetic acid (0.001 M). This is because CD and the unmodified reactions gave faster rate values in acetic acid than it did in toluene + acetic acid (0.001 M) which means the aR and iR is lower as the rate enhancements are compared to the unmodified reaction. This is consistent with results using the state-of-the-art method from Baiker *et al.* which uses acetic acid (see Chapter 3); they found the rate was faster than when done in toluene. Racemic QL and RQL gave very similar rate enhancements and rate values in both solvents. The difference in rate values for CD, QD and DABCO could be due to the different dielectric constants of the acetic acid (6.15) and toluene (2.38).¹⁷ These dielectric constants change the conformation of the molecule in space which in turn can change how they interact with the substrate and can either increase or decrease the rate.

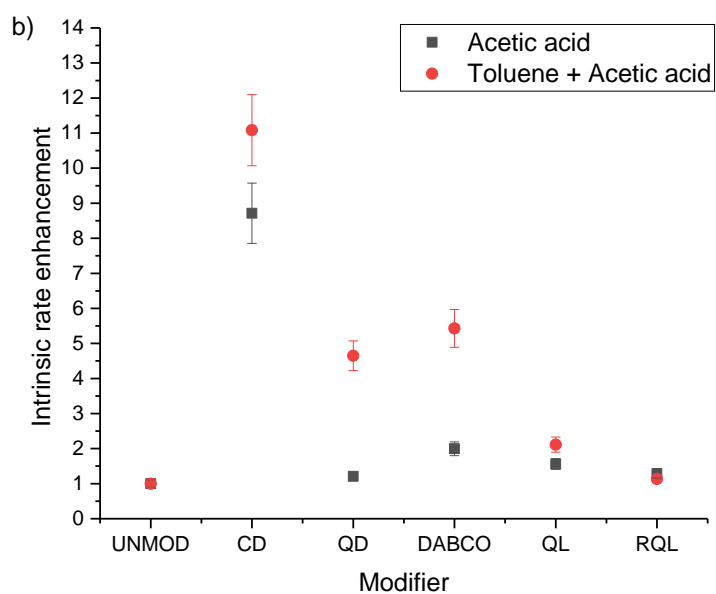
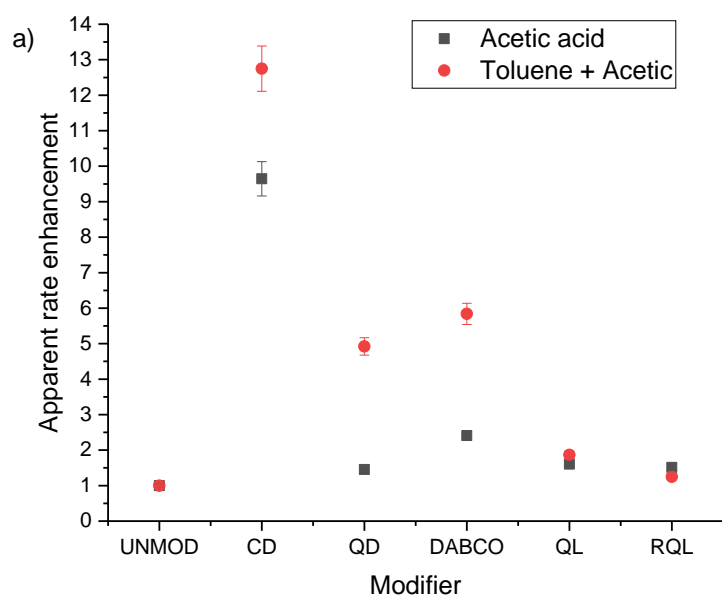


Figure 4.26: aR enhancements (a) and iR enhancements (b) of the different modifiers for the EtPy hydrogenation reaction in both toluene + 0.001 M acetic acid and neat acetic acid, H₂ (20 bar), RT, 5 wt. % Pt / Al₂O₃ (0.06 mmol, 250 mg); EtPy (45 mmol, 5.2 mL); toluene + 0.001 M acetic acid); CD (8.5 μmol, 2.5 mg), CN (8.5 μmol, 2.5 mg). QD (0.9 mmol, 100 mg), QL (0.08 mmol, 10 mg), DABCO (0.9 mmol, 101 mg) and RQL (0.08 mmol, 10 mg)

Table 4.15- Different hydrogenation rate enhancements with different modifiers in different solvent systems for EtPy hydrogenation.

Modifier	aRs		iRs	
	Acetic acid	Toluene (0.001 M acetic acid)	Acetic acid	Toluene (0.001 M acetic acid)
Unmodified	1.0	1.0	1.0	1.0
CD	9.6	12.7	8.7	11.1
QD	1.5	4.9	1.2	4.6
DABCO	2.4	5.8	2.0	5.4
QL	1.6	1.9	1.6	2.1
R-QL	1.5	1.2	1.3	1.1
AQ	3.7		3.6	

Table 4.16 – Rate values of different modifiers' reactions in the two solvents.

	Acetic acid		Toluene + 0.001 M acetic acid	
	lin_fit slope / mmol s ⁻¹	kinetic fit, k2 / mmol s ⁻¹	lin_fit slope / mmol s ⁻¹	kinetic fit, k2 / mmol s ⁻¹
Unmodified	4.0×10 ⁻³	4.9×10 ⁻³	3.0×10 ⁻³	3.5×10 ⁻³
CD	3.8×10 ⁻²	4.2×10 ⁻²	3.8×10 ⁻²	3.9×10 ⁻²
QD	5.8×10 ⁻³	5.9×10 ⁻³	1.5×10 ⁻²	1.6×10 ⁻²
DABCO	9.6×10 ⁻³	9.7×10 ⁻³	1.72×10 ⁻²	1.9×10 ⁻²
QL	6.4×10 ⁻³	7.6×10 ⁻³	5.5×10 ⁻³	7.4×10 ⁻³
R-QL	6.0×10 ⁻³	6.3×10 ⁻³	3.7×10 ⁻³	4.0×10 ⁻³
AQ	1.5×10 ⁻²	1.7×10 ⁻²		

4.12.2 MBF

The same two solvents were also used for the MBF hydrogenation. As can be seen in Figures 4.27, Table 4.17 and Table 4.18 there is a large difference in aRs between the solvents in all the modifiers except for RQL. CD, QD, DABCO and QL gave much higher aRs in toluene + acetic acid (0.001 M) than in neat acetic acid. However, the iRs for QD, DABCO and QL were only slightly higher in toluene + acetic acid (0.001 M). R-QL gave a lower aR and iR for both for toluene + acetic acid (0.001 M) and in acetic acid. For the MBF hydrogenation it can be concluded that CD gives a faster rate in toluene + acetic acid (0.001 M) than in glacial acetic acid as the rate values were much faster for CD in toluene + acetic acid (0.001 M) than glacial acetic acid. The unmodified reaction was much faster in acetic acid than toluene + acetic acid (0.001 M) which has made it look like there is a big difference between QL and DABCO when in reality the rate values are very similar. However, QD gives faster rate values in toluene + acetic acid (0.001 M) than in glacial acetic acid.

Table 4.17 aRs and iRs with different modifiers' reactions in the two different solvents				
Modifier	aRs		iRs	
	Acetic acid	Toluene (0.001 M acetic acid)	Acetic acid	Toluene (0.001 M acetic acid)
Unmodified	1	1.0	1	1
CD	1.3	3.9	1.7	3.9
QD	0.8	2.6	1.1	2.2
DABCO	0.5	1.9	1.5	1.9
QL	0.9	2.6	1.5	2.4
R-QL	0.8	0.5	0.8	0.5
AQ	0.8		1.0	

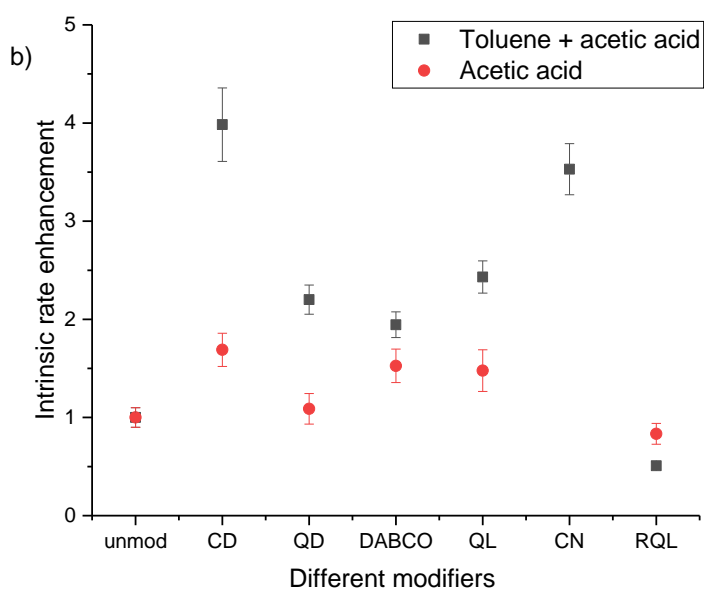
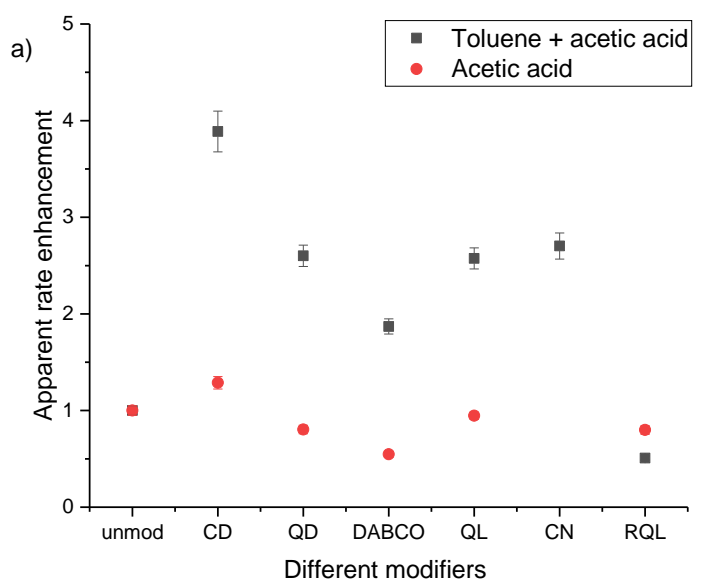


Figure 4.27: The different aR (a) and iR (b)enhancement with different modifiers used in the hydrogenation reaction using the two solvents: neat acetic acid and toluene (0.001 M acetic acid), H₂ (20 bar), RT, 5 wt.% Pt / Al₂O₃ (0.06 mmol, 250 mg); MBF (41 mmol, 5.8 mL); toluene + 0.001 M acetic acid); CD (8.5 μmol, 2.5 mg), CN (8.5 μmol, 2.5 mg). QD (0.9 mmol, 100 mg), QL (0.08 mmol, 10 mg), DABCO (0.9 mmol, 101 mg) and RQL (0.08 mmol, 10 mg)

Table 4.18- Rate values for the modifiers' reactions using the two different solvents.				
	Acetic acid		Toluene +0.001 M acetic acid	
	lin_fit slope / mmol s ⁻¹	kinetic fit, k2 / mmol s ⁻¹	lin_fit slope / mmol s ⁻¹	kinetic fit, k2 / mmol s ⁻¹
Unmodified	8.9×10 ⁻³	9.5×10 ⁻³	5.6×10 ⁻³	6.8×10 ⁻³
CD	1.1×10 ⁻²	1.6×10 ⁻²	2.2×10 ⁻²	2.7×10 ⁻²
QD	7.1×10 ⁻³	1.0×10 ⁻²	1.4×10 ⁻²	1.5×10 ⁻²
DABCO	4.8×10 ⁻³	1.4×10 ⁻²	1.0×10 ⁻²	1.3×10 ⁻²
QL	8.3×10 ⁻³	1.4×10 ⁻²	1.4×10 ⁻²	1.7×10 ⁻²
R-QL	7.0×10 ⁻³	7.9×10 ⁻³	2.8×10 ⁻³	3.5×10 ⁻³
AQ	7.1×10 ⁻³	9.6×10 ⁻³		

4.12.3 EBF

In Figure 4.28, Table 4.19 and Table 4.20 the comparison of the modifiers in the two different solvents are shown. The rate values and aRs and iRs show that CD is much faster in toluene + acetic acid (0.001 M) than in acetic acid. The rate values show that QD was faster in toluene + acetic acid (0.001 M). DABCO behaved similarly in both solvents. QL and RQL gave similar rate values in both solvents. The unmodified reaction was much faster in acetic acid than it was in toluene + acetic acid (0.001 M).

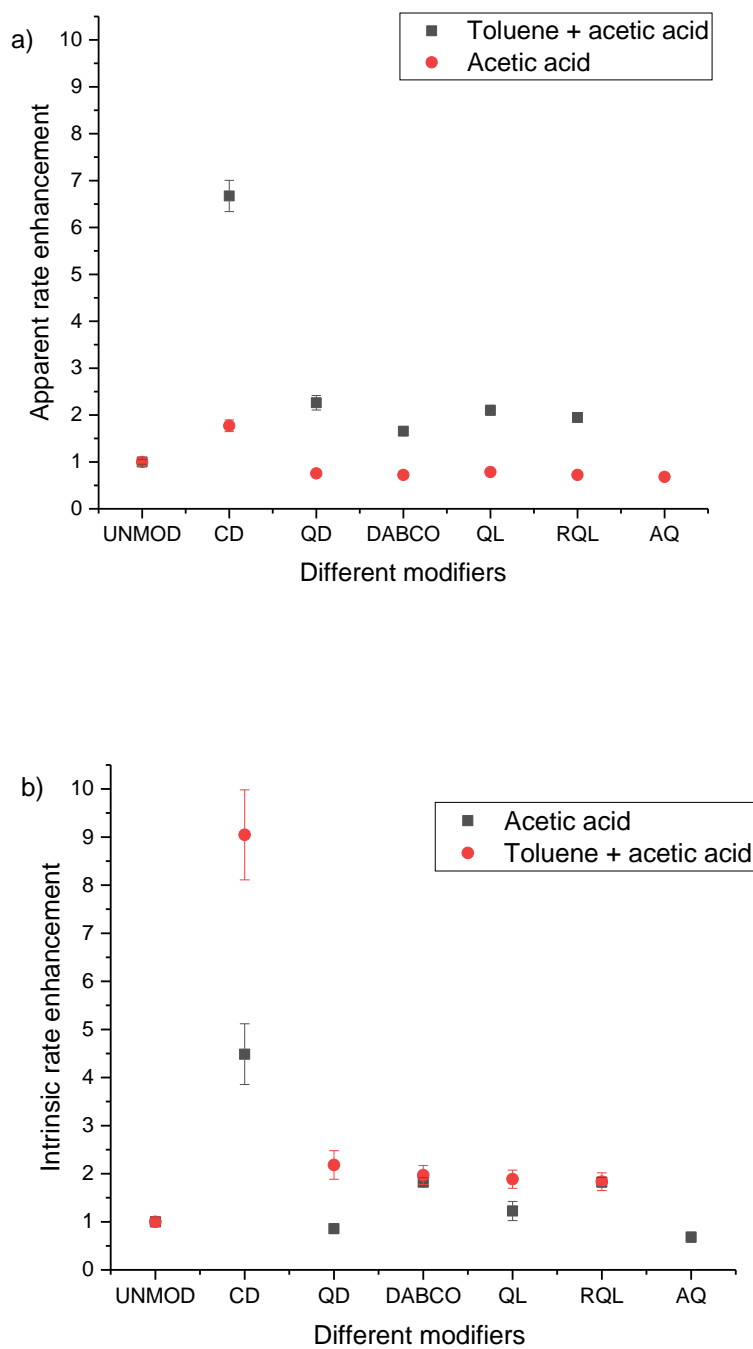


Figure 4.28: The aR (a) and iR (b) enhancements of different modifiers in the two solvent systems (acetic acid and toluene/acetic acid); H_2 (20 bar), RT, 5 wt.% Pt / Al_2O_3 (0.06 mmol, 250 mg); MBF (41 mmol, 5.8 mL); toluene + 0.001 M acetic acid); CD (8.5 μ mol, 2.5 mg), CN (8.5 μ mol, 2.5 mg). QD (0.9 mmol, 100 mg), QL (0.08 mmol, 10 mg), DABCO (0.9 mmol, 101 mg) and RQL (0.08 mmol, 10 mg).

Table 4.19- aRs and iRs of the different modifier reactions in the two solvents.

Modifier	aRs		iRs	
	Acetic acid	Toluene (0.001 M acetic acid)	Acetic acid	Toluene (0.001 M acetic acid)
Unmodified	1.0	1.0	1.0	1.0
CD	1.8	6.7	4.5	9.0
QD	0.8	2.3	0.9	2.2
DABCO	0.7	1.7	1.8	2.0
QL	0.8	2.1	1.2	1.9
R-QL	0.7	1.9	1.8	1.8
AQ	0.7		0.7	

Table 4.20- Rate values of the different modifiers' reactions using the two solvents

	Acetic acid		Toluene +0.001 M acetic acid	
	lin_fit slope / mmol s ⁻¹	kinetic fit, k2 / mmol s ⁻¹	lin_fit slope / mmol s ⁻¹	kinetic fit, k2 / mmol s ⁻¹
Unmodified	8.6×10 ⁻³	1.0×10 ⁻²	6.4×10 ⁻³	7.7×10 ⁻³
CD	1.5×10 ⁻²	4.5×10 ⁻²	4.3×10 ⁻²	6.9×10 ⁻²
QD	6.5×10 ⁻³	8.7×10 ⁻³	1.4×10 ⁻²	1.7×10 ⁻²
DABCO	6.2×10 ⁻³	1.9×10 ⁻²	1.1×10 ⁻²	1.5×10 ⁻²
QL	6.7×10 ⁻³	1.2×10 ⁻²	1.3×10 ⁻²	1.4×10 ⁻²
R-QL	6.2×10 ⁻³	1.9×10 ⁻²	1.2×10 ⁻²	1.4×10 ⁻²
AQ	5.8×10 ⁻³	6.9×10 ⁻³		

4.13 Conclusion

In this chapter the influence of the different modifiers used throughout this project on the rate of reaction was discussed in comparison to the unmodified hydrogenation reaction. For the three substrates EtPy, MBF and EBF the different modifiers (QD, QL, CD, CN and DABCO) gave rate enhancements of varying magnitude in toluene +0.001 M of acetic acid. There were large differences when using the different solvents; using neat acetic acid for several of the modifiers, in the concentration ranges used, gave similar rates to the unmodified reaction with no rate enhancements observed in MBF reactions and only slight rate enhancements observed for the EBF hydrogenation. This suggests that for these substrates (MBF and EBF) the rate is solvent dependent. However, for the EtPy hydrogenation the solvent changed the rate enhancements slightly but still gave a rate enhancement nonetheless.

It was found that all the modifiers tested and shown in this chapter gave rate enhancements. Most of them gave a rate enhancement of around 2 and it is unclear why this is. A possible reason for QL giving better rate enhancements at the lower concentrations than the other modifiers is because the OH group may have hydrogen bonded with the substrate. However, there does not seem to be a clear reason why QD gave a better rate enhancement than DABCO as there are two basic nitrogens on DABCO which intuitively would increase the rate enhancement, not decrease it. It would be needed in the future to test a QD molecule without the nitrogen to see if a rate enhancement is obtained without the basic nitrogen.

Concerning the origin of the rate enhancement it looks like the 1:1 modifier: reactant model that stabilises the half-hydrogenated state is the most likely explanation. The reason being that the ‘cleaning’ of the catalyst surface theory would not work for MBF and EBF. Also, through rate calculations it was found that QL and DABCO enhance the adsorption of the EtPy which would be in more agreement with the 1:1 modifier: reactant model.

4.14 References

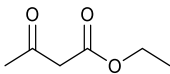
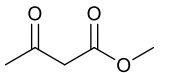
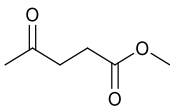
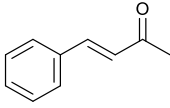
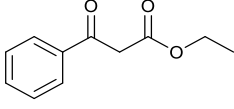
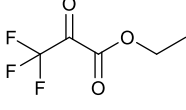
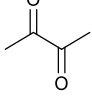
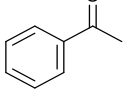
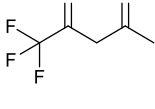
1. Chemical Book, https://www.chemicalbook.com/ChemicalProductProperty_EN_CB7199624.htm, (accessed 3 August, 2022)
2. PubChem, <https://pubchem.ncbi.nlm.nih.gov/source/hsdb/5556#section=Boiling-Point>, (accessed 3 August, 2022)
3. B. Minder, M. Schürch, T. Mallat and A. Baiker, *Catalysis Letters*, 1995, **31**, 143–151.
4. A. Baiker, Progress in asymmetric heterogeneous catalysis: Design of novel chirally modified platinum metal catalysts. *J. Mol. Catal. A: Chem.* 1997, **115**, 473–493.
5. B. Minder, M. Schürch, T. Mallat, A. Baiker, T. Heinz, A. Pfaltz, *Journal of Catalysis*, 1996, **160**, 261-268
6. E. Toukinity and D. Murzin, *Journal of Catalysis*, 2006, **241**, 96-102.
7. D. Jenkins, A. Aalabulrahman, G. Attard, K. Griffin, P. Johnston and P. Wells, *Journal of Catalysis*, 2005, **234**, 230-239.
8. J. Margitfalvi, E. Tálas and M. Hegedûs, *Chemical Communications*, 1999, 645-646.
9. G. Bond, P.A. Meheux, A. Ibbotson, P.B. Wells, *Catal. Today* 10, 1991, 371–378.
10. D. Fierri, T. Burgi, *J. Am. Chem. Soc.* 2001, **123**, 48, 12074–12084
11. T. Bürgi, A. Baiker, *Accounts of Chemical Research*, 2004, **37**, 909-917.
12. E. Tálas, F. Zsila, P. Szabó and J. Margitfalvi, *Journal of Molecular Catalysis A: Chemical*, 2012, **357**, 87-94.
13. J. Margitfalvi, E. Tálas, E. Tfirst, C. Kumar and A. Gergely, *Applied Catalysis A: General*, 2000, **191**, 177-191.
14. H. U. Blaser, H. P. Jalett, W. Lottenbach and M. Studer, *Journal of the American Chemical Society*, 2000, **122**, 12675–12682.
15. H.-U. Blaser, H.-P. Jalett, M. Müller and M. Studer, *Catalysis Today*, 1997, **37**, 441–463.
16. J. Margitfalvi, E. Tálas, F. Zsila and S. Kristyán, *Tetrahedron: Asymmetry*, 2007, **18**, 750-758.
17. Dielectric constants of common solvents, https://depts.washington.edu/eoopic/linkfiles/dielectric_chart%5B1%5D.pdf, (accessed April 2022).

Chapter 5

Extending the Pt-cinchona system to other reactants

Following on from the work using EtPy, several other reactants were selected to use in the Pt-cinchona system to assess if rate enhancement could be achieved using the conditions used previously in this reaction setup. The substrates chosen possessed similar structure motifs to EtPy with respect to functional groups, such as carbonyl and ester moieties. These substrates were selected because of the similar structure to EtPy but also because of the availability. The aim was to investigate whether the rate enhancement found in EtPy using the modifiers in the previous chapters could be repeated. Some of the substrates had been reported to have had rate enhancements using different catalyst-modifier setups to the one used in this reaction.

The substrates tested can be classified into groups: Beta-diketone, gamma-diketone single ketone and F-containing ketone. While testing other substrates (Table 5.1) only one concentration of modifier was used for each reaction and the modifier amounts were not optimised. In the EBF and MBF reactions a broad range of modifier concentrations were used and only some of these gave rate enhancements so it is possible that different amounts of modifier could significantly change the rate in these substrates. The modifiers used previously in this project (QD, QL, DABCO) were tested on these substrates (EBF and MBF) as the modifiers contain aspects of the CD structure and some of these substrates have been previously reported to have had a rate enhancement observed on addition of CD.

Table 5.1- The structures for the substrate in Chapter 5	
Substrate	Structure of substrate
Ethyl acetoacetate (EAA)	
Methyl acetoacetate (MAA)	
Methyl levulinate (ML)	
Benzylideneacetone (BA)	
Ethyl benzoylacetate (EBA)	
Ethyl trifluoroacetate (EFP)	
2,3-butane-dione	
Acetophenone (AP)	
1,1,1-trifluoro-2,4-pentandione (TP)	

5.1 Hydrogenation of β -diketo esters

5.1.1 Ethyl acetoacetate

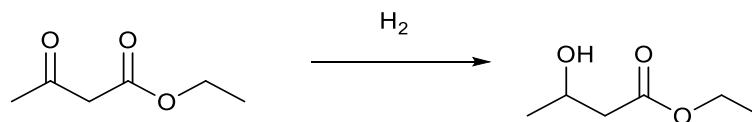


Figure 5.1: EAA hydrogenation

Ethyl acetoacetate (EAA) (Figure 5.1), a β -diketo ester has a similar structure to EtPy. β -diketo esters like EAA and methyl acetoacetate have been hydrogenated using nickel catalysts modified with tartaric acid to find optically pure products previously.¹ However, work on β -diketo esters being hydrogenated in Pt-cinchona system has not been found. The most accepted mechanism for the rate enhancement is that the adsorbed protonated modifier (CD) attracts and stabilizes the half-hydrogenated substrate (EtPy) where the OH bond on the CD further attracts and stabilizes the substrate through hydrogen bonding (see Chapter 1 for more details). The implication based on this mechanism is that a small structural deviation from EtPy (i.e., another CH_2 in ethyl acetoacetate) should result in a rate enhancement (Table 5.2). An apparent rate enhancement of 0.8 was calculated and an intrinsic rate enhancement of 1.3 was found for the EAA reaction with CD. The same modifiers were used in the EAA hydrogenation to see if similar enhancements were observed as it is structurally like the EtPy substrate.

Modifier	lin_fit slope / mmol s ⁻¹	aR	kinetic fit, k ₂ / mmol s ⁻¹	iR
CD	2.0×10 ⁻³	1.2	2.7×10 ⁻³	0.9
QD	5.0×10 ⁻⁴	0.3	1.5×10 ⁻³	0.5
DABCO	1.2×10 ⁻³	0.7	2.2×10 ⁻³	0.7
QL	9.9×10 ⁻⁴	0.6	9.9×10 ⁻³	0.3
Unmod	1.7×10 ⁻³	1.0	3.0×10 ⁻³	1.0

The hydrogenation rate values of the different modifiers in the EAA hydrogenation reaction showed that all the modifiers poisoned the reaction (Table 5.2 and Figure 5.2). This is interesting as the substrate only differs from the structure of the EtPy molecule by a CH₂ group, but this is enough for the modifiers to not enhance the rate; such a small steric difference can change the function of the modifiers completely.

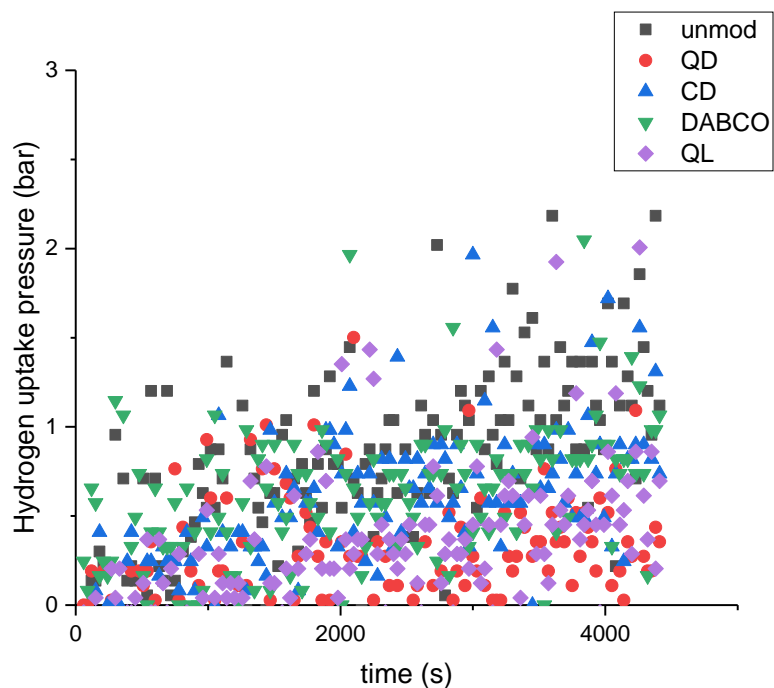


Figure 5.2: Hydrogen uptake graphs of EAA using different modifiers, unmodified (black), QD (red), CD (blue), DABCO (green) and QL (purple); Reaction conditions: H_2 (20 bar), RT, 5 wt.% Pt / Al_2O_3 (1.25 mmol, 250 mg); EAA (41 mmol, 5.3 mL); toluene + 0.001 M acetic acid); CD (8.5 μmol , 2.5 mg), QD (0.9 mmol, 100 mg), QL (0.08 mmol, 10 mg), DABCO (0.9 mmol, 101 mg).

5.1.2 Methyl acetoacetate hydrogenation

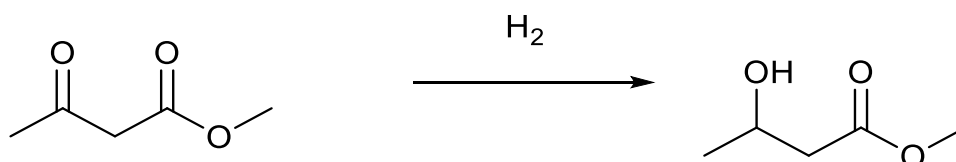


Figure 5.3: Methyl acetoacetate hydrogenation

Methyl acetoacetate (MAA) (Figure 5.3) is a beta keto ester that is mainly used in the synthesis of pharmaceuticals. The MAA hydrogenation has been studied extensively using Raney Nickel catalysts. These hydrogenation studies show that MAA is influenced by the modifier tartaric acid.²

As the MAA hydrogenation can be influenced by a modifier the effect of CD and the achiral tertiary amines using a Pt catalyst would be interesting to investigate. MAA was used because of its similar structure to methyl pyruvate and methyl pyruvate has been reported to give a rate enhancement using CD.^{3,4} However, there was no rate enhancement when using CD and it reduced the rate, similar to the EAA hydrogenation (Table 5.3). The hydrogenation modified with CD gave an apparent rate enhancement of 0.6 and an intrinsic rate enhancement of 0.2. The same modifiers were used to investigate potential rate enhancements in the MAA hydrogenation. It would be interesting to see what would happen if achiral tertiary amines were added to the reaction. There are no prior publications of this reaction using these modifiers and so the results presented here are novel.

Modifier	lin_fit slope	aR	kinetic fit, k2	iR
	/ mmol s ⁻¹		/ mmol s ⁻¹	
CD	1.6×10 ⁻³	0.6	1.6×10 ⁻³	0.2
QD	5.9×10 ⁻⁴	0.2	5.9×10 ⁻⁴	0.1
DABCO	1.6×10 ⁻³	0.6	1.6×10 ⁻³	0.2
QL	1.1×10 ⁻³	0.4	1.3×10 ⁻³	0.1
Unmod	2.9×10 ⁻³	1.0	8.5×10 ⁻³	1.0

The hydrogenation rate values for each of the different modifiers showed that all the modifiers poisoned the methyl acetoacetate hydrogenation (Table 5.3 and Figure 5.4). As there are no previously reported results for these modifiers in the methyl pyruvate hydrogenation it was not possible to make any comparisons.

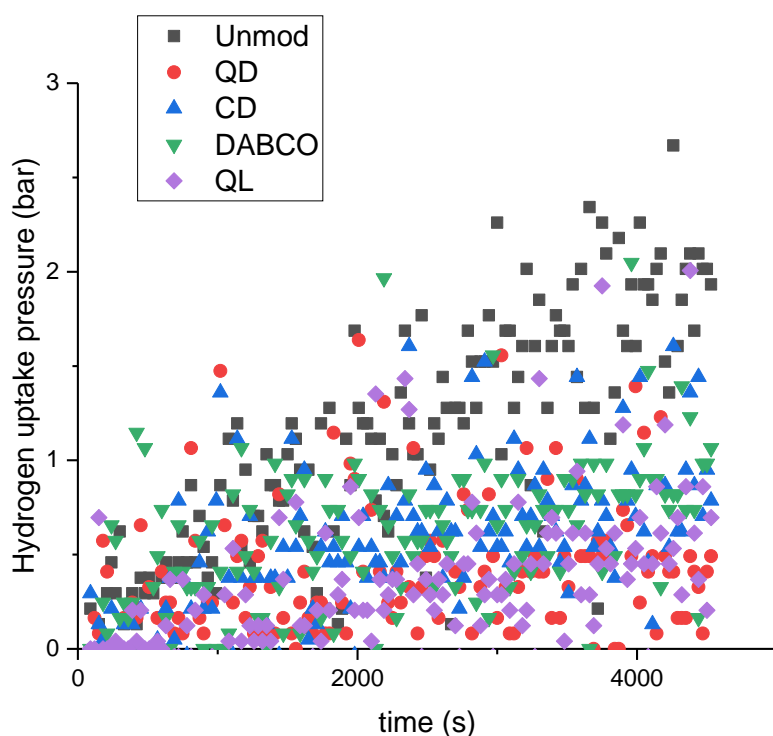


Figure 5.4: Methyl acetoacetate hydrogenation using the different modifiers, unmodified (black), QD (red), CD (blue), DABCO (green) and QL (purple); Reaction conditions: H₂ (20 bar), RT, 5 wt.% Pt / Al₂O₃ (1.25 mmol, 250 mg); MAA (46 mmol, 5.3 mL); toluene + 0.001 M acetic acid); CD (8.5 μmol, 2.5 mg), QD (0.9 mmol, 100 mg), QL (0.08 mmol, 10 mg), DABCO (0.9 mmol, 101 mg).

5.1.3 Ethyl benzoyl acetate hydrogenation

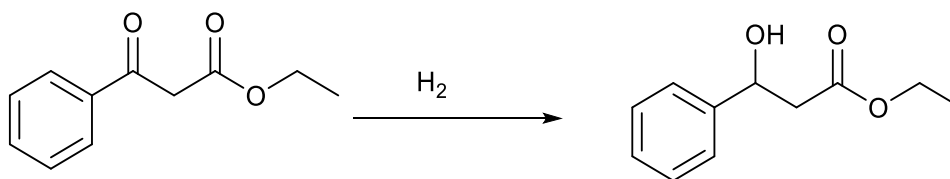


Figure 5.5: Ethyl benzoylacetate hydrogenation

Ethyl benzoyl acetate (EBA) (Figure 5.5) is the β -diketoester version of EBF and, as stated previously, CD gives a significant rate enhancement in the EBF hydrogenation. The hydrogenation of EBA has been studied as the need for enantiomerically pure alcohols for the production of agriculturals and pharmaceuticals is high.

Sterk *et al.* used chiral ligands to achieve an ee of 98% and a slight increase in rate on a ruthenium catalyst, although no rate data was presented.⁵ The apparent rate enhancement of CD was 0.5 and the intrinsic rate enhancement was 0.6 (Table 5.4).

Table 5.4- Hydrogenation rate values and rate enhancements using different modifiers in the EBA hydrogenation reaction.				
Modifier	lin_fit slope / mmol s ⁻¹	aR	kinetic fit, k2 / mmol s ⁻¹	iR
CD	1.1×10 ⁻³	0.5	1.8×10 ⁻³	0.6
QD	1.3×10 ⁻³	0.6	3.8×10 ⁻³	1.2
DABCO	2.0×10 ⁻³	0.9	2.7×10 ⁻³	0.8
QL	7.7×10 ⁻⁴	0.3	2.3×10 ⁻³	0.7
Unmodified	2.2×10 ⁻³	1.0	3.2×10 ⁻³	1.0

All the modifiers investigated poisoned the ethyl benzoylacetate hydrogenation reaction (Table 5.4 and Figure 5.6); even though it is very similar to EBF structurally there was no rate enhancement. This shows that only very specific structures of substrates actually have a rate enhancement when using these modifiers. These results are novel.

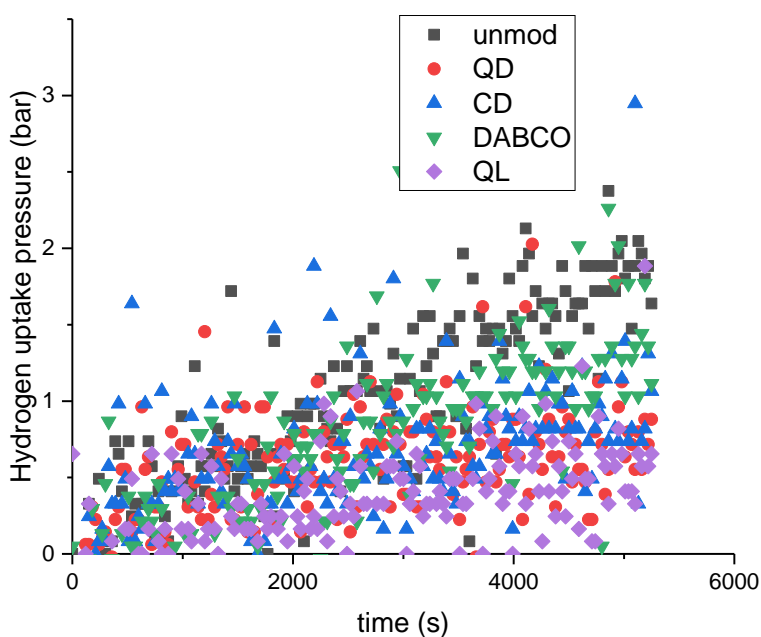


Figure 5.6: Hydrogen uptake graph of ethyl benzoylacetate hydrogenation: unmodified (black), QD (red), CD (blue), DABCO (green) and QL (purple); Reaction conditions: H₂ (20 bar), RT, 5 wt.% Pt / Al₂O₃ (1.25 mmol, 250 mg); EBA (46 mmol, 7.9 mL); toluene + 0.001 M acetic acid); CD (8.5 μmol, 2.5 mg), QD (0.9 mmol, 100 mg), QL (0.08 mmol, 10 mg), DABCO (0.9 mmol, 101 mg).

5.2 γ - diketo ester

5.2.1 Methyl levulinate hydrogenation

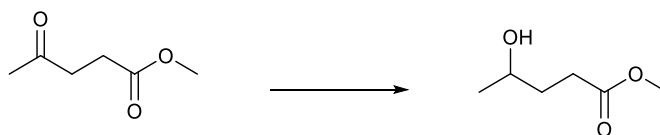


Figure 5.7: Methyl levulinate hydrogenation

Methyl levulinate (ML) (Figure 5.7) is a short chain fatty ester with properties such as non-toxicity, high lubricity and flashpoint stability. They are similar to methyl esters and are used as additives for petrol and diesel.⁶ The hydrogenation of methyl levulinate has been reported a few times previously.⁷ However, ML being tested in a Pt / Al₂O₃/cinchona system has not been reported before. ML was used as it is the gamma keto ester version of methyl pyruvate. The CD modified reaction gave an apparent and intrinsic rate enhancement of 0.6. ML is the gamma diketoester version of methyl pyruvate and methyl pyruvate has a rate enhancement when CD and QD are used. Therefore, it was tested with the other modifiers used in this project to see if there is any rate enhancement (Table 5.5).

Table 5.5- the hydrogenation rate values and rate enhancements using different modifiers in the ML hydrogenation				
Modifier	lin_fit slope / mmol s ⁻¹	aR	kinetic fit, k2 / mmol s ⁻¹	iR
CD	1.3×10 ⁻³	0.6	4.0×10 ⁻³	0.6
QD	1.2×10 ⁻³	0.5	3.5×10 ⁻³	0.5
DABCO	4.1×10 ⁻⁴	0.2	4.9×10 ⁻⁴	0.1
QL	3.4×10 ⁻⁴	0.2	3.8×10 ⁻⁴	0.1
Unmod	2.1×10 ⁻³	1.0	6.3×10 ⁻³	1.0

As seen as in Table 5.5 and Figure 5.8 no rate enhancement was observed after adding any of these modifiers. However, the rate was very low using the condition of this project in the unmodified reaction and even after two hours the hydrogen pressure had not decreased by much meaning that only a small amount of the substrate had been hydrogenated. Perhaps the conditions needed to be changed. However, using the conditions which were standard to all the previous work, none of the modifiers increased the rate of reaction, nevertheless.

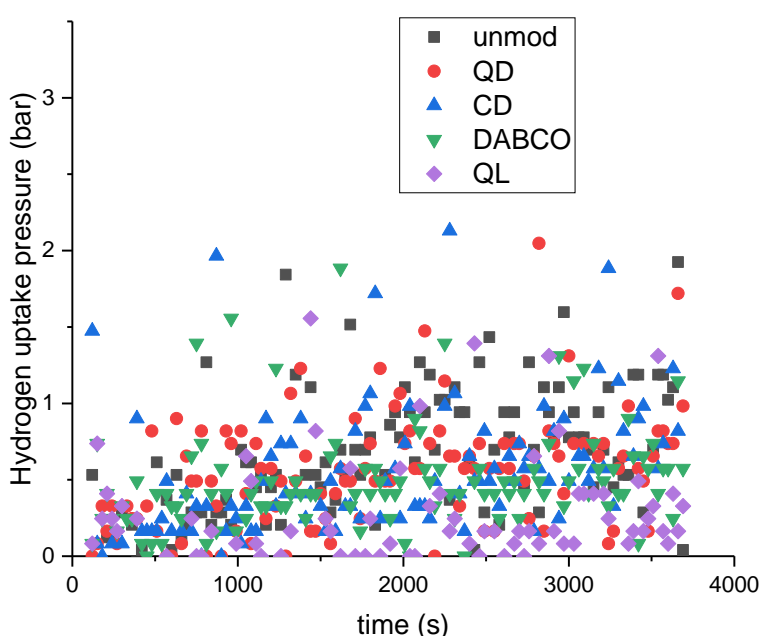


Figure 5.8: Hydrogen uptake graph of methyl levulinate hydrogenation: unmodified (black), QD (red), CD (blue), DABCO (green) and QL (purple); Reaction conditions: H₂ (20 bar), RT, 5 wt.% Pt / Al₂O₃ (1.25 mmol, 250 mg); ML (64 mmol, 7.9 mL); toluene + 0.001 M acetic acid); CD (8.5 μmol, 2.5 mg), QD (0.9 mmol, 100 mg), QL (0.08 mmol, 10 mg), DABCO (0.9 mmol, 101 mg).

5.3 Simple ketones

5.3.1 Acetophenone hydrogenation

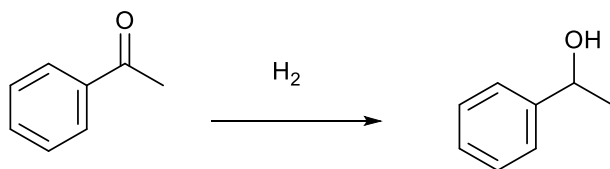


Figure 5.9: Acetophenone hydrogenation

Acetophenone (AP) (Figure 5.9) was chosen for this project as it is the simplest ketone that has an aromatic ring. It is synthesised from the industrial process for phenol synthesis from isopropyl benzene, selective decomposition of cumene hydro peroxide, or the oxidation of ethylbenzene.⁸ The AP hydrogenation is used to create important products such as 1-cyclohexylethanol in the manufacture of polymers and 1-phenylethanol for fragrances and pharmaceutical. It is also used as a raw material for synthetic resins.⁹ Therefore enhancing the method for the hydrogenation of this useful substrate is of paramount importance.

The hydrogenation of AP in heterogeneous catalysis has been studied using CD and cinchonine where a slight rate enhancement has been reported using a platinum on carbon catalyst.¹⁰ Also, CD has been reported to give a rate enhancement on an Ir/SiO₂ catalyst.¹¹ Interestingly, Baiker *et al.* found that on addition of cinchona alkaloids the reaction rate decreased.¹² CD poisoned the reaction by giving a 0.2 apparent rate enhancement and 0.2 intrinsic rate enhancement. The other modifiers that have been used in this project were also tested in order to see if there is any rate enhancement as CD has been reported to have given a rate enhancement previously and so the individual parts of CD could potentially give rate enhancements themselves (Table 5.6).

Table 5.6- The hydrogenation rate values and rate enhancements found using different modifiers in the AP hydrogenation reaction				
Modifier	lin_fit slope/ mmol s ⁻¹	aR	kinetic fit, k2 / mmol s ⁻¹	iR
CD	6.9×10 ⁻⁴	0.2	8.2 ×10 ⁻⁴	0.2
QD	5.8×10 ⁻⁴	0.2	6.6×10 ⁻⁴	0.1
DABCO	2.2×10 ⁻⁴	0.1	3.9×10 ⁻⁴	0.1
QL	7.4×10 ⁻⁴	0.2	1.0×10 ⁻³	0.2
Unmodified	3.7×10 ⁻³	1.0	4.6×10 ⁻³	1.0

All of the modifiers poisoned the reaction rate compared to the unmodified reaction (Table 5.6 and Figure 5.10). No previous publications have been found describing the attempted rate enhancements of AP hydrogenation using any of these modifiers and so the findings are believed to be novel. It is not known why the modifiers do not induce a rate enhancement as the protonated nitrogen should still stabilize the half-hydrogenated AP.

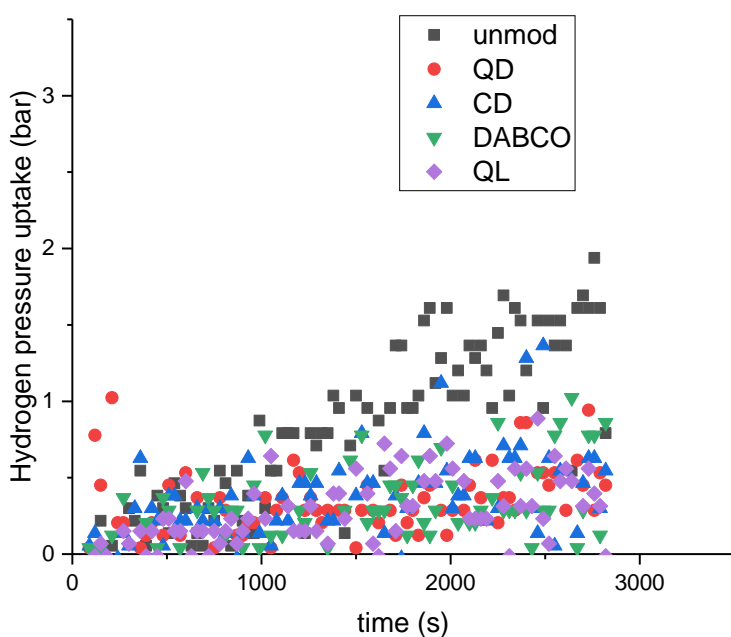


Figure 5.10: Hydrogen uptake graph of A: unmodified (black), QD (red), CD (blue), DABCO (green) and QL (purple); Reaction conditions: H_2 (20 bar), RT, 5 wt.% Pt / Al_2O_3 (1.25 mmol, 250 mg); acetophenone (42 mmol, 4.9 mL); toluene + 0.001 M acetic acid); CD (8.5 μmol , 2.5 mg), QD (0.9 mmol, 100 mg), QL (0.08 mmol, 10 mg), DABCO (0.9 mmol, 101 mg).

5.3.2 Benzalacetone hydrogenation

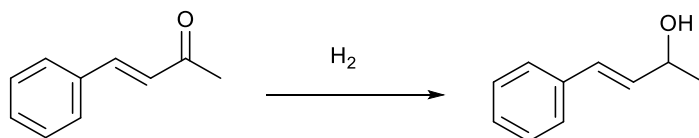


Figure 5.11: Benzalacetone hydrogenation

Benzalacetone (BA) (Figure 5.11) is an alpha, beta-unsaturated ketone and is used as a flavouring in fragrances and food. The hydrogenation of BA has been studied extensively over

different catalysts like Au/ SiO₂ and Ir/SiO₂.^{13,14} Also, chiral diamines have been used to increase the ee and rate in other reports which could mean that the modifiers similar to CD could give a rate enhancement under the conditions of this project.¹⁵

In Figure 5.12 all the modifiers poison the rate. BA was chosen because there is a carbonyl group that can be hydrogenated but also there is a double bond. The apparent rate enhancement given by the CD reaction is 0.5 and the intrinsic rate enhancement is 0.9.

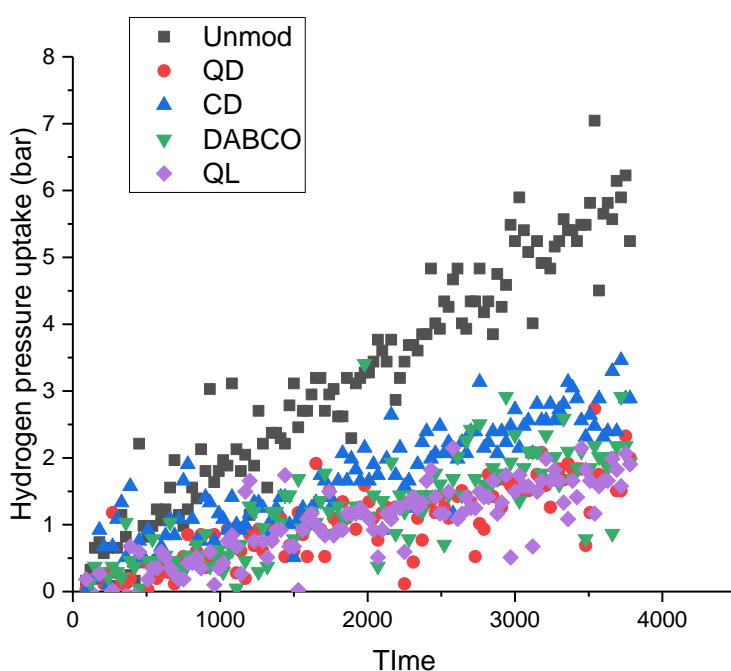


Figure 5.12: Hydrogen uptake pressure of BA hydrogenation, unmodified (black), QD (red), CD (blue), DABCO (green) and QL (purple); Reaction conditions: H₂ (20 bar), RT, 5 wt.% Pt / Al₂O₃ (1.25 mmol, 250 mg); BA (40 mmol, 5.8mL); toluene + 0.001 M acetic acid); CD (8.5 μmol, 2.5 mg), QD (0.9 mmol, 100 mg), QL (0.08 mmol, 10 mg), DABCO (0.9 mmol, 101 mg).

5.4 Diketone

5.4.1 2,3-Butane-dione hydrogenation

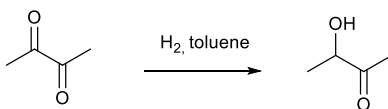


Figure 5.13: 2,3-Butandione hydrogenation

2,3-butane-dione (Figure 5.13) is a very important chemical used in flavourings for food and beverages. It gives foods a buttery flavour.¹⁶ It has been reported that 2,3-butanedione has given a rate enhancement previously using CD.¹⁷ CD in this reaction gave an apparent rate enhancement of 2 and an intrinsic rate enhancement of 1.4.

2,3-Butanedione was tested as it reportedly gave a rate enhancement when using CD modifier. The other modifiers have not been reportedly used in this reaction and could provide rate enhancements similar to the EtPy hydrogenation as there are elements in these modifiers which give rate enhancements (Table 5.7).

Table 5.7- Hydrogenation rate values and the rate enhancements in the 2,3-butanedione hydrogenation reaction				
Modifier	lin_fit slope / mmol s ⁻¹	aR	kinetic fit, k2 / mmol s ⁻¹	iR
CD	1.0×10 ⁻²	1.4	1.6×10 ⁻²	0.7
QD	6.3×10 ⁻³	0.8	1.0×10 ⁻²	0.4
QL	1.6×10 ⁻²	2.1	2.7×10 ⁻²	1.2
Unmodified	7.5×10 ⁻³	1.0	2.2×10 ⁻²	1.0

The hydrogenation rate values using different modifiers in the 2,3-butanedione hydrogenation showed that QL gave a significant apparent rate enhancement (Table 5.7 and Figure 5.14). These results are novel.

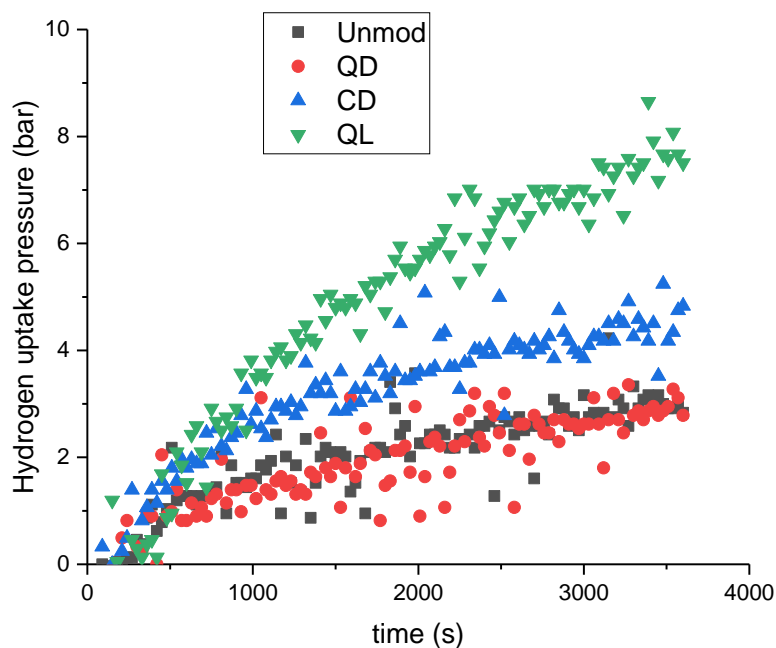


Figure 5.14: Hydrogen pressure uptake (bar) 2,3-butanedione hydrogenation, unmodified (black), QD (red), CD (blue) and QL (green); Reaction conditions: H₂ (20 bar), RT, 5 wt.% Pt / Al₂O₃ (1.25 mmol, 250 mg); 2,3-butanedione (40 mmol, 3.5 mL); toluene + 0.001 M acetic acid); CD (8.5 μmol, 2.5 mg), QD (0.9 mmol, 100 mg), QL (0.08 mmol, 10 mg).

5.5 Fluorine-containing compounds

5.5.1 1,1,1-trifluoro-2,4-pentandione hydrogenation

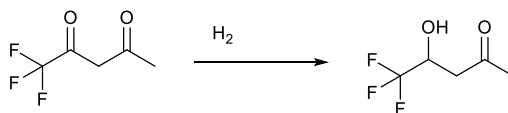


Figure 5.15: 1,1,1-trifluoro-2,4-pentandione hydrogenation

Trifluoro diketones and their corresponding alcohols have gained much attention in the agrochemical and pharmaceutical industries.¹⁸ 1,1,1-trifluoro-2,4-pentandione (TP) (Figure 5.15) is a beta diketone and was chosen because a rate enhancement has been reported using trace amounts of CD as well as the ee (35%). This amount of CD was used because it is the same amount that was in the literature. An apparent rate enhancement of this magnitude would imply that optimising the amount of CD added would show an increase in rate enhancement.^{18,19} However, QD poisoned the reaction (Table 5.8 and Figure 5.16).

Table 5.8- Hydrogenation rate values and the rate enhancements in the TP hydrogenation reaction				
Modifier	lin_fit slope / mmol s ⁻¹	aR	kinetic fit, k2 / mmol s ⁻¹	iR
CD	2.3×10 ⁻³	1.3	4.0×10 ⁻³	0.7
QD	4.3×10 ⁻⁴	0.2	1.3×10 ⁻³	0.2
Unmodified	1.8×10 ⁻³	1.0	5.5×10 ⁻³	1.0

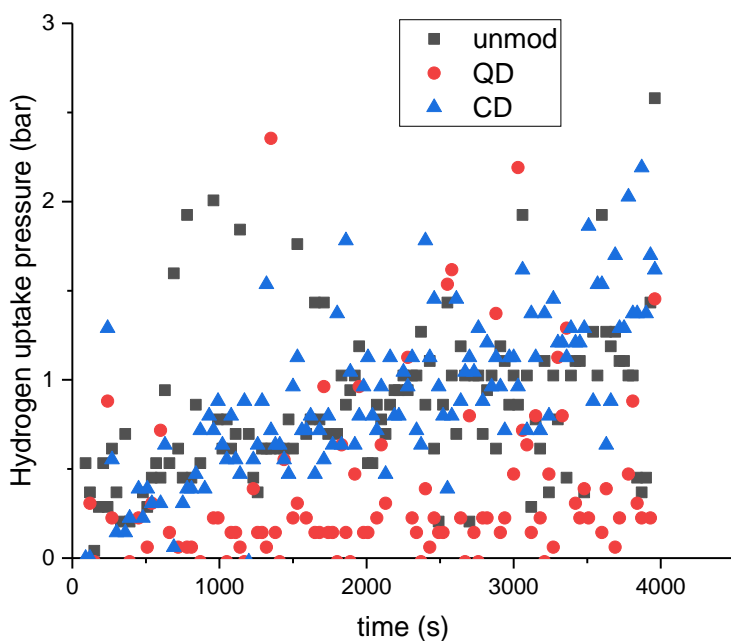


Figure 5.16: Hydrogenation uptake pressure (bar) for the hydrogenation of 1,1,1-trifluoro-2,4-pentandione, unmodified (black), QD (red) and CD (blue): Reaction conditions: H₂ (20 bar), RT, 5 wt.% Pt / Al₂O₃ (1.25 mmol, 250 mg); TP (41 mmol, 5 mL); toluene + 0.001 M acetic acid); CD (17 μmol, 5 mg), QD (0.9 mmol, 100 mg).

5.5.2 Ethyl trifluoropyruvate hydrogenation

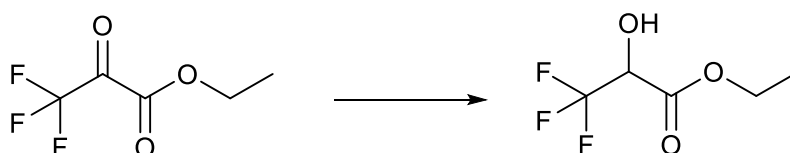


Figure 5.17: Ethyl trifluoropyruvate reaction

Ethyl trifluoropyruvate (EFP) (Figure 5.17) is an important chemical as it acts as a building block for fluorine-containing compounds. It was tested using the modifiers that have

been used in this project. EFP has been tested before using CD, but it did not give a rate enhancement and it gave a very low ee (5%). The reason given for the lack of effect was that NMR studies showed that the CD reacted with the EFP. Therefore, it would be interesting to see if the other modifiers used in this project would give a rate enhancement.²⁰ Unfortunately, a rate enhancement was not observed in the reactions completed in this project. The apparent rate enhancement using CD was 0.3 and the intrinsic rate enhancement was 0.5. This means the reaction was poisoned by the CD. EFP was investigated as a rate enhancement had been reported when using CD in this hydrogenation (Table 5.9).

Table 5.9- Hydrogenation rate values and rate enhancement using different modifiers in the EFP hydrogenation reaction				
Modifier	lin_fit slope / mmol s ⁻¹	aR	kinetic fit, k2 / mmol s ⁻¹	iR
CD	2.3×10 ⁻³	0.3	6.9×10 ⁻³	0.5
QD	2.9×10 ⁻³	0.4	6.7×10 ⁻³	0.5
DABCO	7.4×10 ⁻³	0.9	1.1×10 ⁻²	0.8
QL	3.7×10 ⁻³	0.5	1.1×10 ⁻²	0.9
Unmodified	8.2×10 ⁻³	1.0	1.3×10 ⁻²	1.0

DABCO has a similar rate compared to the unmodified reaction whereas the other modifiers showed no increase in the rate and poisoned the reaction (Table 5.9 and Figure 5.18). More reactions should be carried out in order to see if a faster rate could be achieved using DABCO with different concentrations. These results are novel.

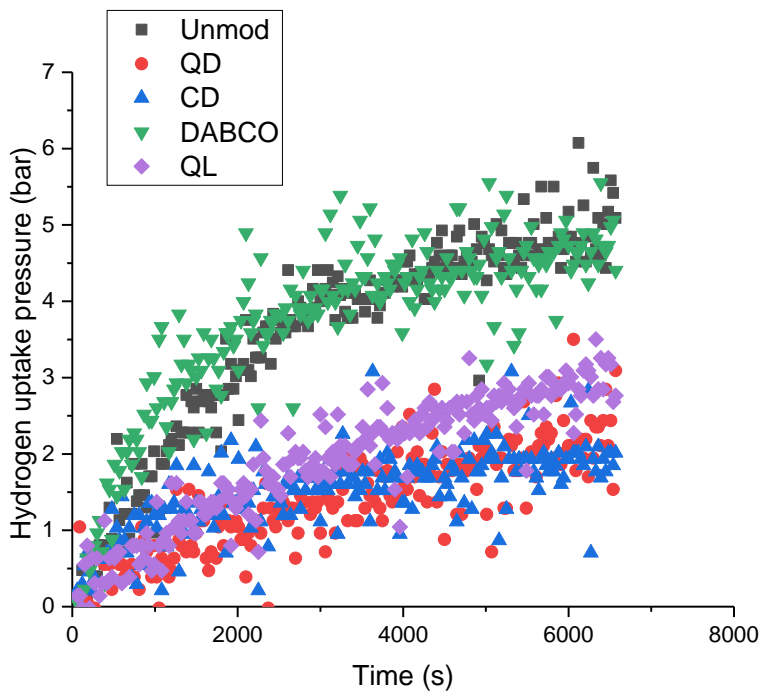
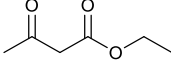
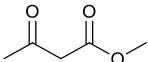
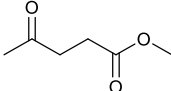
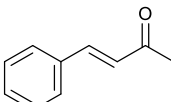
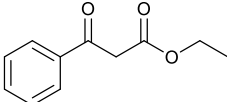
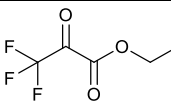
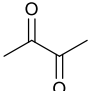
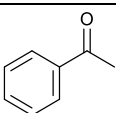
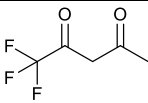


Figure 5.18: Hydrogen uptake graph of EFP hydrogenation unmodified (black), QD (red), CD (blue), DABCO (green) and QL (purple); Reaction conditions: H₂ (20 bar), RT, 5 wt.% Pt / Al₂O₃ (1.25 mmol, 250 mg); EFP (53 mmol, 7.0 mL); toluene + 0.001 M acetic acid); CD (8.5 μmol, 2.5 mg), QD (0.9 mmol, 100 mg), QL (0.08 mmol, 10 mg), DABCO (0.9 mmol, 101 mg).

5.6 Conclusion

Table 5.10- Summary of the reactants, modifiers and the subsequent rate enhancement found					
Substrate	Structure of substrate	Results when CD was added.	Results when QD was added.	Results when QL was added.	Results when DABCO was added.
EAA		Intrinsic rate enhancement was found. Apparent rate enhancement was not.	Reaction was poisoned.	Reaction was poisoned.	Reaction was poisoned.
MAA		Reaction was poisoned.	Reaction was poisoned.	Reaction was poisoned.	Reaction was poisoned.
ML		Reaction was poisoned.	Reaction was poisoned.	Reaction was poisoned.	Reaction was poisoned.
BA		Reaction was poisoned.	Reaction was poisoned.	Slight intrinsic rate enhancement.	Slight intrinsic rate enhancement
EBA		Reaction was poisoned.	Slight intrinsic rate enhancement	Reaction was poisoned.	Reaction was poisoned.
EFP		Reaction was poisoned.	Slight intrinsic rate enhancement	Reaction was poisoned.	Reaction was poisoned.
2,3-butane-dione		There is an apparent rate enhancement and an intrinsic rate enhancement.	Reaction was poisoned.	Significant apparent rate enhancement. Slight apparent rate enhancement.	Reaction was poisoned.
A		Reaction was poisoned.	Reaction was poisoned.	Reaction was poisoned.	Reaction was poisoned.
TP		Apparent rate enhancement was found. No intrinsic rate enhancement.	Reaction was poisoned.	Reaction was poisoned.	Reaction was poisoned.

A summary of the results of the reactions with different modifiers and reactants is shown in Table 5.10. Most of the modifiers at the specific concentration they were tested at were found not to have given a rate enhancement and actually poisoned the reaction. Out of the achiral tertiary amines QL was the only modifier that gave a rate enhancement in the 2,3-butanedione reaction. It is not known why QL gave a rate enhancement in this reaction whereas the other modifiers did not; perhaps the OH group played a role in the reaction. QD gave slight intrinsic rate enhancements to EBA and EFP but then poisoned all the reactions. This could mean that at other concentrations of QD the rate enhancement could have been more significant. CD gave slight rate enhancements in the TP, 2,3-butanedione and EAA hydrogenation but accounting for error these rates overlap, although it shows that CD perhaps could give a rate enhancement if the concentrations were changed.

5.7 References

1. P. Kukula and L. Červený, *Journal of Molecular Catalysis A: Chemical*, 2002, **185**, 195-202.
2. H. Tadao, I. Yoshiharu, *Chemistry Letters*, 1978, **7**, 1195-1196
3. G. Bond, P. Meheux, A. Ibbotson and P. Wells, *Catalysis Today*, 1991, **10**, 371-378
4. I. Sutherland, *Journal of Catalysis*, 1990, **125**, 77-88.
5. D. Sterk, M. Stephan, B. Mohar, *34 Tetrahedron: Asymmetry*, 2002, **13**, 2605-2608,
6. L. Lomba, C. Lafuente, M. García-Mardones, I. Gascón and B. Giner, *The Journal of Chemical Thermodynamics*, 2013, **65**, 34-41.
7. O. Turova, E. Starodubtseva, M. Vinogradov and V. Ferapontov, *Journal of Molecular Catalysis A: Chemical*, 2009, **311**, 61-65.
8. H. Siegel, M. Eggersdorfer, Ullmann's Encyclopedia, vol. A15, Wiley-VCH, New York, 2012
9. M. Casagrande, L. Storaro, A. Talon, M. Lenarda, R. Frattini, E. RodriguezCastellon, P. Maireles-Torres, Liquid phase acetophenone hydrogenation on Ru/Cr/B catalysts supported on silica, *J. Mol. Catal. A Chem.*, 2002, **188**, 133-139.
10. A. Perosa, P. Tundo and M. Selva, *Journal of Molecular Catalysis A: Chemical*, 2002, **180**, 169-175.
11. A. Yang, H. Jiang, J. Feng, H. Fu, R. Li, H. Chen and X. Li, *Journal of Molecular Catalysis A: Chemical*, 2009, **300**, 98-102.
12. R. Hess, A. Vargas, T. Mallat, T. Bürgi and A. Baiker, *Journal of Catalysis*, 2004, **222**, 117-128.
13. H. Rojas, G. Díaz, J. Martínez, C. Castañeda, A. Gómez-Cortés and J. Arenas-Alatorre, *Journal of Molecular Catalysis A: Chemical*, 2012, **363-364**, 122-128.
14. R. Ouyang and D. Jiang, *ACS Catalysis*, 2015, **5**, 6624-6629.
15. X. Lu, M. Wang, L. Zhang, J. Jiang, L. Li, X. Gao, L. Zhang, C. Li and H. Chen, *Tetrahedron Letters*, 2020, **61**, 151661.
16. V. Schaeffer, A. Iannucci, in *Encyclopedia of Toxicology (Third Edition)*, 2014, Elsevier
17. J. Sowa, *Catalysis of organic reactions*, Taylor & Francis, Boca Raton, 2005.
18. S. Diezi, D. Ferri, A. Vargas, T. Mallat and A. Baiker, *Journal of the American Chemical Society*, 2006, **128**, 4048-4057.
19. R. Hess, S. Diezi, T. Mallat and A. Baiker, *Tetrahedron: Asymmetry*, 2004, **15**, 251-257.
20. M. von Arx, T. Mallat and A. Baiker, *Journal of Catalysis*, 2000, **193**, 161-164.

Chapter 6

Computational analysis

6.1 Background to theoretical calculations

In the last few decades, the advancements of theoretical calculations have allowed a greater understanding of reaction mechanisms and have had uses in many industries; for example, hydrogen storage, materials for batteries and environmental studies. Advancements in density functional theory (DFT) have allowed accurate descriptions of catalytic systems that can be compared with experimental results. DFT is a quantum mechanical method that allows the calculations of the electronic structure of atoms, molecules, complexes, solids and their surfaces.¹

Reducing environmental impact and changing from fossil fuels to more renewable energy sources is a significant challenge that will require the design of new catalytic materials. Catalytic properties are determined by the electronic structure of the catalyst material, by changing the physical structure and by altering their composition. Now, because of these advancements in DFT calculations of big complex, extended systems are possible. Based on DFT calculations of reaction barriers and reaction energies the complete kinetics of some catalytic reactions have been evaluated; for example, the ethylene hydrogenation on Pd.²

DFT was created by Kohn and Sham (1965) and Hohenberg and Kohn (1964). They proved that the total energy of an electron gas is a unique functional of the electron density. The minimum value of the total energy functional is the ground- state energy of the system and the density that gives this value is the single-particle ground state density. Kohn and Sham then replaced the many-electron system by a set of self-consistent one-electron equations. This many-electron problem is caused by the electron-electron interactions that happen in multi-atom systems.

6.1.1 Periodic calculations

In DFT calculations, periodic boundaries DFT assumes that the system is periodic and so builds the electronic structure using a finite unit cell which is assumed to repeat throughout space. The unit cell and the whole crystal can be built up by using this unit cell.

To find the electronic potential and the total energy of a system, k-point sampling over reciprocal space is required. Electronic states are only allowed at a set of k- points which are set by the boundary conditions for that solid. The sampling narrows the choice further to only the few that are selected by the user. This allows a compromise between accuracy and computational cost to be made. Electronic states of a finite number of k-points are needed to determine the total energy of the solid. An infinite number of calculations are needed at this potential as the occupied k-states contribute to the electronic potential. Electronic wave functions of k-points that are close together will be almost identical. Therefore, the wavefunction at a single k point can represent the electronic wavefunctions over a region of k space. k-Points are sampling points in the first Brillouin zone which is the specific region of reciprocal space closest to the origin. K-points are needed because of Bloch's theorem which states that in a periodic potential the wavefunctions have a periodic magnitude.³

One k-point in reciprocal space corresponds to an infinite set of planes in real space. The magnitude of error found using k-point sampling can be reduced by using a denser set of k-points. The total energy will converge as a denser set of k-points is used and the error goes towards zero.

According to Bloch's theorem the electronic wave functions at each k-point can be expanded using plane-wave basis sets. Coefficients for the plane-wave basis set with low kinetic energy are more important than those with high kinetic energy so the plane-wave basis set can be shortened by having an energy cut-off as, in theory, an infinite wave basis set would be needed to expand the electronic wave functions. This energy cut-off produces a finite basis

set. There would also be an error in these calculations using the finite basis set but increasing the energy cut-off can reduce this. There are problems using plane-wave basis sets, one of which is that the energy cut-off changes discontinuously with energy cut-off. These occur at different cut-offs in the k-points. The problem can be reduced by using denser k-points sets so the problem can be spread over more basis sets.³

In catalytic systems the adsorption energies are determined by the electronic structure of the surface. Christensen *et al.* illustrate this using transition metals whereby the higher the d-states in energy compared to the fermi level the greater the interaction with the adsorbate states. They explain this by stating that as the d-states get closer to the fermi level the antibonding states can be shifted above it and become empty.⁴

Computational calculations were carried out on the different substrate -modifier- Pt systems in order to find a greater understanding of the mechanism of these reactions. The modifiers were either side-on or end-on (see Figure 6.1) to the Pt(111) surface. The modifier is considered end on if the basic nitrogen is perpendicular towards the Pt (111) surface and side-on if the basic nitrogen is parallel to the Pt (111) surface.

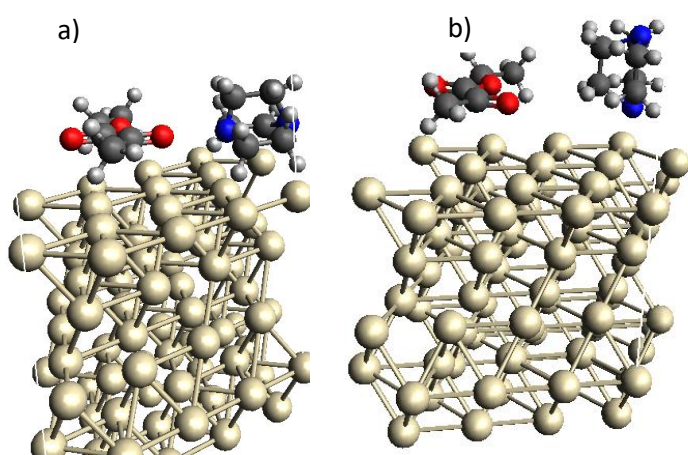


Figure 6.1: a) Side-on on DABCO and b) end-on DABCO with EtPy on the Pt(111) surface.

Atom colours: C: grey, H: white, O: red, N: blue and Pt: white

6.1.2 Molecular calculations

Molecular calculations in computational chemistry are made with the use of basis sets from quantum chemistry produced from hydrogenic-like atomic orbitals, s, p, d etc... Basis sets are a set of functions that are used to represent electronic wave functions. These basis sets refer to the one particle function used to build molecular orbitals. To determine these basis sets either Slater type orbitals (STOs) (Equation 1) or Gaussian type orbitals (GTOs) are used. Gaussian type orbitals are used more often as they are easier to implement computationally.⁵

$$R(r) = Nr^{n-1}e^{-\zeta r}$$

Equation 1: the equation for Slater type orbitals

n= principal quantum number

N= normalizing constant

r= is the distant of the electron from the atomic nucleus

ζ = is a constant that controls the way the wavefunction decays as we move away from the nucleus. The value is affected by the effective charge

STOs are functions used to represent atomic orbitals as part of the linear combination of atomic orbitals molecular orbital method (Equation 1). They have no radial nodes only angular nodes. The ζ controls the width of the orbital. STOs have an exponential decay at long range and agree with Kato cusps condition at short range which states that the electron density of a ground state of a molecular system has cusps at the location of the nuclei. The Kato cusps condition can accurately calculate the electron density near the nucleus. The problem with STOs is that there is no simple analytical solution for the overlap integrals used to describe chemical bonding and so these must be calculated numerically in a practical implementation,

adding computational overheads. They could be approximated to linear combinations of Gaussian-type orbitals instead (Equation 2).

$$R(r) = Nr^{n-1}e^{-\zeta r^2}$$

Equation 2: The equation for Gaussian-type orbital

n= principal quantum number

N= normalizing constant

r= is the distant of the electron from the atomic nucleus

ζ = It is a constant that shows the effective charge of the nucleus, where the effective charge is partly shielded by electrons.

The Gaussian type-orbital accounts for many electron interactions and is much easier to implement in a computational program than the STOs. The smallest type of basis set that can be implemented computationally is a minimal basis set.⁶ However, as valence electrons take part in bonding these valence orbitals are represented by more than one basis function which are called split valence basis sets. Split valence sets are used so that more functions can be used in the important bonding regions between atoms than are used for the core states. This saves computer time.⁷ The split valence basis set used in this project is B3LYP/6-31G(d,p). The number 6 from the basis set represents the primitive Gaussians comprising each core atomic orbital. The d and p of the basis set correspond to polarization functions which are added to describe polarization of electron density of an atom in a molecule as bonds are often polarized. The 3 and the 1 of the basis set show that the valence orbitals are composed of two basis functions each. The fact that there are two numbers after the hyphen means that it is a split valence double zeta basis set.

6.2 Dimer formation

For this project theoretical calculations of dimers have been completed firstly to see if it is likely that dimers are formed in the liquid phase but also to see if they can explain the significance of the rate enhancement experimentally. The calculations were completed by optimising the structure of the individual molecules (modifier and substrate) and then subtracting them from the calculated values of the dimer (Equation 3). If the energy is negative, it is favourable to form in the liquid phase.

$$E_{ads} = E_{Dimer\ complex} - E_{reactant} - E_{modifier}$$

Equation 3- Calculation of the energy of the dimer

Dimers have been previously modelled by Margitfalvi *et al.* using EtPy (Figure 6.2) as a substrate, although they used two conformers of cinchonidine that have not been studied in this project. These cinchonidine conformers are in the open form and they found that four of them were stable. They used the B3LYP/6-31G basis sets for their ab initio calculations.⁸

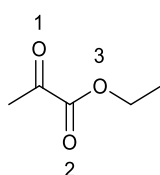


Figure 6.2: EtPy. The numbers are used in the text to explain the oxygen atoms in the structure

Figure 6.2 shows the structure of EtPy with the oxygen atoms numbered for reference when describing the dimer structures studied here. For the dimer calculations in this project the first dimer structure has the N-H of the modifier hydrogen bonded with the C=O (1) bond closest to the end at a distance of approximately 1.5 Å, the second dimer structure is where the

N-H is approximately 1.5 Å distance from the other C=O (2) bond and the third is where the N-H is at a distance of approximately 2 Å from the C=O (3) bond away. The difference in the length (in Angstroms) is due to which oxygen the N-H is bonding to as the carbonyl oxygens can be closer to the N-H bond. N-H cannot get that close to the ester O as there is steric hindrance from the modifier and other atoms in the molecule.

The images of dimers that are shown in section 6.2.2, 6.2.3, 6.2.4 and 6.2.5 are the conformations where the energies are calculated. Once these energies are calculated the optimised energies for the substrate and the modifier are subtracted off to find if the formation of these dimers is favourable (Equation 1). If the value is negative, it is considered favourable.

6.2.1 ETPY

In Table 6.1 and Figures 6.3, 6.4, 6.5 and 6.6 the different energies to make the dimer can be seen. All the dimers have favourable orientations. Margitfalvi *et al.* showed that EtPy and cinchonidine have interactions in the liquid phase via computational calculations and NMR studies.⁹ There has been work reported by Margitfalvi *et al.*⁸ that show dimer calculations with two cinchonidine molecules and a cinchonidine and a EtPy molecule. However, in this project cinchonidine was not used in theoretical calculations so no comparisons could be made.

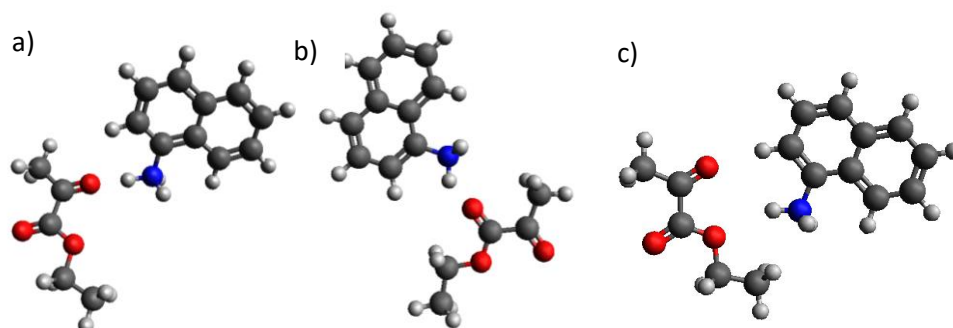


Figure 6.3: The three different dimer structures calculated for EtPy and 4-aminoquinolone, a) 1-EtPy-AQ, b) 2-EtPy-AQ, c) 3-EtPy-AQ

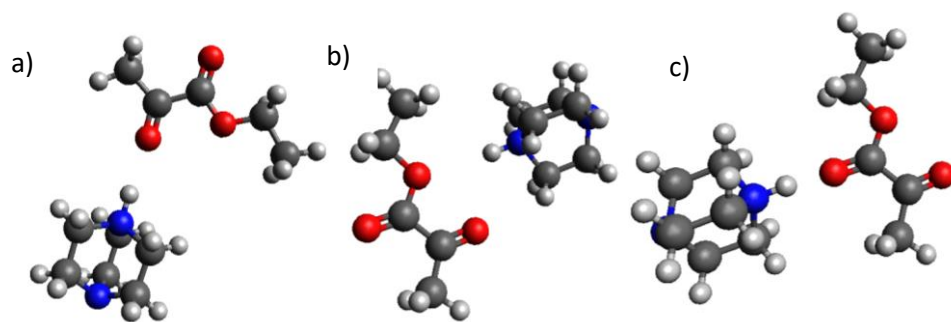


Figure 6.4: The three different dimer structures calculated for EtPy and DABCO, a) 1-EtPy-DABCO, b) 2-EtPy-DABCO, c) 3-EtPy-DABCO

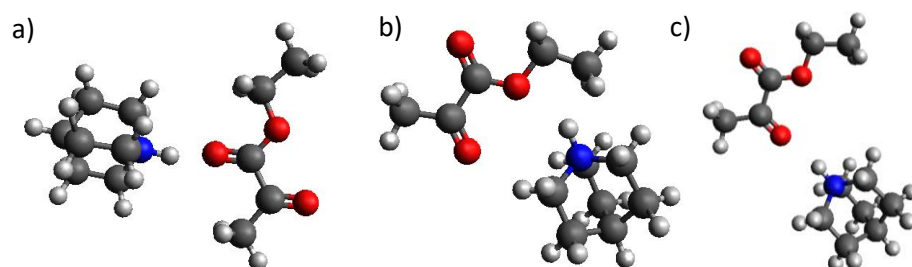


Figure 6.5: The three different dimer structures calculated for EtPy and QD, a) 1-QD-EtPy, b) 2-QD-EtPy, c) 3-QD-EtPy

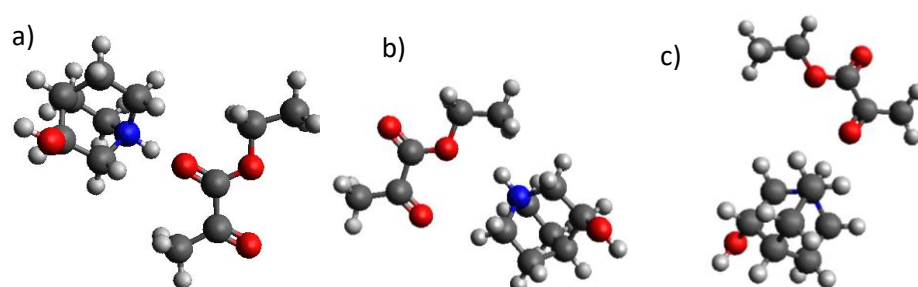


Figure 6.6: The three different dimer structures calculated for EtPy and QL, a) 1-QL-EtPy, b) 2-QL-EtPy, c) 3-QL-EtPy

Table 6.1- Dimer energies with ETPY and each modifier			
Dimer	Energy/ kJ mol ⁻¹		
	1	2	3
EtPy-AQ	-74	-59	-56
EtPy-QD	-61	53	50
EtPy-QL	-35	1	-31
EtPy-DABCO	-101	-101	-78

This work shows that EtPy also has dimer interactions with the other modifiers used in this project (QD, AQ, QL and DABCO). EtPy and DABCO form dimers with the lowest dimerization energies. In this project interestingly the EtPy reactions using DABCO gave the slowest intrinsic rate enhancement compared to QD and QL. The dimer forming with a very favourable dimerization energy led to a lowering of the reaction rate. QL and EtPy were the least feasible to form dimers but it was found to give faster rate enhancements in this project than the QD and DABCO. AQ could not be compared as it was used in neat acetic acid but dimers were likely to form in the liquid phase in this reaction. In these reactions the 1st dimer for each one of the modifiers with EtPy was the most favourable and most likely to occur. There was no correlation found between the dimer energies calculated and the apparent rate enhancement (Figure 6.7).

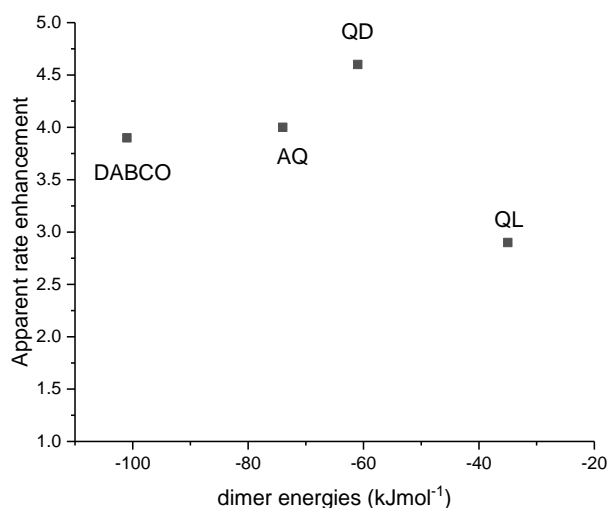


Figure 6.7: The apparent rate enhancement for ETYPY dimers vs calculated dimer energies.

6.2.2 MBF

In Table 6.2 the dimer energies for MBF and the different modifiers can be seen. All the dimer orientations had negative energies and were favourable to form (Figure 6.8, 6.9, 6.10 and 6.11). MBF-DABCO (-214 kJ mol^{-1}) and MBF-QD (-204 kJ mol^{-1}) gave the most negative and the most favourable dimer energies whereas MBF-AQ (-80 kJ mol^{-1}) gave the least negative and least favourable energy. This latter observation may be perhaps because the extra steric bulk of the AQ made it harder to obtain a more favourable dimer.

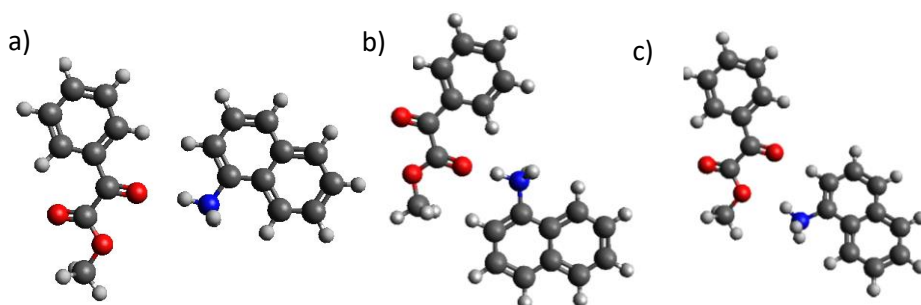


Figure 6.8: The three different dimers' structures calculated for MBF and 4-aminoquinolone,

a) 1-MBF-AQ, b) 2-MBF-AQ, c) 3-MBF-AQ

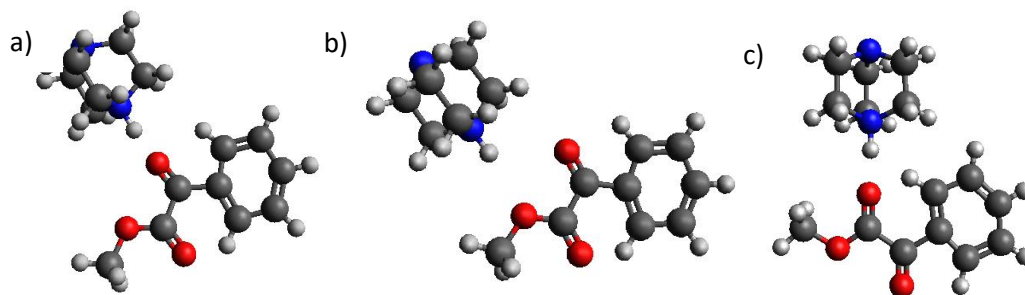


Figure 6.9: The three different dimers' structures calculated for MBF and DABCO, a) 1-MBF-DABCO, b) 2-MBF-DABCO, c) 3-MBF-DABCO

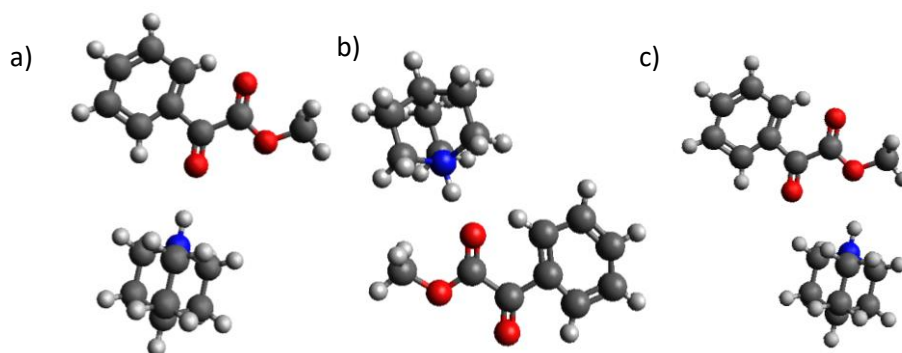


Figure 6.10: The three different dimers structures calculated for MBF and QD, a) 1-MBF-QD, b) 2-MBF-QD, c) 3-MBF-QD

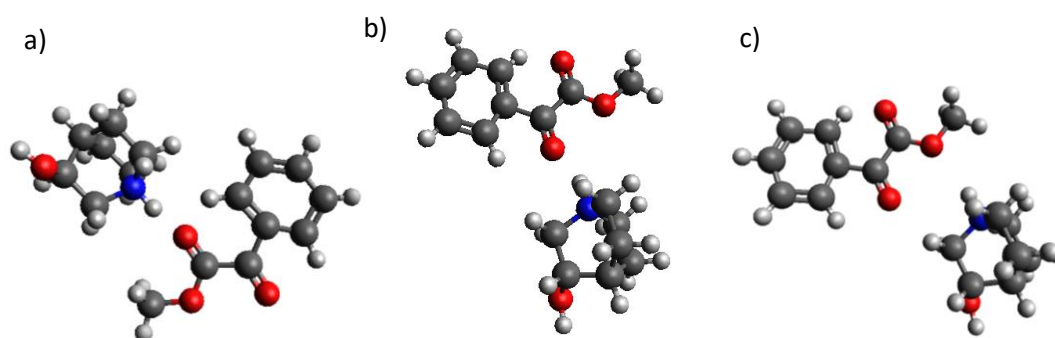


Figure 6.11: The three different dimer structures calculated for MBF and QL, a) 1-MBF-QL, b) 2-MBF-QL, c) 3-MBF-QL

Table 6.2- Dimer energies with MBF and each modifier			
	Energy/ kJ mol ⁻¹		
Dimer	1	2	3
MBF-AQ	-80	-61	-63
MBF-QD	-204	-177	-196
MBF-QL	-194	-161	-187
MBF-DABCO	-214	-192	-172

In these results the dimers MBF-QD, MBF-QL, MBF-DABCO have similar dimer energies, but the rate enhancements found in this project were much greater in MBF-QL than MBF-DABCO and MBF-QD. So, this may not be a suitable calculation for seeing which modifier would give a rate enhancement or not. Interestingly, all the 1st dimer conformations had the lowest energy for their respective MBF-modifier combinations and were the most favourable. There was no correlation found between the dimer energies and apparent rate enhancements (Figure 6.12)

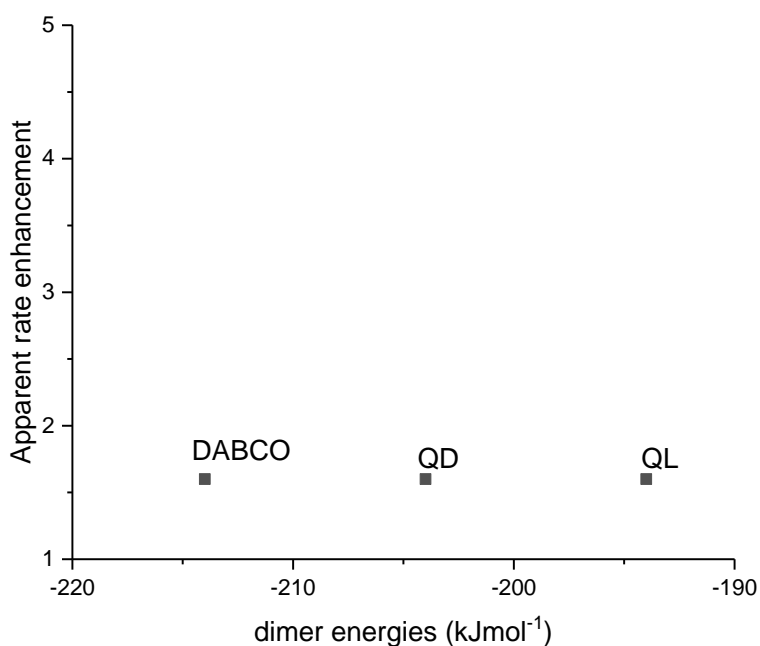


Figure 6.12: The apparent rate enhancement for MBF dimers vs calculated dimer energies.

6.2.3 EBF

In Table 6.3 and Figures 6.13, 6.14, 6.15 and 6.16 the different energies for the dimer formation can be seen. As all the energies are negative it shows that all these dimers can form. The EBF-DABCO dimer has the lowest energy (-143 kJ mol^{-1}) and therefore the most favourable to form whereas the other three dimers EBF-AQ (-110 kJ mol^{-1}), EBF-QD (-113 kJ mol^{-1}) and EBF-QL (-112 kJ mol^{-1}) gave very similar energies when forming the dimer.

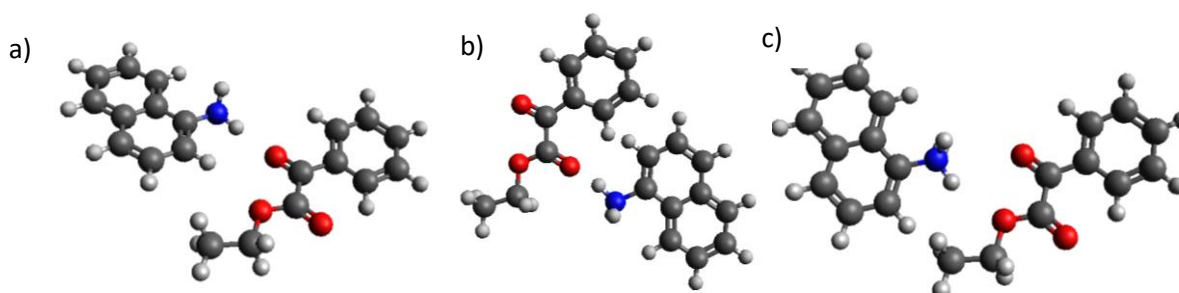


Figure 6.13: The energies of the three different structures calculated for EBF and 4-aminoquinolone, a) 1-EBF-AQ, b) 2-EBF-AQ, c) 3-EBF-AQ

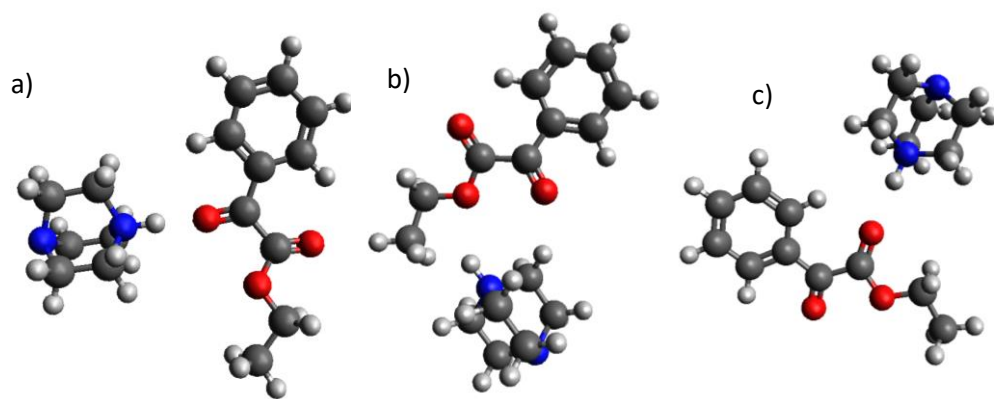


Figure 6.14: The three different dimer structures calculated for EBF and DABCO, a) 1-EBF-DABCO, b) 2-EBF-DABCO, c) 3-EBF-DABCO

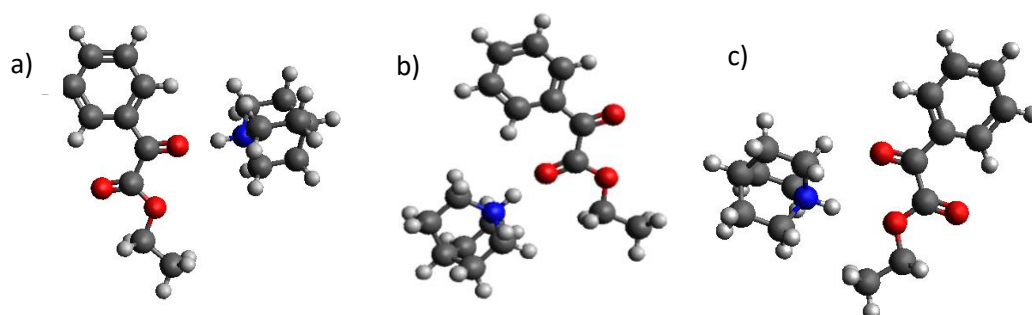


Figure 6.15: The three different dimers structures calculated for EBF and QD, a) 1-EBF-QD, b) 2-EBF-QD, c) 3-EBF-QD

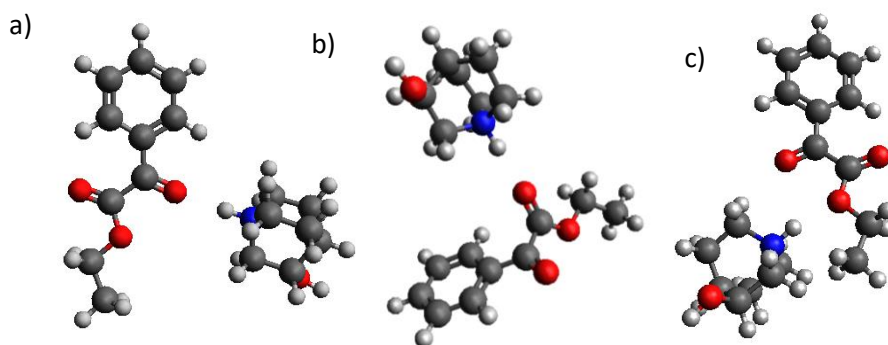


Figure 6.16: The three different dimer structures calculated for EBF and QL, a) 1-EBF-QL, b) 2-EBF-QL, c) 3-EBF-QL

Table 6.3- Dimer energies with EBF and each modifier			
Dimer	Energy/ kJ mol ⁻¹		
	1	2	3
EBF-AQ	-91	-110	-50
EBF-QD	-113	-50	-60
EBF-QL	-112	-58	-25
EBF-DABCO	-84	-52	-143

Interestingly, in these results for EBF-AQ and EBF-DABCO the dimer energies go against the trend of the first dimer conformation being the most favourable as these were the 2nd conformer for EBF-AQ and the 3rd conformer for EBF-DABCO. There has been literature published on the dimer calculations for ETPY and CD ⁸ but not for other modifiers tested in this project so these results are novel (Table 6.3). There was no correlation found between the dimer energies and the apparent rate enhancement.

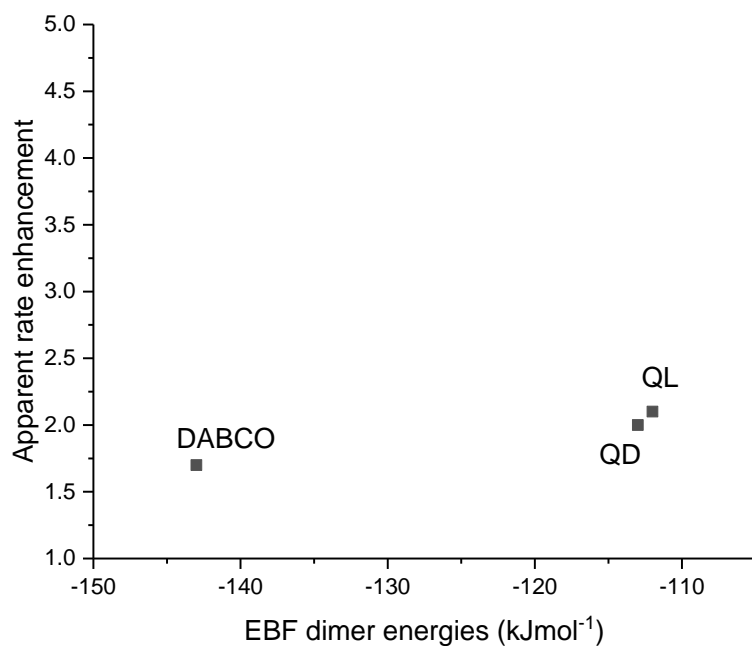


Figure 6.17: The apparent rate enhancement for EBF dimers vs calculated dimer energies.

6.2.4 Ethylacetoacetate

Theoretical calculations of the dimers of ethyl acetoacetate (EAA) were also determined to see if there was any difference between dimers of substrates that give a rate enhancement versus one that does not. Theoretical calculations were completed using the conformers in Figure 6.18, 6.19 and 6.20.

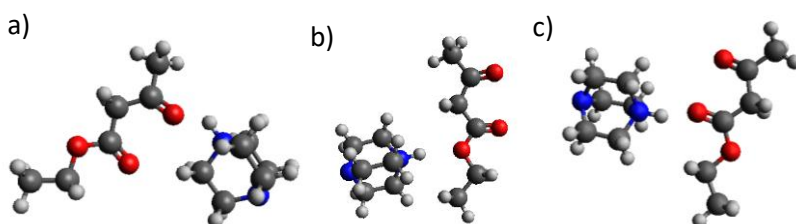


Figure 6.18: The three different dimer structures calculated for EAA and DABCO, a) 1-DABCO-EAA, b) 2-DABCO-EAA, c) 3-DABCO-EAA

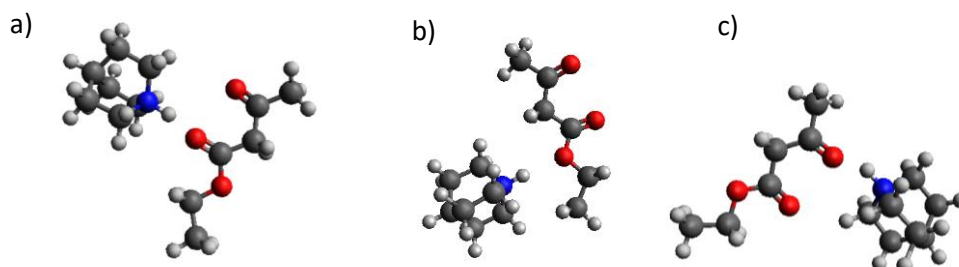


Figure 6.19: The three different dimer structures calculated for EAA and DABCO, a) 1-DABCO-EAA, b) 2-DABCO-EAA, c) 3-DABCO-EAA

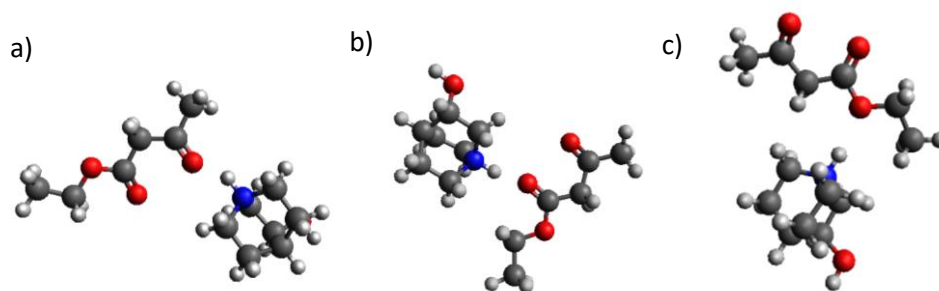


Figure 6.20: The three different dimer energies calculated for EAA and DABCO, a) 1-DABCO-EAA, b) 2-DABCO-EAA, c) 3-DABCO-EAA

Table 6.4- Dimer energies with EAA and each modifier			
Dimer	Energy/ kJ mol ⁻¹		
	1	2	3
EAA-QD	-21	57	-19
EAA-QL	-117	-109	-42
EAA-DABCO	-118	-48	-123

In Table 6.4 and Figures 6.18, 6.19 and 6.20 the different energies for dimer formation can be seen. DABCO again gave the most feasible dimer (-123 kJ mol⁻¹) with QL at a close second (-117 kJ mol⁻¹). QD gave the least feasible dimers (-21 kJ mol⁻¹). As this substrate did not give any rate enhancements in this project, dimer energy calculations cannot be used to predict whether a rate enhancement may occur or not. In these calculations the 1st dimer for all the modifiers and EAA gave the lowest and most feasible energy except for DABCO where the 1st and 3rd dimer conformation were very similar.

6.2.5 Conclusions for dimer calculation

In conclusion, as the EAA dimers calculated energies are also negative it was inconclusive as to whether dimers forming in the liquid phase is a prerequisite to a rate enhancement as the energies did not correlate with the rate enhancements found in this project

other than for EBF where it was found that the higher the dimer energy the higher the apparent rate enhancement. This would mean the less favourable the dimer is to form the higher the rate enhancement so perhaps the dimers forming without the surface may inhibit the rate enhancement.

Both EtPy and EBF gave feasible dimer calculations with each of the modifiers. This shows that not only do they form dimers with CD in the liquid phase they also form dimers with QD, QL and DABCO in the liquid phase also.

A trend found was that the 1st dimer conformation was usually the lowest in energy in almost all the modifier-substrate dimers tested. This is interesting as the carbonyl that the modifier has H-bonded to in this dimer is the carbonyl that is hydrogenated in the reaction. This shows that all the modifiers are very likely to stabilize the half-hydrogenated state of this directed carbonyl which has been proposed as the reason that QD gives the rate enhancement in Bond *et al.*'s work.¹⁰

6.3 Substrate-modifier- surface

Optimised energies were calculated for all the substrate-modifier surface combinations that were used in this project with the substrates EtPy, EBF and MBF. The adsorption energies of the substrate were calculated using Equation 4. The adsorption energies of the modifier were calculated using Equation 5.

$$E_{ads} = E_{Pt+Substrate+Modifier} - E_{Pt+Modifier-Substrate} - E_{Substrate}$$

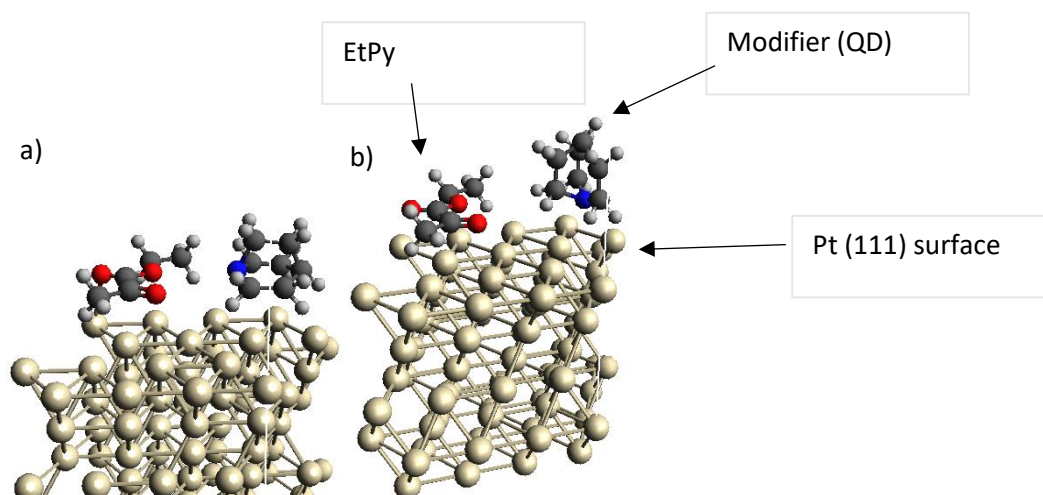
Equation 4- Equation showing how the adsorption energy of the substrate was calculated.

$$E_{ads} = E_{Pt+Modifier-Substrate} - E_{Pt} - E_{modifier}$$

Equation 5- Equation showing how the adsorption energy of the modifier was calculated.

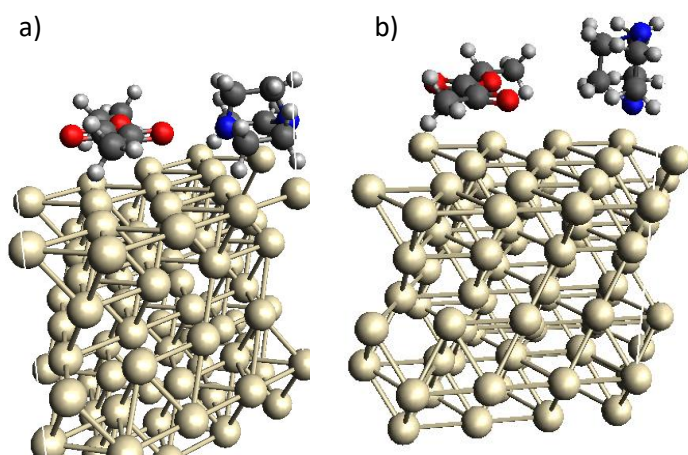
6.3.1 ETPY

The adsorption energies of the EtPy and the different complexes are shown in Table 6.5. The complexes are shown in Figures 6.21, 6.22, 6.23 and 6.24.

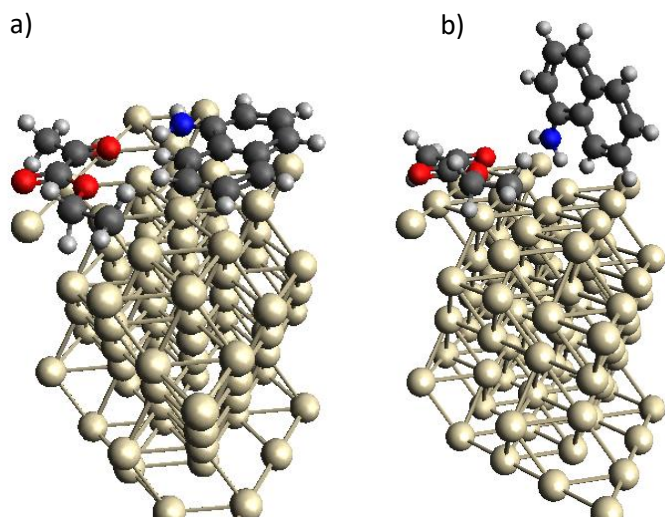


In Figure 6.2: EtPy-QD the two different ways the modifiers can be adsorbed onto the surface:

a) side-on and b) end-on can be seen.

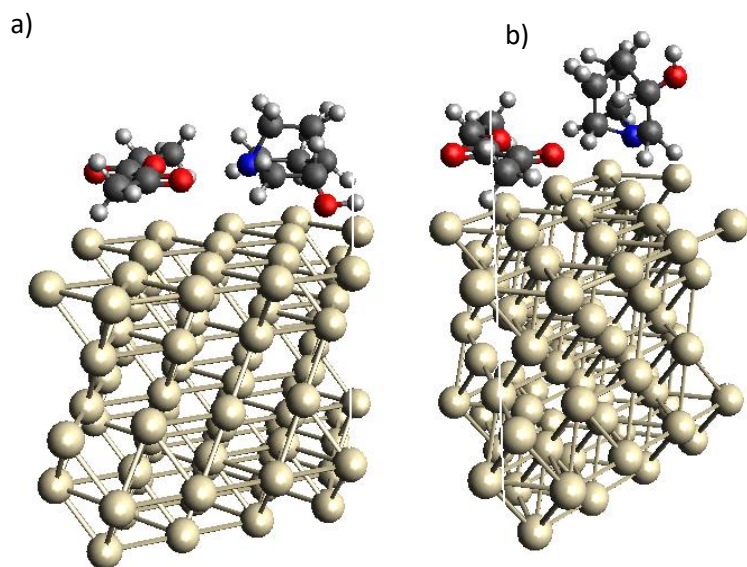


In Figure 6.22: EtPy-DABCO the two different ways the modifiers can be adsorbed onto the surface: a) side-on and b) end-on can be seen.



In Figure 6.23: EtPy-AQ the two different ways the modifiers can be adsorbed onto the surface:

a) side-on and b) end-on can be seen.



In Figure 6.24: EtPy-QL the two different ways the modifiers can be adsorbed onto the surface:

a) side-on and b) end-on can be seen.

Table 6.5- List of adsorption energies of modifiers and EtPy from the different EtPy-modifier complexes.		
Structure	E _{ads} of modifier /kJ mol ⁻¹	E _{ads} of EtPy /kJ mol ⁻¹
EtPy- QD end-on	-191	-135
EtPy- QD side-on	-112	-104
EtPy- DABCO end-on	-190	-141
EtPy- DABCO side-on	-193	-65
EtPy- QL end-on	-189	-142
EtPy- QL side-on	-116	-147
EtPy- 4-AQ end-on	-219	-18
EtPy- 4-AQ side-on	-258	-134
EtPy only, on platinum		-101

Figures 6.21, 6.22, 6.23 and 6.24 and Table 6.5 show the complexes and their energies. If the adsorption energy of EtPy as part of the complex is less than the EtPy on Pt (-101.4 kJ mol⁻¹) alone, this suggests that the modifiers help the EtPy adsorb to the surface. In this Table all the modifiers help the EtPy adsorb onto the surface in one way or another (side- on or end-on). End-on AQ (-18 kJ mol⁻¹) and side-on DABCO (-64.5 kJ mol⁻¹) does not help EtPy adsorb onto the Pt surface. The values shown in the centre column are the adsorption energies of just the modifier on the platinum.

The modifier was tested when it adsorbed end-on and side-on to see which gave a more favourable adsorption energy. It has been stated that side-on adsorption is more stable for pyridine computationally and cinchonidine using Near Edge X-Ray Absorption Fine Structure (NEXAFS) studies under ultrahigh vacuum (UHV).^{11,12} It was found that there is a correlation between the adsorption energies vs the apparent rate enhancement in the EtPy hydrogenation (Figure 6.25). It was also found that the higher the calculated adsorption energies of the EtPy in the modifier-EtPy-Pt complex the higher the apparent rate enhancement.

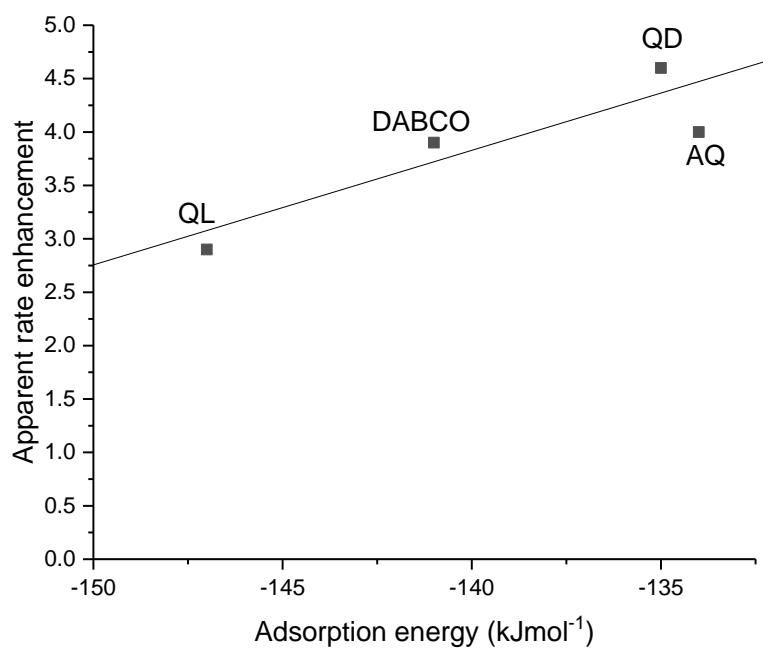


Figure 6.25: Apparent rate enhancement vs Adsorption energies of EtPy when using the different modifiers for the ETPY reaction

6.3.2 MBF

In Table 6.6 the list of adsorption energies of MBF on the Pt can be seen with the different modifiers. In Figures 6.26, 6.27, 6.28 and 6.29 the complexes that were used to calculate these adsorption energies can be seen.

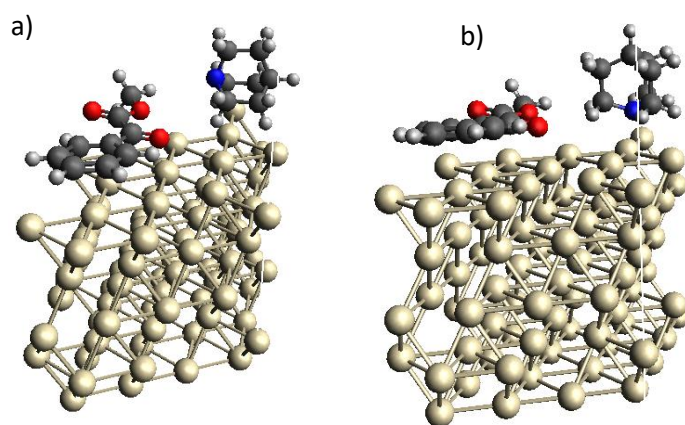


Figure 6.26: MBF-QD-Pt (111): a) QD side-on b) end-on

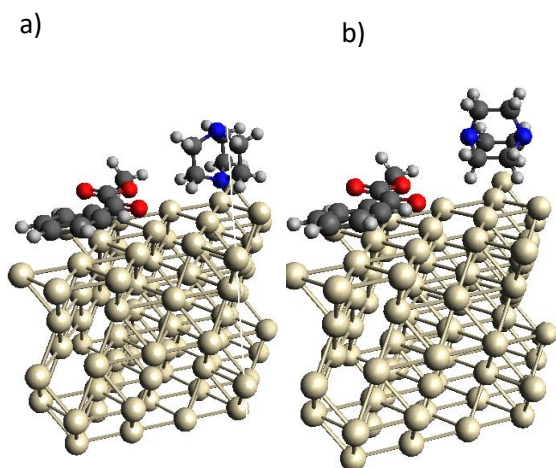


Figure 6.27: MBF-DABCO-Pt (111): a) DABCO end-on b) and side-on

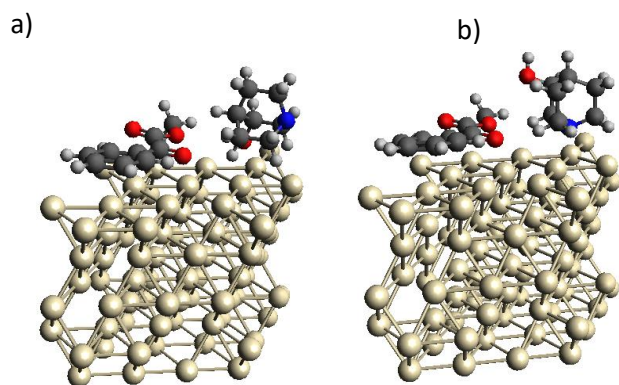


Figure 6.28: MBF-QL-Pt (111): a) QL side-on b) end-on

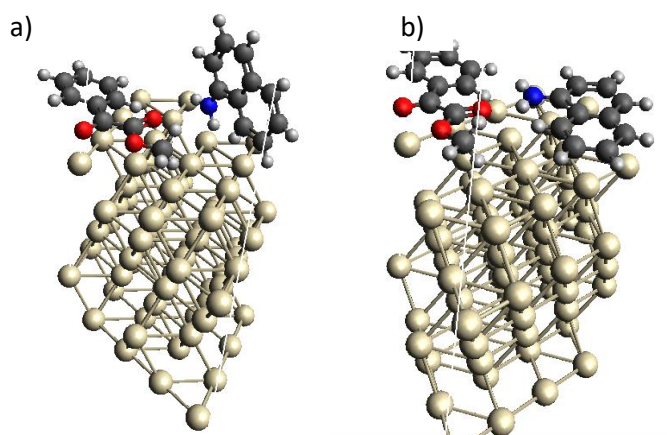


Figure 6.29: MBF-4-AQ-Pt (111) a) 4-AQ end-on b) and side-on

Table 6.6- List of adsorption energies of modifiers and MBF from the different MBF-modifier complexes.		
Structure	E _{ads} of modifier /kJ mol ⁻¹	E _{ads} of MBF /kJ mol ⁻¹
MBF- QD end-on	-192.	-184
MBF - QD side-on	-112	-227
MBF - DABCO end-on	-191	-147
MBF - DABCO side-on	-130	-221
MBF - QL end-on	-184	-185
MBF - QL side-on	-118	-220
MBF - 4-AQ end-on	-109	-247
MBF - 4-AQ side-on	-258	-62
Just MBF on the platinum		-221

Almost none of the modifiers made it more favourable for the MBF to adsorb onto the surface, the exception being end-on 4-aminoquinoline (Table 6.6). This could be as this hydrogenation reaction is solvent dependent as when the reactions were performed in neat acetic acid none of these modifiers (at the one amount tested) gave rate enhancements but in toluene +.001M acetic acid at the same amounts of modifiers rate enhancements were seen. There have been theoretical calculations completed on an MBF and CD system but not for any of the modifiers investigated in this project.¹³ Adsorption energies vs apparent rate enhancement graph (Figure 6.30) show that there is no correlation between the theoretical calculations found and the rate enhancement found in the experimental part of this thesis.

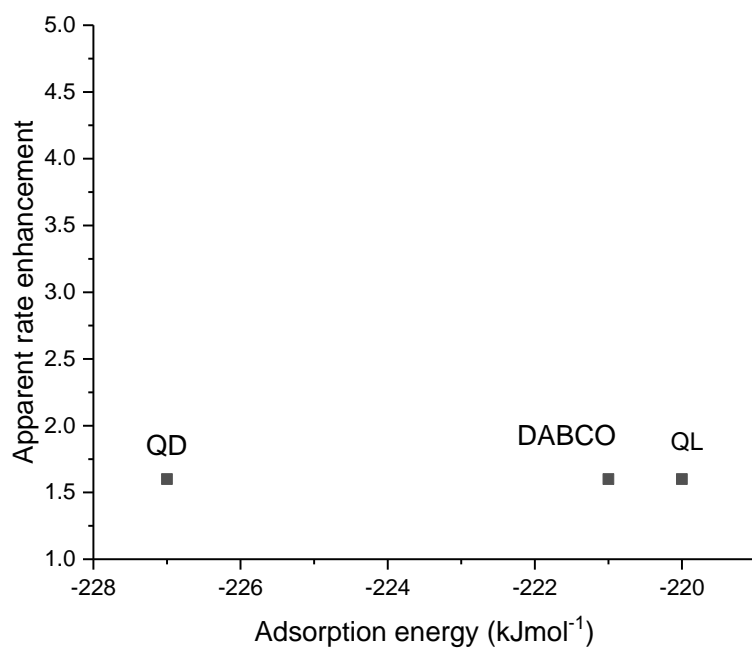


Figure 6.30: Apparent rate enhancement vs Adsorption energies of MBF when using the different modifiers.

6.3.3 EBF

Table 6.7 shows the different adsorption energies for EBF using the different modifiers. The complexes used to calculate these adsorption energies are in Figures 6.31, 6.32, 6.33 and 6.34.

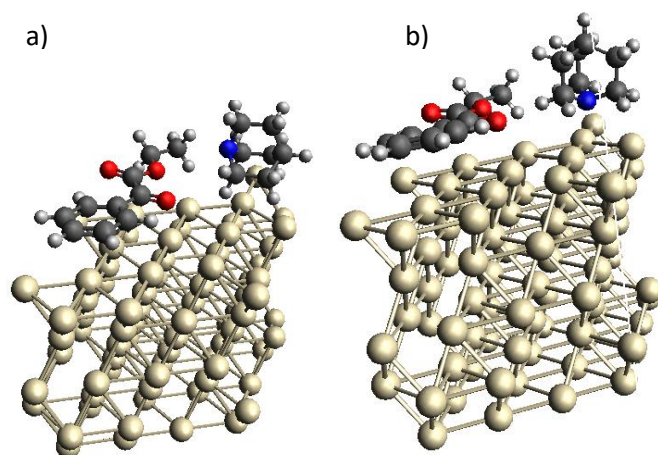


Figure 6.31: EBF-QD-Pt (111): a) QD side-on b) and end-on

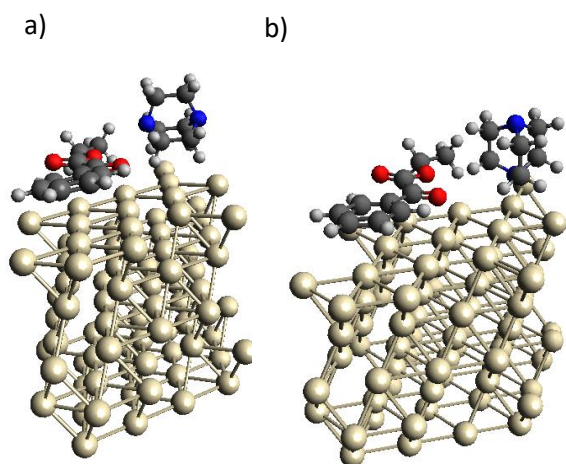


Figure 6.32: EBF-DABCO -Pt (111): a) DABCO side-on b) and end-on

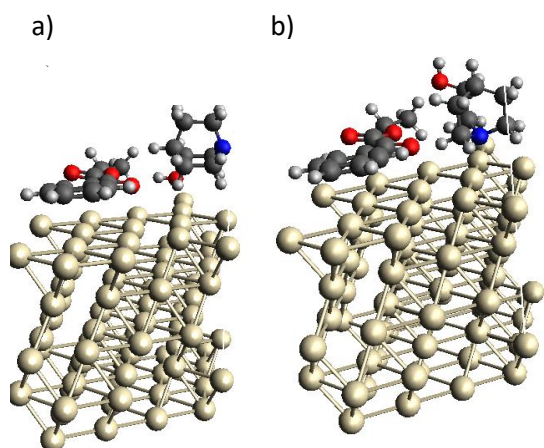


Figure 6.33: EBF-QL-Pt (111): a) QL side-on b) and end-on

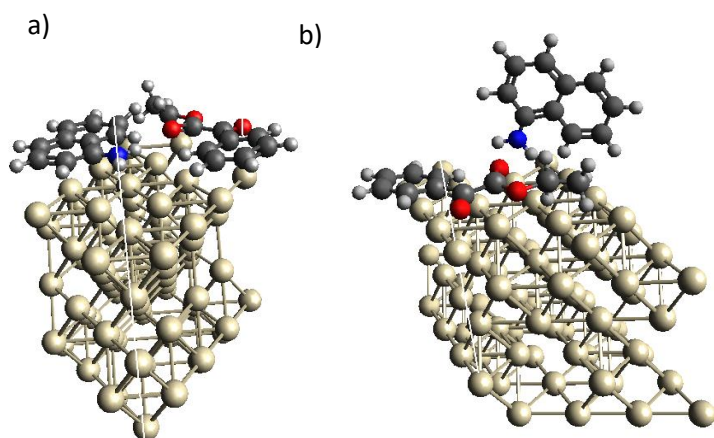


Figure 6.34: EBF-4-AQ -Pt (111): a) 4-AQ side-on b) and end-on

Table 6.7- List of adsorption energies of modifiers and EBF from the different EBF-modifier complexes.		
Structure	E _{ads} of modifier /kJ mol ⁻¹	E _{ads} of EBF /kJ mol ⁻¹
EBF- QD end-on	-192	-218
EBF - QD side-on	-112	-229
EBF - DABCO end-on	-190	-189
EBF - DABCO side-on	-127	-214
EBF - QL end-on	-189	-210
EBF - QL side-on	-114	-224
EBF - 4-AQ end-on	-109	-244
EBF - 4-AQ side-on	-258	-60
Just EBF on Pt		-222

Similar to MBF complexes, none of the modifiers help the adsorption of EBF significantly except for end-on AQ (-244 kJ mol⁻¹) (Table 6.7). This could be seen experimentally as only toluene + .001 M of acetic acid gave rate enhancements in this project and neat acetic acid did not give rate enhancements. However, only one amount of modifier was used in the acetic acid reactions so more reactions in the future would have to be completed in acetic acid at different modifier amounts to get a clearer understanding of this solvent dependency. There was no correlation found between the adsorption energies and the apparent rate enhancement found in this project (Figure 6.35).

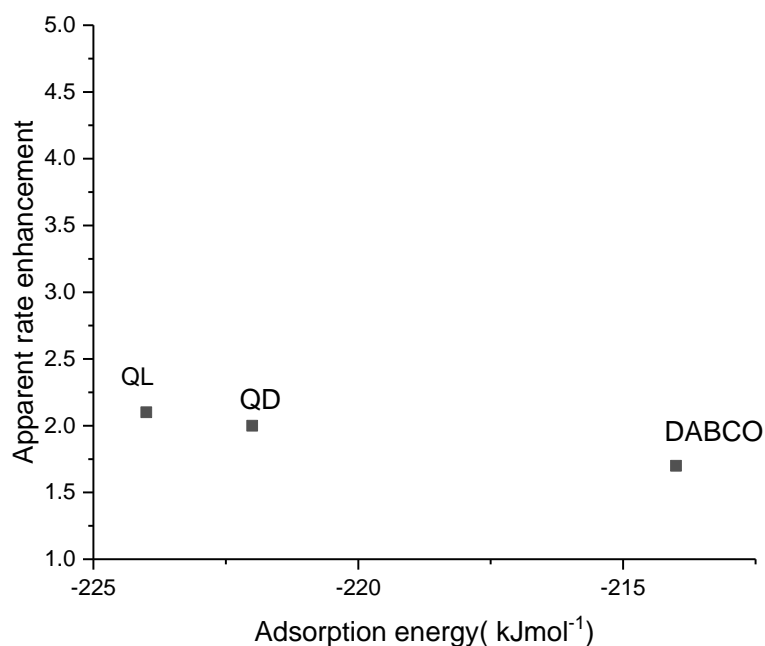


Figure 6.35: Apparent rate enhancement vs Adsorption energies of the substrates using different modifiers for the EBF reaction.

Interestingly, it was found that in the EBF reaction it was DABCO which gave the highest adsorption energy whereas in the MBF hydrogenation it was QD. It is unclear why this occurred as QD and DABCO have very similar structures.

6.3.4 Ethyl acetoacetate

The energies of EAA (Figure 6.36) were also calculated theoretically as in this reaction the modifiers poisoned the rate and so it was interesting to see if this difference could be explained using computational studies (Table 6.8). The complexes that were used for these calculations are shown in Figure 6.37, 6.38 and 6.39. However, only one amount of the modifier was used in each of these EAA hydrogenation reactions and future work using different amounts would be needed in order to get a comprehensive reaction profile of this substrate and these modifiers.

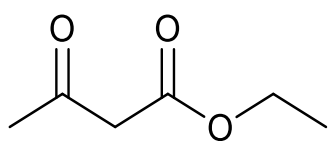


Figure 6.36: The structure of EAA

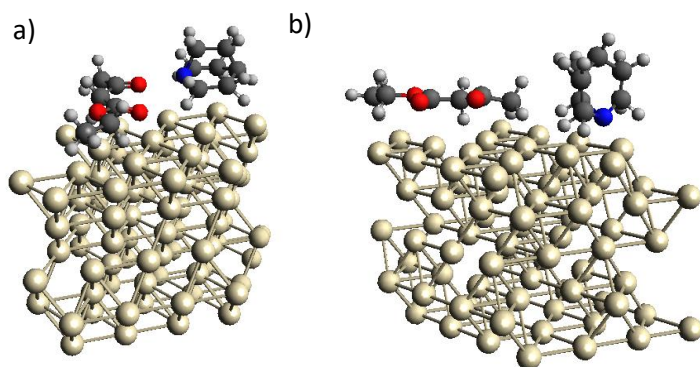


Figure 6.37: EAA-QD-Pt (111): a) QD side-on b) and end-on (left)

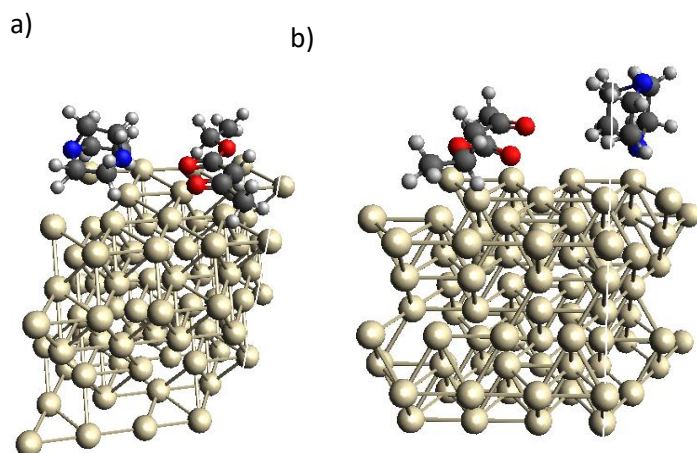


Figure 6.38: EAA-DABCO -Pt (111): a) DABCO side-on b) and end-on

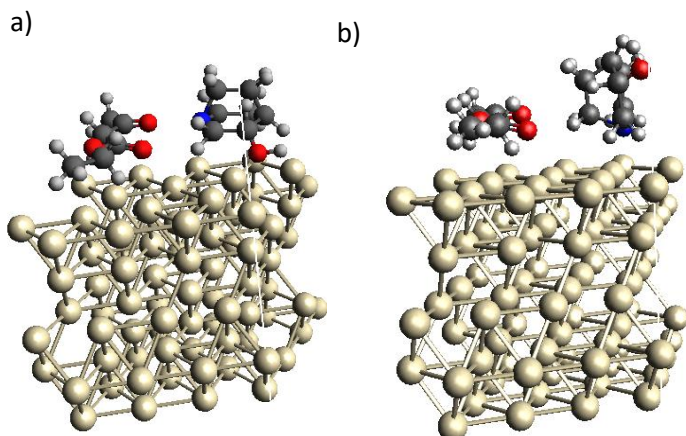


Figure 6.39: EAA-QL-Pt (111): a) QL side-on b) and side-on

Table 6.8- List of adsorption energies of modifiers and EAA from the different EAA-modifier complexes		
Structure	E_{ads} of modifier /kJ mol ⁻¹	E_{ads} of ETPY /kJ mol ⁻¹
Ethyl acetoacetate- QD end-on	-192	-142
EAA- QD side-on	-112	-147
EAA- DABCO end-on	-190	-18
EAA- DABCO side-on	-178	-132
EAA- QL end-on	-189	-184
EAA- QL side-on	-116	-147
Just EAA on platinum		-119

In Table 6.8 the different adsorption energies can be seen. In this Table all the modifiers except DABCO end-on could be shown to help EAA adsorb to the surface of the Pt (111) surface. This shows that all of the modifiers help EAA onto the surface of the Pt(111). The

reason that EAA showed no rate enhancement at the specific concentrations that were completed in this project (see Chapter 3) could be because of a steric issue that the extra CH₂ in-between the two carbonyl group causes. However, at different concentrations of modifier there could potentially be a significant rate enhancement, but more reactions would have to be completed to see if this is the case.

6.3.5 Conclusion for complex calculations

In these set of calculations, it was shown that all the modifiers can enhance the adsorption of EtPy and EAA onto the Pt (111) surface. A positive correlation was found in the calculations for the Pt-EtPy complexes with the rate enhancement. It can be shown that the higher the adsorption energy of the EtPy in the complex the higher the rate enhancement. The modifiers do not significantly help MBF and EBF to adsorb onto the surface. The rates enhancements found experimentally for these substrates cannot be explained through the computational calculations completed during this project.

Dimers have been found to form between the modifiers and the substrates in all cases and in most the preferred co-ordination is to the ketone that is hydrogenated. Also, each modifier is able to enhance the substrate adsorption in at least one configuration. This provides evidence to the 1:1 modifier: reactant model explanation for the origin of the rate enhancement rather than the catalyst 'cleaning' effect.

As the modifiers help EAA adsorb onto the surface this could mean that a rate enhancement could be achieved in EAA if more reactions were done using these modifiers at different amounts. However, these calculations cannot be used to see if a rate enhancement is likely or not.

6.4 Workfunction

The workfunction is the minimum energy required to remove an electron from the surface to a point in the vacuum outside the solid surface (Equation 6) .

$$W = -e\phi - E_f$$

Equation 6- Shows how the workfunction is calculated. W-workfunction, ϕ - electrostatic potential and E_F - fermi energy

Equation 6 shows how the workfunction is calculated. The workfunction was calculated on the surface with all the modifiers adsorbed onto it to see if the modifiers reduce or increase the workfunction. These values are shown in Table 6.9.

Table 6.9- List of work function calculations for each of the different modifiers		
Modifier	Workfunction/ eV	Workfunction/ kJ mol ⁻¹
QD_sideon	3.9	376
QD_endon	4.3	415
DABCO_sideon	4.2	405
DABCO_endon	4.4	425
QL_sideon	4.5	434
QL_endon	4.0	386
AQ_sideon	4.2	405
Pt_(111)_surface	5.7	550

In Table 6.9 the workfunction calculations are shown. When compared to the bare Pt (111) surface (5.7 eV) all the modifiers reduce the workfunction energy. This means it allows an electron to go from the surface to the point in the vacuum more easily when there is a modifier already adsorbed onto the surface. This signifies that the modifier allows the substrate to adsorb to the surface of the Pt (111) surface more easily. After comparing the data given by the adsorption energies of the EtPy, MBF and EBF on the Pt with the modifiers and the workfunction no correlation could be seen for any of the substrates (Figure 6.40, 6.41 and 6.42) with the apparent rate enhancement.

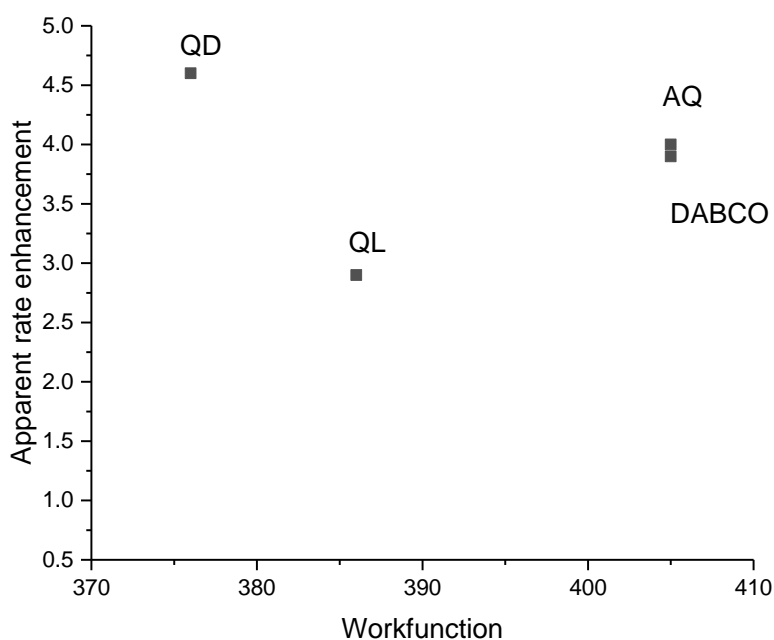


Figure 6.40: Apparent rate enhancement in the EtPy hydrogenation vs workfunction

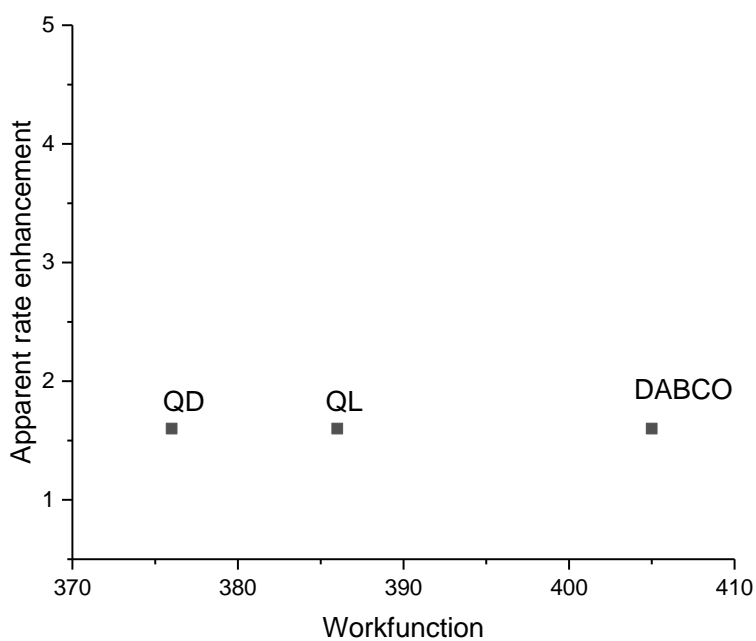


Figure 6.41: Apparent rate enhancement in the MBF hydrogenation vs workfunction

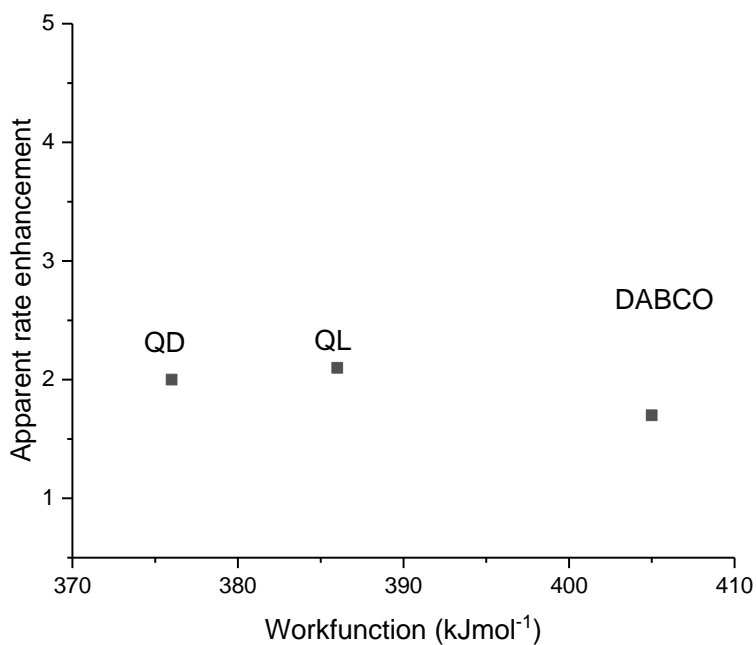


Figure 6.42: Apparent rate enhancement in the EBF hydrogenation vs workfunction

6.5 References

1. T. van Mourik, M. Bühl and M. Gaigeot, *Philosophical Transactions of the Royal Society A: Mathematical, Physical and Engineering Sciences*, 2014, **372**, 20120488.
2. E. Hansen and M. Neurock, *Journal of Catalysis*, 2000, **196**, 241-252.
3. M. C. Payne, M. P. Teter, D. C. Allan, T. A. Arias and J. D. Joannopoulos, *Reviews of Modern Physics*, 1992, **64**, 1045–1097.
4. J. Nørskov, T. Bligaard, J. Rossmeisl and C. Christensen, *Nature Chemistry*, 2009, **1**, 37-46.
5. R. Ditchfield, W. Hehre and J. Pople, *The Journal of Chemical Physics*, 1971, **54**, 724-728.
6. Insilicosci, <https://insilicosci.com/hartree-fock-method-a-simple-explanation/#:~:text=In%20a%20nutshell%2C%20the%20Hartree%20Fock%20method%20is,the%20time-independent%20Schrodinger%20equation%20of%20many-body%20electronic%20systems>, accessed August 2022
7. M. Matin, M. Shaikh, M. Hossain, M. Alauddin, T. Debnath and M. Aziz, *Green and Sustainable Chemistry*, 2021, **11**, 125-141.
8. J. Margitfalvi, E. Tálás, F. Zsila and S. Kristyán, *Tetrahedron: Asymmetry*, 2007, **18**, 750-758.
9. J. Margitfalvi and E. Tfirst, *Journal of Molecular Catalysis A: Chemical*, 1999, **139**, 81-95.
10. G. Bond, P.A. Meheux, A. Ibbotson, P.B. Wells, *Catal. Today*, 1991 **10**, 371–378
11. E. Kolsbjerg, M. Groves and B. Hammer, *The Journal of Chemical Physics*, 2016, **144**, 164112.
12. T. Evans, A.P. Woodhead, A. Gutiérrez-Sosa, G. Thornton, T.J. Hall, A.A. Davis, N.A. Young, P.B. Wells, R.J. Oldman, O. Plashkevych, O. Vahtras, H. Ågren, V. Carravetta, *Surf. Sci.*, 1999, **436**, L691–L696.
13. J. L. Margitfalvi and E. Tfirst, *Journal of Molecular Catalysis A: Chemical*, 1999, **139**, 81–95.

Chapter 7

Summary and Conclusions

7.1 Summary

The purpose of the work described in the preceding chapters was to investigate in mechanistic detail the hydrogenation of EtPy to see how cinchona alkaloid modifiers such as cinchonidine (CD) and its enantiomer cinchonine (CN) provide a rate enhancement for the reaction. Once this mechanism is understood, it may be possible to achieve rate enhancements in similar hydrogenation reactions. In the literature research detailed in Chapter 1, it is obvious that currently the EtPy hydrogenation is not clearly understood even though there has been extensive investigation using cinchona alkaloids.^{1,2,3,4,5,6} Several theories of how the rate enhancement occurs have been put forward but none of these are definitive. There is still room for more work to be carried out in order to see if this reaction could be understood in greater detail.

In the first results chapter (Chapter 3) two different catalysts sourced from Johnson Matthey and Sigma Aldrich were compared using the hydrogenation reactions of EtPy, EBF and MBF. Modifiers CD and CN gave significant rate enhancements over the unmodified reaction in the EtPy hydrogenation and slight rate enhancements in the MBF and EBF hydrogenation. There were differences between the reaction rates achieved over the two catalysts and it became clear that overall, the Johnson Matthey catalyst gave faster rates, with a couple of exceptions. Through characterization of the two catalysts by XRD and TEM the differences in rates were explained by the JM catalyst having smaller nanoparticles, larger pore volume and the SA catalyst having alumina overlay on the Pt.

Reactions were completed using CD and CN modifiers in the EtPy, MBF and EBF hydrogenation and were found to give rate enhancements using both modifiers. Where CD was

used with the three substrates, the rate enhancements initially correlated with CD concentration but hit a maximum. Further increases in quantities of CD produced a lower rate which then plateaued. These results support the reported literature studies that a significant rate enhancement takes place when CD and CN are added to the EtPy, MBF and EBF. Concerning the mechanism of this enhancement it is likely that a 1:1 modifier: reactant complex forms following binding of the modifier to the Pt surface and this enhances the reaction. It is also possible that there is an added effect of cleaning the Pt catalyst surface of oligomers and decomposition products making more binding sites available which could help with the rate enhancement for EtPy hydrogenation.^{7,8,9} For MBF and EBF the rate enhancements almost certainly come from the 1:1 modifier: reactant model as they do not produce condensation products (oligomers, polymers).

To understand the mechanism of the rate enhancement of α -keto ester reduction produced by CD, the molecule was deconstructed into specific structural moieties that each potentially play a role in the rate enhancement mechanism. Chapter 4 describes the influences of the different modifiers on the rate of reaction in comparison to each other and the unmodified hydrogenation reaction. For the three substrates EtPy, MBF and EBF the different modifiers (QD, QL, CD, CN and DABCO) gave rate enhancements of varying magnitude in toluene + .001M of acetic acid. CD and CN gave faster rate enhancements than the achiral tertiary amines at lower amounts. It was found that there were large differences when using the different solvents; using neat acetic acid several of the modifiers, in the concentration ranges used, gave similar rates to the unmodified reaction with no rate enhancements observed in the EBF and MBF reactions. This suggests that for these substrates (MBF and EBF) the rate is solvent dependent. When using EtPy the rate enhancements only changed slightly when using different solvents.

Concerning the mechanism of rate enhancement caused by the achiral tertiary amines, it seems that it is more complicated to resolve than for CD and CN because, unlike the structures of CD and CN, there is no aromatic moiety that can adsorb onto the catalyst surface. Because of the reasons outlined in Chapter 4 and Chapter 6, the most likely mechanism involves the 1:1 modifier: reactant model with stabilisation of the half-hydrogenated substrate as the most likely intermediate. For QD a dimer could also form with the reactant while QD is protonated in the liquid phase, and then the reactant could adsorb onto the surface and QD could stabilize it and / or QD could also adsorb onto the surface. This has been described in Chapter 4, where QD is end-on with the nitrogen and then this nitrogen stabilises the oxygen on the half-hydrogenated EtPy molecule. In the EtPy hydrogenation reactions an added effect could be that the EtPy aldol condensation products are removed by QD as stated by Toukoniitty *et al.* and Jenkins *et al.* (see Chapter 4 for more details).^{10,11} DABCO has an additional basic nitrogen so potentially one nitrogen could adsorb onto the surface while the other one is protonated and stabilizes the substrate. QL contains an O-H group so maybe the nitrogen adsorbs, and the O-H group stabilizes the half-hydrogenated substrate. As discussed in Chapter 4, and briefly summarised here, the way the modifiers work is not clear and there are several likely possibilities and, in some cases, more than one mechanism may be involved.

In Chapter 5 other reactants of a similar structure to the α -ketoesters used in Chapter 3 and 4, were tested. Most of the modifiers poisoned these reactions and gave no rate enhancement. Of the achiral tertiary amines used, QL was the only modifier that gave a rate enhancement in the 2,3-butanedione reaction. It is not known why QL gave a rate enhancement in this reaction whereas the other modifiers did not but perhaps the -OH group on QL played a role in the reaction. CD gave slight rate enhancements in the TP, 2,3-butanedione and EAA hydrogenation but accounting for experimental variation these rates overlap. This may show

that CD could potentially give a more significant rate enhancement at different concentrations of CD.

In Chapter 6 the reactions were investigated using theoretical calculations. Dimer and substrate-modifier-surface complex calculation were performed. The data showed a trend where the 1st dimer conformation was usually the lowest in energy in almost all the modifier-substrate dimers tested. This is interesting as the carbonyl that the modifier has H-bonded to in this dimer is the carbonyl that is hydrogenated in the reaction. All of the modifiers were likely to form dimers with all three of the reactants (EBF, MBF and EtPy) which shows that the dimers are formed in the liquid phase; perhaps this gives evidence to the dimer forming in the liquid phase and then adsorbing to the surface. EAA dimers calculated energies were negative so overall it was inconclusive as to whether dimers forming in the liquid phase is a prerequisite to a rate enhancement as the energies across all the substrates did not correlate with the rate enhancements found in this project.

The complex calculations showed that all the modifiers can enhance the adsorption of EtPy and EAA onto the Pt (111) surface. This enhancement of adsorption energy of EtPy alone was found to not be enough to enhance the rate as there was no rate enhancement in the EAA reaction. This implies the modifier adsorbing to the surface is not enough to enhance the rate and there must be another interaction as well which implies the modifier may stabilize the half-hydrogenated carbonyl. Through these calculations it was found that the modifiers do not significantly help MBF and EBF to adsorb onto the surface. The rate enhancements found experimentally for these substrates cannot be fully explained through the computational calculations completed during this project.

7.2 Future work

More reactions should be completed where the modifier has already been adsorbed onto the catalyst surface prior to addition of substrate. This could be done by adding the modifier to the Pt catalyst in a solvent and checking via IR analysis that the modifier has adsorbed and then adding the reactant and starting the reaction. This would be used to investigate whether the dimer interactions in the liquid phase are an important part of the mechanism of the rate enhancement. If a rate enhancement was observed this could rule out dimer formation in the liquid phase being a reason for the rate enhancement.

For the QL modifier the -OH group could be substituted with a methoxy group in order to see if this has an effect on the rate enhancement. If this reduces the rate enhancement, then it would show that the O-H group interacts with the substrate and helps stabilize the substrate through hydrogen bonding, providing insight into the mechanism.

In order to see if the rate enhancement could be due to competitive adsorption the adsorption energy of ethyl lactate on the Pt(111) surface could be found and compared to the other ethyl pyruvate and achiral tertiary amine adsorption energies. This would be able to determine if the modifiers just remove the product and help speed up the reaction in that way. This is because if the adsorption energy is more negative for the modifier compared to ethyl pyruvate and ethyl lactate then the modifier could knock both of those modifiers off the surface and enhance the rate that way.

Adsorption isotherms could be completed on the Pt / Al₂O₃ catalysts, specifically one measured using the whole catalyst and one with just the alumina. This would be used to see how much achiral tertiary amine and EtPy can be adsorbed onto the nanoparticles. This would be important to know so that if the plateau seen in most of the achiral tertiary amines, rate

enhancements are due to not enough space on the catalyst for the modifiers and the reactants to adsorb.

7.3 References

1. T. Burgi, A. Baiker, Heterogeneous enantioselective hydrogenation over cinchona alkaloid modified platinum: mechanistic insights into a complex reaction. *Acc. Chem. Res.* 2004, **37**, 909–917
2. Baiker, A. Progress in asymmetric heterogeneous catalysis: Design of novel chirally modified platinum metal catalysts. *J. Mol. Catal. A: Chem.* 1997, **115**, 473–493.
3. Z. Guan, S. Lu and C. Li, *Chinese Journal of Catalysis*, 2015, **36**, 1535-1542.
4. H. Blaser, M. Garland, H. Jallet, *Journal of Catalysis*, 1993, **144**, 569-578.-
5. B. Minder, T. Mallat, K. Pickel, K. Steiner and A. Baiker, *Catalysis Letters*, 1995, **34**, 1-9.
6. Xin.You, *Studies in Surface Science and Catalysis*, 2000, **130**, 3375-3380
7. G. Bond, P.A. Meheux, A. Ibbotson, P.B. Wells, *Catal. Today* 10, 1991, 371–378.
8. D. Jenkins, A. Aalabulrahman, G. Attard, K. Griffin, P. Johnston and P. Wells, *Journal of Catalysis*, 2005, **234**, 230-239.
9. Baiker, A. Progress in asymmetric heterogeneous catalysis: Design of novel chirally modified platinum metal catalysts. *J. Mol. Catal. A: Chem.* 1997, **115**, 473–493.
10. E. Toukoniitty and D. Murzin, *Journal of Catalysis*, 2006, **241**, 96-102
11. D. Jenkins, A. Aalabulrahman, G. Attard, K. Griffin, P. Johnston and P. Wells, *Journal of Catalysis*, 2005, **234**, 230-239.

10. Acknowledgements

I would like to express my sincere gratitude to my supervisor Prof. Graham Hutchings for allowing me to undertake this project and letting me work in his research group. Also, Special thanks to Dr. Nicholas Dummer for providing the help and guidance I needed to allow me to complete this project.

The computational section of this thesis could not have been completed without the help of Dr. David Willock who provide the training, help and guidance needed to finish this section of the project. Also, the TEM images were produced and analysed by Dr. Thomas Davies so a big thanks to him for his help. The analysis of the catalysts could not have been done without him.

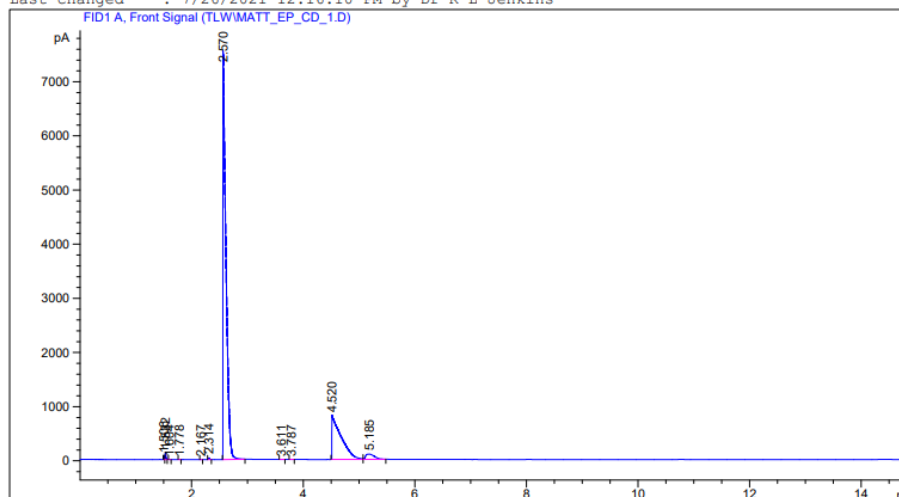
I would like to thank my fellow chemists who worked with me throughout my PhD: Anna, Alba, Simon, Joe and especially to my former flat mate Tom. I would like to thank my Mum, Dad and brother, Luke, and my friend Cristina for supporting me through this time and my friends outside the lab for making this a memorable experience.

11. Appendix

EP CD GC

ata File C:\CHEM32\1\DATA\TLW\MATT_EP_CD_1.D
ample Name: Matt EP_CD_1

```
=====
Acq. Operator   : Dr R L Jenkins
Acq. Instrument : Instrument 1           Location : Vial 101
Injection Date  : 7/26/2021 11:02:56 AM Inj Volume : 0.2 µl
Acq. Method     : C:\CHEM32\1\METHODS\EE ROB.M
Last changed    : 7/23/2021 4:31:13 PM by Dr R L Jenkins
Analysis Method : C:\CHEM32\1\METHODS\EE ROB.M
Last changed    : 7/26/2021 12:16:10 PM by Dr R L Jenkins
=====
```



```
=====
Area Percent Report
=====
```

```
Sorted By      : Signal
Multiplier     : 1.0000
Dilution       : 1.0000
Sample Amount  : 1.00000 [ng/ul] (not used in calc.)
Use Multiplier & Dilution Factor with ISTDs
```

Signal 1: FID1 A, Front Signal

Sample Amount: 1.0000 [ng/ul] (NOT USED IN CALC.)
Use Multiplier & Dilution Factor with ISTDs

Signal 1: FID1 A, Front Signal

Peak #	RetTime [min]	Type	Width [min]	Area [pA*s]	Height [pA]	Area %
1	1.506	BV	0.0119	43.61169	57.34044	0.11504
2	1.532	VB	0.0120	97.27020	126.67094	0.25658
3	1.604	BB	0.0146	4.22264	4.62653	0.01114
4	1.778	BB	0.0170	2.84083	2.55074	0.00749
5	2.167	BB	0.0161	2.66233	2.56643	0.00702
6	2.314	BB	0.0210	36.78172	28.63943	0.09702
7	2.570	BB S	0.0453	2.71690e4	7493.61035	71.66620
8	3.611	BB	0.0340	5.45503	2.55030	0.01439
9	3.787	BB	0.0315	2.81658	1.39589	0.00743
10	4.520	BV	0.1442	9517.47461	803.43195	25.10508
11	5.185	VB	0.1293	1028.36084	95.74997	2.71260

Instrument 1 7/26/2021 12:41:46 PM Dr R L Jenkins

Page 1 of 2

Data File C:\CHEM32\1\DATA\TLW\MATT_EP_CD_1.D

Sample Name: Matt EP_CD_1

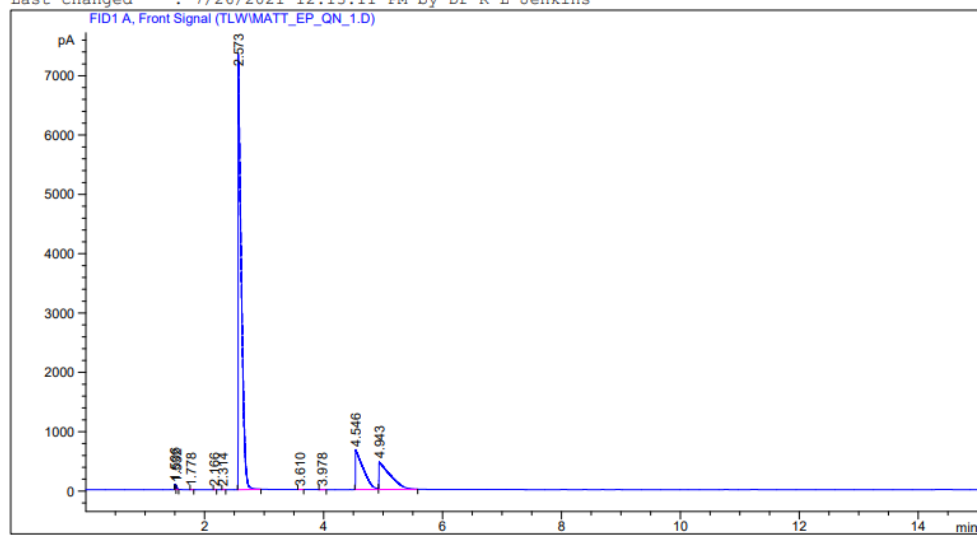
Totals : 3.79105e4 8619.13296

*** End of Report ***

EP QD GC

Data File C:\CHEM32\1\DATA\TLW\MATT_EP_QN_1.D
Sample Name: Matt EP QN_1

```
=====
Acq. Operator   : Dr R L Jenkins
Acq. Instrument : Instrument 1          Location : Vial 102
Injection Date  : 7/26/2021 11:58:12 AM
                                           Inj Volume : 0.2 µl
Acq. Method     : C:\CHEM32\1\METHODS\EE ROB.M
Last changed    : 7/26/2021 11:20:54 AM by Dr R L Jenkins
Analysis Method : C:\CHEM32\1\METHODS\EE ROB.M
Last changed    : 7/26/2021 12:13:11 PM by Dr R L Jenkins
=====
```



=====
Area Percent Report
=====

```
Sorted By      :      Signal
Multiplier     :      1.0000
Dilution       :      1.0000
Sample Amount  :      1.00000 [ng/ul] (not used in calc.)
Use Multiplier & Dilution Factor with ISTDs
```

Signal 1: FID1 A, Front Signal

Signal 1: FID1 A, Front Signal

Peak #	RetTime [min]	Type	Width [min]	Area [pA*s]	Height [pA]	Area %
1	1.506	BV	0.0125	72.35081	89.17332	0.19086
2	1.532	VB	0.0126	48.67881	59.38628	0.12841
3	1.778	BB	0.0170	2.92108	2.61935	0.00771
4	2.166	BB	0.0172	5.07852	4.85704	0.01340
5	2.314	BB	0.0206	7.64008	6.09766	0.02015
6	2.573	BB S	0.0463	2.57643e4	7113.80469	67.96445
7	3.610	BB	0.0325	3.42854	1.63596	0.00904
8	3.978	BB	0.0411	4.73257	1.77258	0.01248
9	4.546	BV	0.1102	6033.20264	662.85297	15.91518
10	4.943	VB	0.1561	5966.16016	457.71259	15.73832

Totals : 3.79085e4 8399.91242

Instrument 1 7/26/2021 12:13:12 PM Dr R L Jenkins

Page 1 of 2

Data File C:\CHEM32\1\DATA\TLW\MATT_EP_QN_1.D
Sample Name: Matt EP QN_1

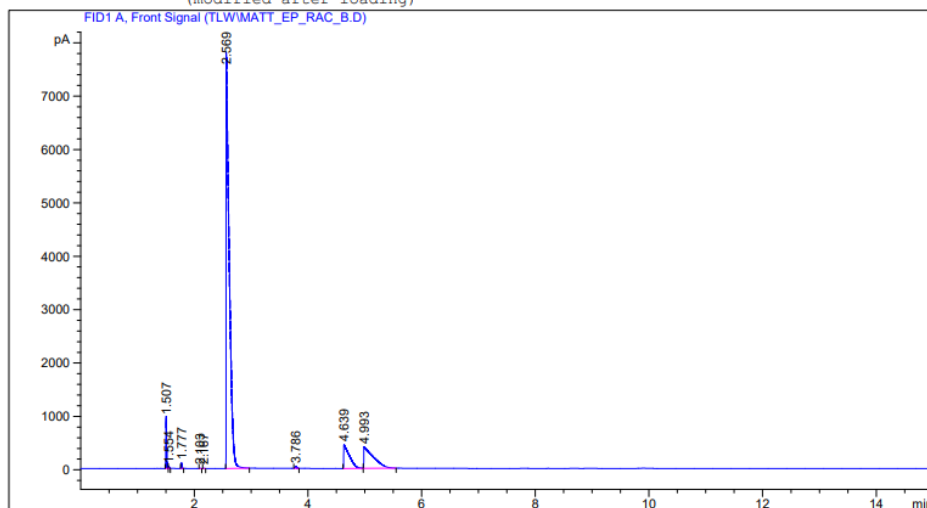
=====
*** End of Report ***

EP racemic unmodified

Data File C:\CHEM32\1\DATA\TLW\MATT_EP_RAC_B.D
Sample Name: Matt EP EE_B

```
=====
Acq. Operator   : Dr R L Jenkins
Acq. Instrument : Instrument 1          Location : Vial 101
Injection Date  : 7/23/2021 2:43:07 PM
                                           Inj Volume : 0.2 µl

Acq. Method     : C:\CHEM32\1\METHODS\EE ROB.M
Last changed    : 7/23/2021 2:41:15 PM by Dr R L Jenkins
                  (modified after loading)
Analysis Method : C:\CHEM32\1\METHODS\EE ROB.M
Last changed    : 7/23/2021 2:58:06 PM by Dr R L Jenkins
                  (modified after loading)
=====
```



Area Percent Report

```
=====
Sorted By      : Signal
Multiplier     : 1.0000
Dilution       : 1.0000
Sample Amount  : 1.00000 [ng/ul] (not used in calc.)
Use Multiplier & Dilution Factor with ISTDs
=====
```

Signal 1: FID1 A, Front Signal

Peak #	RetTime [min]	Type	Width [min]	Area [pA*s]	Height [pA]	Area %
1	1.507	BV	0.0139	805.40607	950.13568	2.16289
2	1.554	VB	0.0132	32.93699	37.62446	0.08845
3	1.777	BB	0.0149	95.44390	101.99364	0.25631
4	2.103	BB	0.0167	1.10228	1.01329	0.00296
5	2.167	BB	0.0173	1.98920	1.88788	0.00534
6	2.569	BB S	0.0462	2.84817e4	7698.03711	76.48654
7	3.786	BB	0.0301	78.55328	41.54491	0.21095
8	4.639	BV	0.0879	3085.32104	444.90173	8.28551
9	4.993	VB	0.1435	4655.08496	403.73575	12.50105

Instrument 1 7/23/2021 2:58:06 PM Dr R L Jenkins

Page 1 of 2

Data File C:\CHEM32\1\DATA\TLW\MATT_EP_RAC_B.D
Sample Name: Matt EP EE_B

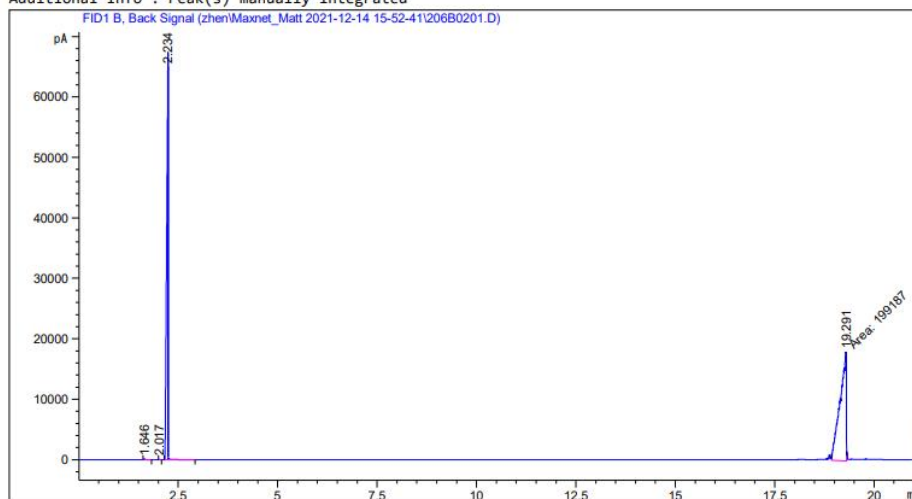
Totals : 3.72375e4 9680.87444

*** End of Report ***

EBF CD

Data File C:\Chem32\1\Data\zhen\Maxnet_Matt 2021-12-14 15-52-41\206B0201.D
Sample Name: EBF CD

```
=====
Acq. Operator   : SYSTEM                      Seq. Line :    2
Acq. Instrument : GC                        Location  : 206 (B)
Injection Date  : 14/12/2021 16:22:27       Inj       :    1
                                           Inj Volume: 1 µl
Acq. Method     : C:\Chem32\1\Data\zhen\Maxnet_Matt 2021-12-14 15-52-41\ep hydrog 3.M
Last changed    : 14/12/2021 16:16:57 by SYSTEM
                 (modified after loading)
Analysis Method : C:\Chem32\1\Data\zhen\Maxnet_Matt 2021-12-14 15-52-41\ep hydrog 3.M (
                 Sequence Method)
Last changed    : 14/12/2021 17:38:06 by SYSTEM
Additional Info  : Peak(s) manually integrated
=====
```



=====
Area Percent Report
=====

```
Sorted By      : Signal
Multiplier     : 1.0000
Dilution       : 1.0000
Use Multiplier & Dilution Factor with ISTDs
```

Signal 1: FID1 B, Back Signal

Peak #	RetTime [min]	Type	Width [min]	Area [pA*s]	Height [pA]	Area %
1	1.646	BB	0.0178	170.46944	134.19923	0.04678
2	2.017	BB	0.0164	88.06572	82.70338	0.02417
3	2.234	BB	0.0361	1.64919e5	6.60706e4	45.26161
4	19.291	MM	0.1841	1.99187e5	1.80313e4	54.66655
5	21.170	BB	0.0275	3.20029	1.73803	0.00088

GC 21/03/2022 10:59:38 SYSTEM

Page 1 of 2

Data File C:\Chem32\1\Data\zhen\Maxnet_Matt 2021-12-14 15-52-41\206B0201.D
Sample Name: EBF CD

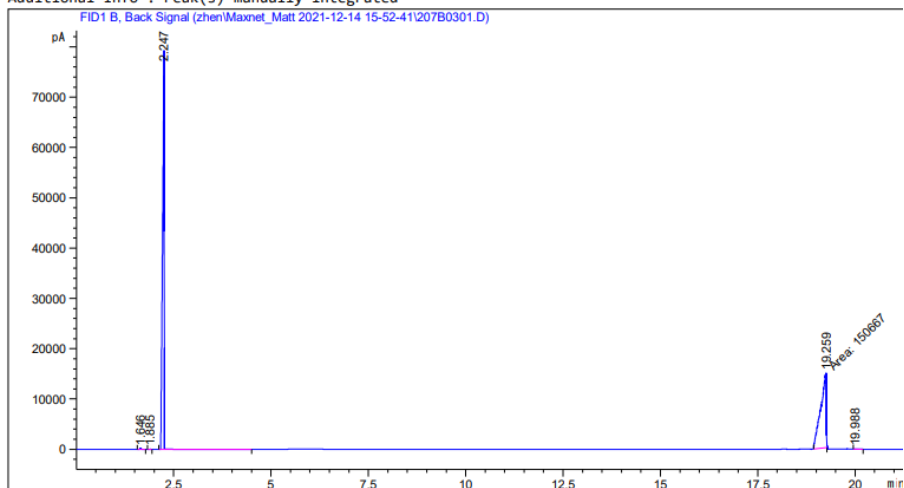
Totals : 3.64368e5 8.43205e4

=====
*** End of Report ***

EBF DABCO

Data File C:\Chem32\1\Data\zhen\Maxnet_Matt 2021-12-14 15-52-41\207B0301.D
Sample Name: EBF DABCO

```
=====
Acq. Operator   : SYSTEM                      Seq. Line :    3
Acq. Instrument : GC                          Location  : 207 (B)
Injection Date  : 14/12/2021 16:49:34        Inj       :    1
                                           Inj Volume: 1 µl
Acq. Method    : C:\Chem32\1\Data\zhen\Maxnet_Matt 2021-12-14 15-52-41\ep hydrog 3.M
Last changed   : 14/12/2021 16:43:58 by SYSTEM
                (modified after loading)
Analysis Method: C:\Chem32\1\Data\zhen\Maxnet_Matt 2021-12-14 15-52-41\ep hydrog 3.M (
                Sequence Method)
Last changed   : 14/12/2021 17:38:06 by SYSTEM
Additional Info : Peak(s) manually integrated
=====
```



=====
Area Percent Report
=====

```
Sorted By      : Signal
Multiplier     : 1.0000
Dilution       : 1.0000
Use Multiplier & Dilution Factor with ISTDs
```

Signal 1: FID1 B, Back Signal

Peak #	RetTime [min]	Type	Width [min]	Area [pA*s]	Height [pA]	Area %
1	1.646	BB	0.0179	217.84044	171.10654	0.05801
2	1.885	BB	0.0191	33.25408	25.64199	0.00886
3	2.247	BB	0.0403	2.24463e5	7.87067e4	59.77554
4	19.259	MM	0.1691	1.50667e5	1.48491e4	40.12336
5	19.988	BB	0.0581	128.55217	29.32505	0.03423

GC 21/03/2022 11:00:14 SYSTEM

Page 1 of 2

Data File C:\Chem32\1\Data\zhen\Maxnet_Matt 2021-12-14 15-52-41\207B0301.D

Sample Name: EBF DABCO

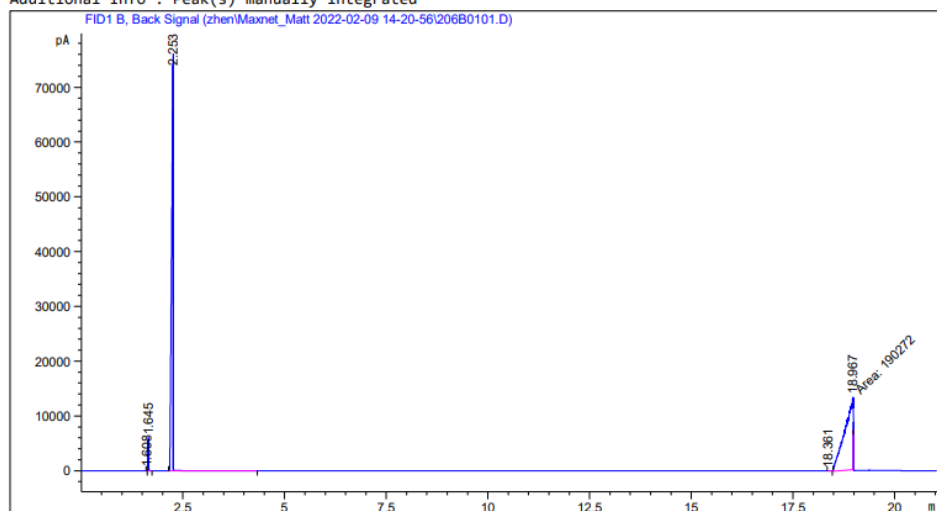
Totals : 3.75509e5 9.37819e4

=====
*** End of Report ***

MBF CD

Data File C:\Chem32\1\Data\zhen\Maxnet_Matt 2022-02-09 14-20-56\206B0101.D
Sample Name: MBFCD

```
=====
Acq. Operator   : SYSTEM                      Seq. Line :    1
Acq. Instrument : GC                        Location  : 206 (B)
Injection Date  : 09/02/2022 14:23:14      Inj       :    1
                                           Inj Volume: 1 µl
Acq. Method     : C:\Chem32\1\Data\zhen\Maxnet_Matt 2022-02-09 14-20-56\ep hydrog 3.M
Last changed    : 09/02/2022 14:21:23 by SYSTEM
                 (modified after loading)
Analysis Method : C:\Chem32\1\Data\zhen\Maxnet_Matt 2022-02-09 14-20-56\ep hydrog 3.M (
                 Sequence Method)
Last changed    : 09/02/2022 14:44:32 by SYSTEM
Additional Info  : Peak(s) manually integrated
=====
```



=====
Area Percent Report
=====

```
Sorted By      : Signal
Multiplier     : 1.0000
Dilution       : 1.0000
Use Multiplier & Dilution Factor with ISTDs
```

Signal 1: FID1 B, Back Signal

Peak #	RetTime [min]	Type	Width [min]	Area [pA*s]	Height [pA]	Area %
1	1.608	BV	0.0110	34.42263	50.39461	0.00852
2	1.645	VB	9.48e-3	3266.32544	5878.82080	0.80877
3	2.253	BB	0.0359	2.10258e5	7.68629e4	52.06169
4	18.361	BB	0.0440	32.79614	9.81737	0.00812
5	18.967	MM	0.2399	1.90272e5	1.32191e4	47.11290

GC 21/03/2022 11:02:11 SYSTEM

Page 1 of 2

Data File C:\Chem32\1\Data\zhen\Maxnet_Matt 2022-02-09 14-20-56\206B0101.D

Sample Name: MBFCD

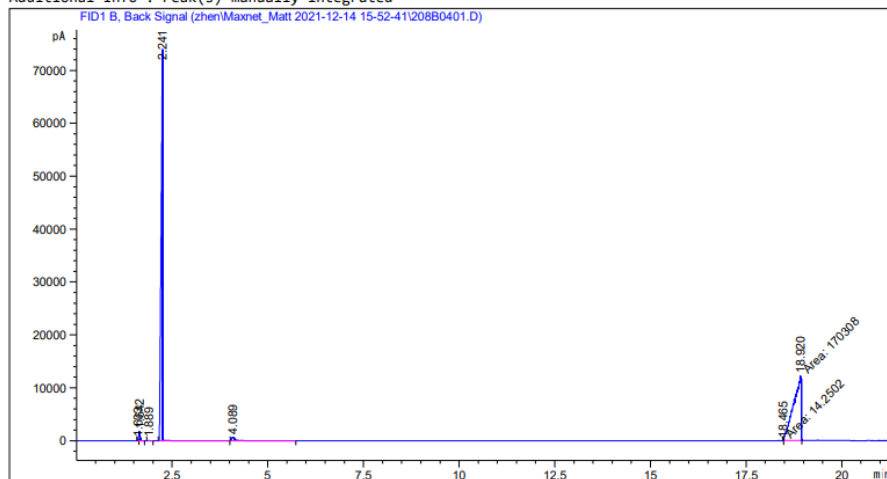
Totals : 4.03864e5 9.60211e4

=====
*** End of Report ***

MBF QD

ata File C:\Chem32\1\Data\zhen\Maxnet_Matt 2021-12-14 15-52-41\208B0401.D
Sample Name: MBF QD

```
=====
Acq. Operator   : SYSTEM                      Seq. Line :    4
Acq. Instrument : GC                        Location  : 208 (B)
Injection Date  : 14/12/2021 17:16:48       Inj       :    1
                                           Inj Volume: 1 µl
Acq. Method    : C:\Chem32\1\Data\zhen\Maxnet_Matt 2021-12-14 15-52-41\ep hydrog 3.M
Last changed   : 14/12/2021 17:11:06 by SYSTEM
               (modified after loading)
Analysis Method : C:\Chem32\1\Data\zhen\Maxnet_Matt 2021-12-14 15-52-41\ep hydrog 3.M (
               Sequence Method)
Last changed   : 14/12/2021 17:38:06 by SYSTEM
Additional Info : Peak(s) manually integrated
=====
```



=====
Area Percent Report
=====

```
Sorted By      : Signal
Multiplier     : 1.0000
Dilution       : 1.0000
Use Multiplier & Dilution Factor with ISTDs
```

Signal 1: FID1 B, Back Signal

Peak #	RetTime [min]	Type	Width [min]	Area [pA*s]	Height [pA]	Area %
1	1.603	BV E	0.0167	168.48572	143.44481	0.04522
2	1.642	VB R	0.0188	2313.63306	1709.01453	0.62090
3	1.889	BB	0.0455	58.63670	20.41423	0.01574
4	2.241	BB	0.0430	1.95816e5	7.14914e4	52.54985
5	4.089	BB	0.0882	3949.81274	596.67371	1.05999
6	18.465	MP N	0.0228	14.25018	10.40119	0.00382

GC 21/03/2022 11:01:40 SYSTEM

Page 1 of 2

Data File C:\Chem32\1\Data\zhen\Maxnet_Matt 2021-12-14 15-52-41\208B0401.D
Sample Name: MBF QD

Peak #	RetTime [min]	Type	Width [min]	Area [pA*s]	Height [pA]	Area %
7	18.920	PM	0.2318	1.70308e5	1.22449e4	45.70449

Totals : 3.72628e5 8.62163e4

=====
*** End of Report ***

Data sheet for the transducer



KELLER

SPECIFICATIONS

SERIES 21 R / 21 SR / 21 MR

PR 21 R/SR/MR ¹⁾	0,5	1	2	5	10	16	bar	vented gauge								
PAA 21 R/SR/MR		1	2	5	10	16	bar	absolute								
PA 21 R/SR/MFP		1	2	5	10	16	30	50	100	160	200	400	600	bar	sealed gauge	
Over Range		2	3	4	10	20	25	50	75	150	250	300	500	700	bar	

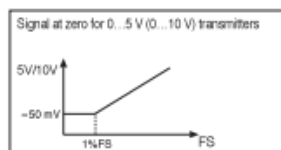
¹⁾ mPm connector only, not cable

²⁾ Zero at 1000 mbar abs.

Signal Output	4...20 mA	0...5 Vdc	1...6 Vdc	0...10 Vdc	0...100 mV
Supply Voltage		8...28 Vdc		13...30 Vdc	6...28 Vdc / 10 Vdc
Current required	max. 25 mA	4 mA max.			2 mA max.
Zero/Span Tolerance	0,5% FS	0,5% FS ^{a)}	0,5% FS	0,5% FS ^{a)}	± 0,1% FS
Configuration	2 wire	3 wire			4 wire
Electrical Connection:	OUT/GND: Pin 1 / White		GND: Pin 1 / Green		GND: Pin 1 / White
mPm 193 or			+OUT: Pin 2 / White		+OUT: Pin 2 / Red
cable 2 m, 4 core			+Vcc: Pin 3 / Brown		+Vcc: Pin 3 / Black
					-OUT: Pin 4 / Blue
Linearity	± 0,2% typ. / ± 0,5% max.				
Total Error Band ^{b)} +18...+22 °C	± 0,5% typ. / ± 1% max.				
Total Error Band ^{b)} 0...+50 °C	± 1,0% typ. / ± 2% max.				
Total Error Band ^{b)} -20...+80 °C	± 2,5% typ. / ± 4% max.				

^{b)} Total error band includes linearity, hysteresis, repeatability, zero/span offsets and temperature effects.

^{a)} Signal at zero = 50 mV → see chart



Operating Temperature	-20...+80 °C (on demand -40...100 °C)
Pressure Port	G 1/4" male
Pressure Media	Compatible with 316L stainless steel
Weight	= 75 g
Electromagnetic Compatibility	CE marked: Fully tested to EN 50081-2 and EN 50082-2
Enclosure Protection	IP 65
Insulation	> 100 MΩ / 500 Vdc
Vibration	20 g (5...2000 Hz, max. amplitude ± 3 mm), according to IEC 68-2-6
Shock	20 g (11 ms)

User Notes: Basic 100 mV transmitters are calibrated at 10 Vdc to produce 0...100 mV signal (nominal), and require a stable voltage supply. They can be operated at 5 Vdc to give 0...50 mV signal or 20 Vdc to give 0...200 mV signal. The circuit is a compensated resistance bridge and is completely passive with no diodes or reactive components. Bridge resistance is 3.5 kΩ nominal. The 6...28 V supply transmitter is fitted with an internal regulator. The mPm connector has a PG7 cable gland entry suitable for cables between 4 and 6 mm diameter. Screw terminals and solder lugs are provided. The G 1/4 pressure connection has an integral Viton[®] seal at the shoulder. Alternatively it may be sealed using a face seal on the flat nose of the pressure port.

Subject to alterations

6/02

KELLER AG für Druckmesstechnik KELLER Gesellschaft für Druckmesstechnik mbH	St. Gallerstrasse 119 Schwarzwaldstrasse 17	CH-8404 Winterthur D-79798 Jestetten	Tel. 052 - 235 25 25 Tel. 07745 - 9214 - 0	Fax 052 - 235 25 00 Fax 07745 - 9214 - 50
--	--	---	---	--

Complies approved to ISO 9001 / EN 29001

www.keller-druck.com

Python script for EtPy and CD Hfitting

```

-- coding: utf-8 --
'''
Created on Thu Sep 30 14:05:15 2021
@author: sacdjw
'''
import numpy as np
import csv
import os
from scipy.optimize import curve_fit
from scipy.signal import savgol_filter
from matplotlib import pyplot

# fit function for initial fitting of linear region
def fitfunc_lin(x,m,c):
    return m*x + c

# fit function for fitting whole of data after origin shift
# Note that the calling routine will send a whole array of times to the
# function, so need to integrate between successive points and return
# arrays that have the same length.
def fitfunc(t,k,Keq,c0):
    # c0 is the final value at infinite time, should correspond to the
    # value of the substrate concentration.
    # c with t is the solution concentration of the substrate at a particular time
    #
    # c0=7.53
    c_with_t=[]
    Hup_val=[]
    dt=1.0

    # loop over the t data
    for ipnt in range(0,len(t)):
        if (ipnt == 0):
            H_next=0.0
            ccc=c0
            t_jump=t[0]
        else:
            H_next=Hup_val[ipnt-1]
            t_jump=t[ipnt]-t[ipnt-1]
            ccc=c_with_t[ipnt-1]

        ni=int(t_jump/dt)

        for iil in range(0,ni):
            denom=1.0+Keq*ccc
            theta1=Keq*ccc/denom
            dH1= k*theta1*dt

            ccc -= dH1
            H_next += dH1

        Hup_val.append(H_next)
        c_with_t.append(ccc)

    return Hup_val

# Read the csv file
row_start=1
t_initial=9000.0
c0_set=7.60
file_stem="ETPY_Huptake"
data_file="hs.csv" % file_stem

fptr=open(data_file,'rt')
csv_data=csv.reader(fptr)
for row in csv_data:
    numrows=len(row)
#
fptr.close()

# Set up a csv file for recording the fitted data
csvout="%s_fitted_params.csv" % file_stem
csv_headers=[ 'Modifier', 'lin_fit slope', 'lin_fit_c', 'kinetic fit - k2', 'stdev - k2', \
              'kinetic fit - Keq1', 'stdev - Keq1', 'kinetic fit - c0', 'stdev - c0' ]
fptr_csvout=open(csvout,'w',newline='')

```



```

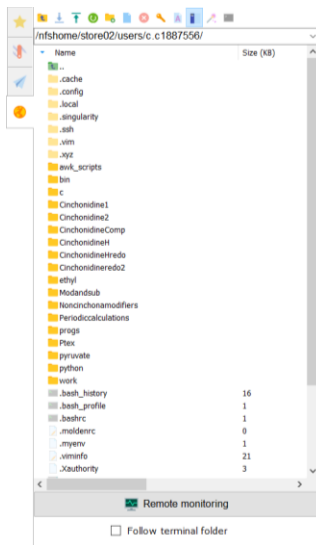
fptr_csvout=open(csvout,'w', newline='')
csvout_writer=csv.writer(fptr_csvout)
csvout_writer.writerow(csv_headers)
# Loop over columns in the data, i.e. the experimental data sets for different catalysts
#
for which_col in range(1,numrows):
    fptr=open(data_file, 'r')
    csv_data=csv.reader(fptr)
    t_data=[]
    Hup_data=[]
    row_num=0
    for row in csv_data:
        # read title
        if (row_num == 0):
            title=row[which_col]
            print(which_col,title)
        # make sure the row contains numeric data
        test_nodect=row[0].replace('.',',',1)
        test=test_nodect.replace('-',',',1).isdigit()
    # collect time and Hup data from csv file
    if (test and row_num >= row_start):
        t_data.append(float(row[0]))
        Hup_data.append(float(row[which_col]))
        row_num = row_num + 1
# Clean the data by rejecting high frequency noise using savgol_filter
window_len=101
poly_order=4
Hup_svgfits=savgol_filter(Hup_data, window_len, poly_order)
pyplot.scatter(t_data,Hup_data, label=title, marker='.', c='black')
pyplot.plot(t_data, Hup_svgfit, "--", color='red', label='svg fit')
pyplot.axis([0, 6000.0, 0, 10.0])
figname='svgfit_%.3g_%.3g_% title

```

```

pyplot.legend()
pyplot.savefig(figname, dpi=300)
pyplot.clf()
# reject outliers with reference to fit
H_tol=0.5
H_tol2=H_tol+H_tol
Hup_clean=[]
t_clean=[]
for iii in range(0,len(Hup_data)):
    H_diff=Hup_data[iii] - Hup_svgfit[iii]
    H_diff2=H_diff * H_diff
    if (H_diff2 < H_tol2):
        Hup_clean.append(Hup_data[iii])
        t_clean.append(t_data[iii])
Hup_data=Hup_clean.copy()
t_data=t_clean.copy()
# capture initial data for initial slope analysis
t_init=[]
Hup_init=[]
for iii in range(0,len(t_data)):
    if (t_data[iii] <= t_initial):
        t_init.append(t_data[iii])
        Hup_init.append(Hup_data[iii])
#print(t_data[0], Hup_data[0])
pyplot.scatter(t_init,Hup_init)
# fit initial data
popt, covar = curve_fit(fitfunc_lin, t_init, Hup_init)
m_fit, c_fit =popt
report_string='Processing column %d, title = %s' % (which_col,title)
print(report_string)

```



```
report_string="Linear fit to 0-nds data from column %d gives slope, m= %10.6f intercept, c= %10.6f" \
    % (t_initial, which_col, m_fit, c_fit)
print(report_string)

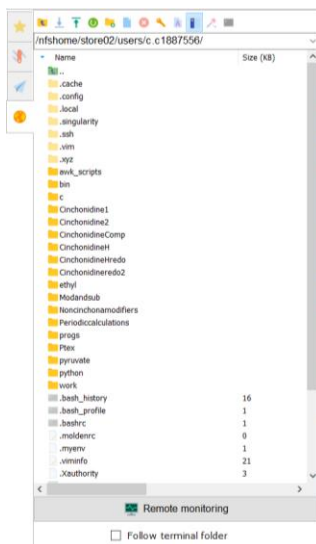
# shift the data along the t axis, rejecting negative time data
t_shift=c_fit/m_fit
report_string="Shifting time origin by %10.6f s will reject negative t data" % t_shift
print(report_string)

t_orig=t_data.copy()
Hup_orig=Hup_data.copy()
t_init=[]
Hup_init=[]
for i in range(0, len(t_orig)):
    t_orig[i]=t_orig[i]-t_shift
    if (t_orig[i]>0.0):
        t_init.append(t_orig[i])
        Hup_init.append(Hup_orig[i])

t_orig=t_data.copy()
Hup_orig=Hup_data.copy()
t_data=[]
Hup_data=[]
for i in range(0, len(t_orig)):
    t_orig[i]=t_orig[i]-t_shift
    if (t_orig[i]>0.0):
        t_data.append(t_orig[i])
        Hup_data.append(Hup_orig[i])

# fit shifted data
popt, covar = curve_fit(fitfunc_lin, t_init, Hup_init)
m_fit, c_fit = popt
stddev=np.sqrt(np.diag(covar))

report_string="Linear fit to 0-nds t-shifted data from column %d gives:" \
    % (t_initial, which_col)
print(report_string)
report_string="Slope, m= %10.6f (stddev %10.6f)" % (m_fit, stddev[0])
```



```
print(report_string)
report_string="intercept, c= %10.6f (stddev %10.6f)" % (c_fit, stddev[1])
print(report_string)

t_line = np.arange(min(t_init), 3*max(t_init), (max(t_init)-min(t_init))/50)
Hup_init_line = fitfunc_lin(t_line, m_fit, c_fit)

# pyplot.scatter(t_data, Hup_data, label=title)
# pyplot.plot(t_line, Hup_init_line, "--", color='red', label='linear fit')
# pyplot.show()
# figname="linfit_%.png" % title
# pyplot.axis([0, 6000.0, 0, 10.0])
# pyplot.legend()
# pyplot.savefig(figname, dpi=300)
# pyplot.clf()

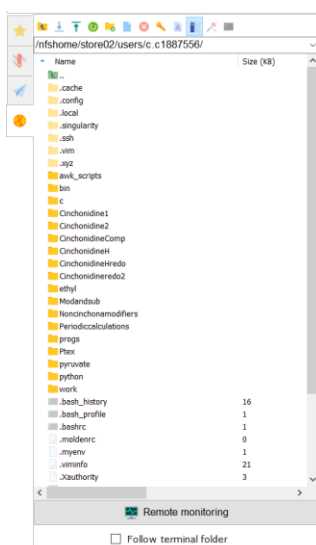
# Now deal with the full function fit to the shifted data
# parameters for the full fit function:
# These are initial guesses that will be fitted
# k1 is the rate constant for hydrogenation
# Keq1 is the equilibrium constant for adsorption of substrate
# min_max_set the bounds, i.e. fitting will not give values outside of these
# bounds.

Keq1= 1.0
min_Keq1= 1.0E-6
max_Keq1= 1.0E6

c0= c0_set
min_c0=0.95*c0
max_c0=1.05*c0

k1= 2*m_fit
min_k1 = 0.5*k1
max_k1 = 1.5*k1

# fit shifted data
limits=(min_k1, min_Keq1, min_c0), (max_k1, max_Keq1, max_c0)
popt, covar = curve_fit(fitfunc, t_data, Hup_data, p0=(k1, Keq1, c0), \
```



```
limits=(min_k1, min_Keq1, min_c0), (max_k1, max_Keq1, max_c0)
popt, covar = curve_fit(fitfunc, t_data, Hup_data, p0=(k1, Keq1, c0), \
    bounds=limits, method="dogbox", x_scale="jac")

k1_fit, Keq1_fit, c0_fit = popt
stddev=np.sqrt(np.diag(covar))

report_string="Kinetic fit to t-shifted data from column %d gives:" % which_col
print(report_string)

report_string="Hydrogenation rate constant k1= %10.6f (stddev %10.6f)" % (k1_fit, stddev[0])
print(report_string)
report_string="Adsorption equilibrium constant Keq1= %10.6f (stddev %10.6f)" % (Keq1_fit, stddev[1])
print(report_string)
report_string="Initial concentration estimate c0= %10.6f (stddev %10.6f)" % (c0_fit, stddev[2])
print(report_string)

csv_row=[title, m_fit, c_fit, k1_fit, stddev[0], Keq1_fit, stddev[1], c0_fit, stddev[2]]
csvout_writer.writerow(csv_row)

print("covariance matrix:")
print(covar)
print()

t_fullfit_line = np.arange(min(t_data), max(t_data), (max(t_data)-min(t_data))/100)
Hup_fullfit_line = fitfunc(t_fullfit_line, k1_fit, Keq1_fit, c0_fit)

pyplot.plot(t_line, Hup_init_line, "--", color='red', label='initial slope fit')
pyplot.plot(t_fullfit_line, Hup_fullfit_line, "--", color='green', label='kinetic model fit')
pyplot.scatter(t_data, Hup_data, label='title', marker='.', c='black')
pyplot.axis([0, 6000.0, 0, 10.0])
pyplot.legend(['Initial Slope fit', 'kinetic model'], title)
# pyplot.show()
# figname="fullfit_%.png" % title
# pyplot.savefig(figname, dpi=300)
# pyplot.clf()

fptr.close()
ptr_csvout.close()
```